Engineering Analysis of Duodenal Digestion

UNIVERSITY OF BIRMINGHAM

SCHOOL OF CHEMICAL ENGINEERING

Ph.D THESIS

Clifford Latty

Supervised by;

Prof. S. Bakalis

Prof. P.J. Fryer

May 2019

For you created my inmost being;
you knit me together in my mothers womb.

I praise you because I am fearfully and wonderfully made;
your works are wonderful,

I know that full well.
Psalm 139: 13-14.

Acknowledgements

First, I want to thank God (YWHW) for His mercies and peace to complete this task and to once again marvel and explore at His handy work, the small intestine. Thank you oh Father, for the past, the present and future that you have prepared for me from the foundations of earth, through your Son, Yeshua. Thank you also for giving me the gift of a daughter (Milani Kanoi Latty) and her mom (Jody Ashton-Latty) on this journey.

I also want to thank my family that supported me from the start of the studies: Edward Williams, Damion Bartley and last but not least my Mum and Dad; Cadeanna and Clifford Latty, and my siblings; Latoya Latty-Calabrese and Aldex Latty, for your love, inspirations, encouragement and support when I needed them the most and in difficult times. I also want to thank my friends, Sydney Brown, Clifton Mcleod and Dr. Reynard Hammond for their unwavering support and words of encouragement throughout my studies, I appreciate it.

Thanks to the PetroCaribe Development Fund (PDF), that have provided the funding for the research and making this experience possible. I want the thank also the key individuals that helped me throughout the project making it a success, my supervisors Prof. Serafim Bakalis and Prof. Peter Fryer for their expertise and support, and suggestions throughout the research. I also want to thank Dr. Ourania Gouseti, Dr. Thomas Moxon, Dr. Georgina Zimbitas. I want to say a special thank you to Lynn Draper, who have been so nice to me and such a wonderful person. I would also like to extend a thank you to Mr. Steve Brookes, at the Physics workshop for making relevant modifications and technical assistance to develop the dynamic duodenal model (DDM). Thank you for your support.

A note to Dr. Gail Baccus-Taylor:

I dedicate this to you; may your soul rest in peace, now and forevermore. I love you Lord, Yeshua.

Abstract

There is a strong interconnection that exists between food structure and gut function and finally health. This work sought to perform engineering analysis of the phenomena occurring during food digestion with emphasis in mixing and reactions limited by mass transfer. Specifically, three (3) in vitro models able to perform food digestion were developed. The salient model developed, Dynamic Duodenal Model (DDM) represented the anatomy and physiology of the human duodenum. The models were used to test the influence of viscosity and intestinal motility on dissolution, mixing and mass transfer of nutrients in the small intestine. Model fluids and real foods (novel breads) passed through the models.

High viscosity fluid systems attenuate sugar uptake, likely due to the reduction in the convective effect of mixing, which also slows starch digestion in breads.

Analysis of the hydrodynamics in the DDM were performed using Positron Emission Tomography (PET), to visualise mixing and mass transfer inside the lumen. The in-vivo lumen flow that occur in the human small intestine during mixing were similarly reproduced in the duodenal model and compared. PET images showed that the rate of axial velocities were associated with the type of particulate systems in addition to viscous effects.

Dissolution profiles of bread boluses were visualised by the structure-mechanics digestion model. Image analyses of the structural changes undergone by boluses suggested that food structure and pH were the main factors driving bolus breakdown and dissolution in digestion.

The main outcomes and implication of this research are the following: (I) Identification of selected wheat varieties with specific arabinoxylan fibre traits for bread making that can influence carbohydrate metabolism and hence glycemic index value for bread (II) Segmentation motility augment mixing and nutrient delivery to the gut wall boundary by means of changes in mass transfer coefficient (III) Development of systematic model that can describe optimised baked breads (gluten free), to alter digestion, and (IV) Visual method that can describe the breakdown pathways undergone by different chewed bolus particulate systems.

The concluding findings contributed more knowledge on some of the factors controlling the physical processes of digestion as well as the effects of different food formulations on nutrient absorption. This may help to develop new lines of structured healthy foods.

Table of contents

List of figures

List of tables

Nomenclature

$C(x,t)$	Drug concentration at any distance along the intestine at time t, mass/m^3
c_1	Concentration in the bulk solution, mol/m^3
c_{1i}	Concentration at the interface, mol/m^3
C_{inf}	Concentration at the infinite, mol/m^3
D	Diameter of the pipe, m
D_{AB}	Diffusion coefficient or diffusivity, m^2/s
D_{mem}	Diffusion coefficient of nutrient through the membrane
F	Frequency of oscillation, s^{-1}
x_o	Amplitude centre-to-peak, m
J	Diffusion flux of material per unit area, mol/m^{2}s
K	Overall mass transfer coefficient, m/s
k_a	Apparent first-order absorption rate constant
k_{bp}	Local mass transfer coefficient, m/s
K_m	Michaelis half saturation constant
k_{rep}	Recipient side mass transfer coefficient, m/s
L	Characteristic length, m
l_{mem}	Thickness of the membrane, m
N_1	Molar flux at the interface, mmol/m^{2}s
Nu	Nusselt number
Re	Reynolds number
Re_n	Net Reynolds number
Re_o	Oscillatory Reynolds number

Rsystem	Resistance from the system
S	Substrate concentration, mol/m^3
Sh	Sherwood number
Sh_n	Sherwood number from net flow
Sh_o	Sherwood number from oscillatory flow
S_o	Initial substrate concentration, mol/m^3
T	Time, s
v_{ave}	Average velocity due to segmentation and peristalsis, m/s
V_{max}	Maximal rate of changing
v_{osc}	Oscillatory velocity induced by segmentation, m/s
W	Lambert *W* function
x, y, z	Position, m

Greek letters

A	Longitudinal spreading coefficient, m^2/s
B	Linear flow velocity, m/s
$\dot{\gamma}$	Shear rate, s^{-1}
ρ	Density of the fluid, Kg/m^3
υ	Mean velocity, m/s
μ	Viscosity of the fluid, Pa.s
μ_{app}	Apparent viscosity, Pa.s

Abbreviations

DGM	Dynamic Gastric Model
GI	Gastrointestinal Tract
PEPT	Positron Emission Particle Tracking
PET	Positron Emission Tomography
PIV	Particle Image Velocimetry
PLIF	Planar Laser Induced Fluorescence
TIM-1	TNO (gastro-) Intestinal Models
TIM-2	TNO Colon Model
SHIME	Simulator of the Human Intestinal Microbial Ecosystem
SIF	Simulated Intestinal Fluid
SIM	Small Intestine Model
STR	Stirred Tank Reactor
TIM	Gastrointestinal Tract Model
VMD	Volume Mean Diameter
OMTC	Overall Mass Transfer Coefficients
PAMPA	Parallel Artificial Membrane Permeation Assay
DNS	3,5-dinitrosalicylic acid
MRI	Magnetic Resonance Imaging
MTC	Mass Transfer Coefficients
USP	United States Pharmacopeia
MR	Modified-release
RDS	Rapidly Digestible Starch
RS	Resistant Starch
SEM	Scanning Electron Microscopy
SDS	Slowly Digestible Starch

Chapter 1

Introduction

1.1 Overview

The principal objective of the research was to perform engineering analysis of the phenomena occurring during food digestion, with an emphasis on mixing and reactions limited by mass transfer. In particular, to develop novel tools that can better describe the effect of food formulations on nutrient absorption to increase understanding of the barriers or "obstruction" to mass transfer.

Carbohydrates are arguably, and without exception, the main source of dietary metabolic energy, every place on earth. Carbohydrates were once only important to provide energy for human nourishment and survival, but in recent times, available carbohydrates have become an important nutritional health marker. Technological advances in agriculture and food engineering has made possible, easy access to foods, while creating a market-driven food-fashion lifestyle economy. As a result, energy intakes have now greatly surpassed the energy requirements of the body, and the “developed world” is currently faced with an obesity endemic (when the body’s mass index is $\geq 30\ kg/m^2$; Berghofer et al., (2008)). The digestion of carbohydrates has now earned new concerns, mainly because it extends its role beyond obesity, causing metabolic syndrome; which clinically leads to the intolerance of glucose. Glucose intolerance is the poor ability to control its postprandial levels, after consumption of carbohydrate-rich meals. Among other linked obesity concerns are diabetes (type 2), different types of cancer, cardiovascular diseases and depression.

Between the period of 2011-2014, 37% of the adult population were clinically obese in the United States (Ogden et al., 2018), while it is predicted to be 42% in the United Kingdom by 2020 (McPherson et al., 2007). The economic burden is immense, with the United States spending a surfeit of 123 billion dollars for diagnosis, direct medical

cost and decreased productivity related to diabetes in 2007 (Ogden et al., 2018; Ogden et al., 2006), while the United Kingdom is estimated to spend £50 billion per annum on society by 2050 (McPherson et al., 2007). As the food industry is responsible for commanding the global food atmosphere, there is a pivotal need for the food industries to be continuously encouraged to help with easing the obesity burden, through product redesign and reformulation, consequently developing "the" new line of foods (Norton et al., 2007). In order for us to develop these types of modern foods to provide health benefits, through site specific delivery of nutrients in the bowels, Norton et al. (2007) have highlighted the need to have comprehensive understanding of the process conditions undergone by a food that affects the food structure, in combination with the material science, physical chemistry and biophysics during digestion. i.e. we will only advance our awareness on the influence of food on human health and wellbeing, when we increase our understanding of food digestion.

Despite the public health awareness of obesity, type 2 diabetes has been surging and has been linked to an approximated 1.5 million deaths that occurred in 2015 (Kam et al., 2016). As a result, there has been recommendations to improve health by increasing exercise and the inclusion of fibre in the diet (Kam et al., 2016). The latter, dietary fibre in the diet, has attracted the food scientists and health professionals due to the range of physiological benefits derived from its consumption. In particular, it; increases satiety, attenuate triglycerides in blood, decrease glucose concentration in blood serum, and furthermore, they have also known to improve colon health (Jenkins et al., 2000; Brownlee, 2011). The British Diabetic Association/Diabetes UK, has recommended at least 30 g per day and the European Association for the Study of Diabetes (EASD), has recommended increase fibre with low glycemic index foods, based on the amount that is needed to safeguard against coronary heart disease. The health effect of viscous dietary fibres to reduce blood glucose levels in the human body has been thoroughly documented over the years (Jenkins, 1977; Torsdottir et al., 1989). However, we acknowledge that no one mechanism can explain why blood glucose concentration is reduced, in the presence of viscous dietary fibres (Dikeman et al., 2006), so the following proposals has been put forward;

- Slowed gastric emptying through increase viscosity, when the bolus enters the stomach (Benini et al., 1995)..
- In the bulk, the luminal content may congeal/ thicken causing reduced contact between enzymes and starch. Starch may also be encapsulated by the viscous agent (Brennan et al., 1996).

- A layer of fluid adjacent to the mucosal surface, also known as the unstirred water layer (UWL), may thicken depending on the mixing conditions, and slow glucose diffusion as it transverse the gut wall barrier (Korjamo et al., 2009 and Pappenheimer 2001b).
- The efficiency of mixing and its reduced convective effects in the presence of viscous dietary fibres has also been postulated as causes of slowed diffusivity (Eastwood et al., 1992 and Tharakan et al., 2010).

Digestion targets the breakdown of the molecular structure that exist within carbohydrates, such as starch, regardless of the form in which it is stored and can vary based on how fast glucose is produced (rapidly digestible; Englyst et al. (1992), slowly digestible starch;Lehmann (2007) and resistance starch; Johnston et al., 2010). Consequently, the structural effect of foods has a major influence on digestion outcomes (Bjorck et al., 1994), such as, the rate at which nutrients becomes bioaccessible (Guerra et al., 2012; Hur et al., 2011). To expand this, if nutrients are locked up and obliged to remain in food structures during the digestion process, they will not be available to be broken down and subsequently transverse the gut wall. Conversely, if they are easily accessible, they will be broken down and released too fast (Guerra et al., 2012), causing an upsurge in blood glucose levels. As a result, carbohydrate-rich foods, such as breads, have been fortified with non-identical forms of fibres (soluble and insoluble) and tested in-vitro to deduce the in-vitro mechanism to make correlation with in-vivo studies.

Figure.1.1 shows the effect of carbohydrate digestion when guar gum at different amounts (2.5, 7.5 and 12.5 g) were added to ~ 45 g of carbohydrate meals that influence blood glucose concentration, in research conducted by Torsdottir et al. (1989).The protocol utilised healthy individuals in the fasted state (12 hours), after which they were fed the above formulated meals. In addition to blood glucose, the gastric emptying times were studied, and correlated to blood glucose responses. It was found that glucose was reduced in the presence of guar but at a threshold; where above 2.5 % guar, there were no noticeable or additional effect in the rise in glucose. It was also concluded that reduced absorption was a consequence of slower gastric emptying rates, even though the author mentioned that, the initial gastric emptying rates were reduced without any significant differences in formulation (rs= 0.83, $P < 0.01$). It is clear that there needs to be a comprehensive understanding of the real mechanism that arise

from the control of carbohydrate digestion in the presence of dietary fibres. Furthermore, the author failed to mention the effect of intestinal events such as the flow and mixing arising in the presence of amylase and chyme.

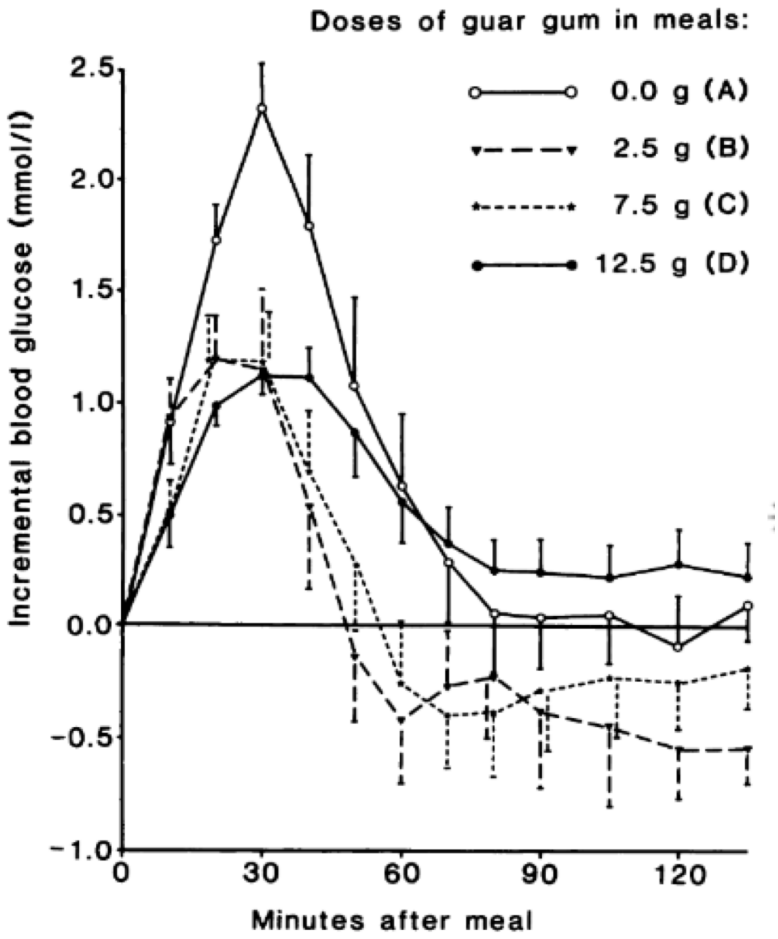

Fig. 1.1 Incremental blood glucose concentration when carbohydrate meals are digested in the presence of varying guar gum concentration. Adapted from Torsdottir et al., (1989).

To replace this experiment by traditional in-vitro methods (static digestion models) would be an extremely complex task for one particular reason - the most appropriate simulation of in-vitro digestion. Even though the methods used to practice digestion have proven to be useful, in-vitro methods rarely simulate the “near real” physiological and biomechanical aspects of digestion when food comes in contact with the gastrointestinal tract (Guerra et al., 2012). This presents a major challenge to in-vitro and in-vivo correlations when enormous efforts that have gone in research on food digestion. Furthermore, a major setback to traditional in-vitro models and methods when specific questions relating to food digestion are surfaced,

such as; “what are the effects of intestinal mixing on these varying food structures during duodenal digestion?”. The fluid dynamics of the small intestine is known to influence the mixing of enzyme secretion with luminal materials and subsequent uptake kinetics in foregut digestion, which is a mass transfer related phenomena (Tharakan et al., 2010). The movement of nutrients from the centre of the lumen to the intravascular fluid (blood plasma) can be described in this way. The flow and mixing during gut mobility are multi-scale processes and are very poorly understood (Lim et al., 2015). Therefore, in spite of the growing knowledge on the benefits of fibres in digestion, selecting the most appropriate physical models to simulate and describe aspects of its’ digestion are essential to the future of food digestion awareness. In particular, understanding the kinetics of carbohydrate digestibility. This will help to elucidate the more detailed mechanism behind the health effects of food, that are more likely to be trusted when comparing in vitro data to real data. Despite these shortcomings, attempts have been made to capture the "entire" digestion processes using single dynamic models such as the TIM1 and TIM2, by TNO (Marteau et al., 1997 and Minekus et al., 1999). The TIM1 and TIM2 models however, lack the capability to reproduce some in-vivo gut contracting mechanisms such as segmentation, (discussed in detail in Chapter 2, Section 2.4.2). The segmentation contracting feature was adopted on the DDM developed in this study, as it is a major contributor to mixing and transfer of nutrients to the lower gut periphery. See Chapter 2, Section 2.5.3 that discusses these limitation on TIM1 and TIM2 models.

1.2 Overall Objectives

In an earlier work, a small intestinal model was a developed by Tharakan et al. (2010), that was able to simulate mixing and mass transfer. It is this work, that is further improved on. In particular, a new model was fabricated, with more physiological and biomechanical relevance to describe in more accuracy, the nature of mixing events undergone by the human duodenum, while it performs digestion. It was able to activate different modes of segmentation, such as regular or irregular contractions, that can occur along the entire gut length, similar to in vivo events, which was not in the older model (SIM- Small Intestinal Model). In addition, it features, a secretions port, where intestinal fluids such as bile and pancreatic fluids similar to in vivo, that allows fluids to enter the lumen. These make important mixing contributions to admix pancreatic fluids containing enzymes with gastric materials for nutrient metabolism. In addition to this objective, an overall approach to the understanding of the in vitro mechanisms controlling carbohydrate digestibility was taken,

which involved structure-function relationships, and resistance to mass transfers. Under this approach, the milestones of the research are as follows:

1. To develop: (i) a biological relevant in-vitro model of the human duodenum which mimicked the main features of the organ and reproduce the motility mechanisms, and (ii) a stirred tank vessel that was capable to investigate in vitro food digestion and absorption. Digestion experiments that were done using the duodenum model were reproduced in the stirred vessel and data compared.
2. To investigate mass transfer rates as a function of mixing regimes (range and type), food formulation and fluid viscosity (fibre type and amount). Thereby, examining the effect these variables may have on resistance to glucose or reducing sugars diffusivity and absorption (mass transfer coefficients).
3. To understand flow and mixing in the dynamic duodenum model (DDM) using pre-established viscosity systems, motility frequencies, and in mixed particulate bread systems (different breads/digesta).
4. To investigate structuring gluten free breads at the baking level to examine its effect on in vitro starch digestion.
5. To develop a new in vitro approach to investigate bolus dissolution kinetics using a range of breads: structure-mechanics-digestion.

This research provides a platform for additional investigation into *in-vitro* modelling of digestion. The work presented here has the potential to guide the understanding of food digestion where a particular breakdown-absorption pathway is desired, leading to design foods that can modulate digestion for health benefits.

1.3 Overview of Thesis Layout

Chapter 2 covers the overview of digestion systems in humans. It then goes onto discuss the literature review of digestion and subsequent absorption of carbohydrates, and the mixing processes involved in its uptake. Lastly, it reviews current in-vitro models used to perform digestion, the need for almost real simulations of digestion, characterising mixing in human and in vitro models, the concept of mass transportation theory as it relates to absorption and digestibility, and food structure: dietary fibres (guar gum and arabinoxylan) in human digestion.

Chapter 3 is the first results chapter, which is concerned with the use of the new novel dynamic duodenal model. Firstly, model fluids were used to test the effect of viscosity and gut movement on absorption, and then finally, bread made up of novel dietary fibres were digested.

Chapter 4 looked at the mixing profiles that were essentially used to perform digestion in Chapter 3. Flows and mixing studies were carried out using visualisation techniques: (i) a molecular imaging technique (Positron Emission Tomography). In particular, the effect of viscosity on mixing, and the velocity profiles in real foods was deduced (ii) residence time distribution technique to establish the type of mixing based on model fluids viscosity.

Chapter 5 looked at the use of newly designed stirred tank reactor equipped with a membrane as an in vitro food digestion tool. The effect of mixing and viscosity on absorption were tested in model fluids, after which bread containing varying fibres were digested. High and low viscosity bread types that were similarly digested in the dynamic duodenal model were compared at the end of this chapter.

Chapter 6 looked at controlling bread digestion from manipulating manufacturing parameters. Consumer preference (high loaf volume) gluten-free bread will be prepared and optimised using a system model and digested in a static dialysis model to test the effect of different bread structure arising, on in vitro starch digestibility and uptake.

Chapter 7 is the final results chapter, which examined various bolus breakdown of breads used throughout the thesis (white bread, wholemeal bread and multi-seed bread). Disintegration rates describing the mechanism of bolus breakdown, under shear forces and no shear as well the effect of the fluids pH will be addressed.

Chapter 8 summarises the conclusions of the thesis and provides recommendations for future work.

1.4 Publications and conferences

Publication:

Thomas Moxon, Clifford Latty, Ourania Gouseti, Serafim Bakalis, School of Chemical Engineering, The University of Birmingham, UK) pp. 35-60 ”From Medicinal Chemistry to Food Science: A Transfer of in Silico Methods Applications” Chapter 3: In-Vitro and In-Silico Models of Digestion: Limitations and Challenge.

Conferences:

Gouseti, O., Latty, C., Moxon, T., Fryer, P.J., Bakalis, S., In-vitro studies of bread digestion: bolus breakdown and digestibility. 5th International Conference of Food Digestion, Renned, France, 2017.

Latty, C., Gouseti, O., Bakalis, S., Bornhorst, G., Bread digestion using dynamic in-vitro gastric and intestinal models. IUFoST, Dublin, Ireland, August 2016.

Bakalis, S., Fourtouni, K., Latty, C., Moxon, T., Gouseti, O., Fryer, P.J., From food engineering to product engineering. EFFoST, Athens, Greece, November 2015.

Moxon, T.E., Latty, C., Gouseti, O., Bakalis, S., Fryer, P.J., Engineering digestion: in-vitro and in-silico methods for studying human digestion. EFFoST, Athens, Greece, November 2015.

Gouseti, O., Jaime-Fonseca, M.R., Latty, C., Moxon, T., Fryer, P.J., Bakalis, S., Engineering digestion: effect of hydrocolloids on mass transfer and nutrient bioaccessibility. 18th Gums and Stabilisers for the Food Industry Conference, UK, June 2015.

Latty, C., Moxon, T., Gouseti, O., Fryer, P.J., Bakalis, S., Novel in-vitro methods to understand mass transfer kinetics in digestion. 12th International Congress of Engineering and Food, Quebec City, Canada, June 2015.

Moxon, T., Latty, C., Gouseti, O., Fryer, P.J., Bakalis, S., In silico modeling of gastric and intestinal processea to study the effects on digestion and absorption of nutrients. 12th International Congress of Engineering and Food, Quebec City, Canada, June 2015.

Latty, C., Moxon, T., Gouseti, O., Fryer, P.J., Bakalis, S., Novel in-vitro small intestine model to quantify mass transfer for different food formulations. 28thConference of European Federation of Food Science and Technology (EFFoST), Innovations in Attractive and Sustainable Food for Health, Uppsala, Sweden, November 2014.

Bakalis, S., Latty, C., Moxon, T., Gouseti, O., Jaime-Fonseca, M., Fryer, P.J., Studying digestion processes for healthier food design: An engineering approach. Institute of Food Technologists (IFT) Annual Meeting and Food Expo, New Orleans, USA, June 2014.

Gouseti, O., Latty, C., Jaime-Fonseca, M.R., Moxon, T., Hari, B., Fryer, P.J., Bakalis, S., Dietary fibre in human digestion: In-vitro and in-silica assessment of the effect of mass transfer on carbohydrate absorption. 12th International Hydrocolloids Conference, Taipei, Taiwan, May 2014.

Latty, C., Moxon, T., Gouseti, O., Fryer, P.J., Bakalis, S., Quantifying the effect of viscosity on food digestibility using in-vitro digestion. 3rd International ISEKI Food Conference, Athens, Greece, May 2014.

Bakalis, S., Gouseti, O., Latty, C., Moxon, T., Fryer, P.J., In-vitro and in-silicamodels to study mass transfer in human digestion for healthier food design. Conference of Food Engineering (CoFE), Omaha, Nebraska, US., April 2014.

Gouseti, O., Latty, C., Moxon, T., Hari, B., Fryer, P.J., Bakalis, S., Dynamic food digestion: Hands-on teach-in. India Partnering Award Meeting, Pune, India, December 2013.

Chapter 2

Literature Review

This review will examine primarily the interconnection between food structure (dietary fibres in food) and intestinal mixing on the ability to modulate starch digestion kinetics for glycemic lowering. As such, an overview of the physiology of human digestive system is presented. This is followed by a description of the mixing process and nutrient absorption. Subsequently, technological progress of in vitro models that describe the physical processes of food digestion, and the need for "near real" simulation are presented, with an emphasis on work investigating starch digestion. Finally, an overview of dietary fibres and food structure and their effects on digestion, such as guar gum and arabinoxylan are presented. References to chemical engineering analogy on the digestive processes are discussed where connected.

2.1 Overview of digestion and gastrointestinal tract (GIT)

Man's curiosity about digestion dates back to prescientific times (Bloch, 1987), and have concluded that food digestion is the body's way to convert foods to fuel. It does this by processing foods into small and then smaller molecules along the entire length of the gastrointestinal tract. Figure 2.1)., shows the location of the GIT relative to other body organs and Figure 2.2., shows the overall processes that occur in the GIT, which can be observed and studied by engineering applications, where each site on the GIT can be described as a series of batch reactors (Penry and Jumars, 1986). The GIT is the largest organ system in the human body, and it is an extremely specialised tube, extending more than 30 ft in length, having a surface area greater than 1000 m^2 (Hooser et al., 2010; Johnson, 2012). The GIT serves as a unique distinctive interface between the outside surroundings and inside the body, and its principal role is to provide the main gateway to for ingress of chemicals, drugs, water and components found in food, and excretion of solid waste. Interestingly, digestion begins before the food enters the body, due sensorial and organoleptic stimulations by eyes, smell and taste. This is known as the cephalic phase of digestion and is known to stimulate both gastric and pancreatic secretions of up to 50 and 25 % respectively. It works by the following physiological mechanism; nerve impulses are sent to the stomach by route of the vacant efferent fibres when the receptors (chemo and mechanoreceptors) located in the nasal and buccal cavities are stimulated by the brain (thought) or smell of foods (Feher 2012, Liddle 2012). It is noteworthy to mention that even though digestibility describes the efficiency of digesting food, the efficiency is related to the properties of food, such as the microstructure of the components' matrix and the consumer's digestive functions, such as the chewing process mechanisms. These will influence the bolus properties that may modulate digestion onwards differently.

2.2 Mouth

Chewing is the first process of food digestion enabling structural alteration, and size reduction- to tiny particles in solid foods (Chen, 2009). This is because the food mass is subjected to shear, saliva, and propulsion from the tongue. Oral residence time varies, lasting about 2 seconds for liquids and semi-solids, and much longer for solids depending on texture and mouthfeel and the individual (chew cycles). Parts of this thesis has looked at chewing of different food materials, and consequential bolus breakdown. Addition of saliva is essential for solid food processing. Saliva aids bolus lubrication and protection, food dilution and

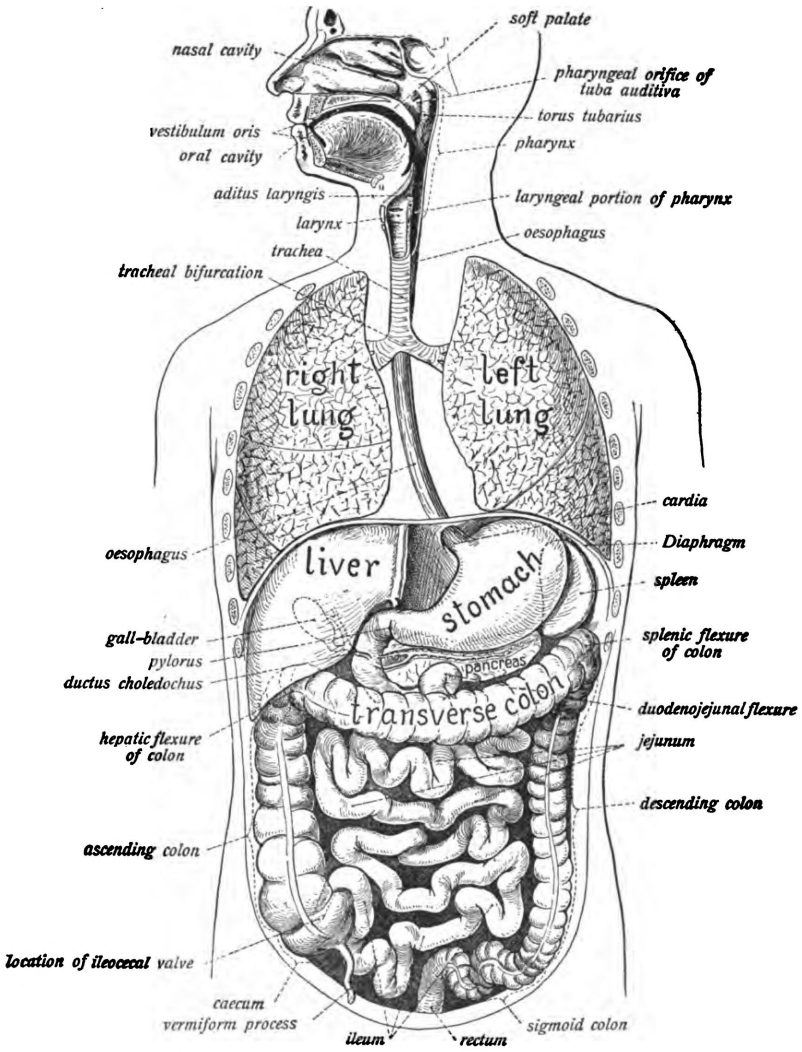

Fig. 2.1 Location of the gastrointestinal tract relative to other main organs in the body. Adapted from Sobotta (1907).

acts as a taste enhancer, while facilitating initial food digestion, by interacting with food components, enabling its structural deformation and breakdown (Chen, 2009; Humphrey et al., 2001). The main stimulus for salivation is food, with about 0.3 - 7 ml saliva secreted in a minute (Edgar, 1990), with the quantity produced ranges about 500 -1500 mL of saliva discharged in 24 hours (Chen, 2009; Humphrey et al., 2001). However, there are several other factors affecting the amount and composition secreted in humans, which influence the final bolus properties (Peyron et al., 2011). The human saliva is a biological fluid, with high complexity, comprising of water (98%), both inorganic and organic compounds (2%), such as antibacterial compounds, electrolytes (sodium, potassium, chloride and bicarbonate), lingual

digestive enzymes (α-amylase, carbonic anhydrase) and proteins (mucus-glycoproteins, peptides-cystatins, statherin, histains, immunoglobulins, proline-rich glycoproteins) and has a slightly neutral pH with an average value of 6.8 (Jenkins, 1978; Johnson, 2012).

After reaching the desired safe to swallowing 'feeling', the food is swallowed, clearing the oral cavity and expelled down the oesophagus (Ertekin and Aydogdu, 2003) by a peristaltic wave-like mechanism. The oral-mastication process is mediated by the central nervous system, controlling the physical and physiological processes, responding to the physical and geometrical properties of the food being chewed (Guyton and Hall, 2012). This is an essential fore step in overall food digestion because further break down in the advancing gastric phase, and subsequent release of nutrients has been linked to the bolus properties derived from oral processing (Chen, 2014; Guinard et al., 1996).

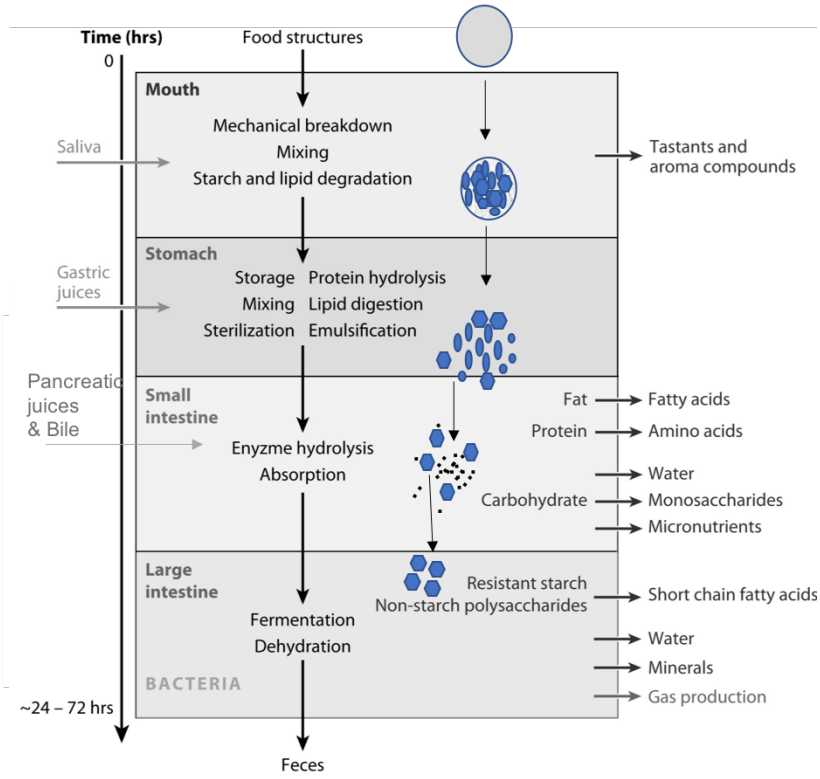

Fig. 2.2 Schematic of the sequence of events of food mass and structure through the mouth, stomach, small and large intestine. Adapted from Topping and Clifton (2001). The compartments can be viewed as a series of chemical reactors (batch processes) from an engineering perspective (Penry and Jumars, 1986).

2.3 Stomach

2.3.1 Stomach's structure and secretion

Once the bolus exits the oesophagus, it enters the stomach, where it begins to accumulate, and now begin a new type of process, under gastric constraints. The stomach is a complex organ as shown Figure 2.3., responsible for mechanical and chemical breakdown the food material (Guo et al., 2015). It is made up of three anatomical regions: the antrum, fundus and body, with two functional regions (Ehrlein et al., 2005), and is about 25-30 cm in length under postprandial conditions (Koziolek et al., 2013). The fundus, is in the proximal part, which acts a reservoir and for the emptying of liquids, connected to the duodenum by the pylorus. Undigested materials are stored here. The antrum is the distal stomach, "multifaceted", performing grinding, mixing, and sieves solid food, and at the same time playing the role of a pump by emptying the chyme (solids) by propelling motions (duodenal delivery) (Guyton and Hall, 2012). This mobility affect disintegration of foods (Urbain et al., 1989). Even with the different regions, the stomach can still be considered as a single vessel, with a heterogeneous environment, concerning the pH and extent of mixing (stirring) (Boland, 2016). When the stomach is empty, it has a free a free capacity of 50 ml, with the diameter of its lumen only minutely larger than that of the small intestine, however when a meal is present, it can hold up to 1.5 L. This is the most stretched organ along the GIT. This is due to the smooth muscles in the fundus and body being able to relax, allowing the stomach's volume to increase and with little rise in pressure (Johnson, 2012; Guyton et al., 2012).

Gastric secretions are important to facilitate the chemical breakdown and fluid mechanical functioning of the stomach. Gastric acid, mucin and gastric intrinsic factors are secreted, as they facilitate, a sterile environment to destroy ingested foreign bacteria, protection of the lining of the stomach's wall and absorption of vitamin B_{12} respectively. The stomach also secretes, electrolytes, water and enzymes such as gastric proteases - pepsin, that breaks down proteins and lipases that break down fats. The cells lining the stomach; gastric epithelium, are made up of three primary cell types (glands), parietal cell - which secrete acid, intrinsic factor, and leptin, the G cell - that secrete gastrin and chief cells - which secrete pepsinogen, gastric lipase, and leptin (Johnson, 2012; Guyton et al., 2012). The parietal cells secrete a highly concentrated dose of HCl at a 160mM (pH 0.8), with the average adult secreting around 2-3 L per day. The pH of the gastric juice is however 2.6. This concentration is known to deactivate salivary amylase in bolus coming from the chewing process, but this range also augments acid hydrolysis of starch (Dona et al., 2010). Regulation of the secretion is achieved the neural, hormonal and paracrine pathways. Secretion of the acid has been

known to occur under three conditions: Cephalic, Gastric, and Intestinal (Mario and Goni, 2014). The cephalic phase which was introduced earlier- occurs prior to occurs prior to food entering the body, while the gastric begins when the food enters the stomach and the intestinal occurs when small fraction amino acids, stimulate the G cells in the small intestine that subsequently secrete gastric in the blood which stimulates the chief and parietal cells (Chang et al., 1996; Johnson, 2012). The latter is importing for maintaining glycaemia through maintaining indirect regulation of blood glucose.

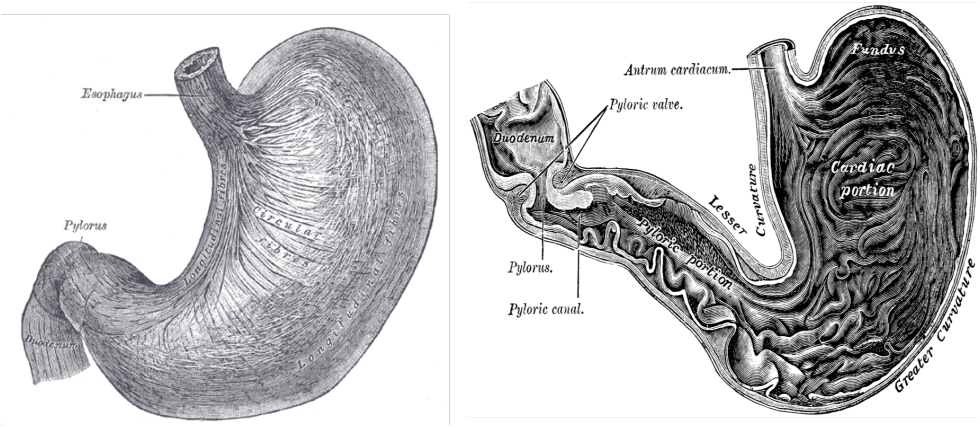

Fig. 2.3 The human stomach showing different anatomical regions. Adapted from (Gray, 1918).

2.3.2 Stomach's motility and emptying

The motility in the stomach is primarily due to peristaltic waves and varies based on fasting or fed states, giving distinctively different patterns, with a single rhythm creating only 3 per minute (20 seconds each) (Bellmann 2016). During the fed state, the movement is described as continuous, while in a fasting state the motility is multiphase in nature. When food is in the stomach, peristaltic waves are initiated, starting from the walls of the stomach and ripples towards the antrum, causing a "terminal antral contraction" (Schulze, 2006) and described by others as, the antral wave contraction (AWC), moving with a velocity profile of 1-4 cm/s towards the antrum antrum (Kong and Singh, 2008). Consequently, the antral lumen occludes, due to the increased contraction width and deepen indentations when mixing the gastric contents that move towards the pylorus. The final antral contraction font inflicts a substantial mechanical force on particulate food matter and therefore is central to the breakdown of solid meals. Forces generated in the stomach have been reported, varying from as little as 0.2N

to a magnitude of 2 N and varies based on meal type and viscosity. These wall forces also generate fluid velocities that are responsible for shear forces in the stomach. For example, an axial force of 10 g is generated from water (0.89 $mN.s.m^{-2}$) and axial force of 7.2 g is generated from 50% sucrose solution (12.4 $mN.s.m^{-2}$) in vivo when a catheter was used test flow rates (Vassallo et al., 1992; Camilleri et al., 1994).

When the pylorus contacts, the sphincter narrows, and the opening is reduced just before the impact of the peristaltic wave. As a result, the chyme is spewed backwards into the regions of the stomach, an activity known as retropulsion (Ehrlein and Scheemann, 2005). Repeated events of retropulsion, and grinding leads to a more consistent chyme in a soft suspension form, because of particle size reduction and homogenisation. Another type of contraction that occurs in the stomach is the antropyloric contractions. These contractions act as a filtering mechanism that "sieves'" the chyme and only small particles (1-2 mm or less) and liquids will flow continuously from the stomach and delivered to the duodenum. These activities have demonstrated the complex events that lead to gastric emptying, rather than simply mixing. Usually, after gastric emptying the fasting motility pattern is restored after which the indigestible larger particulates are emptied (Schwizer et al., 2006; Dressman 1986). Kong and Singh (2008), have led developments to understand the dynamics of mixing in the stomach, and have highlighted the need to further study how material properties such as microstructure and texture of food will affect the kinetics of disintegration under gastric conditions, as they are primarily linked to absorption and glycemic response for different foods. While some studies have investigated the influence of varying manufacturing processes on foods to see the effect on food digestion and glucose response, a deeper examination on the association between the processing of foods and the resulting chemical and physical properties of foods, and its resulting performance during disintegration in the gastrointestinal tract is still deficient.

Gastric emptying has been comprehensively looked at (Janssen et al., 2011; Schulze, 2006). It profiles the volume increases over time in the duodenum, in a changing and momentarily way, i.e., decrease of gastric volume. There are several conditions that influence the rate of gastric emptying's, such as the food caloric density going into the small intestine-duodenum (Moran et al., 1999), osmolality (Vist and Maughan, 1995), viscosity, acidity and, mainly through initiating feedback mechanisms (Delzenne 2010). Figure.2.4., shows the typical gastric emptying of foods by the stomach in normal and diabetic individuals. It shows the same patterns for people with diabetes, except at a slower rate. Liquid meals (10 % dextran solution) are emptied at a faster rate than solid meals (beef). This is due to the sieving function of the antral pump, and the slow solid emptying is linked to the lag stage,

which is a result of the mid-gastric band that retains solids in the stomach, through lower antral activity (Ehrlein et al., 2005; Collins et al., 1991; Camilleri et al., 1985). As mentioned in earlier introduction that carbohydrate digestion is affected by type 2 diabetes has adverse effects on health, and hence the reason for the slower rate of emptying regardless of the meal type (solid or liquid).

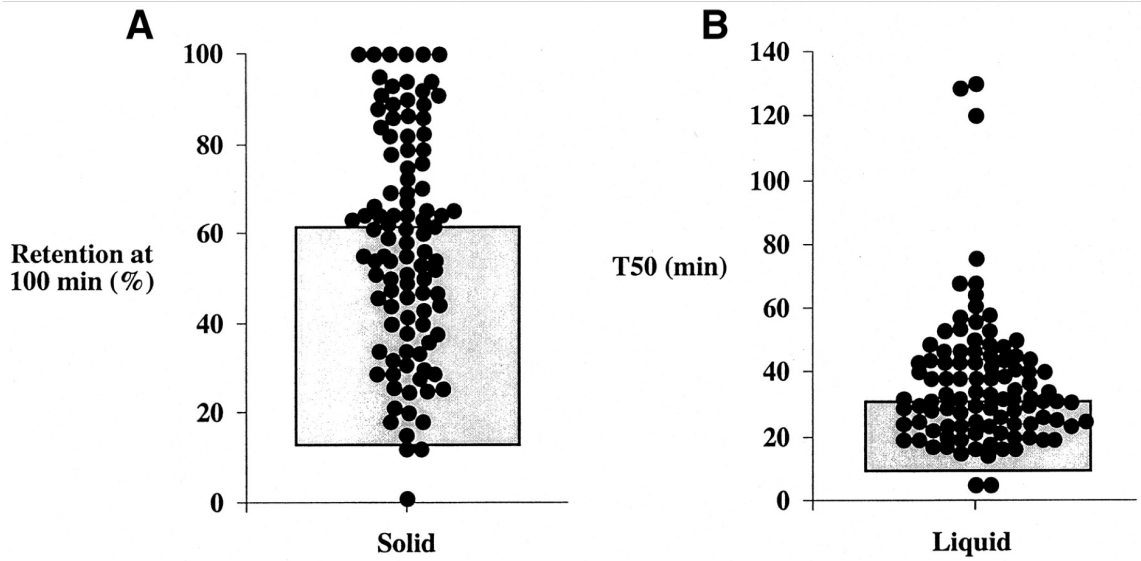

Fig. 2.4 Gastric emptying in normal and diabetic individuals. A -solid meal (beef), B- liquid meal (10 % dextran solution). Shaded area is the occurrence in normal individuals and the dot plots are for the diabetics. Adapted from Jones et al., (2001).

Notwithstanding the many variables that influence gastric emptying, there are efforts done to describe numerically the gastric kinetics of emptying (Meyer et al., 1986; Decuypere et al., 1986). This is important to understand delivery and bioavailability of different food materials, in diets. Models have been proposed, to understand gastric emptying rates (Kong and Singh, 2008a). A well-known approach, and usually, the equation by the first choice is the Siegel's modified exponential power cure. This is developed based on the food fraction retained vs time, see equation.2.1. (Siegel et al., 1988).

$$y_{(t)} = 1 - (1 - e^{kt})^{\beta} \tag{2.1}$$

Where, k is the gastric emptying rate (min-1) and β is primarily used to describe the lag phase. The curve is usually defined by the lag time and half-life. The transit rate through the stomach can differ extensively between individuals, but is usually around 2 to 3 hours (Paintaud et al., 1998).

2.4 Small intestine

The small intestine is 7 metres long starting from the pylorus to the colic valve. It is made up of three anatomical regions: the duodenum, the jejunum and the ileum, in that order. The main function of the small intestine is absorption, taking an approximated 90% of the nutrients and minerals that pass through the gastrointestinal tract (GI) (Guyton and Hall, 2012). The duodenum is the first part - Figure.2.5., ranging from 20-25 cm in length, with a "C" shape structure, and is divided into four parts: superior, descending, horizontal, and ascending orientations, in that order (Mahadevan, 2014; Skandalakis et al., 2009). The superior region (first portion), is the most mobile part of the four, reaching 5 cm in length, starting from the pylorus to the neck of the gall-bladder. It is predominantly covered with peritoneum (membrane lining). The descending region (second portion), is in the range of 7-10 cm in length, starting from the neck of the gall-bladder, with the common bile duct and pancreatic duct perforate it structure about 10 cm below the pylorus. it is uncovered by the peritoneum membrane lining. The horizontal region (third portion) is in the range 5-7.5 cm in length, with the upper surface closely beside the head o the pancreas. The ascending region (fourth portion) is about 2.5 cm long, and the portion that suddenly becomes the jejunum forwardly (Mahadevan 2014).

The balance of the small intestine from the last of the duodenum is the jejunum and ileum. Figure.2.6. shows how mucus in the small intestine varies in thickness along the gut wall. Mucins are secreted by the goblet cells. The jejunum is slightly thinker in diameter, about 4 cm, and more vascular than the ileum which has a diameter of around 3.75 cm. The ileum ranges from 2-4 m in length and ends at the ileocecal valve, the beginning of the large intestine. The small intestine is anatomically designed for optimum uptake having 300 m^2 in absorptive surface area (Helander and Fandriks, 2014). This considerable huge area is a result of the extreme concentration of the meandering surface of the intestines and the arrangements of villi and microvilli (brush border), which is important for digestive mixing and nutrient delivery (Kararli, 1995 and Skandalakis et al., 2009).

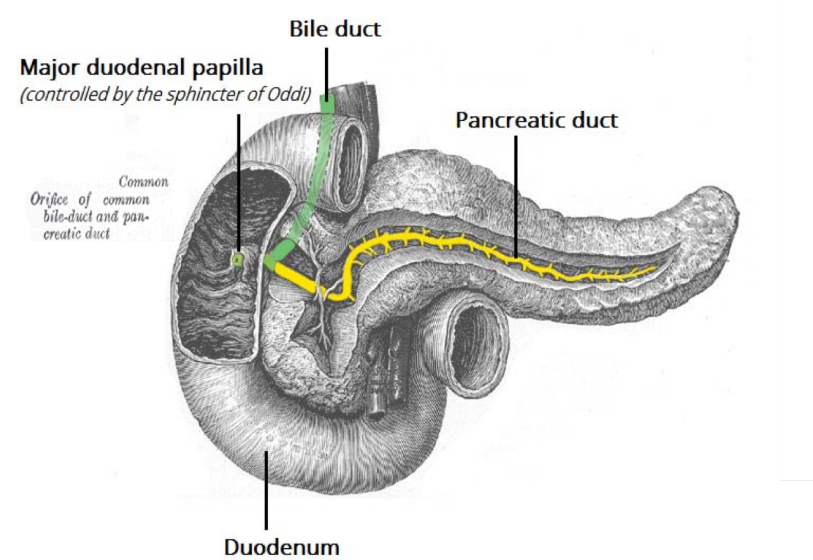

Fig. 2.5 The human duodenum, showing the features that are associated with its digestive function. Adapted from Grey, 1918.

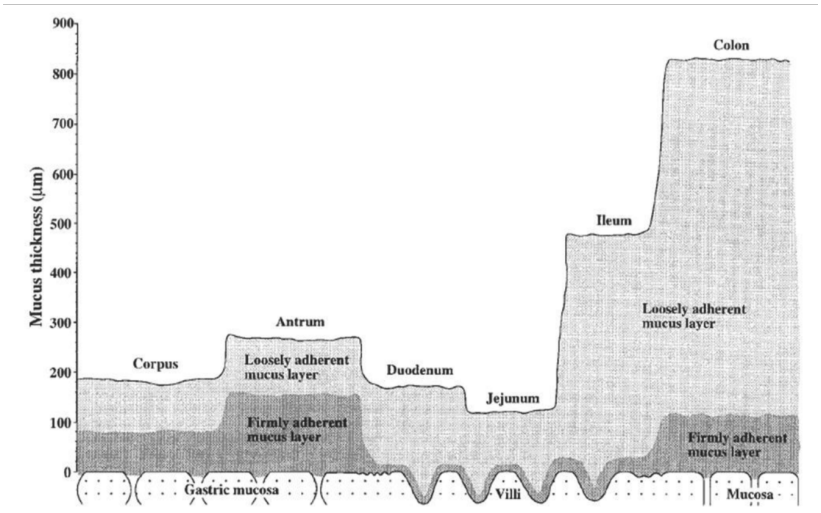

Fig. 2.6 Variation in mucus thickness of a rat GIT: Two (2) mucin gel layers in corpus, antrum, midduodenum, proximal jejunum, distal ileum, and proximal colon. Adapted from Atuma et al., (2001).

2.4.1 Intestinal secretion and carbohydrate metabolism

Carbohydrates are essential constituent in the diet, consisting of simple sugars, complex sugars-starch (polysaccharides) and dietary fibres. Dietary fibres are important for the overall

digestive health (discussed in more detail later in this chapter), and starch provides and important energy source. Currently, the National Health Service (NHS), in the United Kingdom recommends 260 g carbohydrate for daily intake, providing 4kcal (17kJ) per gram, for adults between the ages of 16-64 (NHS, 2018).

Starch is composed of two main fractions: amylose, mainly linear α-D-(1,4)-glucan and amylopectin, a α-D-(1,4) glucan that contains α-D-(1,6) linkages on their molecular structure. Both amylose and amylopectin are embedded in granules ranging from 2 to 100 mm in size, based on the sources and genotype (corn, potato, wheat etc.). The proportion of both differ depending on the starch's botanical origin. The 'waxy' starches has < 15% amylose, 'normal' starches 20– 35% and 'high amylose' starches > 40%. Consequently, starches can be categorised based on their kinetic hydrolysis; (1) rapidly digested (2) slowly digested and (3) resistant, as mentioned in earlier introduction. Once the carbohydrate food mass, is in the mouth, biochemical digestion begins. Where the α-amylase enzyme, called Ptaylin begins to break down complex sugars, by cleaving the -1,4-glycosidic bonds at arbitrary locations, which progressively transform the polysaccharide into maltose, maltotriose and limit dextrins (Johnson, 2014; Butterworth et al., 2011). When the bolus is transported to the stomach via the oesophagus, the acidic phase is traditionally known to deactivate the α-amylase and terminating starch digestion altogether. This is not the case in certainly most situations, as there are in vitro evidence that food microstructure and hence the bolus properties will determine the rate at which this happens, as acid diffusivity into bolus structure varies (Mennah-Govela et al., 2015). Therefore, amylase catalysis my continue for some time, that will play a big role in overall glycemic responses in food. Food particles that have undergone the gastric digestion processes, now the chyme, is propelled in the duodenum as described in earlier section, where a higher percentage of the starch digestion and alteration begins to take place.

Enzymatic digestion in the small intestine happens in two places: in the cavity of the lumen and at the brush border at the epithelial cells, with embedded enzymes. In the small intestine, secretion of the intestinal fluids occur, serving two main functions, to continue enzymatic digestion and neutralise the acidic medium of the chyme coming from the stomach through secretion of bicarbonates which elevates the pH to near neutral. Fluids can be secreted from the pancreas and gall-bladder, via a common duct or from the walls of the intestine. During the digestion process, an approximated 1500 ml of fluids are secreted form the walls each day. This occurs mainly because the villi secrete a number of mineral ions, such as sodium, chloride, and bi-carbonates, into the lumen of the small intestine, as a result water transport towards the digesta via osmosis. This complexity and function has

made it challenging to represent this in-vitro experiments when reporting absorptions, this water inflow to the lumen (osmotic phenomena) is normally left out. Fluids coming from the pancreas, called the pancreatin/pancreatic juice and contains a cocktail of hydrolytic enzymes, pancreatic proteases (trypsin, chymotrypsin, carboxylate-peptidase), and proteins called lactoferrin and pancreatic stone protein, that metabolise the partially digested proteins, and carbohydrates, released in the lumen (Johnson, 2014). An approximated 2~3 L of pancreatic juice is produced per day. It is produced from the Pancreatic acinar cells found in the exocrine glands. Bile acids are also released from the duct, which are made in the gall-bladder, which later emulsify fast, allowing the breakdown by pancreatic lipase (Mahadevan, 2014).

Carbohydrates digestion occurs in several stages: Firstly, the enzymes degrade the amylopectin carbohydrate moiety by targeting the α-1,4-bonds, producing the oligosaccharides-maltose, maltotriose and β-limit dextrins. Secondly, the enzymes, sucrase, maltase and lactase catalyses maltose into glucose, sucrose to yield glucose and fructose, lactose into glucose and galactose respectively. Ultimately, glucose molecules are set free from the oxidising end, leaving the residual 1-6 branch points, that eventually get catalysed by isomaltase. The event usually occurs at the brush border. In healthy individuals, sugar absorption is complete in the in the proximal jejunum (Johnson, 2012). This is know to be an important postprandial hormonal regulation in gastric emptying, occurring by a negative feedback mechanism by osmoreceptors and chemoreceptors in the proximal region of the small intestine. For example, 600m ml of pure water was emptied in 10 minutes, while gastric emptying for glucose solution above 40 g/l was more delayed, when sex (6) healthy individuals were fed with these solutions (Maughan and Vise, 1992). Before glucose can be absorbed into the blood plasma, mixing will be crucial to digestion and delivery of molecules to the brush border for absorption.

2.4.2 Intestinal motility on flow, mixing and glucose absorption

The kinetics of digestion and the absorption of nutrients can be explained by the nutrient behaviour. The nutrient behaviour can be described, by the level of mixing of chyme nutrients in the cavity of the gut (lumen) at the molecular level (μm). This is called micro-mixing, which represents the molecular activity and movements of enzymes and substrates (Baldyage and Bourne, 1986). Therefore, molecular-mixing targets absorption and the associated chemical reactions (Lentle and Janssen, 2008), which could be the critical factors for brush border enzymes found in proximity of the unstirred layer of the villi in the gut walls (Stoll et

al., 2000). It is obvious that without mixing, food and enzyme interaction would be left to be decided by diffusion only and the fate of absorption would be copiously slow. Mixing is therefore critical to the efficiency of the entire digestive processes. Gut mobility of the small intestine provide the impetus to transport and disperse the luminal materials radially and axially. The gut wall contractions patterns differ, in the time scale, and extent of contractile migration activity in which they operate, categorising them as either fasting or postprandial periods (Husebye 1999). Regardless, the patterns observed are a result of the forceful activity of the circular and longitudinal muscles found within the gut walls.

Motility in the small intestine usually occurs by one or either of: (a)peristaltic waves and or (b) segmentation contractions (Guyton and Hall, 2012), Figure.2.7. shows the typical gut motility mechanism that performs mixing. These motions are described by Ehrlein and Scheemann (2005), as slow waves, which are originated from the "interstitial cells of Cajal" located in the intestinal wall, where they move caudally along the length of the intestine. Peristalsis in the small intestine is primarily to provide transport for digesta but at the same time provide some mixing while this is done. The initiated peristaltic contractions are usually weak, 0.2N Ehrlein and Scheemann (2005), moving at a velocity of 0.005 to 0.02 m/s, and very short lived, travelling only 3.5 -10 cm per contraction (Guyton and Hall, 2012). Typically, this flow is unidirectional, caudally (Stoll et al., 2000; Lentle et al., 2008), consequently others, have reported that the rate at which the luminal contents moves caudally through the ileum and jejunum varies in the fasted state from 0.73 ml/ min and in the postprandial state, to 3.0 and 2.35 ml/min respectively (Kerlin et al., 1982).

Unlike peristaltic motions, segmentation contractions propel the digesta in a "to and fro" direction, creating backflow pattern characteristic of mixing resulting in the division and subdivision of the digesta, Figure.2.7-B-C. Segmentation is initiated when a parts of the intestinal compartment is loaded with digesta, and the muscle stretches, then onset localized concentric contraction. Segmentation frequencies vary in the small intestine, ranging from a maximum of 11-12 contractions per minute in the duodenum to a minimum rate of the 9 contractions per minutes in the last part of the ileum. Segmentation, therefore, produces slow migration of the digesta caudally, as the digesta is averagely forced analward more than reverse flow (Johnson, 2014). The rate of transit through the small intestine can vary extensively between individuals but is typically around, or 3-5 hours (Guyton and Hall, 2005). There is another set of gut motility described as the migrating motor complex (MMC), which moves at an initial velocity of 5 to 10 cm/min caudally, and decreases to 0.5 to 1 cm/min (Kellow et al., 1986). The main purpose of this movement is to get rid of the intestinal and digesta residues thereby supressing backflow within the small intestine (Sarna, 1985;

Ehrlein et al., 1987). The engineered model described in chapter three of this thesis has made use of these principles underlying segmentation and peristaltic motility in the gut.

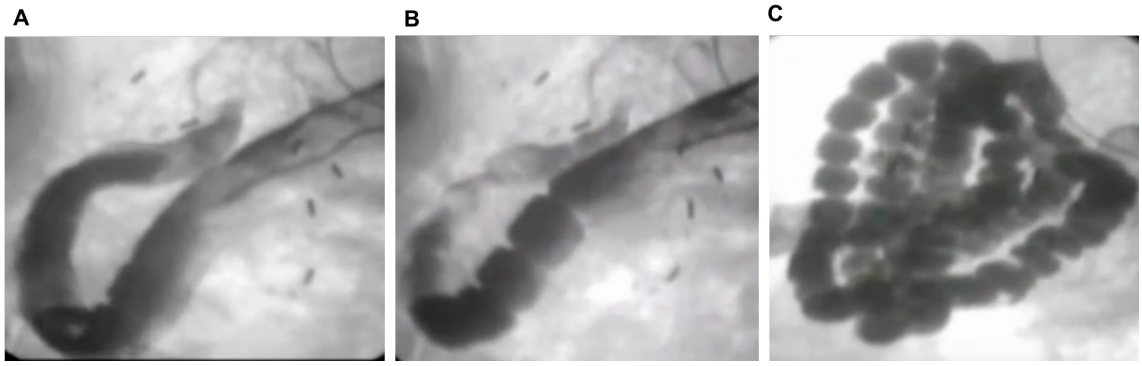

Fig. 2.7 Videofluoroscopy of jejunal intestinal motility along the gut length of a pig: A- peristaltic flow, B- irregular segmentation and C- regular segmentation. Images were reproduced from video provided by Ehrlein and Schemann (2018).

The extent of micro-mixing on nutrient substances can be approximated from the flow behaviour in the lumen cavity. Figure.2.8.shows the flow behaviour generated from segmentation contraction during gut motility, which is predicted using Reynolds number (Re), for fluids- which, describe the relationship of viscous forces to inertial forces within a fluid. The small intestine has been described as plug flow reactors in a series (Jumars, 2000), with conditions that promote mixing and mass transfer in a well-mixed system (homogenous properties), assuming that the system is perfectly mixed in the radial direction and nothing in the axial direction. However, this is not the case, as one can assume that the during segmentation when the circular muscles contract, the formation of vortices are possible, augmenting mixing and mass transfer by both radial and axial dispersion, in different directions and at length scales. Subsequently, the overall mixing can take place by two mechanisms: (1) local mixing included by local flow velocity during contraction and (2) under regularly spaced constriction (regular segmentation), adjacent backflows may collide when contractions are relaxed. If they are done at similar times with like velocities, then their vortices may possibly overlap creating an asymmetry of flow and hence amplify the mixing (Lentle, 2008). This, however, may not be true in all diets conditions .i.e the solid volume ratios and hence the viscosity of the particulate system. As such systems with gell like properties may promote irreversible flows, due to the recovery of the liquid phase into the solid phase during relaxation after compression from segmentation (Lentle, 2005). Therefore, the influence of food properties such as viscosity and food structure on digesta are important to study to deduce

their effect on mixing gut functions. Even so, there is not much proof supporting that these ideal environments arise due to segmentation mixing conditions in vivo.

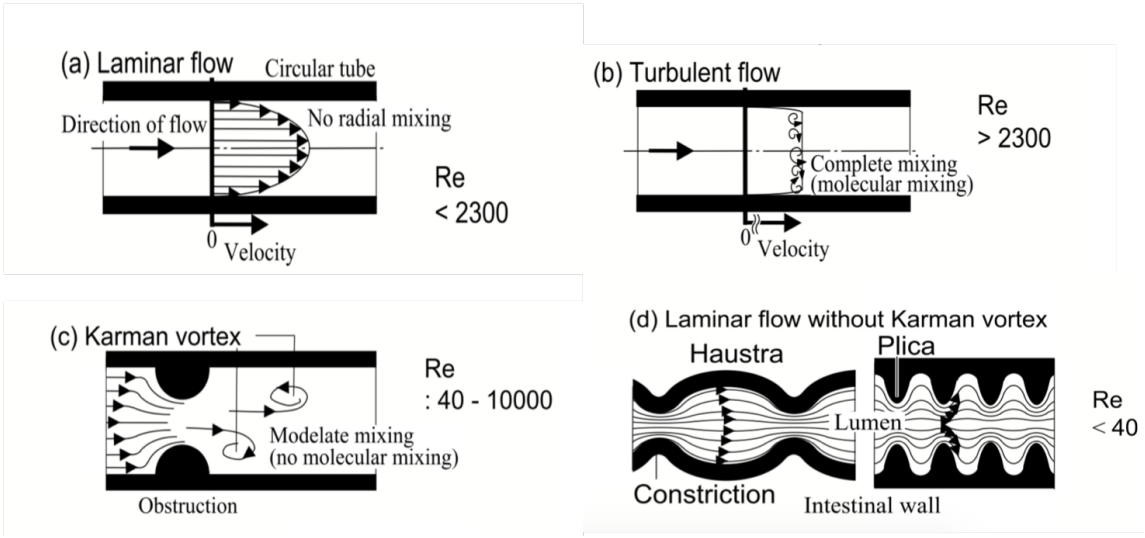

Fig. 2.8 Flow fields generated from gut occlusion in the lumen model: showing nutrient behaviour described by Reynolds number (Takahashi, 2010). When Re is greater than 2300, the flow is described as turbulent, and less that 2300, it describes a laminar flow. Micro mixing occurring during turbulence.

Central to mixing and absorption are the events that occur near the brush borders, and mucosa layer. Figure.2.10.B. shows the structure of the villi -finger-like structures. Flows occurring at this site are poorly understood. As a consequence, the exact mechanisms that augment mixing and mass transfer at this scale are limited in evidence. It is commonly assumed that at this scale, there is a dormant layer, denoted the unstirred water layer (UWL), which has been approximated to be 20-45 μm thick (Levitt, 2013), and is perceived to be the rate-determining step in nutrient absorption. However, Lim et al. (2015), generic two-dimensional (2D) multi-scale models of flow in the gut, has found that the UWL could be responsible for actually stirring rather than being a resistance the nutrient absorption. Therefore, the villi are mechanically active and could be responsible for the secondary flow properties taking place inside the lumen.

Glucose homeostasis is critical to maintain, in order to have proper body functioning. The desired and targeted glucose required in blood plasma is around 4g, less than 7.8 mmol/L (Wasserman 2009). Figure.2.10. shows the intestinal structure and villi. The villi also contain microvilli, which helps to optimise absorption and Figure.2.11. details the mechanism of glucose absorption in the blood before and after consumption of a carbohydrate

meal. Glucose absorption into the bloodstream is by two main mechanisms, either by passive diffusion or and active transport. However, before the molecules are absorbed, the fluid in which they are situated must first flow over some distance as a consequence of gut motion as discussed earlier. If the gut walls are considered as parallel flat plates, the flow of the gut fluid can be simplified to flow in a pipe, from an engineer's view. It can be envisioned tow dimensionally (2D) from Figure.2.8. and 2.9.

One of the root principles of fluid mechanics expressed by Prandtl (1904), was that the effect of the solid boundary on fluid flow is restricted to the layer of fluid directly adjacent to the solid wall (plates), with the exception of fluids that moves with low velocities or those having high viscosities. This is called the boundary layer and analogous to the UWL earlier mentioned, and shear and shear forces (stress needed for a specified displacement) are restricted to this region of the fluid. Outside the boundary layer, probable flow continues (McCabe et al. 2005). In this research the shear stress at the wall membrane (parallel plates) used for absorption is of high importance, because of mass transfer through the membrane wall in the dynamic duodenal model. A relationship exist between shear stress and shear rate (velocity profile), and depends on the type of fluids flowing usually at a constant pressure as observed in Figure.2.9.

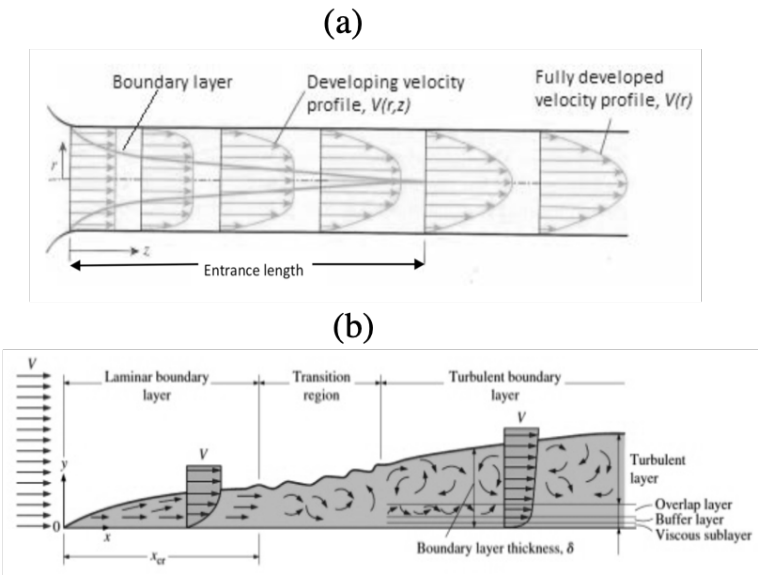

Fig. 2.9 Two-dimensional flow in a circular pipe; (a) development of the velocity profile. V= V (r,z) (b) development of the boundary layer over a flat plate during flow (Cengel et al., 2011).

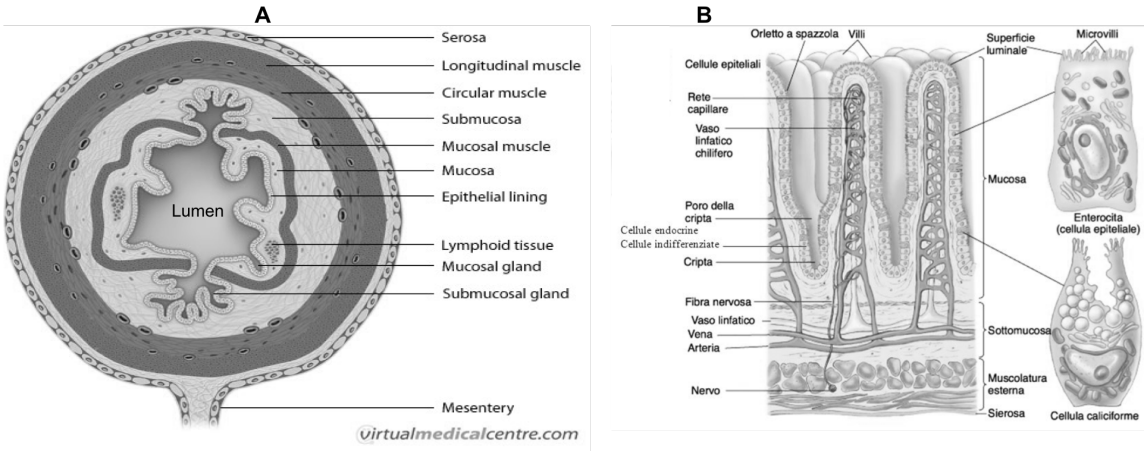

Fig. 2.10 Gut wall; A- cross section, B- Epithelial lining. adapted from Virtual Medical Centre (2018).

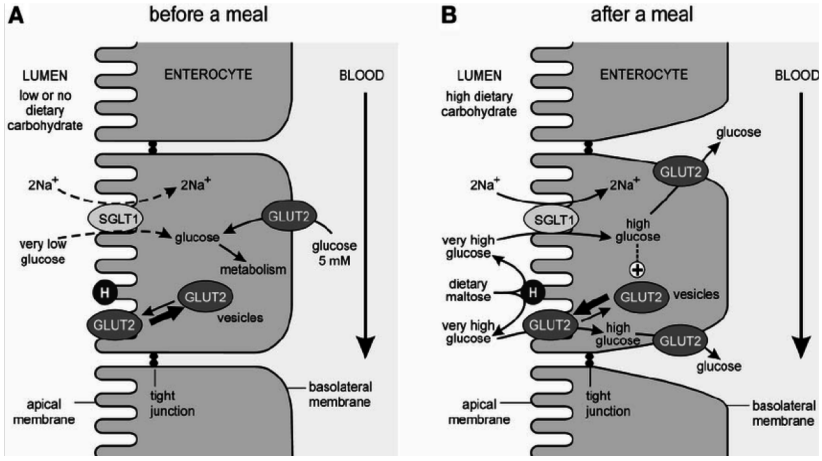

Fig. 2.11 Regulation and mechanism of glucose absorption in the human body-GLUT2 model; A-before meal (no dietary carbohydrate) and B-after meal (high dietary carbohydrate). Adapted from Kellett and Brot-Laroche, (2005).

In engineering perspective, the transfer of nutrients from the lumen into the bloodstream (uptake), can be described in mass transfer terms. The transit of mass from one location to a next, describes mass transfer and is a fundamental backbone of the transport phenomena. A transfer is possible within a single phase or phase interfaces/boundaries in multiphase systems. Mass transfer permits the calculation of mass flux in a conduit system and the allocation of the mass of varying species over time and space in the system, even with the

presence of chemical reactions (Cussler, 2009). The mass transfer coefficient (MTC), model is used in this thesis, assuming that all substance is well mixed with the exception near the interface. Assessment throughout is done based on this thin-film theory (i.e. all activities of flow and mass transfer is at the thin film at the interface) to compute the overall mass transfer coefficient. It is critical to mention that mass movement (diffusion) may also be influenced by the rheology of the immediate surrounding fluid at the micro-scale (μm), rather than the rheology of the luminal fluid at the bulk scale (mm) (Lentle and Janssen, 2008). Even though the micro-rheology concept was beyond this thesis, it is an important consideration for further research when characterizing digestion at the lower end of the length scales (nm). The overall mass transfer coefficient can be computed from equation.2.2.

$$N_i = K\delta C \tag{2.2}$$

Where K is the overall mass transfer coefficient, OMTC (ms^{-1}), *N1*, is the flux ($mol.m^{-2}.s$) and collectively accounts for both convective (characteristic of intestinal motility (Stoll et al., 2000), and diffusional parameters (Cussler, 2009). The concentrations, C_A and C_B are the bulk concentrations in the lumen cavity (where food and enzymes react) and the bulk concentration of the medium absorbing the products (glucose and other reducing sugars) of digestion respectively. The degree of micro-mixing can be approximated by the flow of the lumen contents, which is usually done with the Reynolds number (described below). It is usually common for engineers to correlate mass transfer to some dimensionless groups. Reynolds (Re), Schmidt (Sc), and Sherwood (Sh) are common ones to describe convective mass transfer systems. Re describes flow, Sc describes the diffusion of some kind and Sh number involves the mass transfer coefficient itself (Cussler, 2009). It is noteworthy to mention that mixing and mass transfer in vivo may, therefore, be affected by several factors; the distribution and characteristics of the "continuous" mucus layer (Smithson et al., 1981), the role of the gut wall i.e. the existing villi in the small intestine makeup (Ryu and Grim 1982), and finally, the degree of mixing and distribution of the gut contents can be promoted by motility in the post-prandial state (Lentle et al., 2011; Lentle et al., 2012).

2.5 In-vitro studies on digestion

Performing food digestion ex vivo (out of the body), even though captivating, carries inherent challenges generated by the innate complexities and variability associated with the understanding of both the digestive system as well as the food structure and their interactions,

through ingestion, absorption and to expel. Dissimilar to most pharmacological formulations, foods recipes are multi-component, multi-phase materials with complex structures, and dimensions extending between 8 orders of magnitudes from cm (e.g. first bite) to mm (e.g. sugar granule), μm (e.g. emulsion droplets, starch granules, ice crystals), nm (e.g. plant cell walls) and Angstrom (e.g. single molecules of glucose, water) (Aguilera, 2005; James, 2014). The different food formulations and food structures significantly affect physiological responses during digestion, e.g. enzymatic secretions, feedback mechanisms, satiety perception, residence times, etc., which are therefore difficult to simulate some *in-vitro models,* and almost impossible in others.

The digestive tract is a multi-compartmental system with complex anatomy, structures and functions, and with diverse physiological operating conditions which were comprehensively reviewed earlier. But in addition, it has complex feedback mechanisms, whose role takes control over digestion. For example; the control of satiety which is regulated through a complex, neuro-hormonal brain-gut axis, where signals such as stomach distension or ileal break, where energy detected in the small intestine or ileum are communicated to and stimulate the satiety centers of the brain (Fiszman et al., 2013; Wilde et al., 2011; James, 2014; Lentle et al., 2008; Wey et al., 2014). Likewise, control of gut emptying rates depends on a number of factors, as previously discussed e.g. calorific intake (Calbet and MacLean, 1997) and, the composition of the ingested food (McHugh, 1983 and Brener, Hendrix, and McHugh, 1983) etc. Such controls are advance in their mechanisms, not always well defined and comprehended, and most certainly challenging to reproduce outside of the human body. Adding to this level of sophistication, postprandial responses also vary substantially between and within humans, based on the emotions, hour of the day, amount and type of ingested food, etc. Gidley (2013), investigated controls of duodenal pH of patients with functional dyspepsia during eating and has reported values ranging between 4 and 7 for the 'control' group, indicating the presence of inter-human variability. The human gut also involves many length scales. As also earlier discussed, in particular, the small intestine is the territory where majority of nutrients at molecular dimensions are absorbed- at specific sites in the membrane of the wall, which is matted with villus hair-like projections at the microscale and corrugated into larger villi bodies at the mm scales, all further connected and rooted in forming the tube-like organ (about 3cm diameter). The many length scales, as well as their interrelations, are important in food digestion and present some challenges in simulating them (Wang et al., 2010). Stoll et al. (2000), have indicated that absorption in the small intestine is difficult to mirror *in vitro*, as it is very characteristic of the intestinal walls to perform both macro

and micromixing during the contractions of the tube and movements of the villi respectively, during intestinal motility.

A near real simulation would be ideal and almost complete if the *in-vitro* model would realistically simulate all digestive processes, be easy to use, affordable to operate, produce faster throughput and accurate results, this is not the case, however. It should also be flexible in its functions to allow for any sensitivity analysis or variations in the digestive conditions desired to be studied (such as volume changes and concertation variations). *In-vitro* models which can be either static or dynamic, for food digestion has become progressively trendy since the 1990s and as a result, they have seen substantial progress (Guerra et al., 2012a; Woolnough et al., 2008; Hur et al., 2011). However, *in-vitro* digestion models simulate model conditions, and therefore prudence should be exercised during data interpretations.

2.5.1 In-vitro models

Food digestion in vitro models may consider one or more parts of the digestive paths and may simulate one or more digestive processes occurring after the food enters the alimentary tract. The starting point is the mouth, which initiates and signals the beginning of digestion, and from there, the food transits through to the stomach, then the small intestine, and then the large intestine, in that order. *In-vitro* models for food digestion are, therefore, typically application specific, and should be principally considered for the applications that they were designed. Such as, mouth models designed to study specifically the effect of biting (Meullenet and Gandhapuneni, 2006), mastication (Salles et al., 2007) mixing (Wijk et al., 2011), shearing (Lvova et al., 2012), compression (Loubens et al., 2011; Mills et al., 2011) or the action of the tongue (Benjamin et al., 2012) on different aspects of digestion in the oral cavity, such as taste perception, texture perception, or bolus formation. These models are helpful to unitize and offer insight on different views on food digestion, while simultaneously highlighting the complexities involved and the related challenges in reproducing it. It is valuable to carefully select the *in-vitro* models we use and to understand their capabilities and setbacks during data acquisition and analysis. *In-vitro* food digestion models have been generally cast into two categories: *1) dynamic;* if temporal changes of digestion are incorporated and *2) static;* if they were not (Verhoeckx 2015). The changes may refer to mechanical activities, gut wall contractions (Tharakan et al., 2010a), fluid flow - to and from and within the simulated digestive tract (Vieira et al., 2013).

2.5.2 Static models

Static models uses a fairly diluted digestive intestinal mixture that is fairly well homogenised. When used to perform digestion, static models usually consist of a series of static, batch vessels each imitating a different part of the digestive tract (batch or continuous flow reactors, CSTR) such as oral, gastric, or small intestinal, with their different conditions (pH, temperature, enzymes, etc.) (Guerra et al., 2012). These models lack the time-depended (temporal), processes of digestion and are generally considered advantageous when user-friendliness and when multiple throughputs are required. A prevailing characteristic of static in-vitro model systems is the level of mixing. Mixing is typically performed homogeneously using mixing devices such as magnetic stirrers or shaking incubators (see for example Englyst, Veenstra, and Hudson (1996)). Interestingly, the volumes that those models operate with can vary substantially from microliters (Maldonado et al, 2013), to few hundreds of millilitres (McClements and Li, 2010). They (static models) are highly favoured and offers a lot of flexibility in their operation, allowing for selective regulation of digestive conditions, such as pH changes or enzyme concentrations. This enables systematic investigation of the effect of selected features on food digestion; however, difficulties arise in comparing results from different models that use different conditions of digestion. For instance, European Federation of food safety (2013), described that concentrations of protease in-vitro models used for protein gastric digestion varied by a factor of 100, indicating an enormous range. Woolnough et al. (2008), similarly, reported over 30 different models have been used in 2008 alone to study starch digestion. Further to this is the fact that the models may vary not only in the levels of enzymes used, but also in the type and origin and enzymes obtained from human, animal, or plant origin, may substantially vary in their activities (Benshitrit et al., 2012). Recently there have been attempts in standardising static *in-vitro* models used for food digestion, in an attempt to unite and facilitate comparison between results from different research groups (Minekus et al., 2014). Nevertheless, when similar conditions are used, experimental errors between different laboratories may vary considerably. Studying digestion of specific target groups, such as infants or elderly people, also requires special attention, as the conditions may substantially vary (Thomas et al., 2004; Bourlieu et al., 2014).

2.5.3 Dynamic models

Dynamic models offer the likelihood of merging elements of the temporal profile of digestion, such as mechanical forces and fluid flow (Guerra et al., 2012) together with other physiological conditions (such as pH, type and concentration of digestive enzymes and other secretions,

etc.) in the simulation (Minekus et al., 1999). In the same way, as static models replicate one or more parts of the digestive system, the dynamic system is just as capable. Table 2.1, shows examples of dynamic oral, gastric, and intestinal models developed for food digestion, which simulates the mechanical action of the digestive tract. Table.2.1. indicate some of the prevalent in vitro food digestion models. In some cases, the main purpose of oral digestion is the production a bolus that will then be introduced into a gastric and/or intestinal model for further evaluations (Bornhorst and Singh, 2013). Commercial meat mincers are commonly used to simulate oral digestion depending on the desired application (Hoebler et al., 2002), but there are other, more sophisticated mouth analogues as earlier mentioned that have been specifically developed to study oral digestive processes (Salles et al., 2007; Lvova et al., 2012; Benjamin et al., 2012) etc. Several gastric dynamic models have been developed that incorporate mechanical forces using different techniques. For example, the model introduced by (Chen et al., 2011), utilizes the vertically moving spherical bead positioned in a jacketed tube to mirror gastric fluid flow. The Human Gastric Simulator (HGS), introduced in 2008, by Kong and Singh, mimics gastric mechanical stresses exerted on food digesta through the abrasive motion of small plastic beads in a vessel sitting on a turntable, while, the Dynamic Gastric Model (DGM) mimics gastric wall contractions by the squeezing movement of an elastic conical vessel that sits on a cylindrical container (Wickham et al., 2012). Physical mixing is simulated at representative shear rates, and the model overall simulates food breakdown and transit (Mercuri et al., 2011; Curto et al., 2011). Intestinal motility (segmentation and peristalsis) has been replicated by squeezing a porous cylindrical membrane that simulates the intestinal lumen (Tharakan et al., 2010). In this model, the digesta and enzyme are introduced in the luminal cavity of the membrane, while small molecules such as glucose are allowed to pass to the outer receiving medium.

A multi-compartmental model (TNO's Intestinal Model, TIM1) was introduced in the mid-1990s in the Netherlands, and replicates gastric, duodenal, jejunal, and ileal digestion in the different compartments (Curto et al., 2011; Marteau et al., 1997). A second model (TIM2) was later developed by Minekus et al., (1999), to study large intestine digestion Those models control temperature, pH, and secretions, while replicating peristaltic contractions by a squeezing the walls of a cylindrical tube.

2.5.4 In vitro techniques addressing starch digestion

The digestion and hence the degradation kinetics of starch is a not a simple biochemical process. The quantification of its degradation can be fractionally measured through analytical

Model	Mechanism to produce mechanical element
In-vitro mouth model	Mimics chewing, incorporating and controlling the movement of artificial teeth, jaws, and tongue (Salles et al., 2007).
Dynamic Gastric Model (DGM)	Mimic gastric wall contractions by complex wall motion; gastric motility simulated by squeezing of the conical shaped vessel(Wickham, 2013; Mercuri et al., 2008; Lo Curto et al., 2011).
Human Gastric Simulator (HGS)	Mimics mechanical forces exerted by the stomach by using article-particle abrasion (Kong and Singh, 2008).
In-vitro Gastric Model	Mimics fluid flow in the stomach using compression action between spherical probe and cylindrical wall (Chen et al.,2011).
Dynamic Duodenal Model (DDuo) / Small Intestine Model (SIM)	Mimics segmentation and peristaltic movements of the small intestine by squeezing the walls of a cylindrical shaped membrane at different locations by mechanical action (Tharakan et al., 2010 and Gouseti et al., 2014).
TIM1 (gastric and small intestinal digestion model) (similar apparatus exists for large intestinal simulation)	Mimics peristaltic mixing by squeezing the walls of a flexible tube using pressure (Minekus et al., 1999).

Table 2.1 Dynamic in-vitro models used to perform digestion (-brief listing of well-known models)

techniques which address the rate of starch depletion, the rate of emergence of oligosaccharides chains or rate of glucose emergence. There are a number of factors that influence the kinetics of starch digestion, such as reaction conditions, enzyme/s and most importantly the structure of starch itself. The structure of starch in the native form, vary based on its botanical origins, such as rice, wheat, potato, barley and sorghum, and hence will exhibit different molecular design and physicochemical characteristics, at varying structural scales. Irrespective of the origins, starches has two main components- the amylose residue and amylopectin residue, that is linked by α (1,4) bonds in linear chains, and bonds at α (1,6) branching sites. The structural scale ranges 6 orders of magnitude i.e. from nm to mm, which can be classed in six levels (Ball et al., 1996). Because most of the starch-containing food that is consumed by humans are processed in some way - such as cooking, to add sensorial and textural quality to foods, starch moieties (amylose and amylopectin) undergo structural changes, that conforms during heating, pressure processing and level of hydration forming what is known as gelatinised and retro degraded starches, each having its own structural properties that will affect the overall kinetics of enzymatic starch digestion. The kinetics is influenced because the processes increase the number of polysaccharide chains in the starch to digestive enzymes, and gelatinised starches are more likely to be depleted by ?-amylase than are native starch granules (Mishra et al., 2012; Ball et al., 1996).

Extrinsic factors such as gastrointestinal motility, cooking technique, and the presence of fats and proteins and fibres all affect the nature of starch and hence the GI of food contains carbohydrates (Krezowski et l., 1986; Jenkins et al., 1983). The GI of food is an estimate of the rate at which the available carbohydrate is catalysed in the digestive tract and transverse the cell wall into the bloodstream. i.e. blood glucose levels. This was first described by Jenkins in 1981 (Jenkins et al., 1981). The response of carbohydrate on blood glucose levels are of interest not only to monitor nutrition, but it is also associated with health consequences, as discussed in the early introduction. Measuring digestion of starch by in vivo means are expensive processes, requires many humans as subjects which bring inter-human variability, and time-demanding. Therefore, studies of *in vitro* digestibility as a substitute for the GI tract is an augmented researched focus (Frei et al., 2003; Goni et al., 1997). As such, for nutrition quests, a standard in vitro technique was used by Englyst (Englyst test) to study glucose release to characterise starch fractions, based on the range and kinetics (rate) of their digestions: they have been subsequently categorised as rapidly digested starch (RDS) - the quantity of starch digested in the initial 20 minutes of a typical digestion reaction mixture, slowly digested starch (SDS)- the quantity of starch that is then digested after the RDS but in not more than 120 min, and resistant starch (RS) - starch enzymic hydrolysis is

almost nil (>120 min) (Englyst et al., 1992). This method was utilised to study dietary starch ranging from RS to RDS to deduce the relationship between its digestibility and glycemic response in young males. The study was also extended to understand the effect that these may have on satiety 30 min and 120min after consumption (Anderson et al., 2010). The males were fed tomato soups test meals containing RDS at 10g, 13g, 19g and 41g for whole-grain, cornstarch, high-amylose starch and maltodextrin respectively, and postprandial blood glucose concentration was measured. Blood glucose levels were highest for maltodextrin meals and lowest for whole grain meals. Further food consumption was influenced by higher amounts of RS, which they conclude that its a result of satiety signals in the body, and the method was appropriate to determine food intake thresholds and glycemic response.

Both *in vivo* and *in vitro* digestibility of starch are of colossal importance in understanding the health effects on foods for food and nutritional sciences. For example, studies have also evidence that the amylose portion of starch negatively affects digestibility, where Vesterinen et al., (2001), revealed that by increasing the amylose concentration in starch gels, the extent of degradation was decreased was by α-amylase in 5 minutes, in both in-vitro and in vivo conditions. Minekus et al., (2014) have used, a starch digestion approach to standardise an in vitro design protocol, using a set amount of salivary amylase. Where amylase activity was determined using a starch from potatoes. They have recommended that α-amylase used at an activity of 75 U mL-1, at pH 6.8 is sufficient to perform oral digestion in 2 minutes. However, an older study reproducing in vivo conditions stated otherwise. The study conducted by Hollebeeck et al. (2013), suggested that for the oral digestion salivary stage, only 5 min was sufficient to achieve 5% starch hydrolysis using a surface method, at pH6.9 and α-amylase at a concentration of 1.3 U mL^{-1} (Guyton and Hall, 2012).

Reproducing starch in vivo digestibility, by in vitro methods can be complex, because of the challenges in mimicking in vivo biomechanics of the physical processes. One of the major obvious difference highlighted throughout the discussions so far is between the in vitro model techniques and the in vivo studies is that they are done in stirred tank reactors, which are well-mixed systems. The degree of mixing is completely different from in vivo, and digestibility of starch is known to be strongly affected by the level of shearing (Farhat et al., 2001; Guraya et al., 2001; Shiotsubo, 1983). These studies on starch digestion have definitely led to advances that have helped in the understanding of health effects associated with different structured foods. However, a better understanding of the mechanisms will only be permissible through the use of in-vitro models that can perform digestion to near real expectations, such as the mixing modes and motility patterns to test the effect on dietary carbohydrates supplemented with dietary fibres.

2.5.5 Abilities, setbacks and the future of in-vitro models

Although *in-vitro* models have seen significant progress over the last decades, they currently have a number of limitations and challenges (Hur et al., 2011; Guerra et al., 2012). One such limitation is their biological significance (geometry and physics), and their correlation with *in-vivo* processes correlation, (Hoebler et al., 2002; Wey et al., 2014), and therefore it is our interests to establish methodologies for model validations. Currently, models have been reported that agree quite well (Hettiaratchi, 2012) or less precisely (Hettiaratchi, 2012) with, in-vivo data. In addition, models are needed that will link the various length scales involved in food digestion and identify the controlling mechanisms of digestibility and nutrient bioaccessibility. Harmonization of in-vitro models and standardisation of digestive conditions is, therefore, central and beneficial, as they will allow comparison between the different laboratories. For this, it is crucial to first understand the experimental conditions that we want to replicate. For example, the *in-vivo* biochemistry and the fluid mechanical influences are still not well understood and agreed, such as are the enzyme to food concentrations ratios (Sugano, 2009; Guerra et al., 2012; Hur et al., 2011). There is a need to produce robust models that can be used beyond academic institutions, at a sustainable cost, and modellers of the future are likely to work towards this direction.

2.6 Common techniques used in characterising mixing

In order to evaluate and quantify mixing to some extent, there are several techniques adopted and used in gastrointestinal studies. Imaging application to observe flow and mixing is increasingly attractive since patterns would not be otherwise observed. A wealth of knowledge about mixing is already available on digestion and in particular the stomach and duodenum mechanical functions on an mm length scale (Schulze, 2006). Such as, motility patterns of the gut walls (Schulze, 2006; Camilleri, 1997; Pallotta, 1998; Write et al., 1999; Code and Nelson, 1996; De Schepper et al., 2004), viscoelastic properties (Torgersen, 1942, Gregersen and Kassab, 1996; Kita, 1996; Gao et al., 2003; Kita, 1996), the dynamics of gastric emptying, and electrical and neuronal controls (Meyer, 1991; Meyer et al., 1986; Castedal, Bjornsson and Abrahamsson, 1998; Liau et al., 2001). On the other hand, information about the flow process that transfer's small molecules from macro and complex foods are limited and not well elucidated (Schulze, 2006). Such as the penetration of secretions onto and into foods, particulates from the "solid" phase becoming suspended in the continuous phase, the

scattering or drawn of sheet/film formations for enzyme catalysis, and the replenishing of nutrients at the epithelium boundary. These events are at a disposal for fluid-mechanical considerations i.e., the importance of the discrete flow mechanics to understand digestion is left to be evidence (Schulze, 2006).

These events are captured using various techniques but still has their abilities and setbacks. James Mayer in 1990, had demonstrated a proposal to explain solids and liquid emptying from the stomach, and now, it is possible to assembly flow paths for fluid and particles alike, and compute the shear stresses and efficiency of mixing, which are difficult to be tracked visually (Jeffrey, Udaykumar and Schulze, 2003). Further to this, is the use of Magnetic resonance imaging (MRI) coupled with ultrasonography is used to compute volumes in the intragastric condition and changes in volume that arise during filling and draining/emptying of the stomach. The physical state of the food can also be traced during digestion. This is owed to echo-planar imaging, where Marciani et al., 2001 had conducted the study. It is important to highlight that depending on the design, component and physical material making up of the model, different rigs would require different techniques to study flow and mixing ex vivo. This poses serious challenges for establishing flow and mixing studies in *in-vitro* rigs. For example, a model made of certain metal may cause inference with the study based on the techniques required. Such as a particle image velocimetry (PIV) would require a rig that is transparent, due to tracing metal particles through a laser beam. Additionally, the choice of technique may also be correlated on the aims of the study.

Particle imaging velocimetry is widely used in engineering to look at different flow patterns and used to establish some parameters and derivatives such as velocities and forces from the flow fields (Pianko-Oprych et al., 2009). It has recently been used successfully for studying the flow of solid-liquid suspensions at low concentrations in stirred vessels. When the solid phases increase by modest magnitudes, the PIV method becomes increasingly difficult to use to track and study flow, leading to revert to the use of other methods. PIV was used to understand the forces fields generated, acting on the bolus simulating the shear condition of the stomach. This is covered in Chapter 7, of this thesis, using a transparent in-vitro rig, to visualise the swelling phenomena of chewed bolus under diffusion (self-mixing), and forced convection.

An alternative to study flow and mixing in opaque systems such as the dynamic duodenal model would be to use of positron emission tomography (PET) and positron emission particle tracking (PEPT). PET is widely applicable in medical techniques, mapping spatial concentration of radioactive species added into the body (Phelps, 2006 and Webb 1998; Leadbeater, Parker and Gargiuli, 2011). Likewise, it is applicable to study inanimate objects

or processes such as industrial apparatus and mixing (Parker et al., 1994 and Parker et al., 1995). The work done in this thesis made use of the positron emission tomography (PET) technique, to study the effect viscosity had on mixing, in the dynamic duodenal model, this is examined in Chapter 4. PEPT is a modified version of PET and is used exclusively to understand the dynamics of particle, granular and multiphase flow systems (Parker et al., 1993). Both PET and PEPT uses the gamma-radiation emitted from a positron source which is of relatively high energy and can infiltrate a substantial extent of materials (Leadbeater et al., 2011). The timescale over which data becomes statistically important is greatly lowered and analogous to typical physical and engineering timescales. This makes them suitable to assess mixing with different food materials and the rig's construction materials, under different conditions. Chapter 4**,** have identified mixing profiles based on varying structures of real and model fluids, under similar shearing.

2.7 Dietary Fibres (DF's)

Dietary fibre is comprised of indigestible carbohydrate polymers, or non-starch polysaccharides (NSPs). They are usually present in two forms; soluble hydrocolloids, such as β-glucan, pectin, guar gum, psyllium, and arabinoxylan or insoluble; such as wheat bran, cellulose and hemicellulose - the plant cell wall components and variety of other gums and mucilages (Southgate, 2001). The health effect of dietary fibres in the diet has been observed from early times, and in 1920's bran ingestion lead to a rise in stool weight and laxative effect, which provoke the interest of dietary fibres studies (Slavin, 2013). Consumption of dietary fibres has evidence a range of health benefits, in the management and prohibition of type 2 diabetes, obesity, heart diseases and cancers of the rectum. The heterogeneity of dietary fibres are what allows them to have a range of physiological effects (Table.2.2 synopsis), i.e., different fibres for different responses - not all fibres are not alike, albeit all are indigestible (Slavin and Jacobs, 2009). They are structural different at the molecular scale, having dissimilar monomeric components, the absence or presence of charged groups, linkages and types among the backbone chains (Tungland et al., 2002). Subsequently, they behave very differently, towards the length of the gastrointestinal tract during their transit. Insoluble fibres reduce bowel transit time and allow increase faecal bulk and aids in colonic fermentation (Brownlee, 2011; Brownlee et al., 2006), while soluble fibres delay gastric emptying rates, influence satiety - by changing energy density of foods (Lyly et al., 2009; Pasman et al., 1997; Perrigue, Monsivais and Drewnowski, 2009), lowers serum cholesterol

concentration, slows glucose absorption and enhance immune system (Yamatoya et al., 1997).

In order to tackle high GI for foods, it has become increasingly popular to add soluble dietary fibers (SDFs) to food formulations, as an alternative means to slow digestibility of high GI ingredients (Rasoamanana, 2013). There is a two fold effect of adding soluble dietary fibres to food formulations: (1) alteration of the microstructure within the food matrix - consequently starch will structure and be organised differently and, (2) control the digesta properties once it is consumed, and in contact with secreted oral, gastric and intestinal fluids, thereby affecting gut function differently, as previously mentioned. Using hydrocolloids, primarily those which congeal or gel, amplify the viscosity (Akhtar et al., 2005) and therefore affect the flow of digesta during its transit in the digestive tract. While there is evidence and data to support these claims (the effect of viscosity on gut function), the underpinning means by which they causing these responses still remains to be established. The addition of viscous DFs such as guar gum, arabinoxlyan, alginate and β-glucan is therefore a common approach to maintain physical properties, such as viscosity, in the gut content, when slowing gastric emptying (Burton-Freeman, 2000) and small bowel transit (Kristensen and Jensen, 2011). Figure.2.12. shows, the suggested mechanism soluble dietary fibre operates within the small intestine. The study was conducted to rationalise and deduce the mechanisms responsible for the cholesterol-reducing effects of soluble dietary fibre. It was found that bile micelles, binds to soluble dietary fibre, preventing their re-absorption, from in vivo, ex vivo and in vitro experiments, i.e., a reduction in bile re-cylcling thereby allowing the liver to utilise cholesterol in the production of fresh bile (Gunness and Gidley, 2010).

While it is postulated that, soluble dietary fibres impairs absorption of some nutrients through physical interactions due to vicious effect, thereby reducing postprandial glucose levels, soluble dietary fibres have been extremely important to manage starch digestion. Chapter 3 and 5, of this theses, had looked at food material responses to starch digestion in simulating small bowel digestion. Where, bread was incorporated with different DFs, arabinoxylan and guar gum, and as such, they will be the only two DFs to be reviewed in breadth.

2.7.1 Guar gum

Guar gum is derived from the seeds of the plant *Cyamopsis tetragonoloba*, consisting of high molecular weight polysaccharides of galactomannans, (galactose and mannose groups) Figure.2.13. Guar gum aqueous solutions displays relatively high viscosity even at very small proportions and increase relatively with augmented levels of guar (Morris

Dietary fiber type	Gastric emptying	Satiety	Glucose homeostasis
Guar gum	Delayed in most studies; possible threshold at 5 g	Enhanced in most studies; effect is viscosity dependent, abolished by partial hydrolysis of guar, and modulated by meal fat content	Decreased postprandial glucose levels in most studies; GE delay is main factor; delayed absorption contributes.
Pectin	Delayed with 10g	Enhanced possibly through direct gastric effect	Decreased postprandial glucose when 10 g; possible dose-response relationship
Alginate	Unaffected in healthy normal-weight individuals; delayed in those with stable diabetes	Enhanced only by strong-gelling form independent to GE	Decrease in correlation to GE effect
Glucomannan	No effect	Enhanced satiety, combination with psyllium	No effect
Cellulose	Minor effects (unmodified); delayed (water-soluble)	Enhanced (EHEC)	"Second meal effect" in combination with amylopectin / amylose
Wheat fibre	Unaltered in most studies; delayed by undiluted and coarse bran	Enhanced in most studies; inverse correlation with degree of refinement	Variable effects

Table 2.2 Synopsis of dietary fiber effects on gastric emptying, satiety, glucose homeostasis. Adapted from Vella and Camilleri (2017)

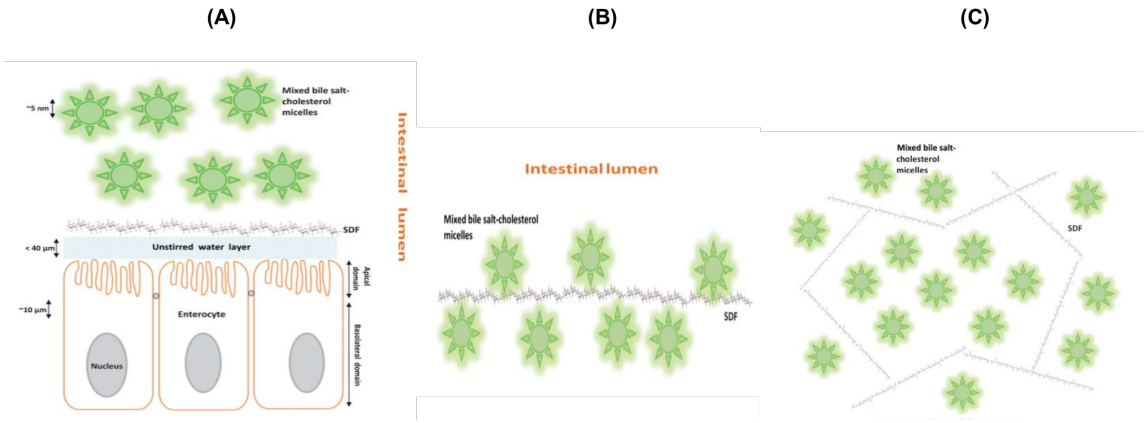

Fig. 2.12 Various functional mechanisms of soluble dietary fibre during small intestinal processes on bile salts: A - barrier formation along the gut wall, B- interaction with mixed bile salts cholesterol micelles and C -entrapment mixed bile salts cholesterol micelles. Adapted from Gunness and Gidley, (2010).

et al. 1981; Robinson et al. 1982). This is a result of enhanced inter-molecular chain or entanglement and reaction which causes the viscosity to rise (Zhang et al. 2005). Even though guar is a water-soluble, most food applications recommend below 1% concentration to accommodate gelling, thickening, stabilizer, emulsifying, and obstruct creaming, syneresis and starch retrogradation (Roberts, 2011). When used in greater quantities, it may also affect other organoleptic food quality attributes, and may also influence gut functions and other physiological functions as the viscosity is amplified. Guar gum in human diets displays a lowering effect on cholesterol and glucose due to its gelling properties. It also assist in decreasing body weight and prevent obesity. Because of the gelling ability of guar gum soluble fibre, higher satiation is gained because of slow gastric emptying. In vitro study shows that presence of guar gum significantly decreases starch digestibility. It acts as a barrier between starch and starch hydrolyzing enzymes (Dartois et al. 2010). But the extent to which these happen are not quantified and therefore requires assessment. With its wide application in human diets, it is worth studying to find out relevant cues on how it affects digestibility of starch.

Brenelli, Campos, and Saad (1997), studied guar gum in vivo to test the effect it has on post-prandial glycemia in humans. It was compared to two other soluble dietary fibres, pectin, and carboxymethylcellulose at similar viscosities. The outcome showed that regardless of the "like" viscosities, guar gum was able to attenuate blood plasma glucose concentrations to a greater extent. Further, when guar was incorporated into potato starch matrix, and in vitro starch digestion studies done for over 3 hours, there was a noticeable reduction in

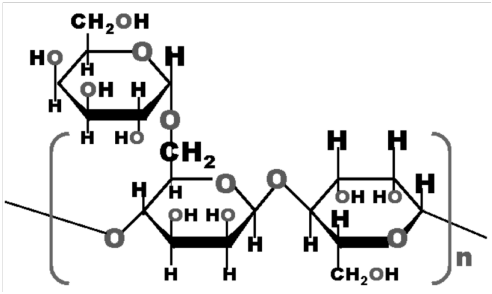

Fig. 2.13 Chemical structure of guar galactomannan backbone (Adapted from Wielinga, 2010.

concentration of starch digested. Gularte and Rosell (2011), have concluded that, it was the guar's ability to obstruct ?-amylase access, thereby being able to pose as a physical barrier. Brennan et al. (2008), incorporated white wheat breads with guar gum at levels of 2.5% and 5% to predict the glycemic indices. Results showed that a reduction of 4 and 13%, respectively were achieved, as a result of guars obstruction to amylase. Pasta digesteion were also studied. Likewise, Brennan et al. (1996) in an earlier structural digestion study conducted have conclude this, where scanning electron microscopy and by fluorescence microscopy were used to study bread matrix that were digested in vivo in pigs. They found that in vitro starch digestion was attenuated to a great extent, and the microscopy studies on the breads structures showed that galactomannan and the wheat starch microstructure were closely intact during the early stage post-prandial period (0–90 min). The results further confirm that galactomannan play the role as a physical 'blockade' to α-amylase and starch interactions. It is expected that in humans, the effect of guar gum (viscosity) on gut function, should meaningfully minimise the increase in post-prandial glycaemia. This many features of guar gum, makes it a highly attractive researched food ingredient, into food systems.

2.7.2 Arabinoxylan

Unlike guar gum, Arabinoxylan (a/x), is a non-starch polysaccharide derived from the cell wall of cereal grains. It is a polysaccharide with its backbone molecule composed of (1 4)-linked β-D-xylopyranosyl units. They can be monosubstituted or disubstituted at the O-3 or O-2 site on the backbone molecule (Figure.2.14 .) by α-L-arabinofuranosyl substituents (Courtin et al., 2002). The type of substitution will depend on the plant origin/ cultivar; for example, mono-substitution is usually found in rye but not typically found in wheat varieties, the location in the intact grain; for example, the outer wheat bran is highly substituted than

the aleurone layer i.e. an a/x fraction of 0.88 and 0.35 respectively, with the endosperm having up to 0.7 a/x (Izydorczyk, 2009; Saulnier et al., 1995). The pattern and level of substitution on the polymer will control the physicochemical properties; solubility, hydration properties and viscosity in water-soluble a/x (Courtin et al., 2002; Saulnier et al., 1995). AX can be water-unextractable as well, which is known to have a deleterious effect on loaf specific volume. However, loaf volume is enhanced by the water-extractable portion, which is around 25% of the endosperm of the grain (Izydorczyk and Biliaderis, 1995). They are water-soluble and forms a highly viscous aqueous solution.

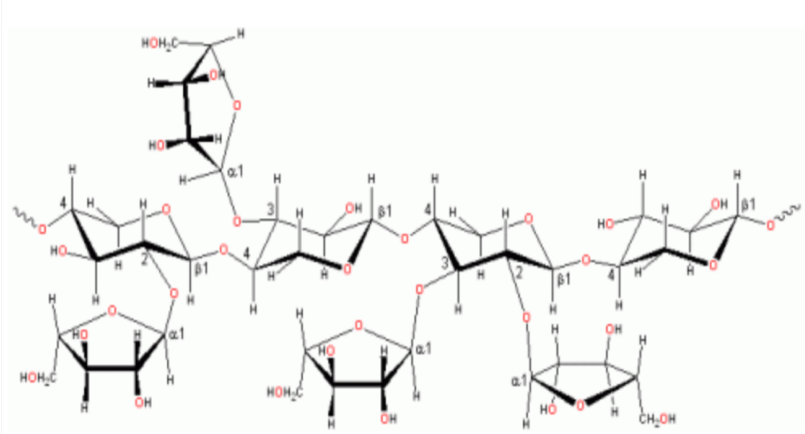

Fig. 2.14 Chemical structure of arabinoxylan consisting of α-L-arabinofuranose residues attached as branch-points to α-(14)-linked D-xylopyranose polymeric backbone (Khattak et al., 2012).

Wheat is one of Uk's most abundant food crop grown and in many varieties. The ingestion of fibres has been liked to health benefits, such as reduced risk in type-2-diabetes, as was earlier discussed. Cereal type diets, those essentially containing bread, form a major part of the UK edibles thereby, providing much of the bodily demanded carbohydrates. White bread forms a major part of this bread demand, even though other alternatives such as wholegrain and wholemeal type bread are encouraged. One functionality of white bread is that they are starchy and are speedily digested to glucose, categorising them as high glycaemic index (GI) foods. This bread contains a very tiny fraction of dietary fibres. The soluble portion (70%), of the dietary fibre arabinoxylan- from wheat has the tendency to be highly viscous and make them an attractive alternative to reduce glucose response to high starch digestibility formulations (breads), reduce triglyceride in healthy individuals, along with others with conditions of impaired glucose tolerances (Garcia et al., 2006; Lu et al., 2004; Mohlig et al., 2005). The means by which these fibre work in the intestinal tract is still left to be elucidated

- albeit evidenced that its repercussion is to alter the viscosity of the contents in the stomach and small intestines, reducing transepithelial absorption into the blood.

Arabinoxylan fractions are studied in healthy humans, in particular, bread formulation to improve postprandial glucose and insulin responses (Lu et al., 2000). Bread types were baked professionally with AX- rich fibre at 7%, or 14% dry-weight basis to a standard white bread recipe, that were palatable to whole-wheat bread at 50%. 30 Normoglycemic subjects, revealed that for bread with AX- rich fibre at 7, and 14%, insulin were 17 and 32.7 % lower respectively, than that of white bread consumption. While incremental area under the curve for glucose was 20.2 and 41.4% lower respectively. A major part of this research had made use of two arabinoxylan fractions, from two unique wheat cultivars to see the effect it poses on in vitro duodenal starch digestibility in bread (the mechanism to control digestion under gut motility), when they were incorporated into the existing white bread formulations.

2.7.3 Bread

Bread is highly the most used (eaten) dietary starchy food around the globe, as previously mentioned, and possess a complex microstructure, comprising of a protein-fat-air-matrix with seeded starch molecules (Figure.2.15.), and elevated glycemic loads, and an important factor in regulating the glycemic response after ingestion (postprandial) (Fardet et al., 2006). Traditional white wheat bread is low in nutrients and minerals, and cause an increase in plasma glucose concentrations, thus making individuals more prone to the risk of metabolic diseases such as type 2 diabetes, CVD and obesity (Fardet et al., 2006). With this strong interconnection between structure and digestibility, it warrants the understanding of digestibility to find ways and means of controlling its digestion. A lot of focus has been placed on reformulation, using alternative low glycemic index (GI), ingredients in order to lower blood glucose response in different bread types (Bharath and Prabhasankar, 2014; Burton et al., 2011). Processing of bread, so that the microstructure can be rearranged, will influence its digestibility. This makes them an attractive staple food to manipulate and regulate blood glucose levels. Bread baking technology revealed that creating breads with more compact structure can regulate postprandial glucose kinetics and hence the metabolic response (Eelderink et al., 2015). And recently, Gao et al. (2015), has attempted to manipulate the bread structure using the same formulation under different processing conditions. Bread is therefore an important food item to study to improve knowledge on food digestion and ways how it can be controlled.

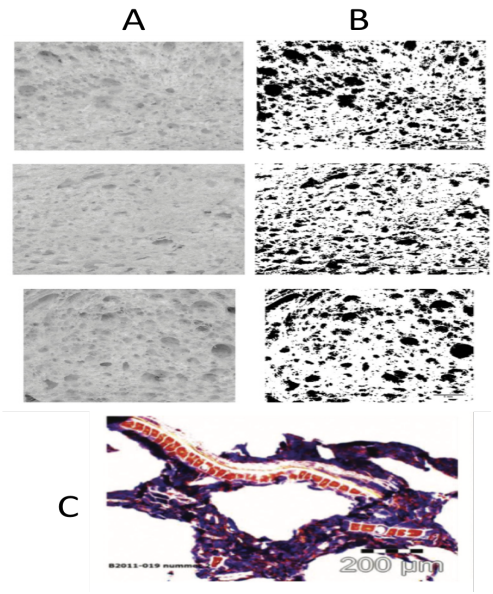

Fig. 2.15 Bread microstructure (a) white breads under different processing (b) binary image of the same white breads (c) gluten protein (red stain) and starch (blue stain) in wheat bread. Images A & B are adapted from Gao et al., (2016), and C from Eelderink et al., (2015).

Summary Comment

The comprehensive review of the literature put forward gives evidence to support the arguments that the effect of viscosity, of dietary fibres and intestinal mixing, are able to regulate glycemic lowering effect in the human diet. However, there are substantial gaps in the mechanistic actions on how the physiological effects are brought about by the living gastrointestinal tract, due to its complexities. As manipulation of bread formulation, with identical starch levels with or without the presence of dietary fibres, can change digestibility, there is a good opportunity to structure bread for control release of sugars. Therefore in order to elucidate how gut mixing modulates dietary fibres to manage and promote dietary carbohydrate metabolism, it is imperative to use in vitro techniques and models through near real digestion approaches.

Chapter 3

A small intestine dynamic model to study the effect of motility on transport and digestion

This chapter was a collaborative effort from the BBSRC grant (BBI0061091) and DRINC. Wheat cultivars with specific genetic traits (for different arabinoxylan contents-for modulating bread digesta viscosity), were first prepared by Rothamstead (crop level) and then milled and processed into bread using standard methods at Campden BRI (centre for baking in the UK). A model stomach at QUADRAM Institute (formerly IFR) was used to simulate gastric digestion. Subsequently, the aliquots were then used to simulate duodenal digestion by myself at the University of Birmingham, using the novel gut model, after developing digestion methods from several in vitro trails and model fluids/foods.

Abstract

An in vitro dynamic intestinal model food system was developed by the gut team (my self, Prof. Serafim Bakalis and Dr. Ourania Gouseti) at the University of Birmingham, that can describe the effect of intestinal motility on mass transfer. The model mimics segmentation and peristaltic motions to induce mixing, similar to in vivo phenomena to simulate in vivo mixing mechanisms. The contribution of mixing to mass transfer during starch digestion in breads and glucose absorption were studied to help elucidate the likely molecular mechanism underpinning glycaemia-lowering contributions of dietary fibres observed in vivo.The aim of this work was to undertake an inter-laboratory experiment to assess the effect of using wheat cultivars with different dietary fibre content on the digestibility of otherwise identical white bread. In preparation of this experiment we conducted: (I) preliminary experiments with non-reactive systems (guar-glucose solutions) to test the effect of viscosity on intestinal digestion in a novel duodenal model (DDM) and (II) preliminary experiments with commercial bread. The main experimental difference between the commercial bread digestions and the arabinoxylan bread digestions is the dynamic (mainly mechanical) element of the gastric digestion. Mixing by segmentation was more important to mass transfer than peristaltic flow, or molecular diffusion, due to the flow kinematics as described by the Reynolds number. The presence of guar fibres increased the viscosity of luminal content. Increase arabinoxylan fractions by 2.09 mg/g (14.4%) result in ~32% reduction in overall mass transportation of sugars during digestion.

3.1 Introduction

There is a demand from food and health professionals in using i*n vitro* techniques to (1) predict *in vivo* absorption of nutrients, and to (2) determine the mechanisms and rates of transfer across the intestinal epithelium barrier (Hur et al., 2011; Guerra et al., 2012). This will allow formulators to be notified about the windows of opportunity in absorption and warn of some of the constraints to formulations when aiming to engineer foods with functionality

and health benefits (Guerra et al., 2012). For example, reduced glycemic index in starchy foods. The small intestine is the key organ to mimic, to understand these phenomena since the majority of the absorption of nutrients occurs in this location in the gut.

The human small intestine is about 6m in relaxed length, consisting of 3 parts: the duodenum, jejunum, and ileum (as mentioned in introduction of the thesis). The duodenum is the first to contact with food coming from the stomach and is about 25-38 cm, in length, lined with villi for absorption (Hall et al., 2011). It is connected to the stomach via a pyloric sphincter muscle that helps to reduce food backflow to the stomach in most cases. It holds a unique orifice common to two distinct ducts, leading from the bile or the pancreas. This is located about 10 cm from the pylorus and secretes bile and pancreatic juices. The small intestine organ is also made up of circular and longitudinal muscles layers, critical in the locomotion of the gut for transporting and admixing digesta with enzymes. The motion in the gut occurs by, peristalsis and segmentation (Skandalakis et al., 2013; Hall et al., 2011). Peristaltic is induced by the longitudinal muscles which propelling the digest caudally, usually at a rate of 0.016 m/min, lasting 3 to 5 cm (Ganong 2005). Segmentation, occurs by the contraction of the circular muscle, creating occlusions, which can occur irregularly or regularly (evenly spaced) along the length of the gut. This repeated constrictions, of the gut wall, cause the digesta to admix with enzymes and bile salts in a forward and backward flow. These contractions occur about 6 every 30 seconds (Hall et al., 2011).

Without physical models that can closely represent digestion “near real”, knowledge of the digestion process will remain insufficient, resulting in poor in-vitro to in- vivo correlations. A lot of effort has been made in times to improve the understanding and functioning of the human gastrointestinal tract and to engineer novel in-vitro models with greater biomechanical and biochemical relevance (Dupont et al., 2015; Dupont, 2016; Zhu, 2011; Guri et al., 2014; Guerra et al., 2012; Hur et al., 2011; Sams et al., 2016; Ulleberg et al., 2011; Alminger et al., 2012). Mixing is crucial to the digestion process in the small intestine bowel, facilitating enzymatic reactions and transportation (Dikeman et al., 2006; Lentle et al., 2010). Most in-vitro procedures simulate intestinal digestion by basicaly mixing food and intestinal fluids using an overhead mixer (Oomen et al., 2003), a shaking or rotating bath (Muir et al., 1992), or magnetic flea stirrer (De Boever and others 2001). Clearly, these procedures highly simplify the mixing process, and will not reconstruct the mechanical forces and the fluid dynamics undergone by the digesta from gut wall contracting forces in the small intestine. Evidence strongly supports that, the environment brought about from fluid-mechanical events occurring in digestion have a crucial function on the medium response to making nutrient becoming biologically available (Lentle et al., 2008; Lentle et al., 2011; Dikeman et al.,

2006). Similarly, until recently, most dynamic models which were used to perform bowel digestions, had rarely account for the interaction effects of segmentation and peristaltic forces on the food digestibility and nutrient transport (Guerra et al., 2012; Gouseti et al., 2014; Tharakan et al., 2010), when reporting product transportation and intestinal absorption.

Some of these complex dynamic models that are able to simulate aspects of intestinal digestion includes the TIM, a gastro intestinal model, simulating peristalsis and absorption (Minekus 1995.), the soft tubular bio-inspired reactor model, which simulate peristalsis frequency and amplitude to understand mass transfer and mixing (Deng et al., 2016; Deng et al., 2014), and the human duodenum model (HDM), which imitate the human duodenum geometry, consisting of ascending and descending regions capable of irregular segmenting patterns to understand transit rate (Wright et al., 2016). These models clearly simulate one or two aspects of intestinal digestion, but not all or almost real. A small intestine model (SIM), developed by Tharakan et al. (2010) was improved by Gouseti et al. (2014); the Dynamic Duo, which was further improved to the dynamic duodenal model (DDM). It has enhanced features and is able to simulate most aspects of small intestinal in-vitro digestion. Longland (1991), has stated that an effective in-vitro model should incorporate the following: sequential and physiological relevant use of enzymes; appropriate pH and simulated GI fluids; the elimination of the digested product; suitable biological transit times and mixing at each compartment for each step of digestion. The improved dynamic duodenal model was designed with these functionalities.

This research explores these effects on these contributions on digestibility and absorption while varying the digest's viscosity, conducted in a newly developed dynamic intestinal model (DDM). Manipulating the luminal content's viscosity by soluble dietary fibres may affect digestibility, and has shown to alter physiologic responses (Roberts et al., 2005; Dikeman et al., 2007; Takahashi et al., 2012; Park et al., 2016; Lund et al., 2005; Haralampu, 2008; Dikeman et al., 2006). The soft tubular material of the dynamic duodenal model allows the walls and inner lumen to be actively engaging in the mixing, reactions and simulated mass transfer during digestion. It also has a pancreatic duct positioned to release intestinal fluids onto the incoming gastric digest. It is therefore an intent to further characterise the mixing in this model to understand how it is related to the digestion efficiencies of bread. This is detailed and studied in Chapter 4 of the thesis.

3.2 The model: design and function

The dynamic duodenal model (DDM): origin

To be able to sufficiently interpret the effect of mixing (segmentation and peristalsis) on digestion and absorption, it would be desirable to have an appropriate biomechanical model reproducing the contraction and relaxation mechanisms for the stirring/churning of the chyme with intestinal fluids and enzymes, within the small intestine (duodenum). The dynamic engineering model of the average adult human duodenum was modelled/constructed according to physiological observations based on MRI images adopted from Kavaliauskiene et al., 2011, (Fig.3.1). The images show the cross sectional views of the small bowels including the duodenum containing digesta (Fig.3.1 (a) and (b)). The images (Fig.3.1 (a) and (b)) were examined to obtain information about the layout (set-up). The aerial planes gave insight about the dimensions, including the lumen's diameter, the patterns, numbers and thickness of the contractile rings in segmentation. These information were taken to the Physics Department at the University of Birmingham, to confirm and amend earlier work done by the gut team, in-order to fabricate the model. Information on gut peristalsis was confirmed by fluoroscope with gallium contrast videos done by Ehrlein (2007). To maintain simplicity of the model, vili were not attempted to be reconstructed.

The dynamic duodenal model (DDM): main body and design

Fig.3.2. shows the dynamic duodenum model (DDM). The main body consist of an aluminium coated stainless steel base, about 350 mm in length. It allows the continuous tubular gut wall (described later on) to rest. There are 8 pillars (50 mm in height each) attached to the base, that supports the platform that secures 8 pistons. The pistons are spaced along the length of the tube on either side of the secreting duct with each piston having a width of 10 mm wide and 10 mm spaced. The secreting duct is 3 mm in internal diameter and located 100 mm from the feed of the pyloric outflow, similar to the distance found between the pylorus and the pancreatic duct found in a typical human small intestinal organ (Kong et al., 2006). These features to date have not been published on any model and they were not available on the older model described by Tharakan et al., (2010). The model described by Tharakan uses inflated cuffs at opposite ends of the tube to induce mixing motility. Even though a good attempt, it was not able to describe the various levels of motility experienced by the living small intestine, such as; irregular or regular segmentation - an important feature based on the residence time of digestion inside the small intestine. Furthermore, it did not have a secretory

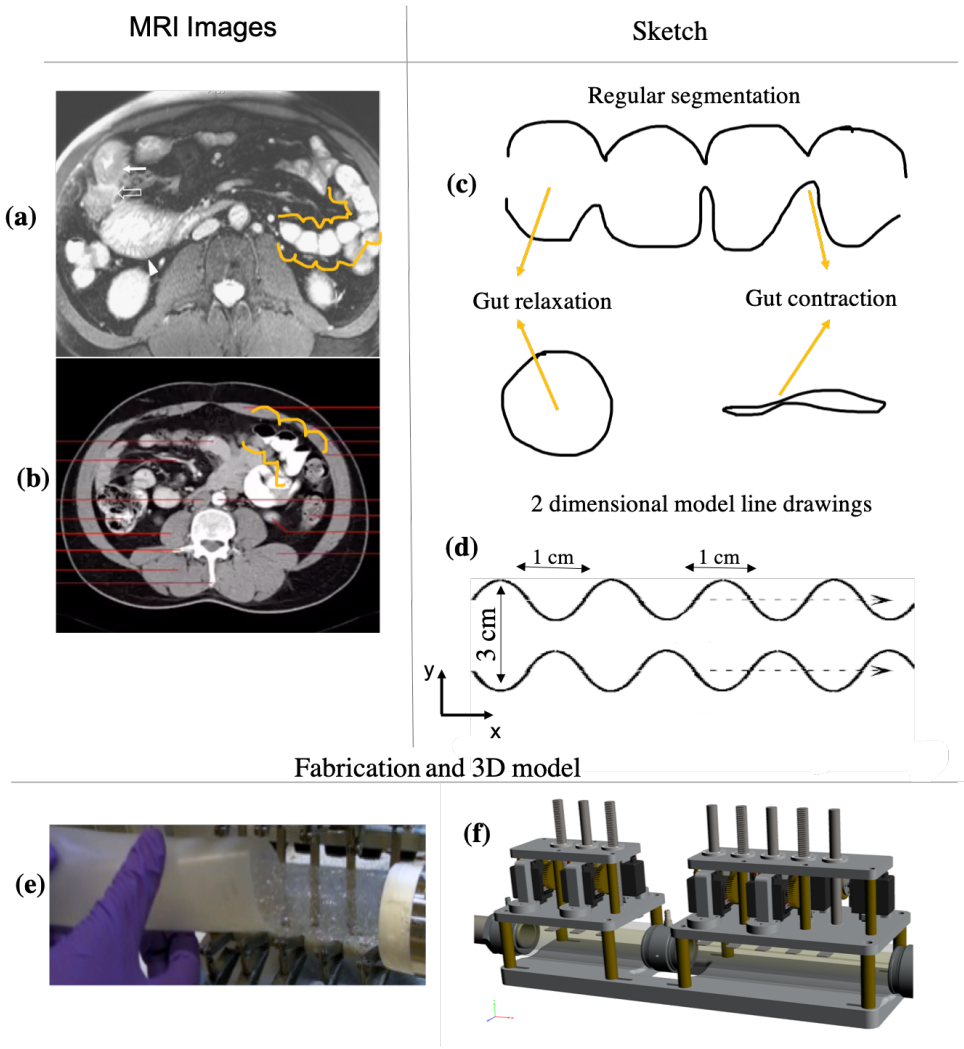

Fig. 3.1 Cross sectional MRI images of the small bowel's segmentation (small intestine): (a) filled lumen and (b) partially filled lumen used in the fabrication of the dynamic duodenal model.

port/duct. Table.3.1., shows the human duodenum features that were adopted and built into the engineered model.

Simulating absorption and mixing

The working mechanisms of the human duodenum were reconstructed and mimicked such that the model comprised of two main compartments;

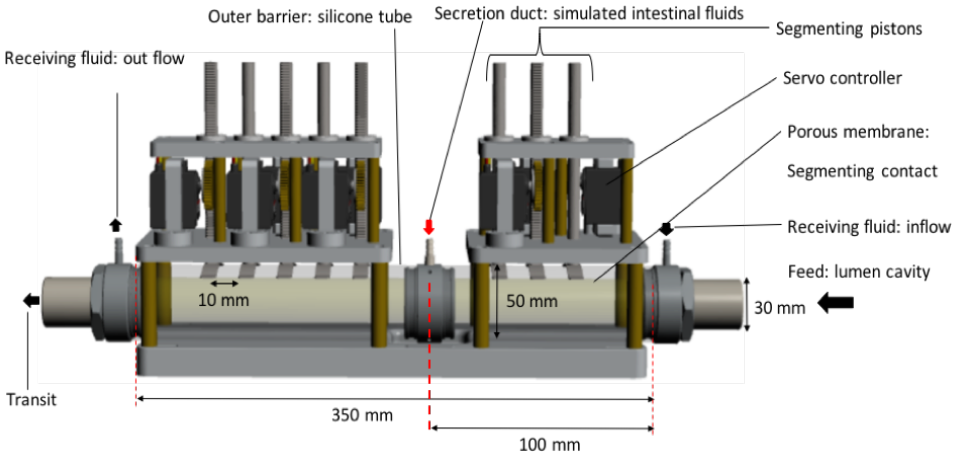

Fig. 3.2 Three-dimensional image of the Dynamic duodenum model (DDM) .

(**1**) A semi-permeable membrane, found inside the flexible cylindrical gut wall. It facilitates diffusion and absorption by acting as an interface, separating the reactor side (luminal cavity; containing digesta and intestinal fluids with enzymes) from the recipient side (absorbing water medium). The semi-permeable membrane is a dialysis tubing made from regenerative cellulose, about 25μm thick with a molecular cut off weight of 3500 daltons. This allow small molecules such as glucose and maltose to pass through, into the recipient zone/fluids, which is recirculated by a peristaltic pump and keep at 37^0C by varying the source flow rates into the model.

(**2**) A flexible silicone outer tube barrier facilitating gut wall movements when pressing pistons induce motility. The pistons are controlled by a parallax servo software (Parallax Servo Controller Interface, Beta version v0.9h). They can be manipulated to induce mixing independently, being evenly spaced (regular segmentation) or irregular spaced if so desired during contraction. For these trials, the contractions were regular for alternative press/squeeze. Their numbers, amplitudes and speed can be controlled to manipulate the rate of segmentation (contraction per minute), and levels of shear. The flexible gut wall movements of peristalsis and segmentation via the pistons in the dynamic duodenal model should be able to apply patterns/magnitudes of shear on the contents in the luminal cavity, similar to that received on the digesta during *in-vivo* motility and transit. These contractions should be similar because of the the lumen diameter and the segmentation frequencies (up to 12 contractions per minute), the

maximum observed in the human body. Furthermore, the presence of segmenting occlusions, means that retropulsions are created, which is observed in in-vivo mixing mechanisms. This means that this model is able to reproduce realistic mixing environments similar to that of the human small intestine in the human body.

Delivery of intestinal contents and recipient fluids

The system was kept at a constant temperature of 37^{o}C with the recirculation of the recipient fluid in the space between the luminal membrane and the outer flexible silicon tube. The recipient fluid was a part of the temperature control system connected to a peristaltic pump, leading the fluid from the tank, maintained at 39^{o}C by a water bath at a flow rate of 120 rpm, to keep the luminal content at the desired 37^{o}C. Material transiting from the gastric phase of digestion were fed immediately to the model's luminal cavity (inner-side of the membrane), through a 90^{0}elbow, 35mm ID (not shown in Fig.3.2), via a peristaltic pump or manually. The load capacity of the lumen ranged from 0.1–0.5 l. A peristaltic pulse then pushes the contents forward, followed by segmenting contractions that do the progressive mixing. Once the digesta is added to the luminal cavity (in full - the feed and exit ends are topped to create a closed system, or continuous- the contents are fed bad to the tank to be recirculated by a peristaltic pump allowing an open system), then, simulated intestinal fluids and enzymes containing and buffer systems, are delivered through a secretion duct (0.003 mm, I.D.). The delivery of the simulated intestinal fluids through the duct can be added manually via syringe or by a mini peristaltic pump at varying flow rates.

3.3 Experimental section

3.3.1 Materials

Guar gum (G4129-500G), glucose, maltose, enzymes and all the digestive materials for the simulated digestive fluids, and other chemicals were purchased from Sigma–Aldrich Chemical Company UK unless otherwise stated. The simulated digestive fluids (sdf), including gastric solutions (sgf), were prepared using a method in previously published manuscripts (Mandalari et al., 2009; Moreno et al., 2005), unless otherwise stated, and the enzymes were added on the day of digestion, dissolved at a room temperature and incubated at 37^{0}C. The ssf, contains 0.15 M NaCl and the pH adjusted to 6.9 using 3-5 drops of 1.0 M HCl, if required (*these small drops were considered to be negligible to the overall*

Feature	Duodenum of human	Dynamic duodenal model
Diameter	Ranges from 4cm at the proximal end to about 2.5 cm distal to the large intestine (Martini, 2006; Guyton and Hall 2005).	3.0 cm (ID- dry)
Length	6 m, small intestine. 25-38 cm, duodenum. (Guyton and Hall, 2005)	35 cm
Surface area	250 m^2 small intestine	0.0715 m^2 (surface area for absorption)
Mixing: Segmentation	11-12 per min (Guyton and Hall, 2005)	Computer manipulated. The range used in the experiments were, 0-12 contractions per minutes.
Flow: Peristaltic	0.016 m/min, Short lived, last 3-5 cm (Ganong 2005)	Computer manipulated, flow is generated from a variable peristaltic pump
Membrane and absorption	Lipid bi-layer epithelium layer of cells, connected tightly	Regenerative cellulose membrane, with molecular cut off weight of 3.5 KDa.
Enzyme duct	7-10 cm from the pylorus (Guyton and Hall, 2005)	15 cm from feed entry (adjustable to 10 cm)
Digesta/ pH	Complex multiphase systems: Highly heterogeneous with varying viscosity (Ellis et al., 1995), pH 5.7-6.4 in duodenum (Ekmekcioglu, 2000)	Complex and simple foods. Simple foods used in this work varied in viscosity from 0.1-10 Pa.s, pH 6.9 in duodenum
Temperature	37^{o}C by the blood	Re-circulation water (0.7/1 L) maintained at 37^{o}C, with variable peristaltic pump

Table 3.1 Features adapted form the human duodenum relevant to perform in vitro digestion to simulating mixing and absorption in the small intestine.

dilution), α-amylase from hog pancreas (50 U/mg) and 6 μg/ml lysozyme solution. The sgf contains 0.15 M NaCl; 3mM $CaCl_2.2H_2O$; 0.9mM NaH_2PO_4; 16mM KCl in 150ml, 0.1 M HCl, pepsin from porcine gastric mucosa - lyophilized powder, 3,200-4,500 units/mg Sigma (P6887). The simulated intestinal fluids (sif), was made up of the hepatic mixed solution (hms), pancreatic mix solution (pms) and modified Krebs Ringer buffer (mkrb). The hms, contains 4 mM Cholesterol; 12.5 mM Sodium taurocholate (hydrate); 12.5 mM Sodium glycodeoxycholate; 146 mM NaCl; 2.6 mM $CaCl_2.2H_2O$; 4.8 mM KCl. The pms contains 125 mM NaCl; 0.6 mM $CaCl_2.2H_2O$; 0.3 mM $MgCl_2.6H_2O$; 4.1 μM $ZnSO_4.7H_2O$ solution, and the mkrb, contains 0.7 mM $Na_2HP0_4.12H_2O$; 4.56 mM KCl; 0.49 mM $MgCl_2.6H_2O$; 1.5 mM $NaH_2P0_4.2H_2O$; 80 mM $NaHCO_3$ solution; 54.5 mM NaCl.

Preparation and characterisation of biopolymer

Aqueous guar gum-glucose model fluids containing; 0.5, 0.75, 1, and 2.5 (%w/v) guar, and glucose (1% w/v: 55 mM) were prepared. The range of guar were selected that represented the shear rates occurring in the small intestine (shear thinning rheology of the intestinal content). Shear rates in the duodenum ranges from 0.02 s^{-1}- 5.8 s^{-1} (Ehrlin and Stockman 1998; de Loubens et al., 2013; Lentle et al., 2013 and Lim et al., 2015). While the luminal content resistance to flow (viscosity) may have a wide range as a result of the solid portion of the food consumed with viscosities ranging from 0.01-10 Pa.s, in in vivo studies (Ellis et al., 1995, Lentle and Janssen, 2008). Gum guar was added to the water, with simultaneous stirring, and the temperature raised and maintained at 80^0C for 10 minutes until fully mixed and allowed to cool at room temperature, then left overnight for complete hydration, before each use. Shear experiments were carried out on the model fluids using a Bohlin Instruments rheometer (KTB 30, Crawley, UK) equipped with a cone-plate geometry 40/1 with a gap size of 1mm. For each test, 5 ml of freshly prepared solution was allowed to equilibrate at room temperature (24^0C) prior to experiments. The viscosities were then measured as a function of shear rates which logarithmically increased from 0.01 to 103 $s^{-1,}$ recorded in Table.3.2. This was repeated in at least duplicates for each concentration of the model solutions.

Preparation of bread

Commercially available white and multi-seed bread (KINGSMILL, soft white thick and multi-seed bread from Allied Bakeries, Vanwall Road, Maidenhead, SL6 4UF; ABF Grain Products Ltd.; Produced in the UK) sourced from local shops, were used for these experiments. The

nutrient profiles of white bread were as follows 100 grams: carbohydrate, 44.1g and protein 7.1g. The multi-seeded bread nutrient profiles were; carbohydrate, 39.1 g and protein 2.1g per 100 grams. For consistent digestion, ~32 grams of carbohydrate regardless of the bread type, were digested. Guar-containing white bread were prepared in the form of dough's using the 125g automatic KENWOOD rapid bake. Gum guar was incorporated into the recipe; 245g water, 13.8g vegetable oil, 350g unbleached white bread flour, 6.5g skimmed milk powder, 5.5g salt, 7.8g sugar, and 3.5g easy blend dried yeast, at a 10% w/w, replacement level for wheat flour. This is a similar method done by Brennan et al. (1996), where they studied guar coated starch structure degradation in different breads. The recipe was added to the dough maker and left to be baked for 3 hrs. The final carbohydrate and protein contents were 44.5g and 6g respectively per 100 g of bread.

Arabinoxylan bread were prepared with different levels of AX from different cultivars, similarly prepared for Smith et al., (2015), that determined gluten protein digestion in AX breads. AX is a by product from flour milling and can be added due its viscogenic properties to bread. Details on its uses and properties are described else where; Smith et al., (2015) and Chapter 2 of this thesis. Grains (Hereward (AX1), and Yumai (AX2)) were provided by Rothamsted Research (Hertfordshire, UK) and grounded at Campden BRI (Gloucestershire, UK) to 81.4% extraction to provide white flour. These were used in the preparation of breads (100g flour, 0.01g ascorbic acid, 1g Bako fat emulsion, 1.5g salt, and 2g yeast) with fungal a-amylase (Bakezyme P180. DSM, Delft, Netherlands) added to 80 Farrand Units (based on Hagberg Falling Number) and water added to the Brabender arinograph (600 line) water absorption value using the Chorleywood bread process. After baking bread, Yumai (AX2), containing 16.65 mg. g^{-1} total arabinoxylan (dw) and a dry matter of 57%. Herward (AX1), contained 14.56 mg. g^{-1} total arabinoxylan (dry weight) and dry matter of 60.6 %.

3.3.2 Performing digestion and absorption in the DDM

Oral and gastric digestions were performed on bread using well established static in vitro techniques as described below.

Model fluids in DDM

The model fluid prepared were fed into the lumen through the feed point of the dynamic model. Trials that requires flow were operated in an open system leaving both entry and exit open for the material to be pumped from the tank. Trials that required segmentation and diffusive only studies required a closed system where the lumen was closed at both ends.

Oral digestion

75 g of white bread were diced into 4cm^3 cubes (roughly the size of bite). 24.5ml ssf warmed at 37^{0}C, containing enzymes; α-amylase, 0.018g and lysozyme 14.7μl and water 50ml, was poured onto the bread and placed in Hammed mincer for 1-3 minutes, to mimic oral processing time, and chewing (Zijlstra et al., 2010; Zijlstra et al., 2009). The mincer has multiple exit diameters of 3mm each. Once the bread samples and required salivary solutions were added incomplete, the timer was started. The chew (bolus) was collected and immediately sent to the gastric digestion stage.

Gastric digestion

The bread bolus (149 ml) coming from the oral phase was placed into a 300 ml, conical flask (stirred tank), and 66 ml sgf, containing 0.093g pepsin, was poured onto it (pepsin to protein ratio of ~ 1:69 was applied), the beginning of the gastric phase. The gastric chyme was placed into a orbital incubator (Stuart orbital incubator SI500) at 37^{o}C, set at 170 rpm and pH 2 for 2 hours in order to provide adequate mixing during digestion. Even though these static mixing techniques are less representative of the mixing of stomach contents in vivo, they are able to reach a fixed pH on the substrates and enzyme functions (Mackie & Rigby, 2015; Minekus et al., 2014).

For arabinoxylan bread (AX1 and AX2), the digestion were done in a Dynamic Gastric Model (DGM) which is designed to simulate near real, the sophisticated mixing, time-space release of nutrients by the stomach's contractions in the the fundal and antral regions (Vardakou et al., 2011; Thuenemann et al., 2015). The DGM can facilitate actual foods, by passing meals at scales relevant to human digestion in vivo (mm - cm scales). The DGM is primed with a pre-release, 20 ml of acid solution-mimicking the fasting state of the human stomach conditions. Following this, enzymes and gastric acid solutions are added at rates that mirror the in-vivo mechanisms. Antral processing takes place by the upward and downward motions of a piston, which has been programmed to release shear forces that are similar to that happening in the body. Samples were collected, through a 15 mm tubing. This dynamic model was used as it has been validated with in vivo digestion data. The trial on each bread was done once, as these bread were specialised and derived from limited raw materials form two cultivars (Arabinoxylan-wheats).

Duodenal digestion

At the end of the gastric phase, the digesta (~215 ml) was released and added to the dynamic duodenal model through the feed point of the lumen. After addition, simulated segmentation and peristaltic motions were initiated. From the secretory port, pancreatic mix solution (57ml), containing room temperature dissolved trypsin 0.126g from porcine pancreas-lyophilized powder, (~780 BAEE units/mg) from Applichem (A4148), α-Chymotrypsin 0.008g from bovine pancreas-lyophilized powder, 350U/mg (11.9 BTEE U/mg) and α-amylase 1.007g were added, along with HMS (20ml) and KRB (80ml) via syringe. Digestion was allowed to run for 2 hours (commercial bread) and 3 hours for speciality arabinoxylan bread. Prior to intestinal digestion, the model luminal membrane was conditioned with 50 ml KRB. The oral through to duodenal digestion were repeated in at least duplicates for commercial bread and once for speciality arabinoxylan bread. Fig.3.3. shows the experimental setup for each run. In total, each digestion ran for ~5 hours for commercial bread and ~ 6 hours fro speciality arabinoxylan breads (oral- gastric).

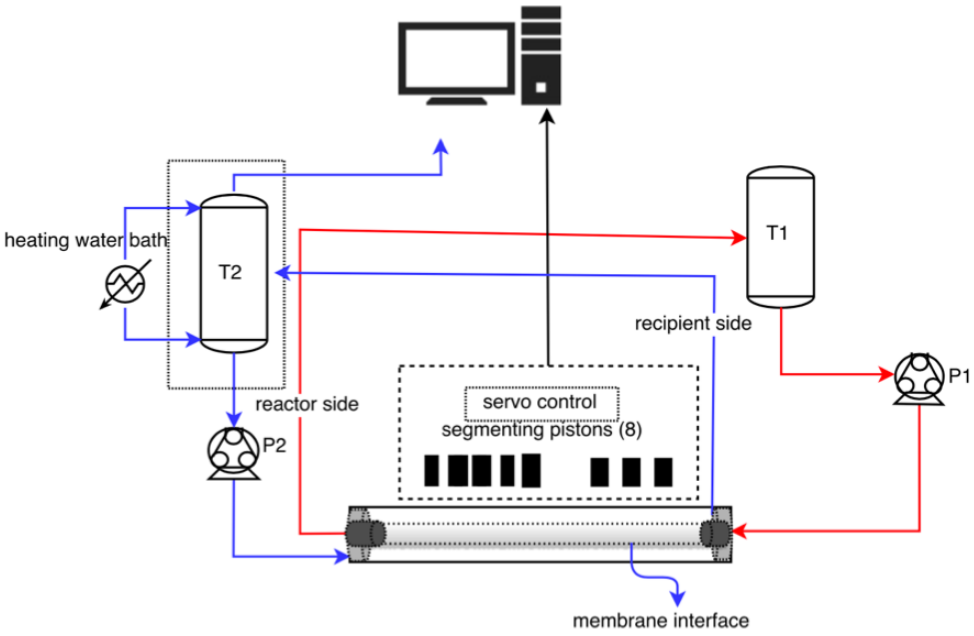

Fig. 3.3 System design schematics for setup using the DDM to perform absorption and in-vitro digestion.T1- for gastric digest outflow usually at pH2, T2- recipient tank for products of digestion for example; glucose and maltose. Servo control; 8 pistons for segmentation motility.

The operating conditions were varied for each trial, to study the effect of the following variables:

1) The effect of viscosity by changing the concentration of guar in the lumenal content.

2) The effect mixing :

a) as influenced under flow: where the peristaltic rate was set at 3rpm and 120 rpm

b) as influenced under segmentation: regular spaced contractions of 0cpm, 6cpm and 12cpm for guar gum model fluids and 2cpm and 6cpm for starch digestions of different bread types.

c) Interaction between flow and segmentation: on guar model fluids

The recipient fluids are sampled (1mL) from recipient tank (T2), to measure the uptake products / reducing sugars (glucose and maltose) of digestion. The effluent/digested materials are collected at the exit end of the model, to be discarded or for further testing.

3.3.3 Reducing sugar determination

Diffusion of reducing sugars across the membrane into the receiving medium was monitored at 5-minute intervals by measuring its concentration using the (DNS) 3,5-dinitrosalicylic acid reagent assay (Miller 1959). DNS test for reducing groups on sugar molecules. The resulting colour change after heating the mixed solution of equal volumes (1ml) of DNS reagent (0.1% dinitrosalicylic acid; 30% w/w potassium sodium tartrate; 0.4M NaOH) and sugar sample at 80 ^{0}C for five minutes was read (the absorbance), using a visible spectrophotometer UV, Libra S12 (Biochrom, Cambridge, UK) at 540 nm. Standard curves were constructed with glucose/maltose standard concentrations ranging from 0.0 -10 mM to determine the reducing sugar concentration from all the absorbance from tested samples drawn. The amount of glucose (from model fluids) and maltose (from bread digestion), in the recipient fluid, is plotted against time, as well as the dependencies of mass transfer coefficient overall (OMTC) on Reynolds number, type of mixing condition and viscosity of the luminal medium. Maltose sugars were converted to starch by using the factor of 0.95.

3.3.4 Analysis of mass transport mechanism across the intestinal wall

The kinetics of mass transfer can be determined by the application of dimensionless analyses, by using the linear region of the diffusion rate plots, observing the characteristic lag phase established before absorption. At the beginning of this linear region, mass transfer can be

said to "truly" begins to take place. i.e., there is a characteristic delay that is associated with some formulations and operating conditions. The transfer of mass in the cylindrical dynamic model can be envisioned as follows:

1. The transfer of molecule from within the bulk of the fluid to the membrane interface; luminal mass transfer coefficient $\left(C_{lumen}^{bulk} - C_{lumen}^{interface}\right)$, (m/s)
2. The transfer from the interface in the lumen membrane to the interface on outer membrane; membrane thickness, X, (m) and diffusional coefficient D, (m2/s). $D\left(\frac{C_{lumen}^{interface} - C_{recipient}^{interface}}{X}\right)$
3. The transfer of molecule from the interface outside the lumen into the bulk recipient fluid $K_{recipient}\left(C_{lumen}^{interface} - C_{recipient}^{interface}\right)$, (m/s)

The overall mass transfer coefficient can estimate from equation (3.1) (Cussler, 2009):

$$N_i = K\delta C \tag{3.1}$$

Where N_i is the molar flux (mmol/m^{2}s), K is the overall mass transport coefficient (m/s) and $\delta C$is the concentration difference at the interface $\left(C_{lumen-interface} - C_{recipient-interface}\right)$, mmol/m^3.

The model goes by the following assumptions:

1. The contents of the lumen are well mixed similar to the mixing tank model.
2. The transferred mass, is proportional to the concentration difference and the area of the interface (Cussler, 2009).

The transport resistance can be interpreted as the sum of the reciprocal of the contributing diffusional resistances and can be used to determine the lumen mass transfer coefficient from equation 3.2:

$$1/K = 1/K_{lm} + l_{mem}/D_{mem} + 1/K_{recipient} \tag{3.2}$$

It is assumed that the resistance to mass transfer from the interface of the membrane to external volume of solution is negligible, since the flow rate of recipient fluid was set at 8 x 10^{-6} m^3/s (120 rpm). The term can therefore be left out from the equation **??** and the equation now becomes:

$$1/K = 1/K_{lm} + l_{mem}/D_{mem} \tag{3.3}$$

Statistical analysis

The trials were done in at least duplicates from freshly prepared samples. The data presented are as means $\pm$ standard deviation, unless stated otherwise, and the statistical significance was set at 0.05 for the probability level.

3.4 Results and discussion

3.4.1 Solution viscosity

All solutions prepared displayed a shear-thinning behaviour; decreasing viscosity with higher increased rate of shear as illustrated by the viscosity flow profiles in Fig.3.4. The resulting raw data was then applied to the 'power-law' model, by using Equation.3.4., because the power law model is able to describe substantially the viscosity non-linear behaviour (relationship) of fluids between extremely low shear rates and larger shear rates, i.e., "zero" shear rate viscosities and relatively large shear rate viscosities. The linear region of the slope for all solutions gave an exponent less than 1 (n-1) as shown in Table.3.2. The zero shear viscosities were recorded in Table.3.2. Regardless of the level of soluble fibre tested, viscosity increased as its concentration in water increased. For example, a 27-fold increase in zero shear viscosity was observed when the concentration moved from 0.5% to 1%, and a 5-fold increase when the concentration moved from 0.75% to 1%. The power law model indicated (Table.3.2) that an enhanced percentage of guar gum (%w/v) in water will result in an augmented shear thinning behaviour during deformation, i.e. the exponent 'n' is reducing, as the concentration increases. This shear thinning type of behaviour may be a result of the components of the guar in the fluids may deform and rearrange to accommodate flow.

$$\tau = K\gamma^n \tag{3.4}$$

Where τ is the shear stress (Nm^{-2}) and γ is the shear rate (s^{-1}), and K and n are the consistency index and an exponent respectively. η is the viscosity (N s m^{-2}), that can be found on the plot in Figure.3.4. (viscosity vs shear rate),

Model fluid: guar gum (% w/v)	Viscosity (Pa.s)	K	n
0.00	0.0089 ± 0.001	-	-
0.50	0.3658 ± 0.147	0.608	0.43
0.75	2.0973 ± 0.222	2.03	0.34
1.00	10.0123 ± 0.877	5.01	0.27
2.50	35.0123 ± 0.877	-	-

Table 3.2 Zero Shear viscosities, and parameter (consistency index (K) and flow behaviour index (n)) fitted for 0.5%, 0.75%, 1% and 2.5% guar gum solutions to the power law model, Equation.3.4, (viscosity versus shear rate).

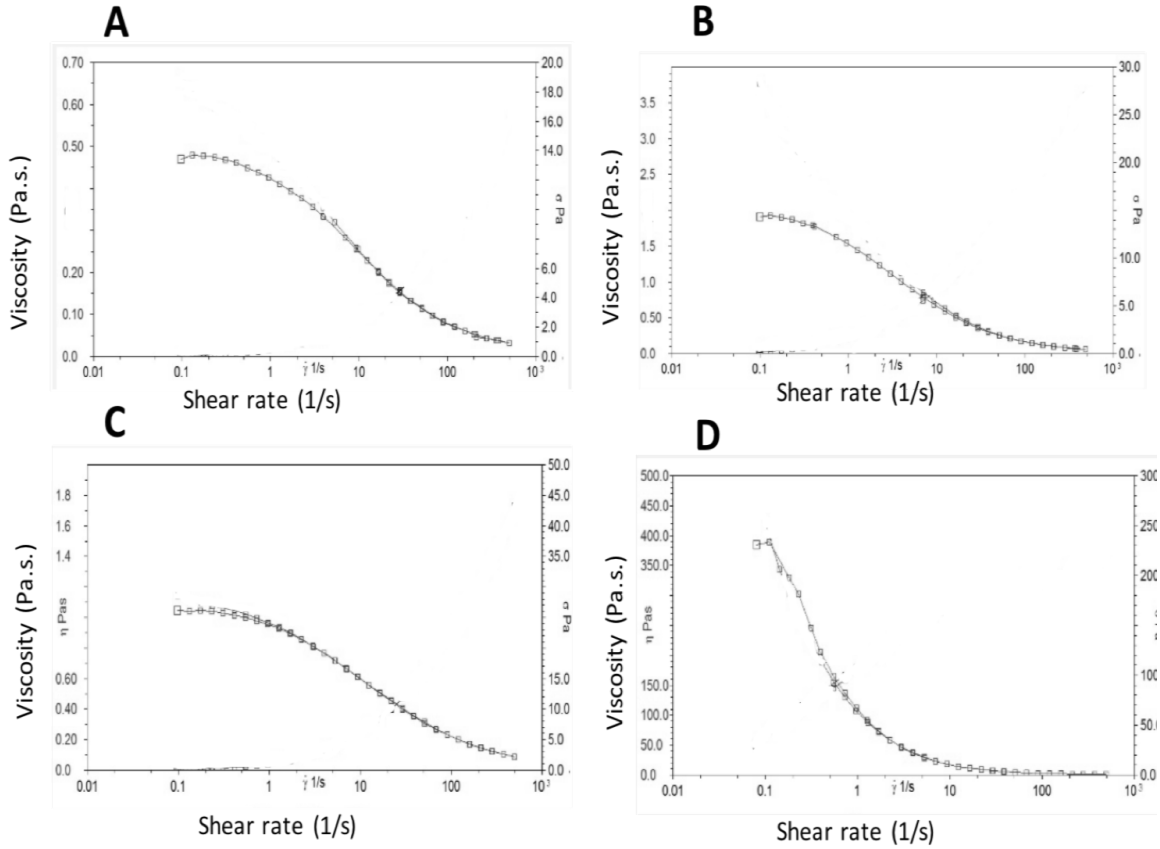

Fig. 3.4 Viscosity flow curves for guar model fluids fitted to the Power law model in Equation.1.4: (A) 0.00% (B) 0.5% (C) 0.75% and (C)2.5%. Raw data plotted are the mean of three readings and error bars are standard deviation of the mean.

3.4.2 Mass transfer coefficient for diffusion of glucose with increasing viscosity

The effect of adding soluble fibre at different guar concentrations and mixing on the transverse of glucose through the membrane are shown in the diffusion rate lots illustrated in Fig.3.5.;(A) Under pure diffusion systems (B) systems under induced mixing by flow (C) systems under induced mixing by segmentation and (D) system by the interaction of simultaneous induced flow and segmentation. The glucose transfer in each system established a lag phase (1-10 minutes) then a linear increase of absorption up to 1 hour. This result shows that the overall mass transfer coefficient as predicted by equation 3.1, decrease with increasing viscosity and increase with mixing via flow and segmentation in the model, which is shown as a function of Reynolds number and viscosity in Fig.3.6. The overall mass transfer coefficient, (k) decreased by 20%, i.e. from $1.52x10^{-7}$m/s for 0% guar to $1.22x10^{-7}$m/s for 2.5% guar under pure molecular diffusive conditions.

3.4.3 Effect of flow

By increasing the flow rate from 3rpm ($2.8X10^{-4}$ m^3/s) to 120rpm ($8.3X10^{-3}m^3/s$) in the 0% guar systems, the overall mass transfer coefficient increased from $1.54x10^{-7}$ m/s to $1.73x10^{-7}$ m/s Fig.3.6.(B). This was 1 and 14% increase from the pure diffusive system ($1.52x10^{-7}$ m/s) for 3 and 120 rpm respectively. However, when the percentage of guar was increased to 1%, the overall mass transfer coefficient decreased regardless of the peristaltic flow speed. For 3rpm and 120rpm the overall mass transfer coefficients were $1.29x10^{-7}$ m/s to $1.34x10^{-7}$m/s respectively. The initial increase in mass transfer is because of the elevated convective mass transfer on the lumen side of the membrane, and the reduction of the thickness of the unstirred water layer that lies adjacent to the membrane wall (boundary layer), because of increased flow rate (Amidon 1980, Elliott 1980, and Tharakan et al., 2010). Even though the flow rate increased 30 folds (2.8X10-4 m^3/s to 8.3X10-3m^3/s), the difference in mass transfer coefficient was surprisingly small, a difference of ~ 0.2 m/s. It is known that the complete nutrient rate of absorption, transepithelial is reliant on the rate of diffusion within the lumen and the membrane transport rate (Takahashi 2011, Levitt et al., 1987 and Tharakan et al., 2010). The increase in fluid flow may have increased the pressure on the stationary layer (solid-liquid interface) which thereby increase its strength slowing mass transfer. The attenuation of glucose mass transfer coefficient when the amount of guar was raised was because of the increased viscosity which may increase the boundary layer thickness, thereby

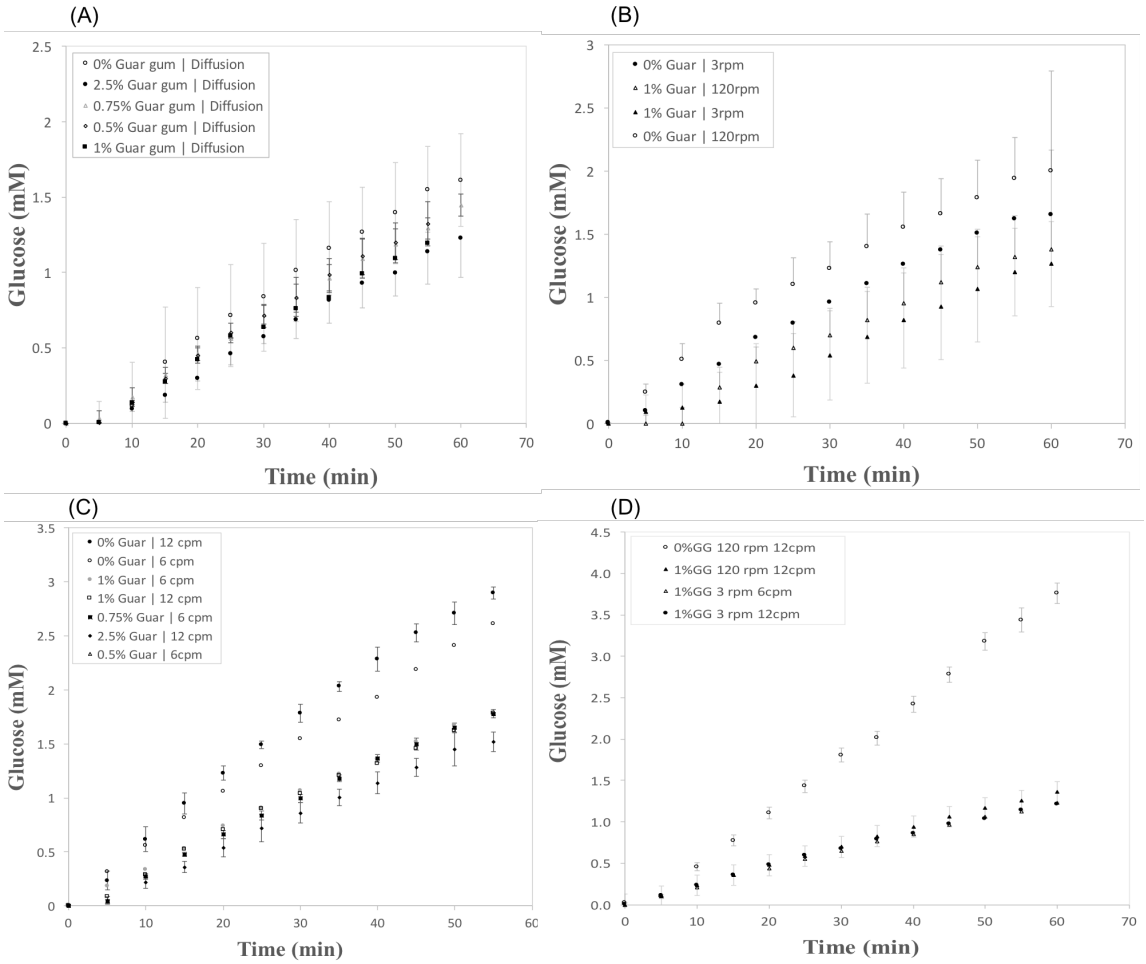

Fig. 3.5 Glucose diffusion rate plots for : (A) molecular diffusion with varying guar concentration, (B) flow rates at 3 and 120 rpm, (C) segmenting rates at, 6 and 12 contractions per minute and (D) the effect of combined flows (3 and 120 rpm) and segmentations (6 and 12 cpm). The error bars show the standard deviation from a sample amount of three.

increasing the diffusional resistance. Increase in peristaltic flow in the small intestine will cause faster transit of bulk material, but the effect on mixing is known to be minimal (Stoll et al., 2000). That is, it causes some mixing, but not to a great extent.

3.4.4 Effect of segmentation

The overall mass transfer coefficient, (k) was greatly enhanced by segmentation, however, a further increase in the mixing frequency had little net effect on overall mass transfer coefficient. Fig.3.6(A). It increased, from $1.52x10^{-7}$ m/s without segmentation to $2.48\ x10^{-07}$ m/s (63%) and $2.73x\ 10^{-7}$ m/s (79%) with segmentation at 6cpm and 12cpm respectively. Even though segmentation improves mass transfer, increasing the viscosity of the luminal content reduce the impact of segmentation, regardless of the mixing frequencies. The values fell to $1.20\ x10^{-07}$, $1.54\ x\ 10^{-07}$, $1.55x\ 10^{-07}$m/s, for 0cpm , 6cpm and 12cpm respectively when the concentration of guar increased to 2.5%. The mixing of fluids in the lumen by segmentation increased the mixing and enhance mass transfer. Segmentation also reduces the unstirred water layer thickness adjacent to the membrane surface, resulting in improved mass transfer efficiency of membrane wall to glucose solutes. Similar conclusions/results were drawn by Fonseca et al. (2016), when starch was digested under segmentation motility in a small intestinal model. Constricted rings from the gut wall contraction disrupts the stationary unstirred layer and induce local asymmetric flow and mixing of the contents at low viscosities (Lentle and Janssen 2011). The flow kinematics is an important part of mass transfer and absorption operation, as to be seen later. When there is mixing, the Reynold's number captures and defines the flow kinematics and differences between different samples really well. Hence, the convection of glucose in the mass transfer operation as displayed in Fig.3.8- as described later. The flow in the small intestine has been established to be laminar in nature (Lentle et al., 2008). Also, the presence of rapid vortices seen almost immediately during each contraction (data not shown: PET data), causes vortical flow and micro-mixing. For this reason, micro-mixing as a result of turbulence is stipulated to contribute more to the transfer of nutrients from the bulk lumen to the epithelium (Takahashi 2011), than diffusion alone, during segmentation.

3.4.5 Interaction of flow with segmentation

The combined effect of flow and segmentation elevated mass transfer Fig.3.6.(C). The greatest enhancement was observed for 0% guar under mixing of 120rpm and 12cpm producing an overall mass transfer coefficient of $3.45X\ 10^{-07}$m/s. Addition of 1% guar resulted in a 64%

reduction (1.22 x 10^{-07}m/s) in mass transfer coefficient, under the same mixing constraints. Surprisingly, the mass transfer was similar for mixing at 3rpm 6cpm for 0% guar, (1.20x 10^{-07} m/s) and 1 % guar (1.08x 10^{-07}m/s) indicating that at high viscosities, mass transfer is reliant predominantly on diffusion and less of convection.

Overall the small amount of glucose transferred under free diffusion was anticipated as well as reduction in overall mass transfer coefficient when the guar fibre was added to in each formulation. In the non mixing systems, the glucose moiety were left stagnant, and will only move towards the membrane interface by free diffusion only. This free diffusivity mechanism works by the thermal random motion of the glucose molecules found inside the fluid. On the external side of the membrane wall, the recipient fluid was circulating at 120rpm and as a result, mass transfer of glucose from the wall to the receiving fluid was not by free diffusion, rather convective diffusion. Therefore, resistance to mass transfer in the recipient fluid can be considered negligible. The added guar gum at increasing levels, increased the viscosity of the bulk luminal content (as stated earlier). This viscous network restricts glucose molecular diffusion by interfering with the random movement thereby decreasing mass transfer and might explain the decrease in overall absorption. This is in accordance with the Cohen-Turnbull theory that explains the movement of particles, with respect to creating free volumes during random motion to allow particles to move through (Cohen and Turnbull, 1959; Duda, 1985) i.e., less free volumes are created in the presence of fluid thickeners, and so particles cannot migrate freely, resulting in an overall decrease in molecule translocation across the membrane.

3.4.6 Fundamental fluid mechanics and mass transfer

The relationship between diffusive and convective transportation of mass at the membrane interface can be understood by deriving the Sherwood number. The lumen side mass transfer coefficient was determined from equation(3.3), and use to predict the *Sh* for each system, using equation (3.5). Where, K_{lm} is the lumen side mass transfer coefficient, (m/s), L is the diameter of the lumen (m), D_{AB} is the diffusivity coefficient, m^2/s, (experimentally determined form Stokes-Einstein equation: 6.90X$10^{-10}m^{2/}s$ for glucose in water at 37^0C).

$$Sh = K_{lm}L/D_{AB} \tag{3.5}$$

As Sherwood number increases, mass transportation increases with increasing mixing (segmentation and peristaltic flow) and reduce with increases luminal content viscosity, as shown in Fig.3.7. All increase were in the same order of magnitude, and as viscosity

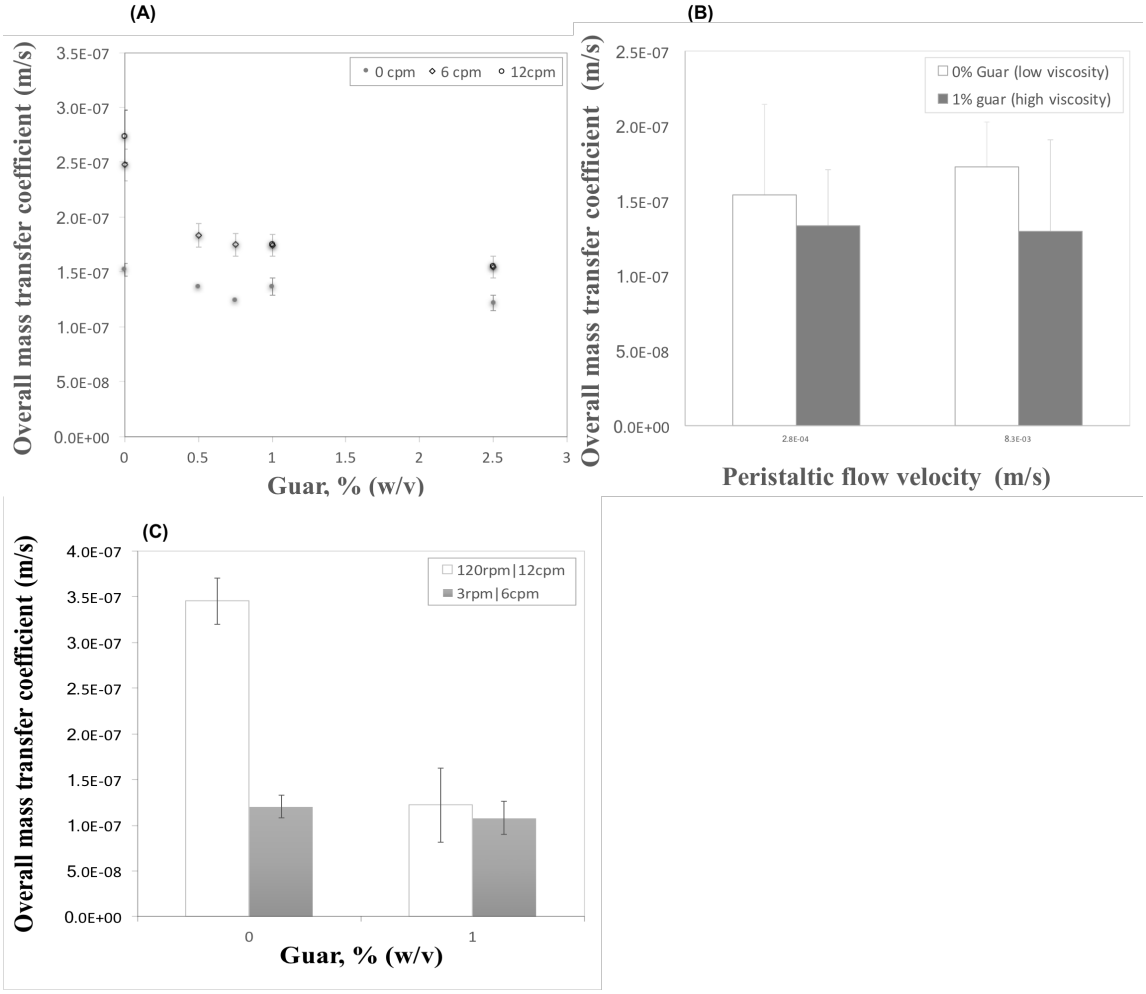

Fig. 3.6 Overall mass transfer coefficient, (k) for different systems: (A) enhanced segmentation and enhanced viscosity, (B) constant flow rate with increased viscosity (C) increase flow, viscosity and segmentation. The error bars show the standard deviation from a sample amount of three.

increases, convective mass transport becomes less important to each system, highlighting the importance of the molecular diffusive mechanisms.

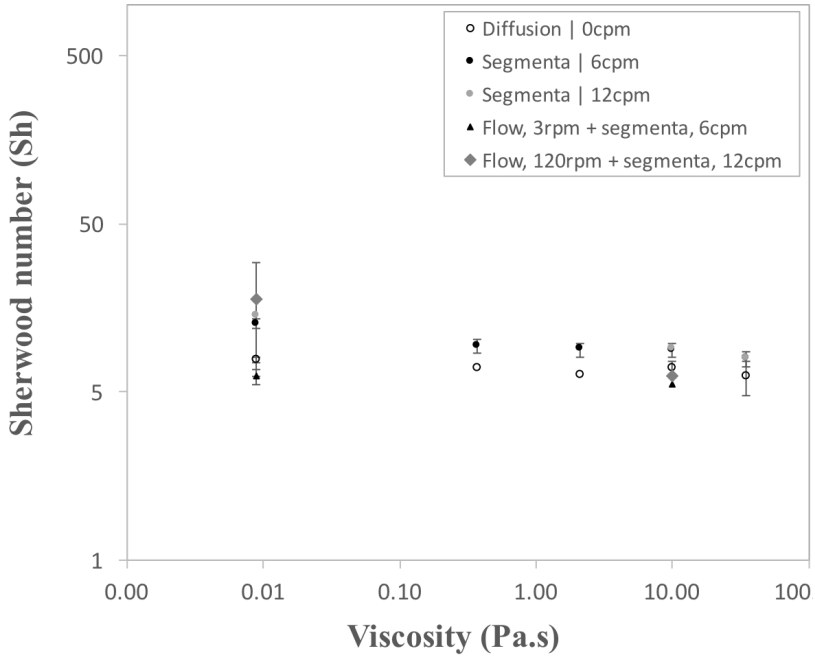

Fig. 3.7 Dependence of mass transfer (Sherwood number) on viscosity under different flow transport conditions. The error bars show the standard deviation from a sample of three.

A conventional way to describe pulsate flows under physiological condition is the dimensionless Womersley number, *Wo,* (Loudon and Tordesillas 1998). *Wo* numbers have been applied to characterise blood flows in arteries (Womersley, 1955). It describes the pulsatile flow frequencies associated with viscous effects and can be estimated from the equation (3.6).

$$W_o = L\left(\frac{\omega\rho}{\mu}\right)^{0.5} \tag{3.6}$$

where ω, is the angular frequency of oscillation (1/s), ρ is the density (kg/m^3), L is the radius of the lumen (m) and μ is the dynamic viscosity (Pa.s). To calculate ω, the frequencies of segmentation (cpm) were used and expressed in rad/sec. i.e. 2. For example: was estimated to be 1.26 rad/sec at 12 contractions per minute (cpm).

Flow in the small intestine has also been frequently characterised by using the Reynolds number. Since the contracting rings during segmentation occurs along the length of the model forming small isolated pockets, the lumen can be visualised in the form of a wave (wave

functions). Therefore, the oscillatory Reynolds number would be appropriate to describe the fluid flow due repeated contractions. It can be estimated from the equation (3.7).

$$Re_{(o)} = \frac{\rho 2\pi f X_0}{\mu} \tag{3.7}$$

WhereX_o, is the centre to peak amplitude (1.75x10^{-2} m), f is the frequency of oscillation, 0.2 s^{-1} (12 cpm/60, 1/T), ρ is the density (kg/m^3), and μ is the dynamic viscosity (Pa.s). Mass transfer rates according to Wo and Re was estimated from the segmentation mixing frequency of at 6 cpm and 12 cpm and plotted in Fig.3.8. below.

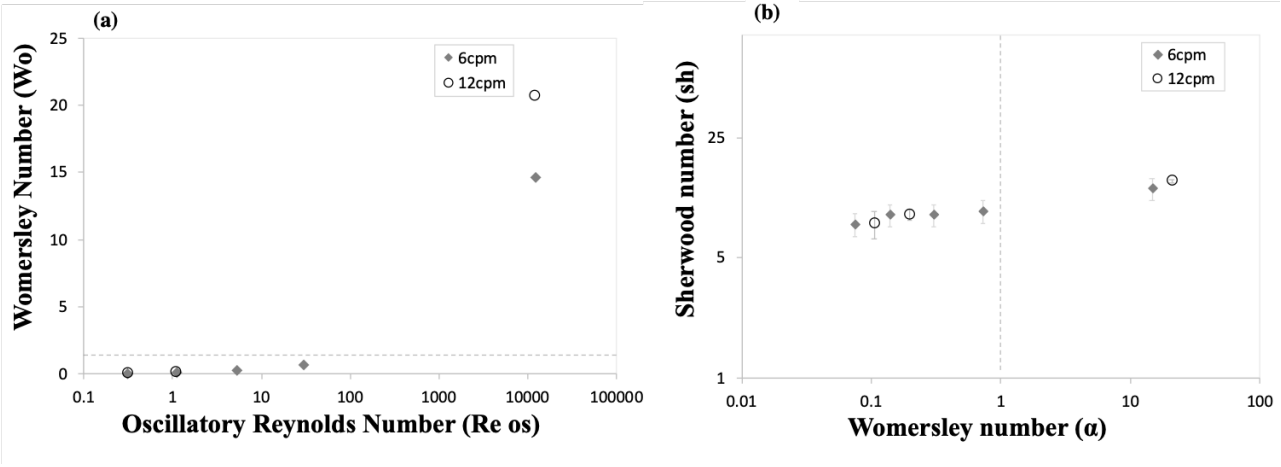

Fig. 3.8 Dependence of mass transfer operations; (a) relationship of oscillatory Reynold's number and Womersley number in segmenting systems and (b) coresponding Sherwood's number as as a function of Womersley number under segmenting systems.

Flow in the small intestinal model ranges from laminar to turbulent depending on formulation (viscosity) and the type and magnitude of induced mixing as shown in Fig.3.8(a). The largest *Re* observed were 1.24 X10^4 and 2.47x 10^4 for 6cpm and 12cpm for 0% guar system respectively. As the system moves above 0.5% guar, there was a significant decline by 4 orders of magnetude in Re number, below 100, suggesting that flows in the model follows a laminar regime as the viscosity increases. This is inline with authors (Love et al. 2013; Jeffrey et al. 2003), which suggest that *Re* numbers in the small intestine does not often times exceed 200. It is therefore expected that mixing by advection and subsequent mass transfer would be limited, in the case of laminar flow, but not in the case of turbulent flows, which promote mixing of the luminal contents.

The corresponding Womersly numbers shows that the Sherwood number mass transfer was independent of it. Fig.3.8.(b). The hashed line on the figure is extrapolated to *Wo* of

1. When *Wo* is above 1, and Re exceeds 1000, mass transfer increases and relies heavily on transient inertial forces suggesting that capturing the importance of higher frequencies of mixing (6 cpm and 12cpm). Below 1, the mass transfer is reduced and conclusively suggesting the increase role of viscous forces in the lumen, and reduced effects of intestinal contractions as the lumen content becomes more viscous. Overall these results highlight that formulation of fluids can manipulate nutrient delivery in the physiological environment. Further, the dynamic model describes that segmenting condition contribute more to mixing than peristaltic flows, influencing nutrient delivery at the membrane.

3.4.7 Digestion of commercial bread and starch kinetics under different mixing conditions.

Under in vivo constraints, the flow and mixing in the small intestine are complex operations involving heterogeneous particles, considering the time-related (temporal) conditions. The materials being digested are faced with different deformation forms at varying shear rates, and at a different location along the GI tract. Therefore, the effect of soluble fibres on mixing patterns of the digested materials, at different locations in the gut, is inevitably complex in nature. As seen in the earlier discussion on model fluids containing guar, the addition of this soluble fibre increase the viscosity of the luminal content. This increase, alters the flow regime, restricting disordered flow (turbulence), which diminish the mixing effects of intestinal contents. In the same way, an addition of this fibre to food formulations will determine the oral and gastric rates of digestion, which will subsequently impede the rate of diffusion and convection of enzymes on to substrate within the heterogeneous food bulk.

The digestion rates of starch in bread were clearly, dependent on mixing of the intestinal model, and formulation as shown in Fig.3.9. Under no shear, and added guar (by 10% soluble fibre), the digestion was profusely slow, compared to mixing (2 and 6 cpm). For example, the mass transfer coefficient was ~2 fold for white bread under no mixing (1.44 $x10^{-7}$m/s) and increased mixing (3.48 $X10^{-7}$m/s) conditions. By substituting the bread with 10% guar, the mass transfer fell, by a third (2.39$X10^{-7}$m/s), even when the mixing frequency was 3 fold (from 2 to 6 cpm). Were it not for the enhanced mixing, the mass transport coefficient would have been extremely low. This demonstrates the effectiveness of guar to act as a modulator in constructing food matrix for improved health conditions regarding improving GI for manufactured foods.

The types of food also impact the rate of starch digestion as shown in Fig.3.9. Multi-seed bread were among the slowest digested bread's and showed the slowest mass transfer

coefficients. When the digestion material was left to the fate of pure molecular diffusion, the rate of mass transfer rate fell by an order of magnitude (5.67X10^{-8} m/s). Under mixing, the mass transfer rate was 2.33 X10^{-7}m/s, in a similar order of magnitude as the white bread for the same mixing condition, but 33% less fast. The form in which the starch is present in the ingested food may impact its digestibility efficiency (Lentle 2011, Lentle 2011a). Additionally, there are other physical impediments that can restrict the rate of starch digestion, such as the plant cell wall. This may be the case for the multi-seeded bread. As they pass through oral digestion, the plat material form the seeds become exposed during the grinding and mixing operations, exposing the soluble fibres in the liquid phase of the digesta. Consequently, the digests's viscosity will be altered and the rate at which amylase catalyse starch will delay or improve the liberation of maltose, dextrin etc.

Overall, it has been cited that, if the activity of amylase can be suppressed through manipulation that deters its diffusion, then there could be some nutritional benefits (Al-Rabadi, et al., 2009), to be gained. Such as, postprandial glycemia lowering responses. The activity of amylase can be described by the overall hydrolysis/kinetics. The kinetic constant, for the kinds of bread were estimated according to equation.3.8., described by Goni, et al., (1997) as shown in Table 3.3.

$$ln[\frac{C_\infty - C_t}{C_\infty}] = -kt \tag{3.8}$$

The hydrolysis behaviour was assumed to follow the first order kinetics, under gut motility shear mixing, where C_t is the concentration of starch passed through the membrane at time, t and C_∞ is the concentration of starch passed through the membrane at the end of digestion (120 minutes), and used to predict the k values. The slowest kinetic, (hydrolysis) constant was established by multi seeded breads, 1.09 X10^{-2} min^{-1} under no mixing. While, white bread under mixing, displayed a the fastest k, 1.2 X10^{-3} min^{-1}, an order magnetude faster that the rest of breads, follwed by the 10% guar containing breads, 2 X10^{-3} min^{-1}. The k for 10% guar in white breads along with the faster mixing frequency highlight the importance of increase viscosity on starch digestion and that the kinetic behaviour is conclusively partially influenced by diffusional restrictions. In addition, the starch forms found in the different breads may have been processed differently for each formulation, giving rise to different starch properties. This may have been translated into different digestibility rates observed in Table 3.3. Similar conclusion have been drawn by Butterworth et al., (2012) and Patel et al., (2014) where digestion rates of starches from different native and gelatinous sources were studied.

Bread/Formulation	No shear: 0 cpm	Low shear: 2 cpm	High shear: 6 cpm
	k (min^{-1})	k (min^{-1})	k (min^{-1})
white bread (wb)	0.0026 ± 0.0002	0.0012 ± 0.0023	-
multiseed bread (msb)	0.0109 ± 0.0021	0.0022 ± 0.0032	-
10% guar bread (gb)	-	-	0.002 ± 0.0003

Table 3.3 Digestibility rate constant (k), for different breads digested after 2 hours in the smal intestine, under different levels of shear mixing (gut motility rates from 0 - 6 cpm).

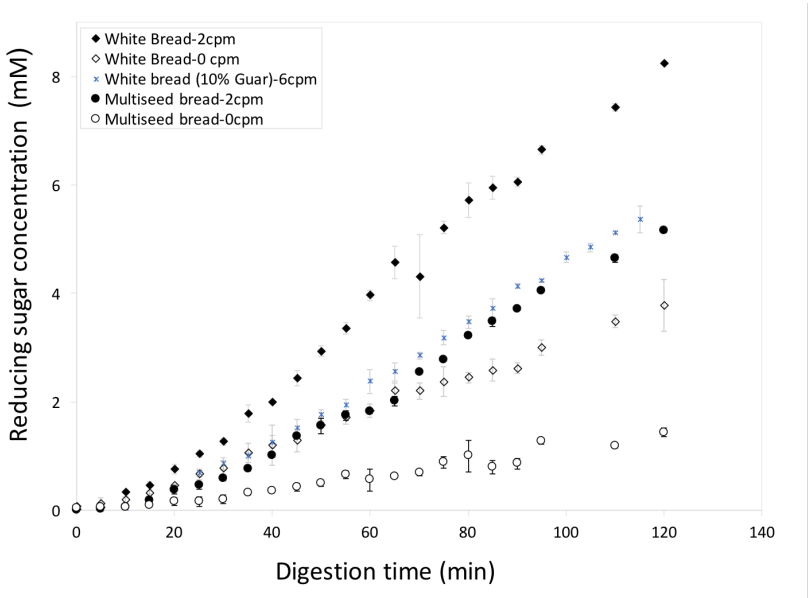

Fig. 3.9 Bread digestion rate plots in the dynamic model under mixing and no mixing conditions: white and multi seeded breads at 0cpm and 2cpm, and white bread substituted with guar 10% at 6cpm. The error bars show the standard deviation from a sample of three.

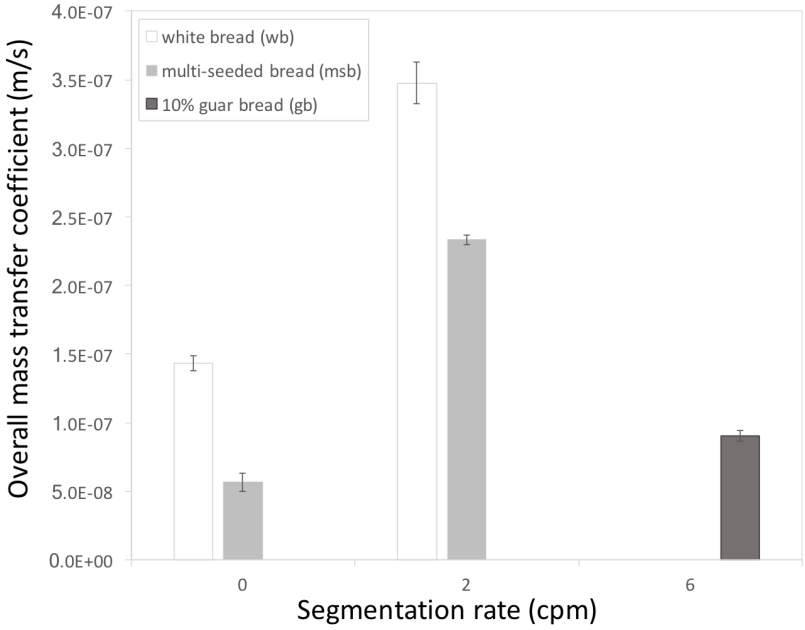

Fig. 3.10 Overall mass transfer coefficient for breads under different mixing conditions.

3.4.8 Effect of Arabinoxylan fibres on bread digestions (Speciality bread).

The endosperm of wheat is made up of about ~2 % w/w arabinoxylan portion, both soluble and insoluble forms. It also integrates with water during dough hydration and binds ~ 20% of it, during bread making (Andersson et al., 1993). It is evident that AX found in grains makes up a significant part of our diet, as indicated in introduction of the thesis, chapter 2, section.2.72.. As a result, the physiological effects have been studied (Lu et al., 2000), and even though the health benefits are well noted in literature, little is known about purified AX and its mechanisms to slow mass transfer during *in-vitro* food digestion and absorption.

Formulating with botanical fibres at different levels, gives different digestive response to reducing sugar absorption, in particular, when digestion is allowed to carry-on. Figure.3.11. illustrates two bread, Yumai (AX2) and Hereward, (AX1) were formulated with incorporated arabinoxylan fibre at 16.65 mg/g and 14.56 mg/g respectively. For the first hour, all bread including the control has similar digestion patterns that make it hard to distinguish between bread types (t_0-t_{60}). However, once digestion prolonged beyond an hour, the bread began to display their own unique digestion patterns up to 3 hours. Increase in fibre content, reduce the rates of absorption. Increased arabinoxylan fraction by 14.4 % (i.e. from 14.56 mg/g to 16.65 mg/g), resulted in a decrease in overall mass transfer rates (~32% decrease), from 4.02 x10^{-07}m/s to 2.73 x 10^{-07}m/s (Figure.3.12). The control bread (white bread with no

arabinoxylan fibre) had the highest mass transfer rate of $5.19x10^{-07}$m/s. Without fibres, the overall rate of absorption is clearly fast and the total sugar absorbed was 8.56 mM (at the end of 2 hours).

When fibres were added, AX1 and AX2, an approximated 8.9 mM and 5.9 mM were transferred to the receiving medium respectively for each fibre, just under 3 hours of intestinal digestion. This is a ~34% reduction in overall absorption in the final amount of reducing sugars when the arabinoxylan values went up by 2.09 mg/g (14.4% increase). This was very similar to in-vivo/clinical studies, that incorporated AX fibres in bread meals to understand the effect on glucose response in normoglycemic individuals, conducted by Lu et al. (2000). They have found that adding increasing AX fibre from 6 and 12 g (50% increase) in bread meals, resulted in a 6% reduction in peak postprandial glucose concentration. The decrease in absorption rates may be accounted for by the expected viscosity of the digesta during intestinal motility. Arabinoxylan fibres are known to increase the viscosity when in the liquid phase (Heaton et al., 1988; Delcour et al., 2012; Li et al., 2017). This viscosity is known to be a major resistance factor, delaying amylase and starch interactions during digestion (Roberts et al., 2005; Ellis et al., 1991; Brennan et al., 1996). There is a strong correlation between the amount of AX fibre and the level of reducing sugar absorbed as prior discussed. However, it is still not well defined whether the effect is from a physical barrier mechanism of the AX fibre or if the fibre function by other means inside the digestive tube. It s also unclear how a the increase in such a small increment (2.09 mg/g) had such a significant impact on mass transfer rates, of up to 34% increase.

The viscosities of the bread digesta were measured with intentions to have precise values, but data had shown (not presented in the thesis), extremely high variability (less viscous to extremely viscous). The digesta has long been acknowledged to have suspended particles and of varying sizes which makes it difficult to estimate. Using the viscosity of the fluid phases when the solid phase have been separated has been practiced, but the approach has been warned against, as disrupting the digesta structure may significantly alter the overall rheological properties (Lentle and Janssen, 2010). Simulated segmentation frequency was carried out at 2cpm. This low frequency of segmentation was selected, as it is was the best way to study digestion of unknown absorption behaviour and also because these samples were also limited. Given that both AX breads went through the similar levels of shear mixing, it evident that the viscosity is responsible for translating breads to different digestion rate profiles. Addition of arabinoxylan fractions has demonstrated that the fibre is capable to modulate digestion and absorption, similar to adding 10% guar biopolymer.

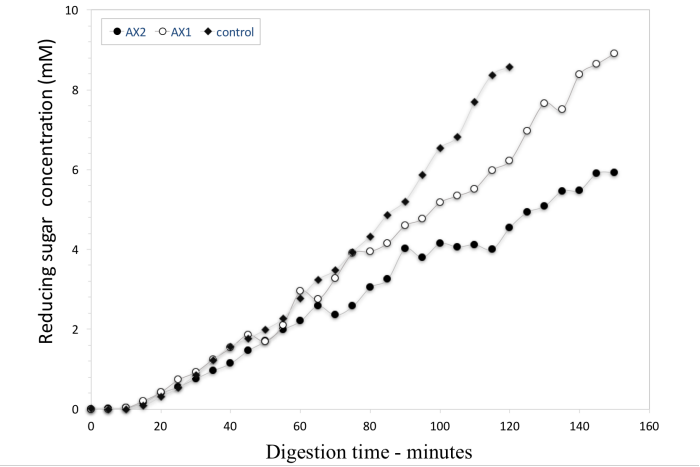

Fig. 3.11 Digestion rate plots of breads baked from different wheat cultivars contain varying levels of arabinoxylan fractions. AX1-14.56 mg/g (Hereward) and AX2-16.56 mg/g (Yumai)

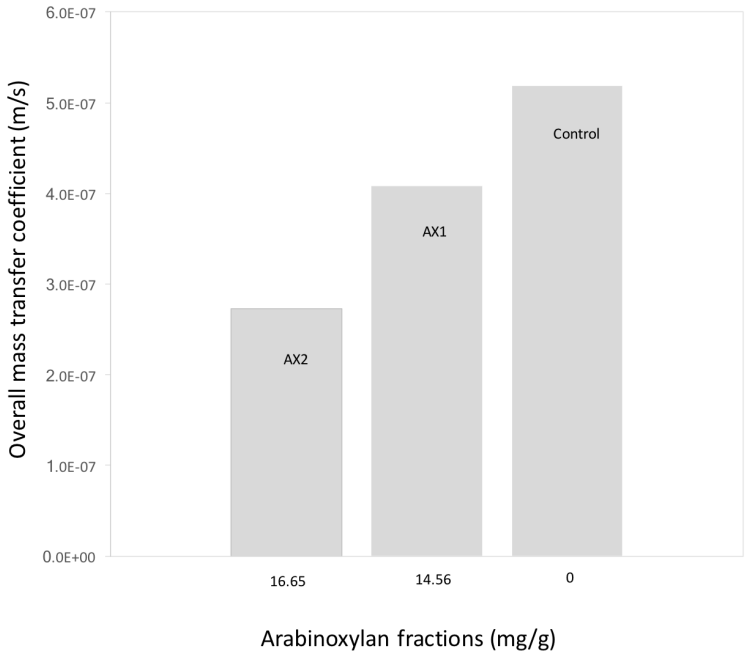

Fig. 3.12 Effect of Arabinoxylan concentration in bread on the overall mass transfer rates during digestion at 2 segmenting frequencies per min in DDM.

3.5 Conclusion

A novel dynamic computer-controlled model of the human duodenum was developed and used to simulate segmentation and peristaltic contractile activities to preform mixing and absorption, during food digestion. The effect of digesta content viscosity and wall motions were investigated. Mass transfer studies using model fluids used in absorption trials indicated that segmentation motility was more important to mixing and mass transfer than peristaltic motility, arising from flow rates. Increasing the viscosity of the intestinal contents, reduce nutrient delivery as well as the effect of mixing. The model was able to digest real foods when they passed through (mm-cm scale), demonstrating how food formulation may affect digestibility differently. The digestion of bread with and without varying soluble fibres confirmed that food formulation can be manipulated to impair diffusional resistance of enzymes, highlighting the importance of segmentation to the overall digestion efficacy of starch. Further, Arabinoxylan is an effective soluble fibre to reduce starch digestion and absorption even in small quantities added to diets. These effects are predominantly observed in the later stages of digestion.

This model promise a good prospect to study in-vitro, the intestinal digestion of foods. However, more investigations are needed for the influence of food material (viscosity) and gut motility (segmentation and peristalsis) mixing on the hydrodynamics in the duodenal model. In particular, the velocities and residence/transit times of the digesta through the lumen of the model to adequately evaluate the performance of food systems for the purpose of digestion. Positron emission tomography (PET) has been proposed and was investigated. Please refer to Chapter 4 for fluid mixing and transport in the gut model to characterise the mixing.

Chapter 4

Fluid mixing and transport process in the gut model

This chapter builds on Chapter 3. The mixing that was used to study bread digestion in the previous chapter and glucose absorption was reproduced, to determine the residence time distribution and fluid velocity profiles in bread systems using molecular imaging techniques.

Abstract

The flow and mixing strategies undertaken by the small intestine to perform food digestion is important to meet the body's energy demand after food consumption. Understanding how the physical properties of foods modulate the mixing in the gut may give insight into the controlling mechanisms regulating the rate at which deposited pancreatic enzymes and other intestinal fluids are mixed with freshly added chyme. Consequently, these mechanisms are strongly interconnected to the enzyme-substrate breakdown of macromolecules to small molecules and their uptake. *In vitro* food digestion models that adapt geometric features of the organs, they wish to simulate, should be able to provide "near-real" flow patterns, during fluid mixing and transport imaging, as if they were the actual organs themselves. Therefore, the dynamic duodenal model should be able to give some insights on the fluid-mechanics that governs gut flow and mixing, to demonstrate the level of mixedness that is achieved when enzymes are deposited onto luminal content. To characterise the mixing phenomena under segmenting and peristaltic motility regimes, model fluids with varying viscosities and real bread systems (white and wholemeal), with varying structural differences, were studied using mean residence time (MRT) and positron emission tomography (PET) techniques for the first time respectively. The axial velocity distribution profiles were estimated from PET, for each bread. Segmentation transport of radioisotope was faster in wholemeal bread, compared to white bread. The increase in model fluid's viscosity caused the mean residence time to decrease and was independent of the motility factor. That is, a 20% reduction under peristaltic only flow and 42% reduction with the synergistic effect of segmentation and peristalsis. The mixedness was improved by 3% for less viscous systems, and 31% more for the most vicious systems when under segmentation, suggesting that segmentation is paramount for efficient food digestion. Overall, the gut model demonstrated that segmentation was less important to mixing in low viscosity fluids at this scale (mm).

4.1 Introduction

The living small intestine has attached to it, an orifice/sphincter, at the major duodenal papilla (ampulla of Vater) that is common to two important ducts, one leading from the gallbladder, containing bile and the other from the pancreas, contains pancreatic fluids (Mahadevan, 2017). It commences, approximately 10 cm from the pylorus of the stomach. In engineering terms, the purpose of an orifice-plate is to regulate fluid flow, by increasing the fluid velocity and reducing pressure (Perry, 2008). In the same way, through constriction of the flexible opening of the sphincter, the passage of intestinal fluids; pancreatic fluids and bile, can be regulated during secretion. The pancreatic fluids is consist of amylases, proteases and lipase, and the bile contains surfactants for fat digestion (Hall et al., 2011). The discharge rate is of high importance to certain postprandial responses such as the body?s blood serum glucose levels, due to the energy demand from ingested carbohydrates such as starch. This makes the common secretion duct/orifice it an important structural feature in the overall mixing process and subsequent digestion phenomena, during gut mobility and should be appropriately considered when simulating mixing in the small intestine.

A body of work has studied flow and mixing of the small intestine by, in-vivo, in-vitro, ex-vivo and in-silico means (for example, Loubens et al. (2013); Lentle et al. (2011); Du et al. (2015)) and see chapter 2 for detail descriptions. These mixing studies equally tried to elucidate the level of turbulence and identify flow streams and predict of eddies generated as a result of the effect of the typical contractile activity, as a single fluid mass. However, no attempt has been made to understand the ?live temporal? mixing strategies when secretion from the orifice are directly mixed with freshly added chyme coming from the stomach. In the human body, bile is typically secreted at a rate of 0.5 L/day (Chang et al., 1996) and pancreatic fluid at a rate of 4.5 ml/min (Argent et al., 1990), when appropriately stimulated. These secretion rates are known to bring about considerable changes in digesta characteristics, in short time periods (Lentle et al., 2011). Consequently, different foods will enable different mixing strategies of the small intestine due to the nature of their chemical and physical properties and will influence how the enzymes are mixed with chyme for enzymatic macro molecule breakdown and subsequent nutrient uptake.

Clinically, the small intestine has been examined by various data imaging techniques including; capsule and double-balloon endoscopy, ultrasonography, magnetic resonance imaging (MRI) and computerized tomography, that can give detail temporal and spatial resolution (Kim Nylund, 2009). Each of these techniques however, has their disadvantages and cannot be applied to some in-vitro models due to their architecture, for example, some

are made of metallic materials that would interfere with a MRI technique. Therefore, other alternative methods have been explored. For example, Fonseca (2011), has studied a small intestinal model to capture temporal flow and mixing images arising from gut motility, using a modified form of Positron Emission Tomography technique (PET), called PEPT, (Positron Emission Particle Tracking), which is based on a molecular imaging technique. However, PEPT tracks a single particle, but the release of enzyme involves a cocktail of enzymes suspended in a fluid, and should be considered as such when trying to detail more accurately the complete flow and mixing profiles, arising from the incorporation of enzymes in freshly added acid chyme, during intestinal mixing. This study consider the use of PET multiple tracking technique. This technique uses isotopes which are positron-emitting, such as Fluorine-18 ($t_{\frac{1}{2}}$ of 109.7 minutes) to label tracers (Cai, Lu, and Pike, 2008). When the isotope (F-18), emits a positron of low energy (0.635 MeV) it travels and annihilate with an electron producing a pair of back-to-back γ-rays (511 keV each) (Parker et al, 2002). This mode of decay, consist of the physical component of PET imaging, which are mapped by detectors/cameras. PET has been one of the most important diagnostic modality tools in medicine, (Wagner, 1991), inclusive of the discovery and development of drugs (Burns et al., 1999). For example, integrating F-18 into radiotracers, such as F-18 into D-glucose to give fluoro-D-glucose ([^{18}F]-FDG), which becomes a radiotracer of glucose metabolism (Fowler and Ido, 2005), permitting the imaging and quantification of biochemical processes.

PET imaging and its variant PEPT, has been applied in process engineering studies (Levenspiel, 1999), by permitting the ability to study processing equipment for pilot studies or laboratory scale studies (Parker et al., 2008). For example, it has been used to study flow and mixing in model food systems with varying viscosities in opaque containers (Bakalis et al., 2003) where the authors were able to estimate the velocity distribution profiles of these fluids, that mimiced the rheology of real foods. PET and PEPT can estimate how well a system is mixed and the rate at which it happens during motility, as the physical phenomena vary widely (Kukukova et al., 2009). As such, it can be applied to the dynamic duodenal model. The mixedness can be defined as the changes in the intensity of segregation which is usually expressed as the normalized coefficient of variation (CoV) in most industrial applications which is used to address mixing at the molecular level (Kukukova et al., 2009).

Under flow, the average time fluid spends in a reactor under different operating constrains, can be used to characterise the mixing in a that reactor. This principle is called residence time distribution (RTD) (Levenspiel, 1999). Dye tracers are used to study RTD and has been applied to bio-inspired small intestine reactors (Deng et al., 2014). Similar tracer based procedures have been used to determine entire gut transit times (Janssen et al, 2007).

However this is complex, trying to accurately evaluating the flow and mixing regimes, even though proven to be very useful in process engineering, can be difficult to measure as mixing occurs at varying length scales. The aim of this study is to use imaging techniques to capture and visualise the fundamental mechanisms of intestinal mixing and flow when fresh enzyme (analogue) is discharged, from the unique duct, onto the inflow gastric chyme in the novel *in-vitro* rig. This will help to highlight the strategies of intestinal mixing when fluids of varying viscosities effect different segregation rates, and residence times.

4.2 Materials and method

4.2.1 Materials

All chemicals were purchased from Sigma Aldrich UK unless other wise stated.

Biopolymer preparation

The procedure in preparing the model fluids and breads were similarly reproduced according to the method section of Chapter 3 of the thesis. In summary: aqueous guar gum solutions containing; 0.5, 0.75, and 1 (%w/v), gum guar supplied by Sigma Aldrich (G4129-500G) were prepared. Gum guar was added to the water, with simultaneous stirring, and temperature raised and maintained at 80 ^{0}C for 10 minutes until fully mixed and allowed to cool at room temperature, then left overnight for complete hydration, before each use. Shear experiments were carried out on the model fluids using a Bohlin Instruments rheometer (KTB 30, Crawley, UK) equipped with a cone-plate geometry 40/1 with gap size of 1mm. For each test, 5 ml of freshly prepared solution was allowed to equilibrated at room temperature (24^{0}C) prior to experiments. The viscosities were then measured as a function at zero-shear rates (s^{-1}). This was repeated in triplicates for each concentration of model solution as recorded in Table.3.2, Chapter 3, section 3.2 of the thesis.

Preparation of bread

Two bread types; white and wholemeal, were procured from the local store. Foods were selected to include breads that may digest differently and may impart different viscosity of the luminal content.

4.2.2 In-vitro digestion

Oral and gastric digestions were performed according to Chapter 3; the first results chapter, methods section of the thesis, and white breads and wholemeal breads were selected for these experiments. The gastric chyme (bread digesta) were then added via the feed entry point on the dynamic model at the onset of the PET experiments.

4.2.3 Residence time distribution (RTD), studies

A pulse response method was carried out, to measure the mean residence time (MRT) and residence time density functions (RTD) (MacMullin and Weber, 1935 and Danckwerts, 1953). The experimental set up is shown in Figure.4.1.A. Riboflavin solution, 0.5ml, was added through the simulated duct with a 5 ml syringe and needle as the initial pulse t(o), to a peristaltic flow of 30 rpm and segmentation of 6 contractions in a minute (6cpm). The intensity of riboflavin dye in the effluent/outflow as a function of time, done at 10s intervals were read using a UV spectrophotometer, at 445 nm. This exercise was done in triplicate and the data set was used to construct the concentration time curves, *C(t)*, interpolated from a standard curve that was constructed using known concentration of riboflavin. At a constant fluid flow the RTD density function *E(t),* can be expressed as equation.4.1, which can be obtained from the *C(t)* curves by dividing by the integral, $\int_0^\infty C(t)\,dt$, (Levenspiel, 1999).

$$E_{(t)} = \frac{C(t)}{\int_0^\infty C(t), \mathrm{d}t} \tag{4.1}$$

4.2.4 Positron emission tomography (PET), studies

Radioisotope solutions (20 ml solutions), were prepared from fluoride ions (F-18), dissolved in water on the day of study to give an activity of 20 mCi. This volume was secreted into the lumen via the in vitro pancreatic orifice (as seen in Chapter 3, section 3.2, which details this part of the model), manually, with a 25ml syringe and needle, onto the material containing in the lumen (500ml), that was closed system at both feed and exit ends with rubber stoppers. Figure.4.1.B., details the set up carried out, and pathways (flow patterns) of the tracer solution were recorded with the PET cameras, to provide the images of the flow profiles under segmentation motility in the lumen of the gut, at the mm scale. After data collection via the PET cameras, 256 x 256 pixels' resolution was extracted and files were vertically integrated and stacked into 10s and 100s time sequences using the *ImageJ*

software. Because the radioactive isotopes activity changes with time, the values were scaled and normalised in order to compare the rates of intensity changes over time between different food model systems and motility treatment.

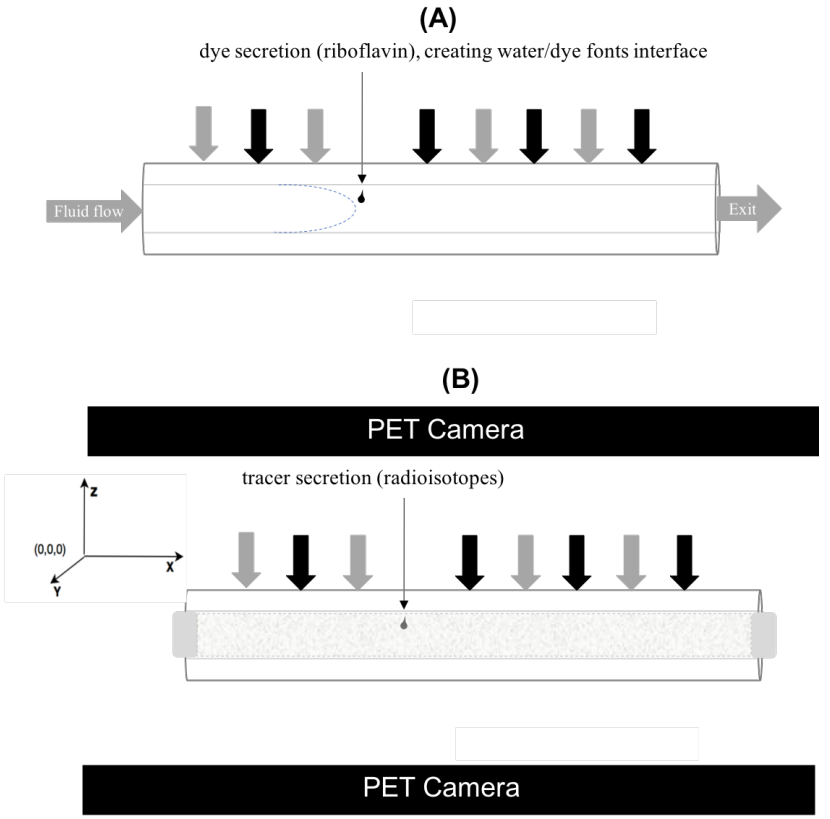

Fig. 4.1 Experimental setup to characterise mixing in the dynamic duodenal model; (A) schema showing in-vitro preparation of the system for perfusion and sampling of the outflow for RTD value estimations and (B) Schematic representation for the experiments conducted for PET (3D coordinate system, x, y and z) with feed and exit ends closed with rubber stoppers.

4.2.5 Data analysis: Coefficient of variation (CoV)

The CoV was determined from the equation.4.4., below as an indication to determine the mixedness in the dynamic duodenal system, during segmentation. This type of analysis has been done extensively on fluids, and Alberini et al., (2014), demonstrated that the CoV can be used as a scale of measurement for mixing. CoV is usually expressed as a ratio of the standard deviation of the intensity of segregation (distribution of concentration in the local mixing area), divided by the concentration of complete mixing (assumed). The scale of

segregation is usually obtained by image analysis as previously described or other imaging techniques. A CoV of zero usually represents complete/perfect mixing (100%) (Kukukova, Aubin, and Kresta (2009); Kukukova et al. (2011) and Alberini et al., 2014).

$$\tilde{X} = \frac{\Sigma}{N} \tag{4.2}$$

$$S = \sqrt{\frac{\Sigma(x-(\tilde{X})^2}{n-1}} \tag{4.3}$$

$$CoV = \sqrt{\frac{\Sigma(x-(\tilde{X})^2}{n-1}} / \frac{\Sigma}{N} \tag{4.4}$$

4.3 Results and discussion

4.3.1 Axial transport in model fluids: effect of segmentation and peristalsis motility on residence time distribution.

Since the dynamic duodenal model is a tubular design, it can be described as a plug flow reactor (Chivers et al., 1994). Therefore, the transit and mixing of fluids having varying viscosities with 'on demand' pancreatic juices in the duodenum of the small intestine can be appropriately described and be represented by plug flow mechanism, during gut movements in digestion. Experiments were performed with both open and closed systems (lumen is closed at both ends or left completely void see Figure.4.1). It is adequate to accept that these approaches (closed and open systems) are well within the physiological range for mixing. For example, the closed system of the model can be envisioned in a similar way as the closed pyloric sphincter that separates the stomach from the duodenum (stomach-duodenum junction) and the closed ileocecal valve that separate the small intestine from the large intestine (Pal.A et al., 2004; Pallotta et al., 1998; Bharucha et al., 2012). Likewise, the transit of chyme between the two valves, at different time points can be treated as an open system. The peristaltic flow was set at 30 rpm (0.9 m/min; flow rate of $2.7\text{x}10^{-06}$ m^3/s), the lowest flow rate that could be achieved by the pump, to match the 1cm/min observed for fluid flow rates in the human small intestine (Hall et al., 2011).

The mean residence time for the duodenal model was measured, to understand how in-vitro mixing mechanism and luminal viscosity regulate axial transport. The gut movement

type (peristalsis and segmentation), had little influence on overall residence time. Figure.4.2. shows the RTD density function *E(t)*, for fluid flow (1% w/v, guar gum: high viscosity fluid) under peristaltic only and combined peristaltic and segmentation motility in the dynamic duodenal model. One of the main feature identified is that both motility conditions of peristalsis (P), and combined segmentation and peristaltic (P&S), has several peaks, with almost equivalent concentrations of riboflavin exiting the lumen (4.3 mg/l and 4.25 mg/l respectively) i.e. there was no significant difference in outflow concentrations for the main peaks. Flow by peristaltic only (grey chart on Fig.4.2) has its main peak ended at about ~45s followed by a delayed smaller peak ending at 85s with an RTD function value of ~0.0355. While combined peristaltic and segmenting motions delivered its main peak (blue chart on Fig.4.2) ending at ~30s (15 seconds faster) and ~40s for the tailing smaller peak with an RTD function value of ~0.0455. Figure.4.3. on the other hand, which utilises low viscosity fluid(0% w/v guar gum) showed peaks ending ~80s, for peristaltic motility (grey chart on Fig.4.3) and ~60s for combined peristaltic and segmentation motility (blue chart on Fig.4.3) which is 20 seconds faster. Both have an RTD function value almost identical even though both had different residence times. With peristaltic having 18% increase in RTD function value (~0.03) compared to combined peristaltic and segmentation which was ~0.0255 (Table.4.1).

It is evident that the E(t) value is a function of viscosity and mixing. E(t) was increased by 18% when the luminal content viscosity increases from low (0.00089 Pa.s) to high viscosity (10 Pa.s) under pure peristaltic flow. Under the combined effect of segmentation and peristaltic gut movements the E(t) value had a significant increase, by 78%, as illustrated in Figures.4.3. and 4.4. from low to high viscosity.

Under perfect conditions, an ideal plug flow reactor would deliver a single pulse (curve) when the effluent concentration is measured. However, this was not the case for the dynamic duodenal model. This deviation is a result of the hydrodynamics effects occurring in the vessel (Levenspiel 1973). The larger early peak of the E(t) curves are followed by the smaller multiple delayed decaying peaks in high viscosity fluids (10 Pa.s) as observed in Figures.4.2 and are suggestive of backmixing occurring during flow. Backmixing occurs when there is strong internal circulation along the fluids path. This is highly controlled by segmentation motion which allows matter to oscillate due to the squeezing and relaxation pulses from the gut wall movements. For low viscosity systems (0.0089 Pa.s), there were no tailing peaks observed under either condition of motility, rather it was a smooth early curve, which suggest a reasonably good plug flow (similar to an ideal plug flow reactor), obeying material

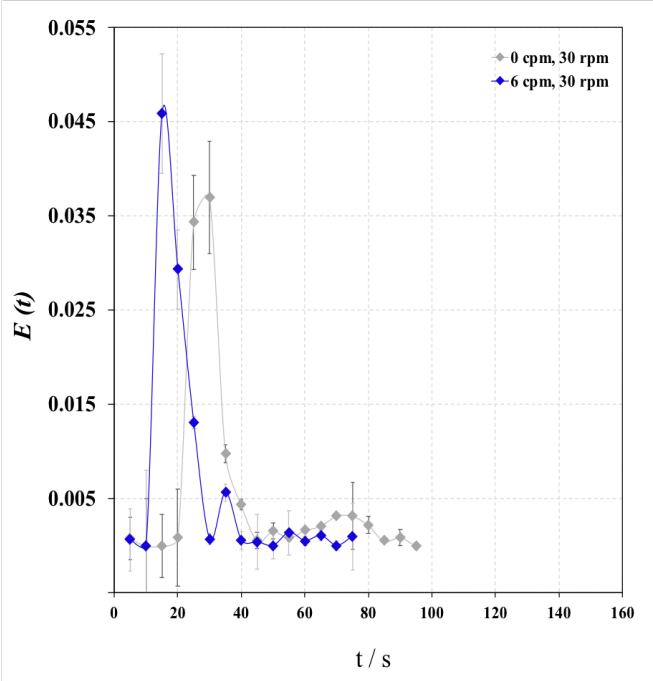

Fig. 4.2 Residence time distribution function, E(t), for peristaltic flow at 30 rpm (0.9 m/min; flow rate of $2.7x10^{-06}$ m^3/s) - grey chart, and peristaltic flow at 30 rpm and segmentation mixing at 6 cpm (blue chart), for high viscosity fluid (1% guar gum solution) in dynamic duodenal reactor model, similar to experiments conducted in Chapter 3, section.3.31. and 3.4.2. of the thesis. Peristaltic flow and segmentation mixing and were simultaneously done for each trial. Error bars are standard deviation of three values

transfer. According to Stoll et al. (2000), peristaltic flow does cause some mixing in the small intestine, but its primary role is axial transport.

The residence time distribution of the riboflavin dye, from the outflow of the dynamic duodenal model, in this study suggest that a turbulent flow regime was present with chaotic vortices occurring at different length scales and duration for the inflow of low viscosity fluids (0.00089 Pa.s), under segmentation. The Reynolds number under segmentation was estimated to be appx.12,348 (Oscillatory Re), from the Equation.3.6. in chapter 3 of the thesis. The Re under peristaltic only flow was estimated to be appx. 590 (laminar flow).

The turbulent regime observations are very similar to results from Loubens et al. (2013), who has similarly characterised mixing in-vivo and ex-vivo using a 10 cm duodenum of euthanized rat (ex vivo), to determine the residence time distribution (RTD-value) using a step response dye method, by collecting and measuring the amount of dye in the effluent every 60 seconds. They had used low viscosity fluids, and had concluded that radial dispersion, was effectively higher than axial dispersion, during contractile activity that cause turbulent

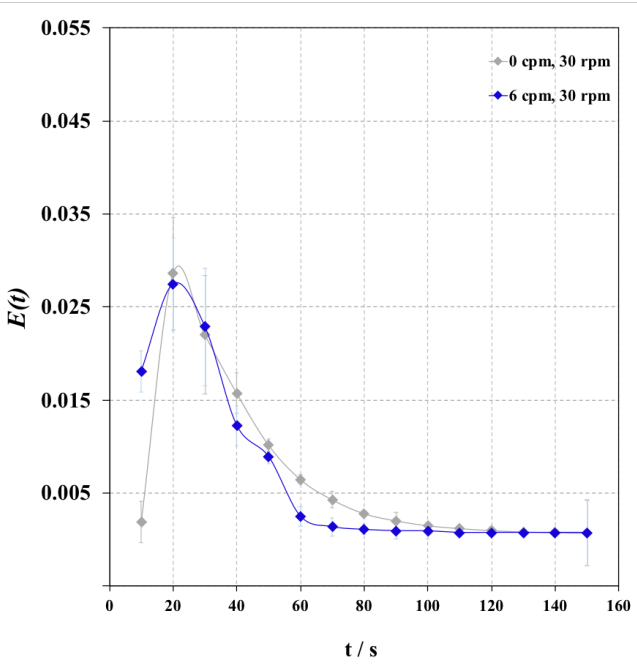

Fig. 4.3 Residence time distribution function, E(t), for peristaltic flow at 30 rpm; (0.9 m/min; flow rate of $2.7x10^{-06}$ m^3/s) - grey chart, and peristaltic flow at 30 rpm and segmentation mixing at 6 cpm (blue chart), for control (water) in dynamic duodenal reactor model, similar to experiments conducted in Chapter 3 of the thesis. Peristaltic flow and segmentation mixing were simultaneously done for each trial. Error bars are standard deviation of three values.

flows (suggestive of recirculation and backmixing). Therefore, it is imaginable that the hydrodynamic circumstances in the living human intestine brings a high degree of turbulence during induced segmenting motility as the typical luminal content in the postprandial state is known to establish low viscosity fluids 0.1 Pa.s (Lentle et al., 2013).

It is evident that fluids passing through the dynamic duodenal model reactor may influence the length of time the dye takes to pass through. Table.4.1.highlight the relationship between flow induced by different motility, and fluid viscous properties. MRT decrease with combined effect of segmentation and peristaltic mixing. However, an increase in viscosity shows a shorter MRT for dyes under the effect of both peristaltic and combined peristaltic and segmentation mixing. Under peristaltic flow (PF), a 20% reduction in MRT was evident. Under combined peristaltic and segmentation flow (PF&S), there was a 42% reduction in MRT, with the combined peristaltic and segmentation flow (P&S) had a profound effect on average time spent in the reactor reducing the MRT more significantly than the increased viscosity. This is primarily due to the ability of the more viscous systems to reduce and slow mass transfer, through reduced convective effect.

Fluid / viscosity (Pa.s)	Gut movement	
	Peristalsis	Peristalsis and segmentation
Water/0.0089 $\pm$ 0.001	42.11$\pm$ 2.1	33.4$\pm$2.1
1% guar gum / 10.0123$\pm$1.877	33.73 $\pm$ 2.0	19.744 $\pm$ 2.1

Table 4.1 Mean residence time (MRT), as a function of viscosity under peristaltic flow and peristaltic and segmentation flow and mixing in the dynamic duodenal model. The two viscosities were selected to cover the range of shear thinning that occurs in the human duodenum (Lentle et al., 2013).

The passage of the riboflavin dye in low viscosity fluids as indicated by their residence time distributions Table.4.1, therefore suggest that, radial dispersion of the dyes were dominant during segmentation, as earlier discussed. Although, both axial and radial flow patterns will contribute to the transport of mass phenomena, radial dispersion by the vortices augment mixing of the luminal material to a greater degree. However, these will be slowed in the presence of high viscosity fluids (10 Pa.s). These hydrodynamic events of flow are important to the digestion and absorption processes promoting material transfer in the gut; modulating the transverse of molecules across the hypothesised unstirred water layer and into the blood stream (Janssen et al., 2007). For example, the slow large peak commencing from the segmenting gut wall movements, in Figure.4.3, in high viscosity fluids, is very suggestive of a predominantly radial flow, from continuous back and forth mixing, which will cause the material to cover larger distances during transit times, which translates into longer mixing times. The peristaltic only flow however, may not have allowed backmixing and thus contribute to shorter mixing times in Figure.4.2.

4.3.2 Axial mass transport in model fluids: effect of segmentation on "enzyme analogue" distribution using PET

The rate of distribution of the radioisotopes is highly influenced by both mixing and the viscosity of the fluid. With the influence of viscosity only becomes important when there is mixing. It is evident from Figure.4.4.II., that, were it not for mixing, distribution of the radioisotope from the site of deposit would still be profusely slow. To track the movement of the radioisotope solution after discharge, a region of interest (ROI) was chosen. The ROI length scale extends 6cm. i.e., 3cm on each side of the point of orifice-duct, (δL=6cm).

Figure.4.4.I. shows the change in concentration of radioisotope (normalised intensity), when segmentation motility was carried out at 11 contractions in one minute i.e. a rate of

change of 0.006m/10s. Blue dots indicate squeezing, red dots correspond to the lack of squeezing. At the end of squeezing (blue data), which is the beginning of relaxation (red data), oscillatory flow is evident. For example, in high viscosity fluids; 1% guar gum; 10 Pa.s, in Figure.4.4.I-A, the initial intensity was 0.6 at the start (0s) of squeezing pulse which fell to 0.5 at the end of the first contraction. During the relaxation pulse (70s); lack of squeezing, the intensity increase to 0.59. Rise and fall in radioconcentration can be described as retrograde or retro-pulsive flow. The more the viscosity is reduced (low viscous fluids: 0.5% guar gum; 0.37 Pa.s), the less discrete these differences become. For example; in Figure.4.4.I-C the initial intensity was 0.39 at the start (0s) of squeezing pulse which fell to 0.31 at the end of the first contraction. During the relaxation pulse (70s); lack of squeezing, the intensity increase to 0.33.

These behaviours may be because of is that the increase in viscosity which results in a decrease in both mass transfer diffusion and diffusion coefficient due to convection, which in turn slows down perceived onward propagation of the tracer. These observations were also highlighted by Wright et al. (2016), who concluded that methylene blue mixing was affected by viscosity and mixing in a duodenum model. Furthermore, Figure.4.4.II(A-C), illustrates that there were little or no changes in concentration, when the same systems undergo self-diffusion as the means of mixing.

Viscosity influences on mixedness in the dynamic duodenal model: CoV's

A common way to characterise the degree of mixing (mixedness) undergone by a system is to determine the intensity of segregation (CoV). The CoV has been used in many industrial application as a means to determine the performances of mixing systems (Levenspiel, 1999; Kukukova et al., 2009), and it can therefore be applied to understand mixing undergone by various constrains in the dynamic duodenal model. The CoV was estimated from equation.4.4, described from the methods section. Different scales of mixing during segmentation were identified for different viscosity of the fluid. Figure.4.5.B., illustrates an overall reduction in the intensity of segregation when segmentation was applied to each system achieving some level of mixedness, but not fully a mixed system. Mixed-ness took a longer time (>100 seconds)to be achieved in the 1% guar gum solution compared less viscous solutions; both 0.5% and 0.7% guar, which had a shorter mixed times, ~50 seconds. There was no significant differences in the CoV's, for 0.5% and 0.7% model fluids. This may be an indication that mesomixing was dominating the mixing process due less resistance in the fluid. For the less

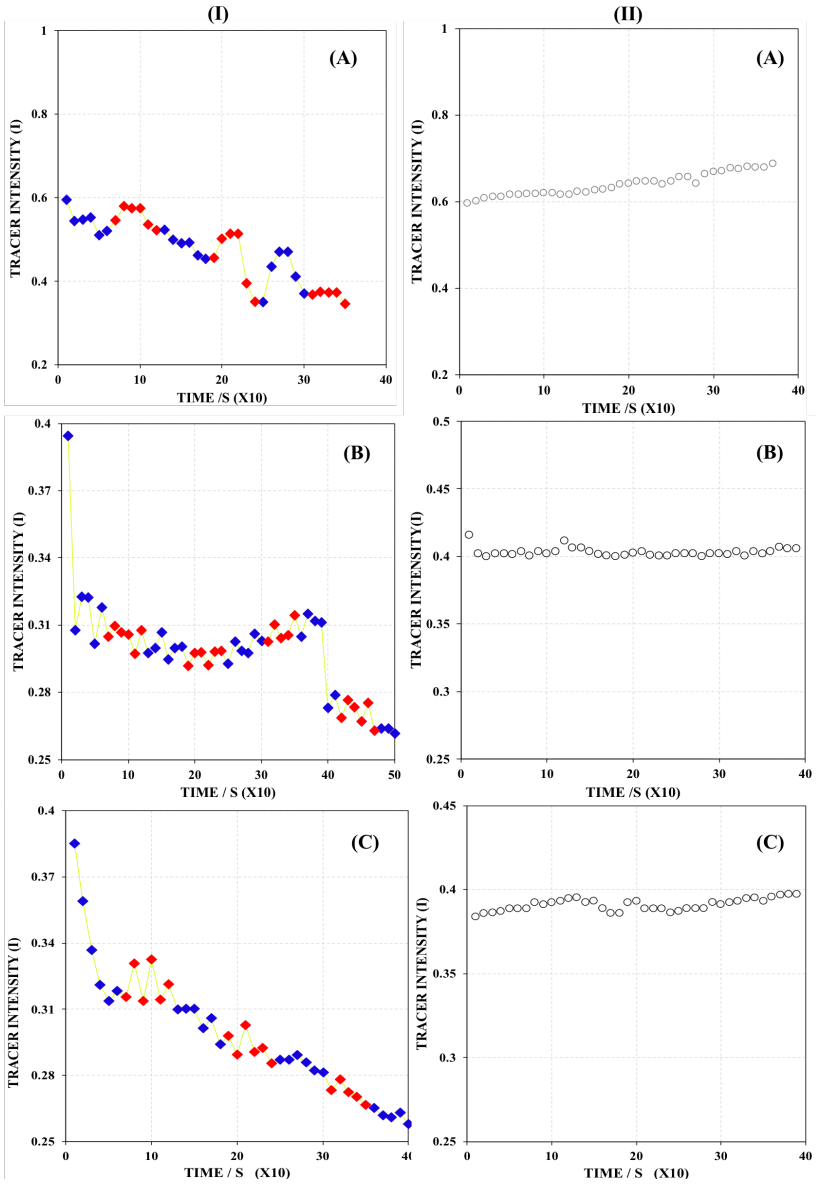

Fig. 4.4 Mass transport brought about by segmentation mixing (I), and self diffusion (II): (A) 1% guar gum (B) 0.75% guar gum (C) 0.5% guar gum. Tracer intensities were measure with length scale of 3 cm to the right (caudal flow) and 3cm to the left (retropulsive flow), at 10 second intervals at the point of secretion i.e., δL = 6cm at δt = 10s. Intensity [I], was normalised (average intensity/total intensity). Red or blue data points indicate segmentation mixing for the duration of 1 minute (11 cpm); ending of the blue is gut wall relaxation and beginning of the red indicate the initiation of gut wall contraction.

viscous systems even without convective forces, mass transport are still achievable to some degree.

Normalised CoV in Fig.4.6., indicated that the coefficient of variation for self-diffusion studies for all model fluids, were higher in un mixed systems than mixed systems for both high and low viscosity fluids. That is, the high viscosity systems were less segregated during diffusion, as clearly expected. Conversely, convective diffusion during segmentation reduces CoV's, thereby improving the mixing. The range between the CoV's for each model fluid, between mixing and non mixing, are widened significantly as the viscosity increases. For 0.5, 0.75 and 1 (%w/v) guar solutions the reductions in coefficient of variation were 3%, 22% and 31% respectively. The small decline for lower viscous solutions are an indication that self-diffusion dominates via molecular permeation due to low resistance to mass transfer in less viscous fluids. Consequently, as the viscosity increases so would be the level of shear that would be required to reduce the high concentration gradients. This is a sophisticated problem and gives very small information about the mixedness of the overall system as it only looks at the rate of removal of radioactive tracer fluids from the region of interest, ROI.

Overall, the CoV was high for low viscous fluids, (macro mixing), and low for high viscous fluids (meso mixing). It is indicative that less viscous model fluids would have longer meso-mixing patterns than macromixing patterns. These less viscous systems will allow longer sustained eddies that does not die out quickly upon the onset of convective segmentation forces promotes more turbulence. While for high viscous fluids, macromixing makes the mixing process longer. Beyond the first 100 seconds mixing is done through micro mixing as it enters the dissolution stage. Similar results are seen in stirred tank reactors by Hartmann et al. (2006) and Hartmann et al. (2006)a, who studied the dissolution of particles.

4.3.3 Propulsion and mixing: oscillatory flow strategies in the model fluids.

Three flow strategies; spreading, segmenting and oscillating, were identified, from 1% guar model fluids, during the application of segmentation on gut wall movements (contraction and relaxation). All intestinal mixing experiments in the dynamic model were done with the feed and exit ends closed, at 11 cpm as shown in Figure.4.1.B. Figure.4.7., shows images that were captured using PET, from the onset of segmentation with the following flow strategies;

(i) Spreading

The flows occurring in this stage is expected to be laminar in nature as they striate and spread. The laminar flows of spreading can be moderately observed from the photo1 in Figure.4.7, during the compression action of the gut wall to form concentric rings. The

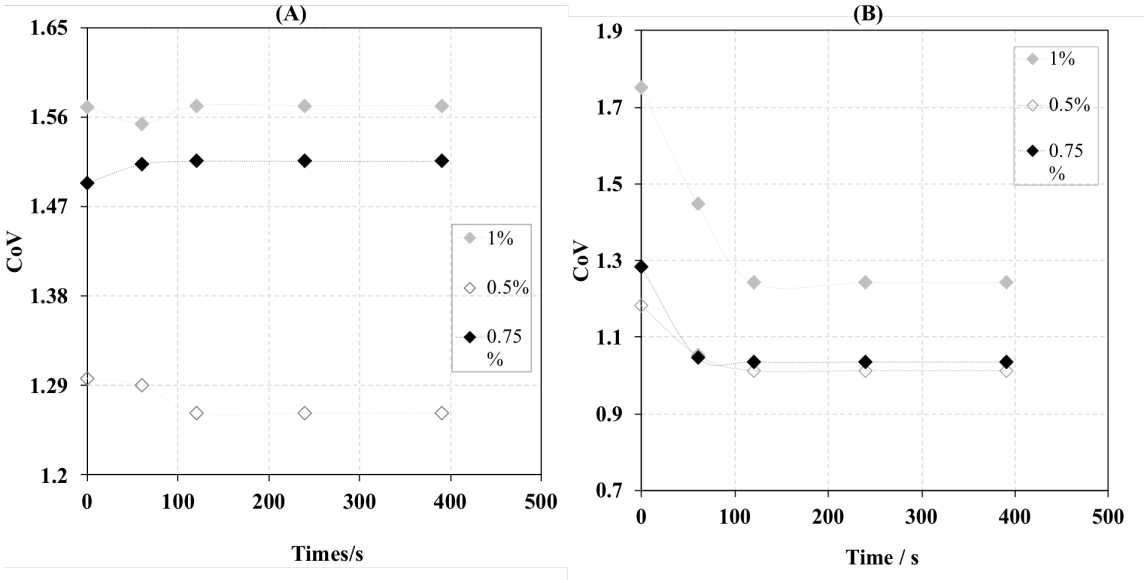

Fig. 4.5 Relationship between intensity of segregation (CoV) and viscosity on mixing and self-diffusion studies: (A) self- diffusion and (B) segmentation

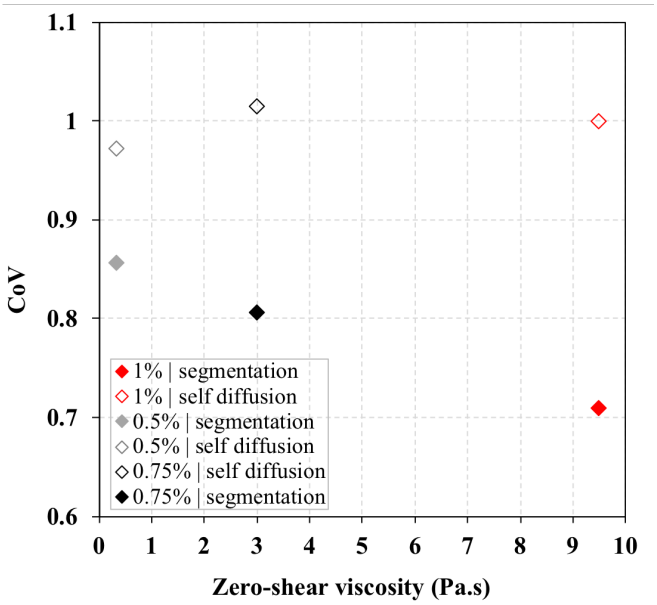

Fig. 4.6 The level of "mixedness" in each system as a function of viscosity and segmentation. The CoV was normalised by dividing the final segregation by the initial segregation; CoVf /CoVi.

compression of the gut wall caused the radioisotope solution to striate along the axial plane. Once the occlusions are completed, concentric rings are formed within 0-10 seconds (photo 2),

similar to in-vivo events (segmenting). This displaced and deformed radio-tracer forms tiny discrete isolated pockets along the length of the intestine, and promote mixing by transferring the tracer solution towards both ends of the luminal cavity. The spreading characteristic may have been possible to observe because of the viscosity of the luminal content (1% guar gum). Highly viscous digesta requires more mixing to remove the concentration gradients to increase segregation (as earlier discussed) of both the enzyme fluids and digesta materials. Therefore, the pattern of spreading may not be readily observed in fluids that displays more Newtonian like behaviour during flow (liquid-liquid systems).

(ii) Oscillation

Flows during this stage was expected to be turbulent, and was evident as described by the oscillatory Reynolds number, previously estimated (>12000) in section 4.1., for 1% guar gum solution under segmenting mixing conditions. It was also anticipated that during the gut wall relaxation sequence, the displaced material will try to regain their position and orientation, following the deformation principle. However, not all the mass (tracer fluid), is returned *in-situ* during this reverse flow for relaxation as seen occurring in images 2 to 4 in Figure.4.7. This form of segregation enhance mixing by reducing the concentration gradient of the radioisotope as confirmed by Figure.4.4.-A in earlier discussion. The the repeated squeezing and lack of squeezing will increase oscillatory flow mixing that will enhance mass transfer axially. Oscillatory flow mixing is known to deliver other clearly defined process enhancements such as improved heat transfer and narrow residence time distribution as discussed earlier in section.4.1. results (Lee et al., 2001).

4.3.4 Mixing process in real foods

The mixing strategies and overall mixing profile is highly influenced by the bread digesta type. The selected bread types: white and wholemeal, with essentially different structures and physical properties went through the two stage digestion process from oral (1-3 minutes) to gastric (2 hours), similarly to the methods used to prepare bread digest in chapter 3, section 3.3.1 and 3.3.2. After 2 hours of gastric digestion, the resulting gastric bread chyme (paste-like, jelly fluid with obvious suspended particles- data not shown) at 37^0C, were added to the lumen of the dynamic duodenal model to test the effect of intestinal motility on mixing (concentration and rate). All intestinal mixing experiments in the model were done with the feed and exit ends closed, at 11 cpm, with 520ml of luminal content (section.4.and Fig.4.1).

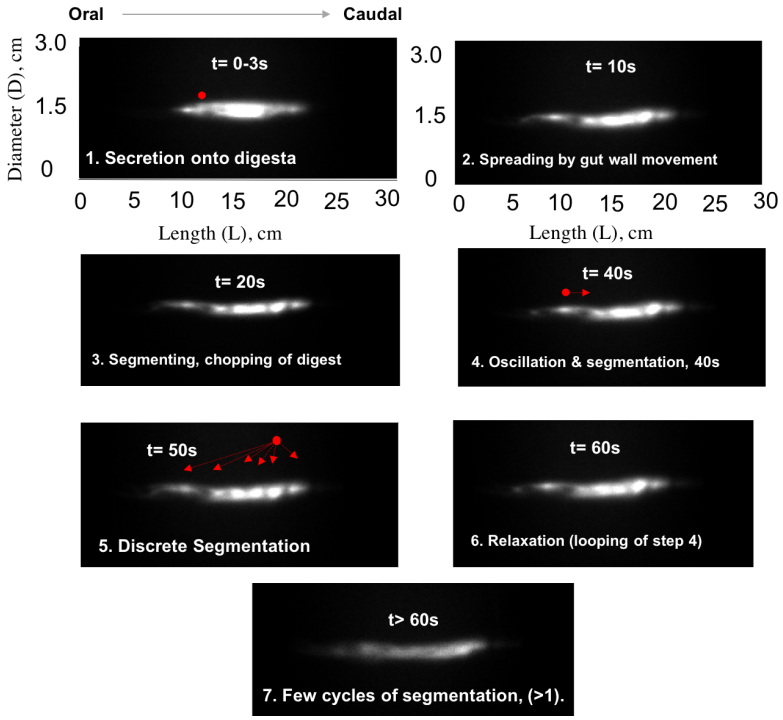

Fig. 4.7 Flow profiles generated in dynamic duodenal model during one cycle of segmentation (11cpm) in high viscosity fluid system (1% guar gum; 10 Pa.s). PET images/frames were captured over 1 minute period of mixing. The first photo shows the time of deposition of the radioactive tracer (red dot). The length of the tube is 35 cm in length with a diameter of 3 cm.

The PET trajectories and resulting flow patterns of the F-18 radioisotope in the 'x'and 'y'coordinates as a function of time (2D), for each bread type, were recorded in Fig.4.8. In the first 100s, the radioisotope solutions was less dispersed (δL,10cm) in white bread compared to whole meal bread, (δL,15cm). This suggests that enzymes would spread over larger distances in whole meal bread digestion than white breads under the same mixing constrains in the dynamic duodenal model. This can be explained by the relative cohesive forces holding the different breads together. It is expected that white bread would have a higher cohesive force holding the particles together and therefore display a more viscous characteristic that wholemeal bread.

Shorter time frames (10s) from the PET images were extracted as shown in Fig.4.9, to reveal the relative axial velocity profiles for each bread system. Axial flow, in both aboral and back flow were used to estimate the distances covered over 11 contractions per minute, and illustrated in Fig.4.10. The relative linear velocities were then rudimentary modelled from equation.4.5. Where, V_{ax} is the axial velocity, and δx is the change is distance from time zero to time final (60s).

$$V_{ax} = \frac{\delta x}{\delta t} \tag{4.5}$$

Wholemeal bread allowed a faster transport of radioisotope solution through its content in both directions compared to white breads over 1minute. I.e. The axial velocity for wmb, was estimated to be of $2.42\text{x}10^{-3}$ m/s and for wb, it was $2.0\text{x}10^{-3}$m/s, both in caudal flow. While, for the backflow, it was $1.0\text{x}10^{-3}$ and $8.33\ \text{x}10^{-4}$ m/s for wmb and wb respectively. The faster mixing in wmb, may be a result of the differences in food structures, and therefore chyme properties. One explanation for this may a result of the particulate system that exist in both types of digesta, in the small intestine. Evidence has suggested that, phase separation can occur, during mixing and transit, where the solid particulates and liquids may move relative to each other (Lentle et al., 2011). This makes the physical interaction between these two phases complex when the two bread are compared.

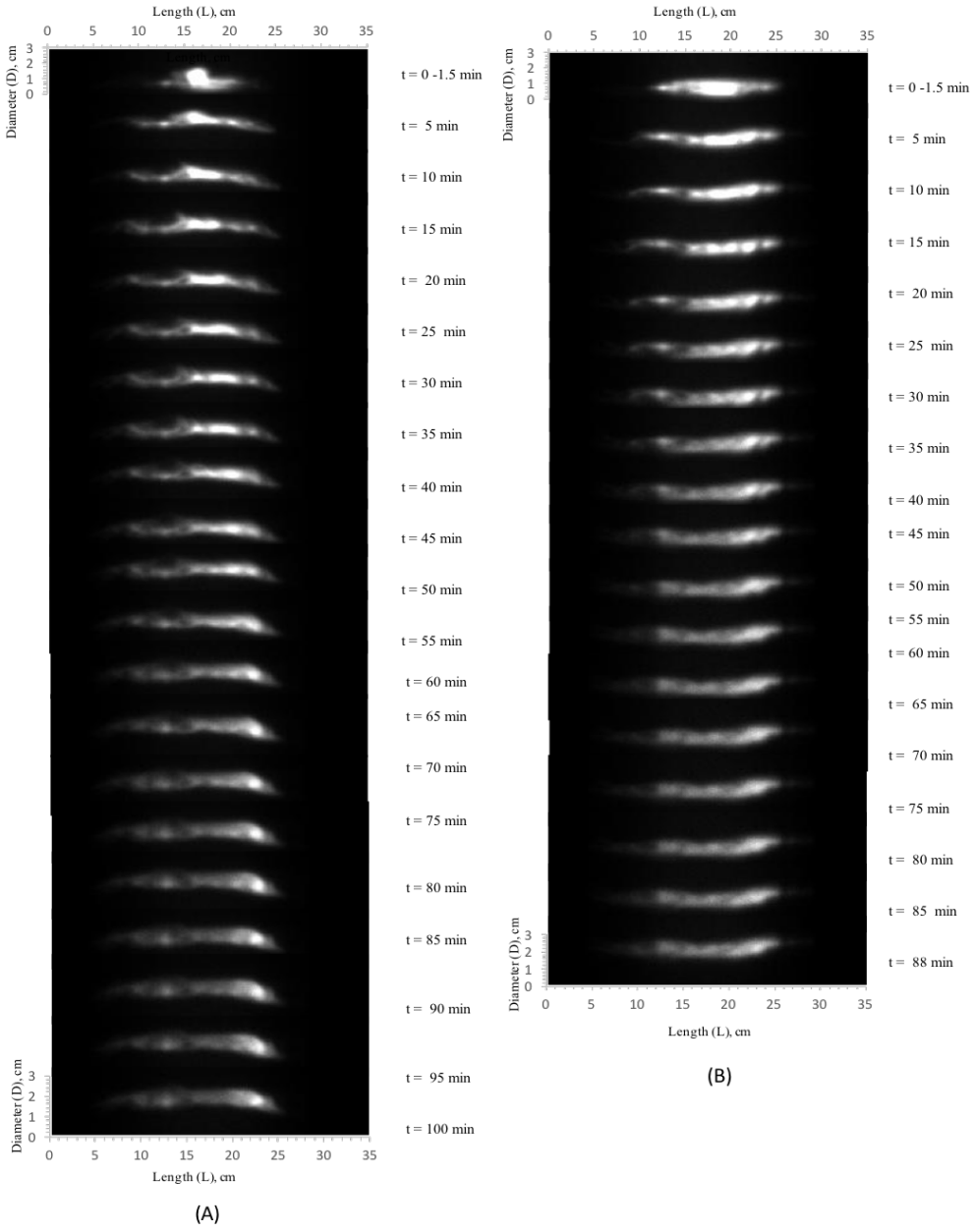

Fig. 4.8 Flow profiles generated from radioisotope particles (F-18), in motion at 5 minute intervals, during segmentation (11 cpm), for breads that went through 2 stage digestion (oral and gastric) (A) white bread and (B) whole meal bread. The length of the tube is 35 cm in length with a diameter of 3 cm.

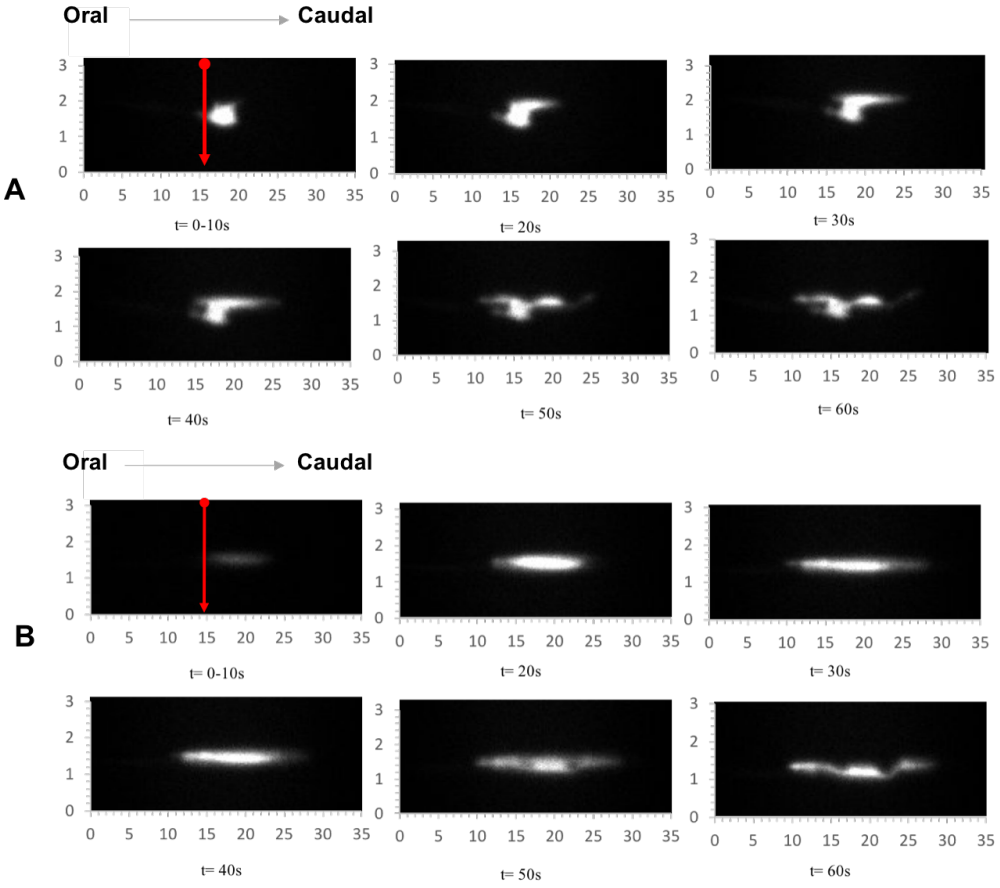

Fig. 4.9 Flow profiles generated from radioisotope particles (F-18), in motion at extracted 10 seconds intervals during intestinal mixing (segmentation at 11 cpm) for breads that went through 2 stage digestion (oral and gastric); (A) white bread and (B) whole meal bread. The length of the tube is 35 cm in length with a diameter of 3 cm

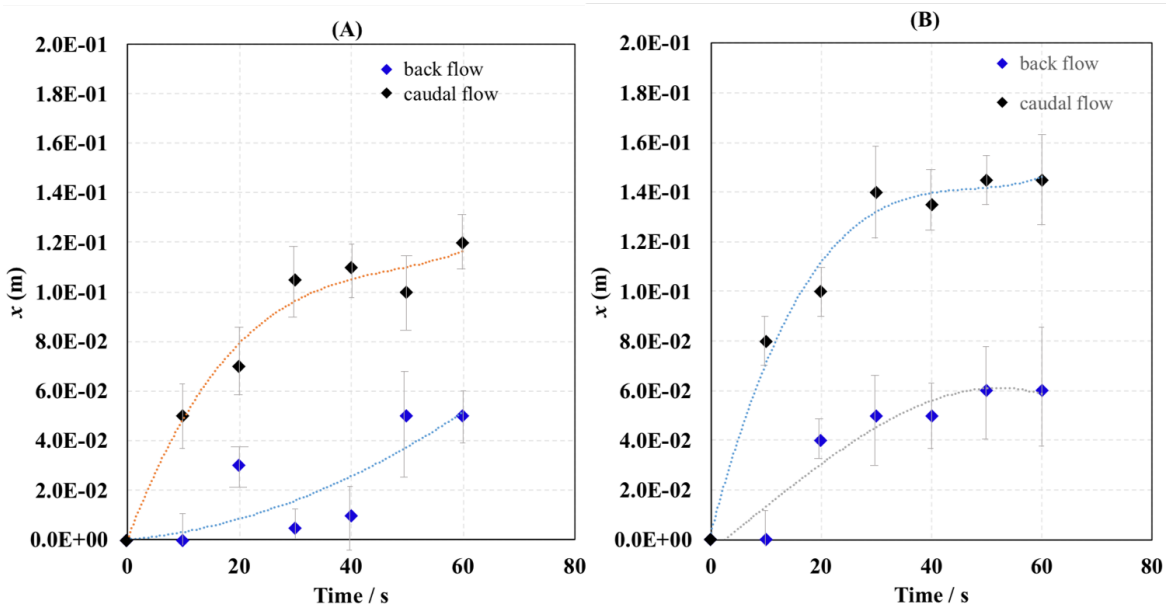

Fig. 4.10 Characteristic axial radioisotope distances permitted by bread type (essentially different structure): (A) white breads and (B) whole meal breads, as a result of segmentation intestinal mixing. Blue data points are flow distances that occurs backwards from the point of secretion and red data point are forward flow from the same point of application. Retropulsive flow (eddies) are seen as rise and fall along the time stamp. The travelled distances were estimated using Fig.4.9, where the backflow distances were measured to the left of the point of injection (redline) and caudal flow distances were to the right of the point of injection, indicating the resistance and progressive flow through each system.

4.4 Conclusion

By manipulating intestinal motility, mixing profiles were identified by using PET. PET was a good choice to visualise the fluid dynamics, but PEPT may also be applied in future studies, to track eddies more precisely, to understand more of the speeds and formation of vortices during turbulent and laminar mixing. Mixing is faster achieved in wholemeal breads, mainly because of the type of particle system (less resistance to fluid flow. For example, finely ground wheat bran in wholemeal bread is known to disrupt the gluten network that is found throughout the bread matrix, unlike white wheat bread that would have its gluten structure more or less better intact (Hemdane et al., 2015). Similarly, breads prepared to have different densities gave different bolus apparent viscosities when chewed (Bleis et al., 2016). The strategies to achieve the degree of 'mixedness', are primarily governed by the motility factor, with viscosity only becoming important only during mixing, as transport of mass is extremely slow regardless of the level of viscousness. The mean residence times indicated that the combined effect of peristalsis and segmentation, decrease the transit speeds of materials (dye), compared to peristaltic mechanism alone, and importantly, shorter transit times for dyes in the more viscous digesta. In the case using PET to characterise some of the mixing, spreading is dominant in high viscous mediums, during the initial stages of segmentation. It is evident that mixing brought about by segmentation in a closed luminal system has a profound effect on material transportation in the dynamic model. The coefficient of variation (cov) is less for more mixed systems and indicates that segmentation enhances mixing, by increasing segregation. The coefficient of variation also indicates that for less viscous or more Newtonian-like mediums, segmentation is less important for mixing as mixedness is not increased significantly. However, since the cov was done by using a defined region, some details may have been lost regarding the entire dynamic model. Therefore, a full description of the mixing can be done in the future. Overall, the application of these two techniques to understand mixing has identified ways in which the dynamic duodenal system can be manipulated to promote mixing in the case of enhancing or retarding the digestion of starchy foods.

Supplemental materials

The following are links for time-lapse of the PET videos:

1% Guar gum 11cpm, https://vimeo.com/261711010.
1% Guar gum 0 cpm, https://vimeo.com/261711007.
0.75% Guar gum 11cpm, https://vimeo.com/261711004.
0.75 % Guar gum 0 cpm, https://vimeo.com/261711003.
0.5% Guar gum, 11 cpm, https://vimeo.com/261710998.
0.5% Guar gum, 0 cpm, https://vimeo.com/261710995.
Wholemeal bread,11 cpm 500 ml (52 x100s), https://vimeo.com/267384930.
White bread, 11cpm 500ml (60 x100s), https://vimeo.com/267384743

Chapter 5

A unique stirred tank reactor in vitro model for food applications

In this Chapter, in vitro digestion were performed on breads which are essentially the same, but with different type and levels of dietary fibres (soluble and insoluble). Digestion of high and low viscosity breads were compared at the end of the Chapter. Also, an attempt was made to compare the digestion between the dynamic duodenal model and the stirred tank reactor in-vitro food model, of the same breads (high and low viscosities). The main experimental difference between these two models is the element of mixing. The design of the stirred tank model was done by myself (ad hoc - to describe mass transfer), and bran fibre breads were prepare and provided by Fred Gates from Campden BRI - the centre for bread making in the UK.

Abstract

The amount of force brought on to food structure during digestion is one of the most important factors that determine the rate and extent of digestibility and subsequent nutrient uptake rates. *In-vitro* techniques have vastly used simplistic static stirred tank reactor models for evaluating digestibility by means of measuring bioaccessibility. But, not being able to quantify the mixing forces in those models makes the link between external forces on the digestibility and the uptake processes on special food materials poorly understood. Furthermore, the amount of stirring and force, on the presence of different dietary fibres, can give insights into the details controlling the micromixing for the reducing effects for blood glucose levels observed at the molecular scale in vivo. We have developed a new digestive system, a rather unique modified stirred static reactor vessel, enabling the description of mass transfer. Following this approach, we have performed enzymatic digestion of starch in speciality bread systems, containing soluble guar and insoluble wheat bran dietary fibres, when the same stirring rates from non-bioactive maltose systems of guar and xanthan soluble dietary fibres were reproduced. The increase in wheat bran content 2 fold, had a negative effect in attenuating sugars during bread digestion, unlike the bread containing guar, which reduces the overall mass transfer rates by 13.3%. Overall, the new model has illustrated that the fate of starch digestion and absorption in bread, in the gastrointestinal tract is not only dependent on the amount of mixing as described by the Power number but also reliant on the amount and how different fibres are distributed throughout the food structure.

5.1 Introduction

The ongoing health awareness has influenced the design of novel foods, by incorporating new and resourceful uses of functional integrants such as dietary fibres. Recently, trendy foods such as bread, are predominately being used as carries to deliver these fibres into various diets (Wyrwisz, 2015; Collar et al., 2006; Houghton et al., 2015). Dietary fiber is made up of non-digestible carbohydrates and the components such as plant cell wall

polysaccharides (lignin) and can be extracted and classified in two broad categories; (1) soluble fibres such as β-glucans, and isolated gums (biopolymers) and (2) insoluble fibres, for example, soy hulls and wheat bran (Marlett 2001). Even though much digestion studies have been done on soluble fibres, little attention has been paid on particulate fibres especially when the cell walls are not completely altered (Singh et al., 2014; Berg et al., 2012), such as wheat bran (Grundy et al., 2016). The health effect of dietary fibre in the human diets are well documented, such as; actively encouraging a healthier bowel function, decreasing cholesterol and manage blood glucose concentrations (Angioloni et al., 2011; Edwards et al., 2015). Depending on the source, dietary fibres can display different physical and chemical properties, triggering a range of different physiological responses, when consumed (Slavin, 2005; Munoz, 1982; Dreher, 2017; Leeds, 1982; Kritchevsky, 1982). In particular, when in contact with liquids, they thicken, with the amount of thickening varying due to the chemical makeup and concentration of the available fibre (Gidley, 2013). Similarly, the viscous effect, is ?played-out? during food digestion, and have been closely associated with regulation of post-prandial glycemic index, delayed gastric emptying and longer transit times along the small intestine (Grundy 2016).

The mechanisms behind the dissemination of nutrients from foods containing varying dietary fibres during digestion have led to different health benefits at large, but are still left to be elucidated (I. Bjrck et al., 1994; Grundy et al., 2016; Kendall et al., 2010). We also acknowledge that a single mechanism will be insufficient to decipher in details, how these fibres manipulate complex food digestion and other functions of the digestive tract, as well as the linkages between the processes and postprandial responses (Lairon et al., 2007). As a result, a lot of focus has been placed on understanding the digestive processes by using a wide array of in-vitro techniques, with higher emphasis been placed on dynamic in-vitro model systems in recent times (Hur et al., 2011; Dupont, 2016; Savoie, 1994; Guerra et al., 2012a). This approach allows a more temporal study of digestion, incorporating biomechanical aspects relevant to match the physiological features and biochemical environments that are important to simulate near real digestion and absorption at various stages of food intake and transport along the gut tract. The biomechanical features in these dynamic models enable clarity on some mechanism during intestinal digestion, such as effect of orientation and geometry on transit time in duodenum (Wright et al., 2016), and the effect of digesta viscosity on mass transfer rates during digestibility and absorption (Jaime-Fonseca et al., 2015; Gouseti et al., 2014). However, one of the main disadvantages to researchers investigating the relationship between food and health is the easy access to these complex invitro models, that are most times developed for interlaboratory studies and mostly restricted to certain

organisations (Guerra et al., 2012). These models are also costly and time consuming to use. Consequently, there should be more focus on invitro techniques and ways that can quickly evaluate digestibility by simplified interpretation of bioaccessibility and bioavailability, in early and preliminary studies. This approach may be useful, especially for studies that may require observation for positive or negative tests (yes and no?s). There have been attempts to harmonised this approach Minekus et al. (2014), by route of static modelling of digestion, but almost all of these models do not allow for the forces during mixing, to be measured by design.

Gut motility is crucial in the entire digestive processes, from mixing of food components with intestinal fluids and enzymes to the transportation of food along the gut cavity, and transfer nutrients across the epithelium barrier into the bloodstream (Hall et al., 2011). The role of mixing on digestion, is usually studied in the form of, the effect of segmentation and peristaltic frequencies (Tharakan et al., 2010a; Gouseti et al., 2014; Wright et al., 2016) and the effect of stirring rates (Dhital et al., 2014; Jaime-Fonseca et al., 2015), and have been well documented. However, not being able to directly quantify the forces changes in the flow streams limits this approach and is a major main drawback to understand potential small intestine digestibility in relation to shear forces. The simulation could expand to include other useful parameters such as the amount of energy or power that is required or placed in the system to perform the overall digestive operation. An understanding of the energy requirement may be useful when comparing different food materials under the same mixing effect.

Herein, we report a newly developed modified stirred tank reactor to perform food digestion. The design of the model integrates the advantages of a simple stirred tank and the sophistication of incorporating a membrane-based interface and measured shear forces. Similarly, Chivers et al. (1994) and Penry et al. (1987) has described the human gut to have analogous features similar to chemical reactors. In particular, the stomach can be modelled as a continuous stirred tank reactor (CSTR), the small intestine as a plug flow reactor (PFR). In the same way, Jaime-Fonseca et al. (2015) have recently use stirred tank reactor to study digestion of starches, during duodenal digestions. This stirred tank reactor model however, does not include a membrane which limits its application to; (1) understand the effect of forces on mixing and on mass transfer across a membrane and (2) the system does not allow products of digestion to be moved to a next compartment, such as simulated blood plasma for uptake. As a result, the substrates, enzymes and products are active in the same medium which can alter enzyme activity resulting in inhibition of enzymes during digestion, leading to poor simulations. To demonstrate the capabilities of the newly developed tool, model

fluids were studied and compared, before subsequent digestion of complex food systems. The main intent of the work was to demonstrate that a stirred tank reactor (STR?s) used as an in-vitro tool, can be used to understand the biological and physical portents arising during novel bread digestion and absorption.

5.2 Design and modification of a stirred tank reactor to perform digestion.

The stirred tank reactor model with a membrane (str)

This *in-vitro* model was designed as a stirred tank chemical reactor (str), intended to simulate mixing, absorption and digestion Figure 5.1. describes the geometry and features of the str. This model mimics induced mixing in a luminal cavity, and absorption from a recipient side. The luminal cavity is capable to hold a maximum volume of 0.3L, having a semipermeable membrane to separate the luminal contents from the recipient side. Addition of digesta was done overhead, and a liquid fill height of 47 mm is generally observed for fluids whilst performing digestion and absorption and the surface area of absorption is ~0.02 m^2. To induce shear mixing, a radial flow paddle - Ruston turbine, 50 mm diameter, with 3 blades was used when performing digestion. The volume of the recipient side holds a maximum of 0.35L (water receiving fluid) and the recipient fluid is well mixed by a magnetic flea, that rotates at ~120rpm, to homogenise the nutrient absorbed in the solution. The temperature of the system was maintained by a jacketed recirculating water, kept at 37^0C from a water bath Fig.5.2. The sampling of fluids from the recipient volume was done overhead. The coordinate ratios for the system is described as: D_a/D_t (0.67), H/D_t (0.63), E/D_a (0.3), W/D_a (0.5), and L/D_a (0.5).

The model goes under the following assumptions:

1. The system will be well mixed
2. The system does not operate under steady state
3. The resistance to mass transfer from the membrane interface to the recipient fluid is negligible, as the magnetic flea rotates at 120 rpm.

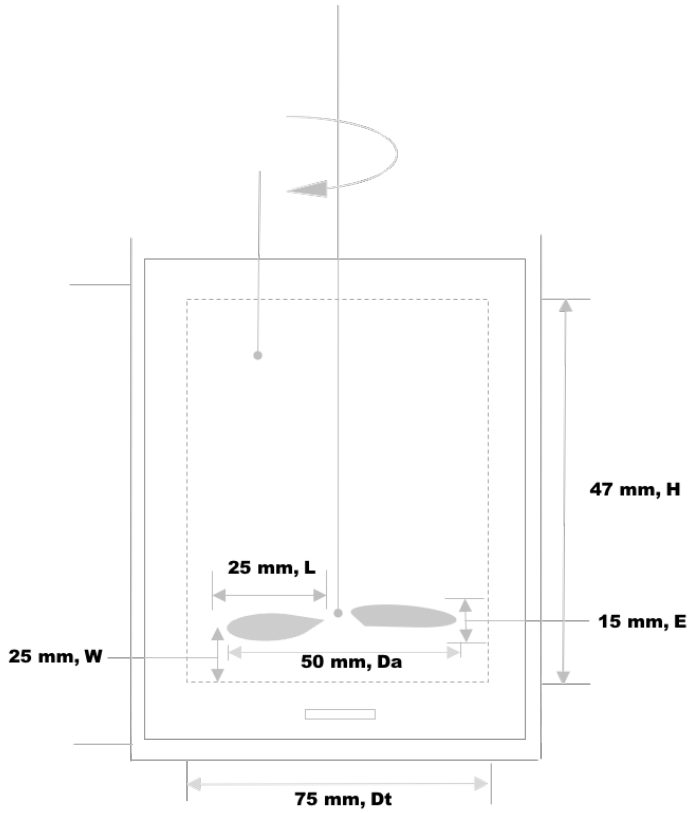

Fig. 5.1 Cordinate system (not drawn to scale) of the stirred tank reactor used for digestion: modified with a membrane for absorption during digestion. Where, Dt-effective tank diameter, Da-impeller diameter, H-effective fluid height, E-impeller height from tank bottom, W-impeller thickness, and L-blade length.

5.3 Materials and method

The digestion techniques were similarly reproduced from the protocol and methods developed and used in Chapter 3, Section 3.3 of the thesis (experimental outline). Any changes made to the procedures are otherwise stated, as follows;

5.3.1 Preparation of materials

The materials used in these studies were sourced from Sigma–Aldrich Chemical Company UK unless otherwise stated. Xanthin gum, Guar gum (G4129-500G), maltose, enzymes and all other materials for the simulated digestive fluids, and other chemicals. The simulated digestive fluids (sdf), including gastric solutions (sgf), were prepared using a protocol in previously published papers (Mandalari et al., 2009a; Moreno et al., 2005a), unless otherwise

Model fluid	concentration (% w/v)	Zero-shear Viscosity (Pa.s)
guar, gg	0.1	0.002 ± 0.004
	1.0	10.03 ± 1.877
xanthan, xg	0.1	2.41 ± 0.084
	1.00	56.01 ± 0.212

Table 5.1 Zero shear viscosities for xanthan gum and guar gum model fluids

stated, and the enzymes were added on the day of digestion, dissolved at a room temperature and incubated at 37^0C. The ssf, contains 0.15M NaCl and the pH adjusted to 6.9 using 3-5 drops of 1.0 M HCl, if required (*these small drops were considered to be negligible to the overall dilution*), α-amylase from hog pancreas (50 U/mg) and 6μg/ml lysozyme solution. The sgf contains 0.15 M NaCl; 3mM $CaCl_2.2H_2O$; 0.9mM NaH_2PO_4; 16mM KCl in 150ml, 0.1 M HCl, pepsin from porcine gastric mucosa - lyophilized powder, 3,200-4,500 units/mg Sigma (P6887). The simulated intestinal fluids (sif), was made up of the hepatic mixed solution (hms), pancreatic mix solution (pms) and modified Krebs Ringer buffer (krb). The hms, contains 4 mM Cholesterol; 12.5 mM Sodium taurocholate (hydrate); 12.5 mM Sodium glycodeoxycholate; 146 mM NaCl; 2.6 mM $CaCl_2.2H_2O$; 4.8 mM KCl. The pms contains 125 mM NaCl; 0.6 mM $CaCl_2.2H_2O$; 0.3 mM $MgCl_2.6H_2O$; 4.1 μM $ZnSO_4.7H_2O$ solution, and the mkrb, contains 0.7 mM $Na_2HP0_4.12H_2O$; 4.56 mM KCl; 0.49 mM $MgCl_2.6H_2O$; 1.5 mM $NaH_2P0_4.2H_2O$; 80 mM $NaHCO_3$ solution; 54.5 mM NaCl.

Preparation and characterisation of biopolymer

Aqueous xanthan and guar gums-maltose model fluids containing; 0.1, and 1 (%w/v) guar and xanthan, and maltose (1% w/v: 29 .2 mM) were prepared. Gum guar was added to the water, with simultaneous stirring, and the temperature raised and maintained at 80^0C for 10 minutes until fully mixed and allowed to cool at room temperature, then left overnight for complete hydration, before each use. This was reproduced for the xanthan gum solutions. Shear experiments were carried out on the model fluids using a Bohlin Instruments rheometer (KTB 30, Crawley, UK) equipped with a cone-plate geometry 40/1 with a gap size of 1mm. For each test, 5 ml of freshly prepared solution was allowed to equilibrated at room temperature (24^0C) prior to experiments. The viscosities were then measured as a function of shear rates which logarithmically increased from 0.1 to 103 s^{-1}. This was repeated in at leasts duplicates for each concentration of model solution and tabulated in Table 5.1.

Preparation of bread

Standard control white bread and uniquely made, 10% and 20% bran bread, were provided by Campden BRI, United Kingdom. The nutrient profile of the bread was as follows 100 grams: carbohydrate, 44.1g and protein 7.1g for white bread, and carbohydrate, 23g and protein 5 g for both bran bread. Guar-containing white bread was prepared in the form of dough's using the 125g automatic KENWOOD rapid bake. Gum guar was incorporated into the recipe; 245g water, 13.8g vegetable oil, 350g unbleached white bread flour, 6.5g skimmed milk powder, 5.5g salt, 7.8g sugar, and 3.5g easy blend dried yeast, at a 10% w/w, replacement level for wheat flour. The method was done comparable to Brennan et al. (1996). The recipe was added to the dough maker and left to be baked for 3 hrs. The final carbohydrate and protein contents were 44.5g and 6g respectively per 100 g of bread. For each digestion,~32 grams of carbohydrate was used.

5.3.2 Performing digestion and absorption in the STR

For all the studies the simulated intestinal fluids (sIf), for oral and gastric digestion were performed on breads using well established static models.

Model fluids in STR

The model fluid prepared were fed into the lumen directly by overhead filling. Trials that required flow were operated with the propeller immersed in the fluids. Trials for diffusive only studies did not require the impeller in the fluids.

Oral digestion

37.5 g of white bread were diced into 4cm3 cubes (roughly the size of bite). 12.25ml ssf warmed at 37^0C, containing enzymes; α amylase, 0.009g and lysozyme 7.25 μl and water 25 ml, was poured onto the bread and placed in Hammed mincer for 1-3 minutes, to mimic oral processing time, and chewing. Once the bread samples and required salivary solutions were added incomplete, the timer was started. The chew (bolus) was collected and immediately sent to the gastric digestion stage.

Gastric digestion

The bread bolus (74.5 ml) coming from the oral phase was placed into a 300 ml, conical flask (stirred tank), and 33 ml sgf, containing 0.047 g pepsin, was poured onto it (pepsin to

protein ratio of ~ 1:69 was applied), the beginning of the gastric phase. The gastric chyme was placed into into a orbital incubator (Stuart orbital incubator SI500) at 37^{o}C, set at 170 rpm and pH 2 for 2 hours.

Duodenal digestion in modified str

At the end of the gastric phase, the digesta (~107.5 ml) was released and added to the stirred tank reactor overhead. From the secretory port (Figure.5.2), pancreatic mix solution (28.5ml), containing room temperature dissolved trypsin 0.063g from porcine pancreas-lyophilized powder, (~780 BAEE units/mg) from Applichem (A4148), α-Chymotrypsin 0.004g from bovine pancreas-lyophilized powder, 350U/mg (11.9 BTEE U/mg) andα-amylase 0.5035 g were added, along with HMS (10ml) and KRB(40ml). Samples were taken as necessary, to obtain the relative densities, and reported in Table.2.2. The mixing was initiated from the impeller set at, 30, 200 and 400 rpm. Digestions were allowed to run for 2 hours. Prior to intestinal digestion, the model luminal membrane was conditioned with 25 ml krb. The oral through to duodenal digestion were repeated in at least duplicates and Figure 5.2. shows the experimental setup and components for each digestion run. In total, each digestion ran for ~5 hours (oral- gastric).

5.3.3 Reducing Sugar Determination

Reducing sugars transported across the membrane was measured at 5-minute intervals using the (DNS) 3,5-dinitrosalicylic acid reagent assay test for reducing groups of sugar molecules (Miller 1959). The resulting colour change after heating the mixed solution of equal volumes (1ml) of DNS reagent (0.1% dinitrosalicylic acid; 30% w/w potassium sodium tartrate; 0.4M NaOH) and sugar sample at 80 0C for five minutes was read (the absorbance), using a UV visible spectrophotometer Libra S12 (Biochrom, Cambridge, UK) at 540 nm. Standard curves were constructed with glucose/maltose standard concentrations ranging from 0.0 -10 mM to determine the reducing sugar concentration from all the absorbance from tested samples drawn. The amount of glucose (from model fluids) and maltose (from bread digestion), in the recipient fluid, is plotted against time, as well as the dependencies of overall mass transfer coefficient on Reynolds number, type of mixing condition and viscosity of the luminal medium.

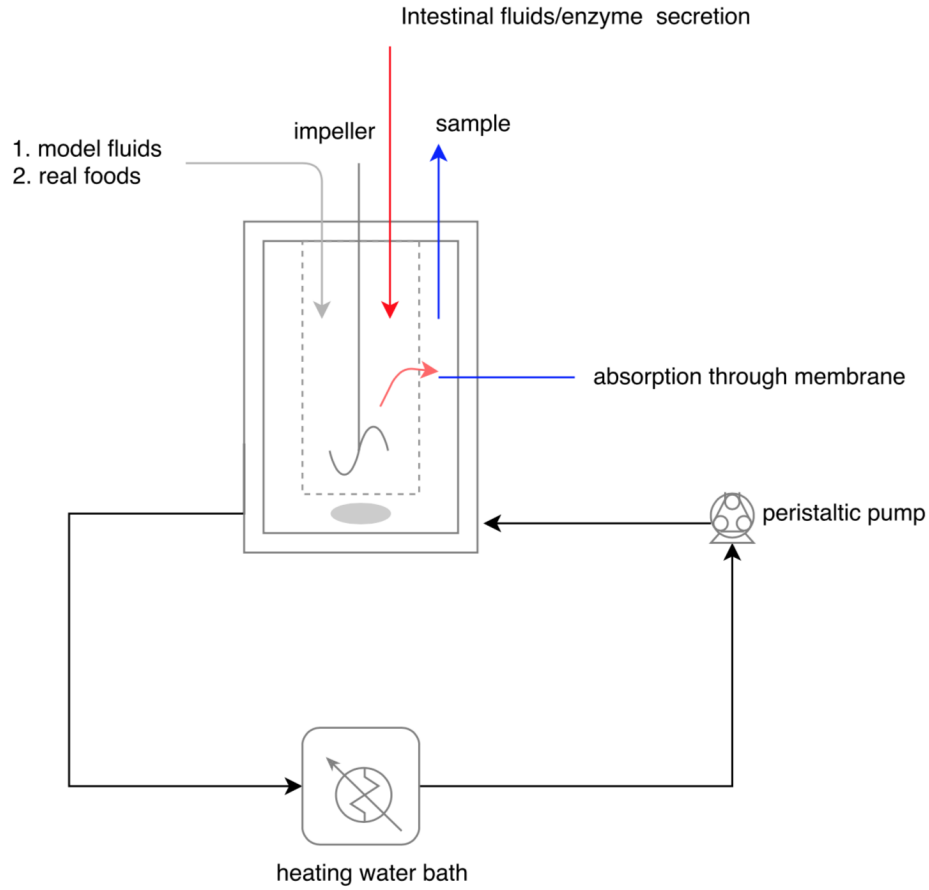

Fig. 5.2 Schema setup of digestion in the stirred tank reactor modified with membrane to track absorption.

5.3.4 Analysis of mass transfer coefficients and operational fluid dynamics

The coefficient of mass transfer was estimated as described by Tharakan et al., (2010), used in Chapter 3, section.3.3.4, of the thesis also. Briefly, the flux, N_i (mmol/m^{2}s), was derived from the diffusion rate plots and this value was divided by the concentration difference, delta C (mmol/m^3) across the membrane to predict the mass transfer coefficient, K (m/s) according to equation.5.1.;

$$N_i = K\delta C \tag{5.1}$$

As part of a stirred tank reactor system, the power draw from the impeller (power transferred to the fluid), and the tip speed are two important economic factors when selecting

the ideal mixer. The power transferred to the liquid is the product of the impeller speed, and torque and can be estimated from equation.5.2.; Where, N is the impeller speed (s^{-1}), and $M\tau$ the torque (N.m).

$$P = 2\pi NM\tau \tag{5.2}$$

Similarly, the power number (Po), which is dimensionless number, describing the ratio of resistance forces to inertia forces, can be estimated from equation.5.3. and the tip speed from equation.5.4. ; Where P, is the power draw from the impeller (W), ρ, is the fluid density (kg/m^3), D is the impeller diameter (m), and U_t is the tip speed (m/s).

$$P_o = \frac{2\pi NM\tau}{\rho N^3 D^5} \tag{5.3}$$

$$U_{tip} = \frac{\pi DN}{60} \tag{5.4}$$

To characterise the flow kinetics of each system, the Reynolds number gives a good indication to predict the flow patterns under each condition. It was estimated according to equation.5.5.; Where, N is the impeller speed (m/s), D is the diameter of the impeller (m), ρ, is the density of the fluid (kg/m^3) and μ, is the viscosity of the fluid (Pa.s).

$$R_e = \frac{D^2 N\rho}{\mu} \tag{5.5}$$

5.4 Results and discussion

5.4.1 Viscosity of soluble fibre solutions

The shear viscosity, obtained from Table.5.1., shows that, at the same concentration for both solutions, they are dependent on shear rate, and can be considered to be shear-thinning fluids. However, guar solutions (gg) were less resistance to shear (0.002 and 10.03 Pa.s, for 0.1% and 1 % w/v respectively), regardless of the concentrations compared to xanthan gum (xg) solutions (2.41 and 56.01 Pa.s for 0.1 and 1% xanthan gum respectively), and are thus less viscous. These results were also inline with the results section of Chapter 3 of the thesis, section.3.4.1, which indicated that the model fluids of guar gum becomes shear thinning as

the shear rate increases. Similar phenomena, of thinning behaviour for food digesta has been observed in vivo, that occurs in the small intestine (de Loubens et al., 2013).

5.4.2 Effect of shear mixing on maltose diffusion during mass transport: Non reactive systems (model fluids)

The lag phase of absorption is dependent on the level of fibres in the fluid as observed in Figure 5.3 .(A)., Xanthan solutions tend to display longer lag phases than guar solutions for similar concentrations, regardless of the mixing conditions. Additionally, the rate of maltose absorption depend on the mixing as seen in Figure 5.3. For example, under mixing conditions, an increase of 17.5 % for total maltose absorbed form the 0.1% xg solution over 2 hours at 30 rpm was observed. Similarly, maltose absorbed from the 0.1% xg solution was raised to 66.5% under the same conditions of mixing speed and time. The rate of maltose absorption is also dependent on the viscosity of the solutions. For example, there was a reduction in maltose absorbtion from 39% for the gg and 52% for xg solutions when the concentration increases form 0.1 to 1% of the fibres. These phenomena are similarly observed when the overall mass transport coefficient (omtc), predicted by equation.5.1., was plotted as a function of Reynolds number as described by equation.5.5., for both diffusive and convect maltose transport, as Illustrated in Figure 5.4. Where, the estimated omtc increases, when the mixing speed of the impeller increases, as well as the decreasing concentration of xg fibre, i.e. form $1.85X10^{-7}$m/s to $2.69X10^{-7}$m/s for 0.1% xg and from $1.21X10^{-7}$m/s to $1.73X10^{-7}$m/s for 1% xg, (Figure 5.4.(B)). For example, there was a 35 and 36 % fall in the omtc under no mixing and mixing (30 rpm) for xg at 0.1% and 1% xg respectively. However, further increase in agitation from 30 to 200 rpm did not significantly increase the the omtc (14% and 24% increase for 0.1 and 1% xg respectively) and interestingly, the omtc for both 0.1 an 1 % in the guar solution at increase from 30 to 200 rpm showed a mild decline. This is suggestive of the different physical properties that guar and xanthan gum solutions possesses, which helps to define the flow dynamics (Reynold's number) and are important elements during mixing which subsequently affects the advection of maltose in the mass transportation process.

Xanthan fibres may reduce absorption of sugars more effectively than guar fibres because of the viscoelastic effect that is lacking by the guar fibre (Mart et al., 2018). This mens that it would require more exposed shear for longer periods of time to break the bonds that may release the sugars for more rapid diffusion. Therefore when formulating, replacing either fibre at the same concentration, may not give the same effect, as both fibres display different

molecular mechanisms due to their viscosities. Similar observations were made by Fabek et al., 2014, where he studied xanthan gum and guar gums model food viscosities before and after in vitro digestion. Where, they found that consistency index K, was larger for xanthan than guar model foods over a range of shear rates (30-200 s^1), suggesting that xanthan is able to retain more of its viscosity over the span of intestinal digestion (Fabek et al., 2011).

5.4.3 Effect of shear mixing on enzymatic digestion bread systems

It is clear from model fluid studies that the effect of viscosity is a determining factor in absorption, similarly, it is expected that viscosity should play a role in enzymatic systems, but may not be in the same operational mechanisms. There is a positive effect of mixing on bread digestion that cancels out the impeding effect of increasing the wheat bran fibre, as shown in Figure 5.5.A-C. At low shear mixing (U_{tip}; 0.08 m/s), there was little differences observed on the digestibility rate plots for bread incorporated with 10 and 20 % wheat bran as illustrated in Figure.5.5.(A). However, both had faster digestion rates than white bread without any fibre, at the same level of shear mixing. Conversely, at higher shear mixing U_{tip}; 0.5 and 1 m/s, Figure 5.5..B-C., the differences are very obvious, where breads in the presence of 20 % bran, displayed higher digestion and absorption rates with overall mass transfer rates occurring at 9.03 $x10^{-07}$ m/s and 1.04 $x10^{-07}$ m/s i.e., 6.4 and 26 % faster than when the bread were in the presence of 10% bran, and 76 and 93 % faster when no fibre is in the system (white bread) as depicted in Figure 5.6..

These trends were merely anticipated, as breads that are incorporated with bran fibres are known to weaken the gluten network during bread development (Hemdane et al., 2015; Gan et al., 1992). A weak gluten network would mean that under small shear forces, starches would be exposed to the continuous phase at a faster rate, leading to faster mixing and enzymatic digestion of starch. However, it was expected that even with a weak gluten network, the bran fibres would have absorbed the surrounding fluids. Hemdane et al. (2015),, have found that wheat bran has the ability to absorb a significant amount of liquid, and increasing the insoluble solid particles should increase the digesta viscosity (Takahashi et al., 2004). This hydration phenomena of the bran would thereby increase the viscosity of the intestinal contents which would slow digestion and absorption. It is obvious that though this might be the case, the effect of a diminished gluten matrix which should hold starch may play a more dominant role (especially for 20 % inclusion) during digestion than the small effect of increased viscousness by fluid absorption by the wheat fibre. Additionally,

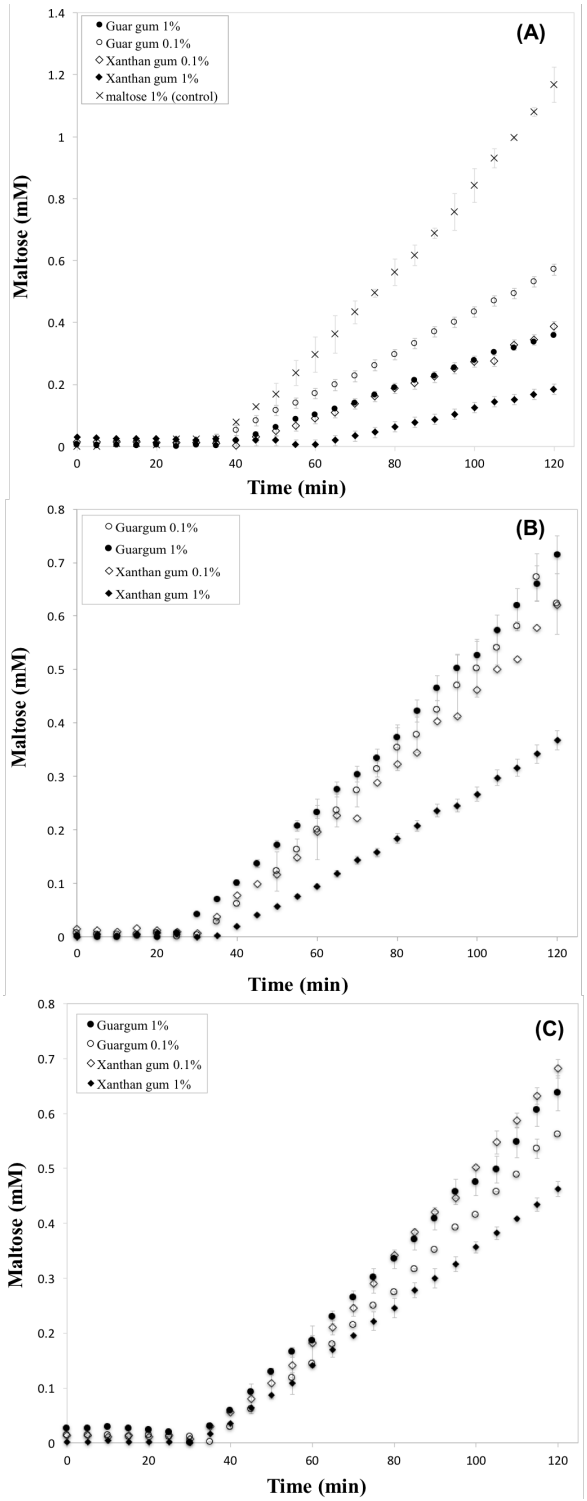

Fig. 5.3 Diffusion rate plots for soluble fibres; guar and xanthan gum model fluids in str: (A) no mixing (B) 30rpm and (C) 200 rpm

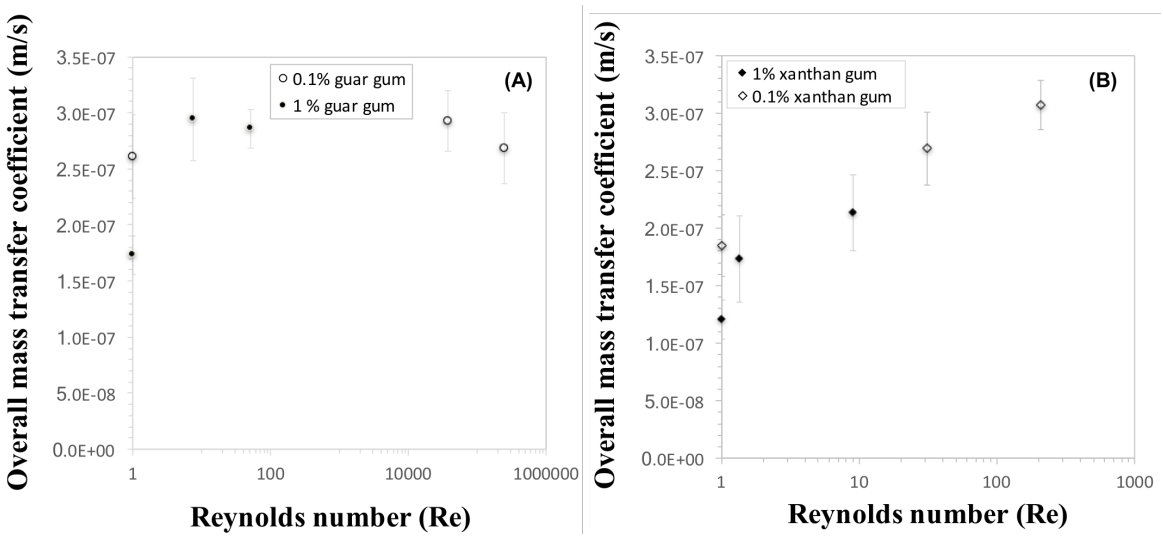

Fig. 5.4 Dependence of overall mass transfer coefficient on Reynolds number under each soluble fibre systems : (A)- guar gum, and (B) - xanthan gum

the treatment of bran, which is widely practised in bread making may help improve bread structure and therefore the functionality during digestion due to imparting different physical properties (Ralet et al., 1990; Hemery et al., 2010).

The presence of the soluble fibre guar was more effective to attenuate the overall absorption/mass transfer rate of sugars than bran insoluble fibres. In fact, white bread digestion and absorption in the presence of 10% guar, diminished consequential mass transfer rates, regardless of the level of shear introduced to the reaction (impeller tip speed) as illustrated in Figure 5.6. However, the lower the level of shear mixing, the more effective guar is in attenuating digestion and absorption. In particular, there was a 59 %, 20% and 13 % reduction in the coefficients of mass transfers ($1.15x10^{-07}$ m/s, $4.03x10^{-07}$m/s and $4.69x10^{-07}$m/s), for 0.08, 0.5 and 1 m/s tip speeds respectively, highlighting the importance of shear rate/forces on material during digestive reactions. The delaying of digestion and absorption using guar may be a result of the behavioural impact of the guar fibre during the dough and bread formation. Brennan et al., (1996), have found that the guar fibre (galactomannan) may have a dual function during digestion compared to other soluble dietary fibres. First, soluble guar may trap starch molecules preventing its complete dispersion during the bread making process, thereby making it difficult for enzymes to digest if they are concentrated in isolated discrete pockets. Secondly, the mucilage coating throughout the protein gluten complex may act as a physical barrier against mechanical stresses and enzymatic diffusivity, where the shear forces may not be sufficient to overcome the barriers, during intestinal transit.

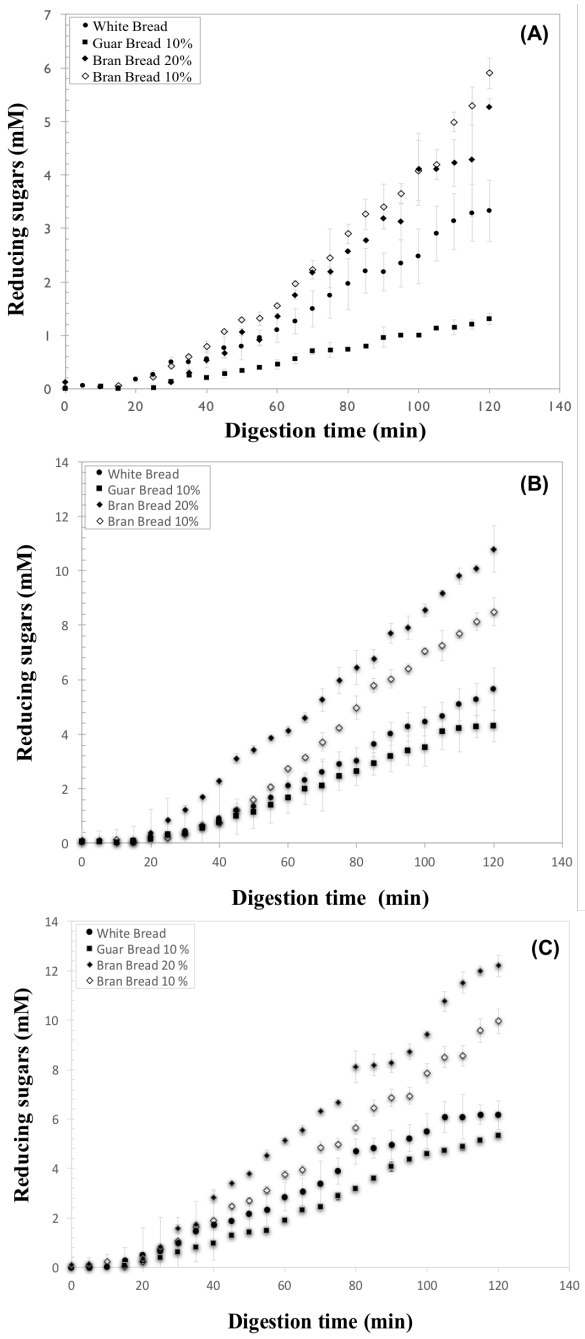

Fig. 5.5 Digestion rate plots for breads with: soluble fibre (guar-10% w/w), insoluble fibres (bran 10 and 20 % w/v) under varying impeller speeds: (A) 30 rpm (U_{tip}- 0.08m/s) (B) 200 rpm (U_{tip}- 0.5m/s) and (C) 400 rpm (U_{tip}-1m/s)

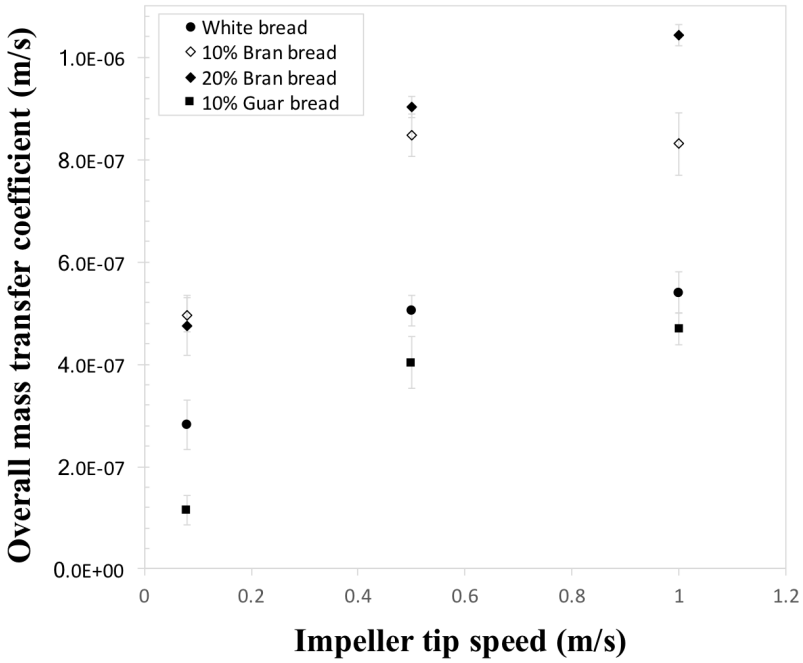

Fig. 5.6 Reliance of overall mass transport coefficient on impeller tip speed in the diffusing medium during digestion of breads with varying fibre type and content.

5.4.4 Effect of food formulation on torque behaviour during small intestinal digestion.

Torque values were determined from the start of digestion for up to two hours, the range of importance for the effect of shear on in vitro intestinal digestion studies. To study the impact of the interaction of shear forces on food materials, intestinal fluids with hypothesised highest (white breads containing 10% guar w/w)) and lowest (white bread with no fibre addition) viscosities were chosen, similarly to model fluids that had increased viscosity when the amount of fibre is increased.

In general, the torque fell at the beginning of digestion, and even though gradually levels off, it never establishes a constancy regardless of the stirring rates as displayed in Figures.5.7. Interestingly, at low mixing tip-speeds (0.08m/s), there was no clear difference in torque observed between either type of intestinal contents; 10% guar substituted nor white bread material, as shown in Figure.5.7.A. However, the digestibility rate plots were extremely different, Figure.5.7., and white bread had faster absorption rate, subsequently, faster overall mass transfer coefficients, highlighting the importance of luminal viscosity in modulating digestion and absorption, as seen in Figure.5.6.

Conversely, at higher mixing tip-speeds - 0.5 and 1 m/s, the torque pattern among each intestinal fluid type became clearer and could be distinguished, as shown in Figure.5.7.B and C. Intestinal contents containing the guar displayed consistently higher torque values throughout, with "zero -shear torques" displaying 8% and 6% higher forces for mixing tip-speeds of 0.5 and 1 m/s respectively, than intestinal contents made up of only white bread i.e. $2.16X10^{-01}$ Nm and $2.61X10^{-01}$ Nm respectively. This increased mixing has a negative impact on viscosity, concerning digestion, increasing the overall mass transport coefficient values, therefore, shortening the gap between the more viscous and less viscous intestinal fluids. This is a strong indication of the importance of increasing shear rates on intestinal digestion and absorption rates. The levelling off of the torque levels in most cases may be because of the - thinning behaviour of the intestinal materials, as the digestive reactions proceed and the required power draw is reduced. This suggests that white bread may require less energy from the body during in vivo digestion compared to guar substituted bread.

The Power number which is analogues to the Reynolds number can help to describe the flow kinematics, and the energy requirements of each system, especially in multiphase materials where the rheology can be too complex to define. Figure.5.8. shows the reliance on mass transfer rates on the Power number. The power number was estimated from equation.**??**. using the initial torque from the impeller (zero-shear torque). As the power number increases, there is a decline in overall mass transport rates, regardless of the material (in the presence of 10% guar) of intestinal fluids. However, white bread in the presence of 10% guar showed slower mass transport rates throughout, with slightly overall higher power numbers (<2%).

This was within expectations: the lower the power number, usually indicative of more turbulent regime flows, which was in the case of the bread without fibres. The reason for such differences, may be explained by the complex rheology of each fluid type. By theory, it can be assumed that the fluids that has a greater internal resistance will have higher viscosities which would require more torque during shearing, regardless of the rate of shear mixing. This highlights the significance of the energy requirements for different food materials a during the mixing process of digestion in-vitro. According to Lentle et al., (2008), some foods may exhibit viscoelastic properties which may require different level of shear forces to deform the materials in order establish flow. This may be the case of the material contains 10 % guar. According to Alloncle et al. (1991), guar hydrocolloid interaction with starch can increase the viscoelastic behaviour, which may be the case of guar with bread intestinal contents.

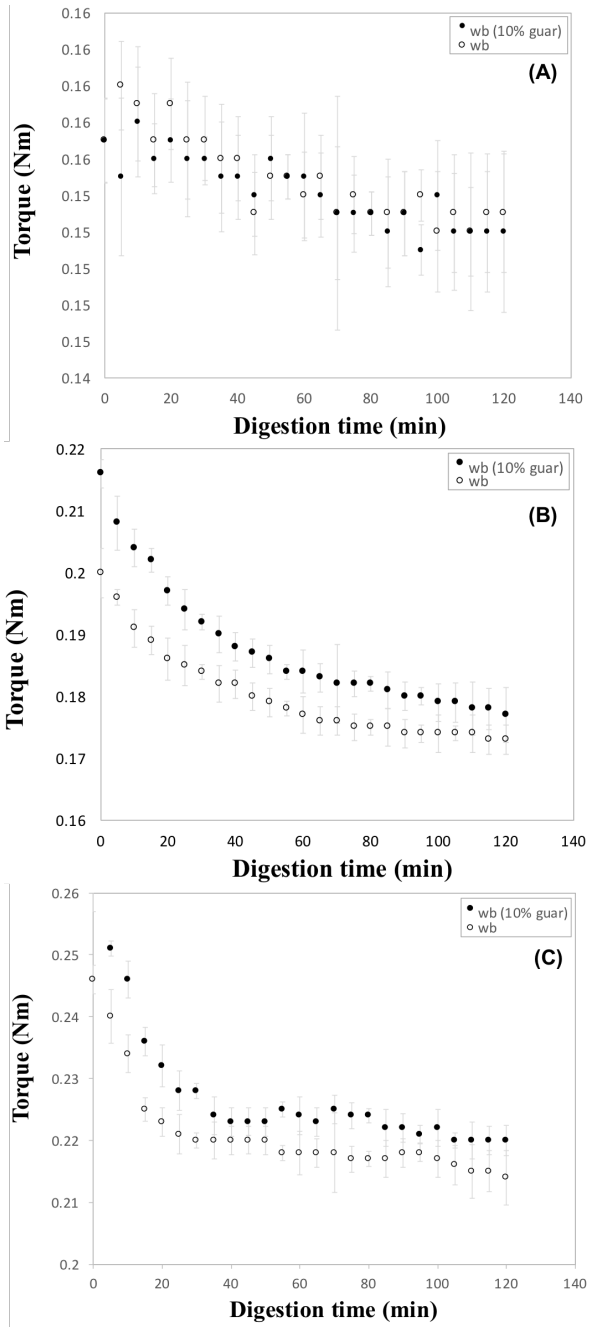

Fig. 5.7 Effect of bread type on torque requirement during digestion under different impeller tip mixing speeds: (A) 0.08m/s (B) 0.5 m/s and (C) 1 m/s . wb- white bread

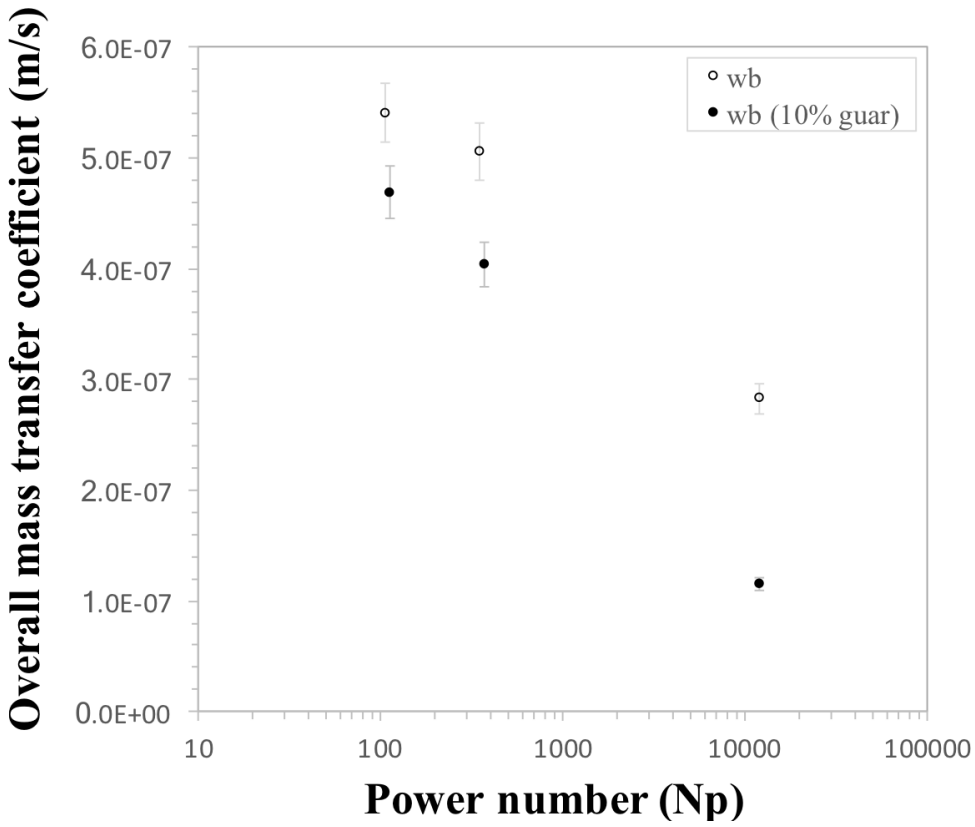

Fig. 5.8 Dependence of overall mass transfer coefficient on Power number on the diffusing medium in bread digestion in str

Operating parameters	Dynamic model	Stirred vessel
Type of mixing	Squeeze flow (dis-continuous)	Spindle (continuous)
Recipient fluid volume (m^3)	0.0007	0.00035
Surface area of absorption (m^2)	0.04	0.02
High level mixing	6cpm	400rpm (1m/s)
Medium level mixing	-	200rpm (0.5m/s)
Low level mixing	2cpm	30rpm (0.08m/s)

Table 5.2 The operating features of the stirred vessel (STR) and dynamic model (DDM) used during in vitro digestion of white bread (low viscosity bread) and bread's with guar added at 10% in recipe (high viscosity bread).

5.4.5 Comparing in vitro digestion in two models (dynamic and stirred vessel).

Table.5.2. shows the features and operating conditions for the dynamic duodenal and stirred tank reactor models during bread digestion. The bread reported and compared here, are bread types that were digesting from Chapter 3 of the thesis. High viscosity bread types were formulated with 10% guar in their recipe and low viscosity bread types had no dietary fibre added to their recipe (controls). Figure 5.9 shows the overall trends when the data were plotted for the results from the two models when maltose concentration was normalised as a function of absorption area (m^2). It is evident that high mixing speed (frequencies) resulting in larger and faster overall nutrient uptake, regardless of the model used. Furthermore, digestion in the stirred vessel resulted in larger maltose concentration absorbed irrespective of the shear rates and bread formulation. For the low viscosity bread kinds (unmodified breads- no dietary fibre) however, there was an overlap in absorption rates, when mixing was at its lowest (30 rpm (0.08m/s)) for the stirred tank reactor and mixing was at its highest (2cpm) for the dynamic duodenal model, in Figure.5.9.A. In fact, these bread digestions were almost identical in linear progressive absorption.

Figure.5.9.B, shows the effect of adding dietary fibres (10% guar) in the formulation. It was clear that absorption during bread digestion were slower for these fortified breads than their unmodified counterparts. A reduction in 13, 24 and 19.4 % were observed for 1, 0.5 and 0.08 m/s mixing speeds respectively, at the end of the digestive process. For digestion in the dynamic duodena model, there was a 35% reduction in final absorption. What is interesting about this aspect is that tripling the mixing frequency from 2 cpm to 6 cpm, was still not effective against the reducing effect of adding guar, to reduce absorption during breads digestion. Mixing at the highest level (1 m/s) in the stirred tank reactor in the

presence of guar bread, resulted in twice the amount of maltose transferred into the recipient fluid (97 g/l) more compared to mixing at the highest level (6cpm) in the dynamic duodenal model (45 g/l).

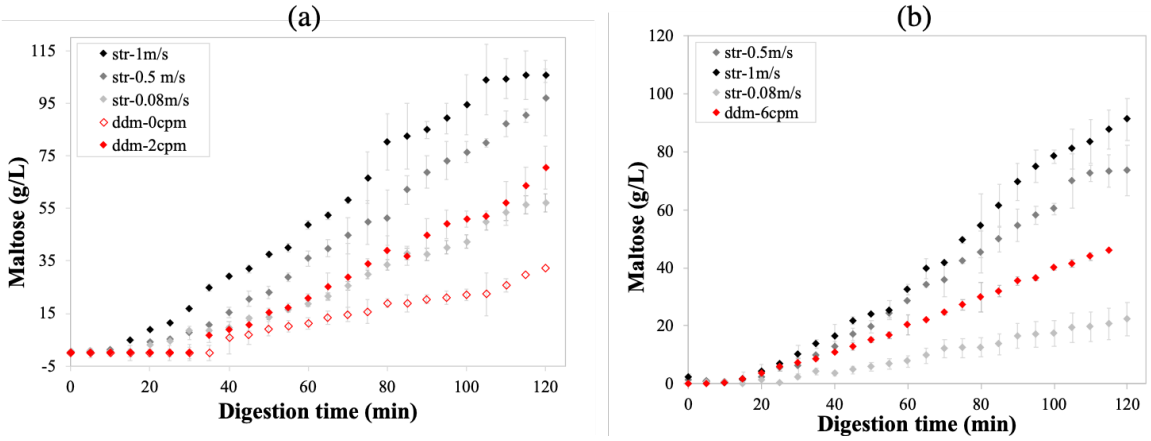

Fig. 5.9 The effect of mixing on bread digestion in the dynamic model and the unique stirred tank reactor model: (a) white bread digestion (low viscosity/controls) and, (b) white bread with 10% guar gum in the recipe (high viscosity). Rpms' were converted to tip speeds (m/s). Maltose concentrations were normalised to mass concentrations (g/l) by then dividing through by the surface area for absorption m^2, converted from the molar concentrations (mmol/l) by using the relative molecular mass of maltose (342.29 g/mol). Maltose concentration (g/L) was then plotted vs digestive time.

As mentioned earlier that the main difference between the two models is the element of mixing and as previously described earlier in this chapter is that the stirred tank reactor is able to describe the power requirements needed to perform mixing, indicating the overall energy applied to the system. The overlap of the absorption results suggest that the total energy used in the mixing process by both systems might be similar, provided that the constraints are more or less the same and the resistance for mass transfer between both systems are negligible at that level of mixing. One explanation for the differences observed between the two models may be the type of mixing undergone by the digesta during the breakdown and absorption process. Mixing in the dynamic duodenal model is via a squeeze flow type, which enhance more axial flow and hence axial mixing, while, a Rushton turbine found on the stirred tank reactor enhances radial mixing in its vessel. This type of radial mixing can work by two mechanisms or simultaneously, by speeding up enzyme diffusivity where enzyme substrate complex are formed at a faster rate leading to faster digestion kinetics, and or, the resulting products of digestion (maltose) are convectively diffused to the membrane interface more

easily and frequently due to the un bottom mixing effect. It can also be hypothesised that further dissolution of digesta particles (to nm scales) due to shear forces of the continuous phase will alter the luminal content's viscosity. Compared to the squeeze flow- the repeated mixing may take a longer time to achieve the same amount of shear and hence will conduct slower digestion and subsequent absorptions. Additionally, the overall absorption derived when mixing speed was 0.5 m/s was not significantly different from the digestion conducted at 1 m/s. i.e. 97 g/l vs 105 g/l. This can be explained by the fact that rotations quicker than 300 rpm (1.5 m/s), allows digestion particles to rotate with the continuous phase (main fluid) due to the centrifugal forces (Yoon et al., 2001). Subsequently, the contact between particles and the impeller may decrease, reducing the relative shear forces (Liao and Lucas, 2010). It can therefore be said that optimum digestive ability that can be obtained, will be no greater than 2 m/s using this food digestion in vitro system *in-vitro* system.

5.5 Conclusion

An in vitro stirred reactor vessel with continuous agitation modified with a membrane was fabricated to provide a new digestion system. In non reactive food systems (model fluids), the extent of mass transfer rates were reduced in the presence of soluble dietary fibres, guar and xanthan gums. However, the range of xanthan model fluids were more effective in reducing maltose absorption for similar range of guar model fluids. Overall, this suggest that xanthan gums may give better control over starch digestion and absorption than guar gums when formulating at similar concentrations. In the reactive systems, under the enzymatic digestion of bread, raising the percentage of wheat bran (insoluble fibre) in the recipe was more deleterious to absorption in-vitro, implying that there are more benefits to be gained in using guar as an effective modulator in starch digestion, for different bread recipes.

To evaluate the impact of more realistic duodenal intestinal mixing on starch digestion in breads, the breads were subjected to two different enzymatic digestive mixing methodologies; (i) continuous agitation and (ii) squeeze-flow mixing (segmentation of gut walls) in dynamic duodenal model. The digestion/absorption rates were significantly different for both mixing methodologies. It is also very clear that the effect of segmentation or "perfect mixing" has a salient influence over the final extent of maltose absorbed (starch digested).

Even though the stirred vessel does not reflect the mixing of in vivo duodenal contents, it was able to improve the contact between starch substrates and intestinal fluids including enzymes, thereby setting the pH to constant value (optimum pH). This may explain why enzyme related activities are translated into faster digestibility of breads in the stirred vessel.

Furthermore, the higher the power number (energy requirement in the system), the slower the rate of mass transfer. However, incorporation of bread with 10% guar, indicated that for the same power number, the rate of mass transfer will decline.

Both novel *in-vitro* models promise advances in predicting the digestive behaviours of food in designing target release foods for health benefits. However, in vitro models that simulate mixing will affect digestibility and hence absorption differently. I.e., Radial mixing (stirred vessel) was more important to mass transfer, than axial flow mixing (dynamic model), as indicated by the relative amounts of mass transferred in the stirred tank reactor as compared to that of the dynamic duodenal model. For example, maltose (g/L) was 38 % higher for white breads in the stirred vessel at 1/ms than 2cpm in the dynamic model (Figure.5.9.A.).

Chapter 6

Manipulating food structure at the manufacturing level to strategise on in vitro starch digestion: Optimised approach.

This chapter was funded by Infogest, COST action FA 1005. In this chapter, gluten-free breads were developed under optimised processing conditions. The breads were prepared at the University of Thessaloniki, Greece. Dr. Athena, helped in the design of the experiments, and conducting the in vitro starch digestion was aided by Dr. Angelica. The manufacturing of the breads, and performing digestion and data analysis of the study was done by myself. Review of the presented data were done by Prof. Serafim Bakalis and Dr. Ourania Gouseti.

Abstract

A mathematical system model that describes the optimised water ratio, for production of gluten-free bread (gfb), to increase loaf specific volume (essentially, hypothesised a different microstructure that may reduce in-vitro starch digestion) using cornstarch and rice flour through direct experimental manipulation of the proofing period was developed. The main effect was observed under the hydration factor, while there were little net effects of the interaction between hydration and dough fermentation times, to increase loaf specific volumes. The water content and dough proofing times influenced the final mechanical properties of each loaf. In-vitro starch digestibility in the bread was highest under 100% hydration level and 40 minutes proofing time, having a mass transfer coefficient of 1.53×10^{-07} m/s, 1 order of magnitude faster than all other bread, reflecting a 45% starch digestion. Bread produced with 69% hydration levels and 40 minutes proofing times, had mass transfer coefficients of 6.47×10^{-08} m/s. The derived model demonstrates good capabilities in predicting gluten-free loaf specific volumes under the condition of varying water ratio and proofing rate.

6.1 Introduction

One of the oldest and most consumed foods globally is bread - and in many forms (Ridgwell, 1986). However, not everyone can biologically utilise the prolamins proteins released from wheat in bread during digestion. This condition is clinically defined as an auto-immune disease of the small intestine (Celiac disease), accounting for 2% of the population in Europe (Mustalahti et al., 2010). Hypersensitivity, and subsequent inability to utilise these proteins, become detrimental to the intestinal absorption phenomena (Zuidmeer et al., 2008). Which, frequently cause perilous malnutrition due to the malabsorption-resulting from, the caudal flow of nutrients along the bowels (Gil-Humanes et al., 2014; Stankovic et al., 1995). To circumvent this issue, food and nutritional sciences have tried to use wheat starch in the diet as a substitute of wheat flour, in bread. However, this has also posed problems, as the gluten's, gliadins fragments remaining in the wheat starch will still trigger an allergic reaction, in

many consumers (Shan, 2002). The most notable approach is, therefore, to reformulate without wheat or products of wheat that will not pass on these proteins during the bread making process, and subsequently in the gastrointestinal tract

Alternative ingredients has been proposed and tested to obtain gluten-free breads (Arendt et al., 2008; Mandala et al., 2011). For example, the use of cassava starch (Gallagher et al., 2004), corn starch, rice flour (Yu et al., 2013) and hydrocolloids such as xanthan, pectin and carboxymethylcellulose (Anton et al., 2008). Attempts have also been made to include a mixture of theses alternatives (L et al., 2004; Lazaridou et al., 2007), with their rheological properties studied (Demirkesen et al., 2010). The major challenges with the introduction of these new raw materials in the existing recipes are: the uncertain responses to processing technologies during the bread making process; the final sensory attributes as perceived by the consumer, such as, colour and mouth feel (texture) (Gambaro et al., 2002) and; the performance of the food material during digestion, such as postprandial glycemic responses and protein absorption (Berti, 2004; Segura et al., 2011; Wolter et al., 2014; Giuberti et al., 2016). If these challenges were to overcome, then unique gluten free breads would be attractive for commercial prodution and their digestibility patterns could also be mapped. Subsequently, to some degree, breads could be manufactured with already predetermined digestibility rates, and some post-prandial responses such as blood sugar levels, could be structured in their early formulation.

Water and flour are central ingredients in bread making (Cauvain et al., 2008). Water dictates the quality and economic attributes in the process, and constitutes an approximated 35% of the final baked bread and around 40% of the dough's initial weight (Cauvain 2003). During the formation dough, and all the ingredient are added and mixed together, the water medium: dissolves all soluble solids, hydrates flour proteins and allows yeast to be dispersed in the continuous phase (Shewry 2009). In the final baked breads, water also acts as a plasticiser. During the eating process, the bread?s freshness is assessed during chewing (compression). Consequently, the more water that remains in the bread, the softer and more appealing the bread will be to the consumer, making it more delightful and acceptable (Gould, 1998). It is therefore important to strike that balance of the water levels needed in the starting recipe. The water influence on proteins network also plays an important role in the final bread properties (Primo-Martt al., 2006). It influences the textural properties, and hence final micro-structure, through air entrapment, giving rise to breads with different porosity and hence different densities (specific volumes). In wheat, the gluten proteins constitutes about 10-15% (Goesaert et al., 2005) and are responsible for the viscous effect during the dough?s formation, elasticity and strength (Shewry et al., 2002). When substituting

alternative ingredients to replace wheat flour, the substitute?s proteins or components must be able to perform similarly in processing, giving rise to similar textural effects, for example, the use of rice flours.

The enzymatic break down of starch during digestion, can be altered by several factors, such as; the presence of macro nutrients (proteins) and micro nutrients (minerals), the granule structure of starch's, and the overall physical structure of food including particle size and densities (Fardet 2006). There are evidence that the particle size in food structures and hence disintegration may influence gastric emptying in vivo and in vitro, which may impart different glycemic responses (Hernot et al., 2008; Kong et al., 2008). Where gluten free breads are concern, there is limited information on how manufactures could customise the processing parameters and starting ingredients for derived health benefits , vis a vis regulation of the glycemic response-during starch digestion. However, reports about how flour particle size influences loaf specific volumes and glycemic index under different hydration rates have been reported by Hera et al. (2014).

For gluten free breads to meet the sensory and nutritional needs of the consumer, it is imperative that the interaction of alternative active ingredients and the processing conditions from the formulators and the manufacturer, lead to final products that are comparable to the traditional wheat bread standards, that appeals to the consumers. With any new product development (NPD), experimentations must be at a minimum, to save cost, and optimise the outcome and objectives. This study aims to understand the starch digestibility mechanisms behind employed processing conditions (water ration and proofing times), under optimised specific volume of gluten free breads, that may lead to beneficial health - for starch digestion control.

6.2 Materials and methods

All chemicals and enzymes used in the trials were sourced from Sigma Aldrich: Greece, unless otherwise stated.

6.2.1 Experimental design

Three responses were measured when gluten free recipe, were hydrated with different water ratios and dough's fermenting proofing times: crumb moisture content (%), specific volume (cm3/g), and the texture profile analyses (TPA), which includes; hardness (N), cohesiveness, resilience and chewiness (N.s). Table.6.1. shows the conditions for randomised full factorial,

Treatment/condition	Water content % (w/w)	Proofing time (min)	Temperature (^{0}C)
1	100	30	180
2	100	40	200
3	100	20	200
4	74	20	200
5	74	40	200
6	69	20	200
7	69	40	200
8	69	30	200
9	59	40	200
10	59	20	200
11*	79.5	30	200

Table 6.1 Experimental design to bake gluten free breads(gfb) with different specific gravity * base values

design for each trial. The independent variables were, water content (59, 69, 74, 79.5, and 100 %), and dough's proofing times (20, 30 and 40 min). They were administered to find out the extent to which they could modulate bread structure (specific volume) and consequently starch digestion from the resulting breads. The water content is crucial for flour hydration and fermentation in the dough for gluten free bread performances (Marco 2008, Schober 2009). Water content was the amount of water in percentage as g/105g (rice flour and corn starch) added to each recipe. 59% was the minimum amount of hydration that is required for the dough to mix (consistent). In the development of the predictive model for simple first step optimisation response surface method, using *R-Studio software*, a water content of 79.5% and dough proofing time of 30 minutes were selected as the base values. They were selected as mid points between the minimum and maximum, independent variables. In-vitro digestion of starch was conducted on breads (treatments; 1-9) to understand the effect of specific volumes may have on overall digestibility and mass transfer rates. All experiments were done in triplicates and expressed as the $\pm$ standard deviation.

6.2.2 Material preparation

Preparation of breads

A kitchen mixer, with dough hook, operated at 50 rpm, process the dough for 10 minutes following the formulation: corn starch 50g, rice flour 50g, Inulin 6g, yeast 2g, sucrose 1g, salt

1g, sunflower oil 2g, and water (62g, 73g, 78g, 83.5g and 105g) to a final carbohydrate content of 82g/100g bread (dry basis). Dough portions of 167g, were transferred to aluminium pans and fermented in a pre-warmed proofing unit, at 37 C, for 20, 30 and 40 minutes. Proofed doughs were then transferred to the pre-warmed oven to bake at 180 or 200 C with steam, for 40 minutes (Table.6.1.). The loaves were then removed and were allowed to cool at room temperature for 1 hour. Loaves that were not used on the same day were wrapped in thin film to prevent moisture loss. All analytical measurements were made no later than 24 hours. Three batches were done for each recipe. Three commercial brown wheat breads were also purchased from stores to aid comparison (controls).

Preparation of simulated intestinal fluids/enzyme and glucose standard solutions

The main simulated intestinal fluid used, was done according Symons et al. (2006). Sodium phosphate buffer contains; 20mM NaH_2PO_4; and 10mM NaC, adjusted to pH 6.9. The 200mM sodium acetate buffer, contains 11.6 ml glacial acetic acid, fixed to pH 4.5 using 30ml 2N NaOH. The GOPOD reagent contains; 50mM potassium dihydrogen orthophosphate; 10mM p-hydroxybenzoic acid; 0.02 w/v % sodium azide; > 12.000 U/1 glucose oxidase; > 650 U/I peroxidase; 0.4 mM 4-Aminoantipyrine; 05 mg Glucose oxidase (Sigma G-7016, 500.000 Units, 115,000 U/g); 3.6 mg of peroxidase from horseradish (Sigma Type II. P8250-50KU at 276.2mg); and 80 mg of 4-Aminoantipyrine The pH was adjusted to 7.4 using 1N KOH.

The pepsin solution was prepared from porcine gastric mucosa, Sigma-Aldrich, P7012.2190 Units/mg solid, Mw 35 KDa, 5 mg/ml in 0.9 % NaCl. The α-amylase solution was prepared from porcine pancreas, Megazyme, 150000 Units/g solid, Mw 51-54 kDa, 5mg/ml in the phosphoric buffer solution describe earlier. The amylosglyucosidase solution was prepared from amyloglucosidase from Rhizopus mold; Sigma, 11600 U/g, Mw 68 kDa, 1mg/ml in distilled water. And, the invertase solution was prepared from invertase, Megazyme, 300 U/mg of solid (5 g), 200 mg/ml in distilled water. α-D-glucose standard solution, 1mg/ml was prepared; using 100 mg for monohydrated glucose dissolved in 100 ml distilled water, and used to prepare standard solutions at concentrations of 75, 50, and 25 μg/0.1 ml.

6.2.3 Characterisation of baked gluten free breads (gfb)

Specific volume and moisture content of the crumbs

The weight, g and volume, cm^3 were determined and used to estimate the specific volume (cm^3/g) for each loaf. The loaf volumes were estimated according to AACC (AACC 2000)

approved method 10-05, through displacement of rapeseed. The moisture of the crumb was also estimated according to AACC (AACC 2000) approved method 44-15A.

Texture profile analysis (TPA)

To determine the mechanical properties of the gluten-free crumbs, the texture measurements (hardness, cohesiveness, resilience and chewiness) of the crumbs, were done. These TPA were selected, as they are considered to have fundamental impact on the physical and chemical process of digestion. The cylinder probe compression method was followed, where the centre of each bread crumb were uniaxially compressed, withdrawn and then repeated to simulate two "back to back" bites (two cycle compression test), using the appropriate compression probe. Each crumb used in these tests were diced into thick slices of 27mm lengths pieces, taken from the centre of each breads, after removing the crusts. The gluten free bread samples were compressed to 40% of its initial height of 60 mm. The Texture Analyzer test speed was set to 1 mm/s, and the trigger force was 9.8N. Measurements were done in four replicates. The profiles of hardness, cohesiveness, resilience were provided from the instrument and chewiness was calculated form the expression; chewiness (N.s) = hardness (N)* cohesiveness* springiness. The TPA analyser measure the cohesiveness as "the as the positive force area during the second compression portion to that during the first compression", the springiness/elasticity as "the height that the food recovers during the time that elapses between the end of the first bite and the start of the second bite, the hardness as the "the peak force during the first bite/compression cycle" (Pons and Fiszman, 1996).

6.2.4 Performing in-vitro bread digestions

Oral digestion was not simulated, because the method by Symons and Brennan (2006) assumed that particle sizes smaller than 3mm are not chewed during meal consumption, but directly swallowed and enter directly in the gastric phase of digestion. As such, gluten free breads studied were sampled by using 5g weights and the digestion initiated at the gastric phase described below:

Gastric digestion

The method by Symons and Brennan (2006), was followed with the following exceptions; bread crumb samples 5g, equivalent to ~2 g available carbohydrate, from each condition in Table.6.1., and commercial wheat breads, were crushed using piston and mortar and then pass through a sieve, to achieve particle sizes of 0.2 cm^3. Each sample was added to sodium

phosphate buffer (35ml) and the pH adjusted to 1.5 with HCl 1N. Pepsin, 2 ml; 730U/g starch-(pepsin, 5mg/ml), was added and digesta was placed in a shaking water bath, set at a 1.5 scale, and kept at 37^0C for 30 minutes.

Small intestine digestion and starch determination

After gastric digestion, the digesta was adjusted to pH 6.9 with NaOH 1N, transferred to 270 mm long ultrafiltration membrane, with molecular cut off weight of 1200–14000 Da and who's flattened width is 76 mm in diameter. The membrane was primed with 30ml, sodium phosphate buffer, prior to the start of intestinal digestion. The membrane acts as the simulated intestinal wall. Small molecules that are produced during digestion can pass though the pores, whereas large biopolymers such as starch remain in the lumen. Subsequently, enzymes; α-amylase (0.44ml; 110 Units/g starch), and invertase (0.1ml; 600 Units/g starch) were added to digesta (65ml) in the membrane, sealed and then placed in a 500 ml duran container, containing sodium phosphate buffer (435ml) the absorbing medium. The duran containing digesta was placed in a water bath, and kept at 37^0C for 5 hours, as displayed in Fig.6.1. 1 ml of the absorbing medium (solution surrounding the membrane) was sampled in duplicates, at 20 min, 2, 3, 4 and 5 hour intervals, and measured by GOPOD reagent method to track glucose absorption and then expressed as percentage starch hydrolysis Symons and Brennan (2006). Briefly, amyloglycosidase 0.1 ml (1mg/ml), 0.1 ml sodium acetate buffer, and 0.1 ml water were added to 0.2 ml of the samples collected from the time points from the absorbing medium, incubated for 15 minutes at 50^{o}C. GOPOD reagent, 3 ml was then added and further incubated at the same temperature for 20 minutes. Absorbances were read at 510 nm and glucose concentration estimated from the coefficient of the calibration curve. In vitro starch digestion (%), was expressed as (g glucose/100g of total digestible carbohydrates). For glucose determination between 2-5 hours, 0.2 mil of the collected sample (1ml) are diluted with 0.4 ml distilled water, as the concentration of glucose is expected tube to large for the spectrophotometer detection. Conversely, the sample collected at 20 min of digestion were not diluted accordingly.

6.2.5 Analyses of mass transfer coefficient and statistical analyses

All trials were done in triplicates. The data presented are as means $\pm$ standard deviation, unless stated otherwise, and the statistical significance was set at 0.05 for the probability level. The mass transfer coefficient was estimated from the method done by Tharakan et al. (2010) - and chapter 3 of the thesis. Briefly, the molar flux of glucose absorbed was divided by the the

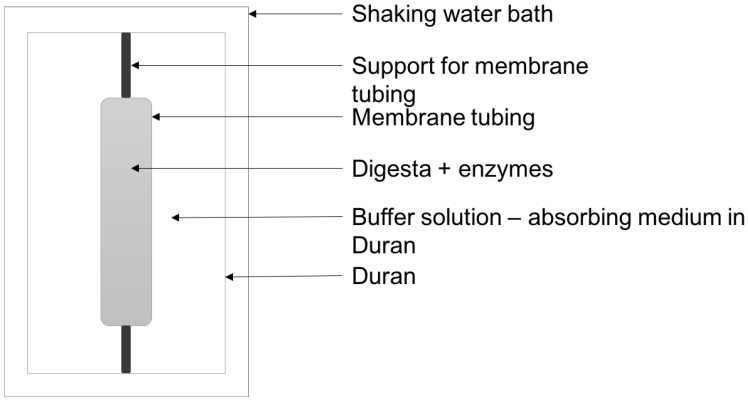

Fig. 6.1 Experimental setup for static *in-vitro* small intestine digestion performed at 37^0C, for 5 hours.

concentration difference at the interface of the intestinal wall (membrane) to derive the overall mass transfer coefficient, K from equation 6.1. Where N_i is the mass flux (mmol/m^{2}s), K is the overall mass transport coefficient (m/s) and $\delta C$is the concentration difference at the lumen membrane interface $\left(C_{lumen-interface} - C_{recipient-interface}\right)$, mmol/m3. For example, for the first trail, the molar flux of glucose was 3.6x10^{-04} mmol/m^2.s and the concentration of the glucose in the membrane interface was 5.57x10^{03} mmol/m^3, which gives an predicted overall mass transfer coefficient of 6.47x10^{-08} m/s.

$$N_i = K\delta C \tag{6.1}$$

6.3 Results and discussion

6.3.1 Effect of hydration on crumb moisture content and loaf specific volumes

The moisture content in gluten free bread crumbs were dependent on the dough's proofing time and water level ratio in the dough formulation as illustrated in Figure.6.2 and 6.3. The longer the proofing time the lower the moisture content in the crumb. For example, at 59 % hydration, the crumb moistures were 41.01 and 40.01% when the doughs were proofed for 20 and 40 minutes respectively. This same phenomena was observed at the 74% water ratio hydration level, where the crumbs moisture contents were 43.36 and 45.67% for 20 and 40 minutes of proofing times respectively. This was a 5% percent decrease by for an

extra 20 minutes of proofing time, compared to the 2.5% decrease at the 59% hydration level. Interestingly, the 69% hydration level, the longer proofing time displayed significantly, more moisture than the shorter proofing time. i.e. a 7% increase. Doughs hydrated at 100% water, had the highest crumb moisture contents in their breads, reaching 47.1% in total moisture, at 40 minutes of proofing time.

Figure.6.3. also Illustrates the dependence of specific volume of breads when the proofing times and water contents were varied. The longer the doughs proofting times and higher the water ratio hydration (>59%), the more the specific volumes of loaves increases. For example, at 59% hydration, the specific volumes were 1.87 and 1.93 cm^3/g for 20 and 40 minutes of dough's proofing times respectively, indicating a 3% raise by extending the proofing time for an extra 20 minutes. Similar trends continued when the water ratio hydration levels were increased. At , 69 and 100% hydration levels, the raise in specific volume when the proofing times were doubled were, approximately, 40 and 20% increase in specific volumes. (i.e. from 1.97 to 2.76 cm^3/g at 69% hydartion level and from 2.98 to 3.56 cm^3/g at the 100% hydration level). Similarly to the phenomena that occurred in the final moisture at 69% hydration of the crumb, occurred for the 74% hydration level, where the highest proofing time displayed a lower specific volume for loafs i.e. 4% decline in specific volume (from 3.42 cm^3/g to 3.27 cm/g). Similar results were experimentally obtained from, Hera et al. (2014), when the water ratio, ranged from 70 to 110% resulting in specific volumes of 3.06-5.24 cm^3/g in gluten-free breads that uses only rice flour as the wheat flour replacement.

Observed from Figure.6.4. is the relationship between the final moistures (dependent variable) and specific volumes "(co-independent variable)" for 1 -hour- old gluten free breads. Expectedly, the higher the specific volumes the higher the crumb moisture content will be. In order to have higher moisture content in the crumb, the condition must be set to achieve higher desired specific volumes during the fermenting proofing times. This is described later in the optimisation approach to maximise loaf specific volumes. The phenomena occurring suggest that for every 1 unit of specific volume increase (1 cm^3/g) would result in 2% and 4% increase in crumb moisture, for 40 and 20 minutes of proofing times respectively, between 59 - 74% hydration levels, under normalised approximations.

6.3.2 Effect of specific volume on breadcrumb texture profile analyses

The crumb texture of a bread can be described as a moist-soft foam, and the distribution of pores affects its texture. The breads were physically characterised and Figure.6.5. shows the the varying bread crumb structures that are produced under each treatment. The sizes

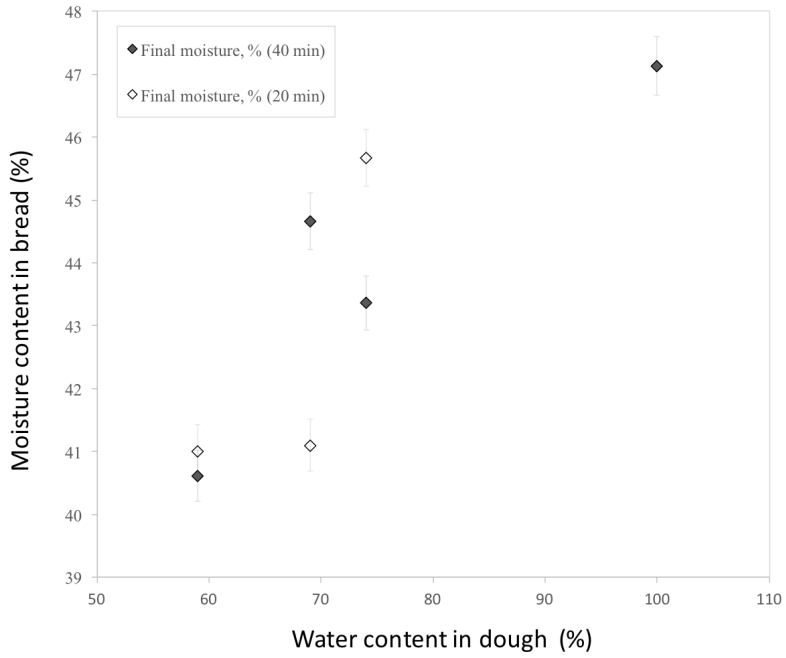

Fig. 6.2 Changes in moisture content of the bread (%), depending on proofing times and water content of the dough.

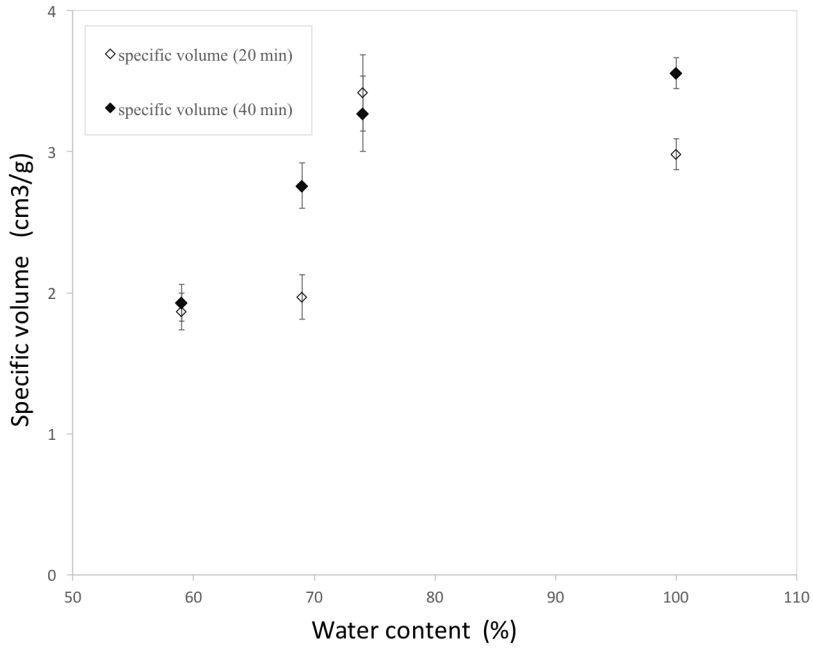

Fig. 6.3 Dependence of specific volume on water content of the dough, for different water ratio hydration levels in gfb recipes.

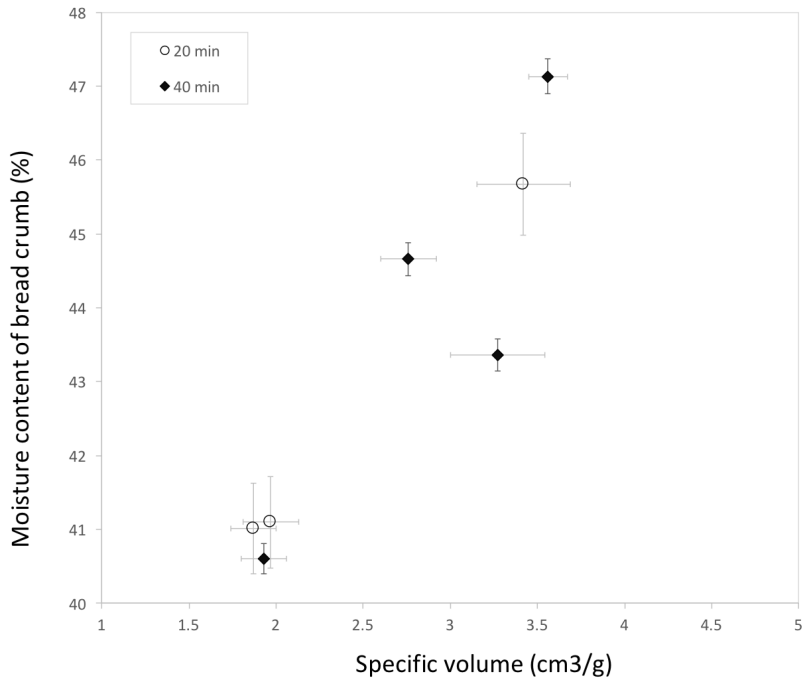

Fig. 6.4 Relationship between final moisture content (%) of gfb crumb and specific volume (cm3/g.

and the amounts of air pockets varied based on the water content of the doughs and proofing times, giving rise to different porous structures and hence specific volume. Figure.6.5.-1. shows larger and smaller air pockets that are non uniform, while Figure.6.5.-2. shows more uniform consistent air pockets. Figure.6.5, photos; 5, 8 and 9 , shows a more dense layered structure, with elongated air pockets and not the typical circular ones. These vastly different soft-faom structures, may give rise to different porosities and essentially, different loaf specific volumes.

The texture profile analyses were conducted via instrumental deformation, on the crumb of the gfb, as depicted in Figure.6.6., to highlight the significance of improving hydration and proofing times on mechanical properties of 1-hour-old loaves. These texture profiles were selected as they are believed to play a significant role in the physical and chemical processes of digestion. Hardness is primarily related to the level of softness of how a material feels. In general, hardness increases as the hydration level is lowered, regardless of the proofing rate (Figure.6.2.). Hardness was highest at 69 and 59% water ratio hydration level for 20 and 40 minutes proofing times respectively. This indicates that breads formulated at theses conditions has increased their bond strength within the rigid foam. At 100% hydration, the

hardness was at the lowest at approximately, 8.7 N, compared to 128.2 N at 40 minutes of proofing time for 59% hydration.

Typically, as breads (wheat breads) become older, the crumb becomes harder which is accompanied by loss of resilience and cohesiveness (Macritchie, 1992). Cohesiveness can be described as the internal resistance of the food structure (crumb), while resilience is indicative of the crumb's elasticity (springiness). In this case, the gluten-free breads were approximately 1-hour- old, and the cohesiveness, resilience and chewiness, increase with decreasing hydration regardless of the dough's fermenting proofing times. The low resilience at low water content 59% hydration, indicate the low level of crumb elasticity (Onyango et al., 2011). Furtemore, this ia a result of the diminished intramolecular interactions among the recipe, because the starting ingredients competes for water in the recipe. It must be acknowledged that the cooling phenomena after baking gives rise to complex operations such as heat transfer, moisture migration-from centre crumb to crust of loaf and the final micro-structure of bread matrix that influences its overall mechanical properties going rise to the overall differences observed in TPA (hardness, cohesiveness, resilience and chewiness) for these gluten-free breads.

Figure.6.7. shows the correlation between specific volume on chewiness for increased hydration and proofing times. Chewiness is selected because it collectively integrates the forces/energy during simulating bites. As the loaf's specific volume increases, the chewiness decreases, and occurring independently of the proofing conditions. Above specific volume of 2.5 cm3/g, the chewiness diminishes and become independent of proofing rates and water ratio hydration levels. It can be said that specific volume becomes limiting in perceived sensory perceptions.

The influence of water portions in the dough was noticeable in the volume of loaves acquired (Fig.6.3.).. It is considered that there is a plasticiser effect based on water level, that are important for flexible properties of the dough mixing, during gluten free bread making process (Marco, 2008 and Hera 2014).. It must be noted that the longer the proofing time, the more fermentation will take place to develop the dough, an therefore the greater will be the water requirements, for yeast activity on air pocket formation. This can rationalise the reason for the low specific volume reached by the breads under 59 % dough water content and 20 min proofing time. Furthermore, over hydration of the dough was reported to lead to loafs with big holes (Han et al., 2011), which was observed (Fig.6.5.-1.), which had 100% water content.

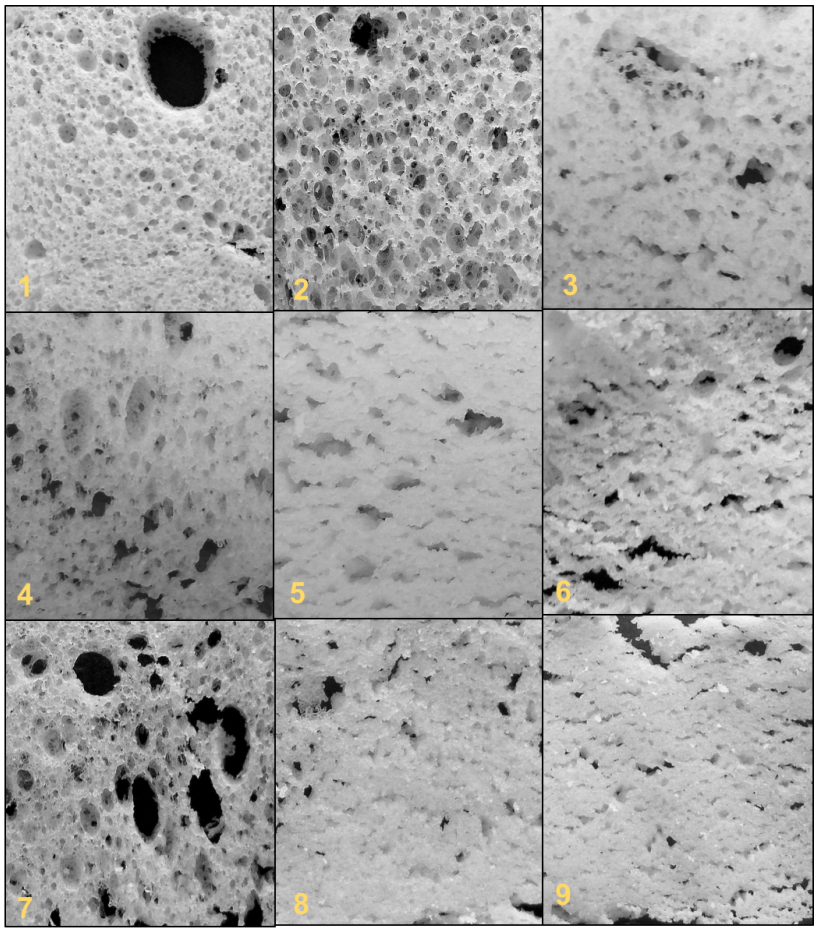

Fig. 6.5 One (1) hour old, crumb structures of gluten free breads resulting from treatments 1-9.

6.3.3 Intestinal digestibility of starch in gluten free breads

It is desirable to manufacture breads that reduce post-prandial glycemic responses and hence diminished rate of starch digestion in order to improve health. Figure.6.9., displays the starch digestion rate plots in gluten-free breads over 5hours. They were further classified into highly, medium and slowly starch digested profiles as observed in Figure.6.10. While, Figure.6.8. illustrates the digestion rate plots for glucose and wheat bread controls/standards performed in the same conditions as the gluten free breads. The crumbs moisture content and proofing time -as it relates to the loaf's specific volume had a profound effect on bread digestibility rates. Breads that digested under condition 2 (100% hydration (100%H), and 40 minutes proofing time (40 PT)) displayed the fastest starch digestibility rates, with approximately 45% of its starch digested (Fig.6.9.). This correlates to the fastest overall mass transfer rate occurring

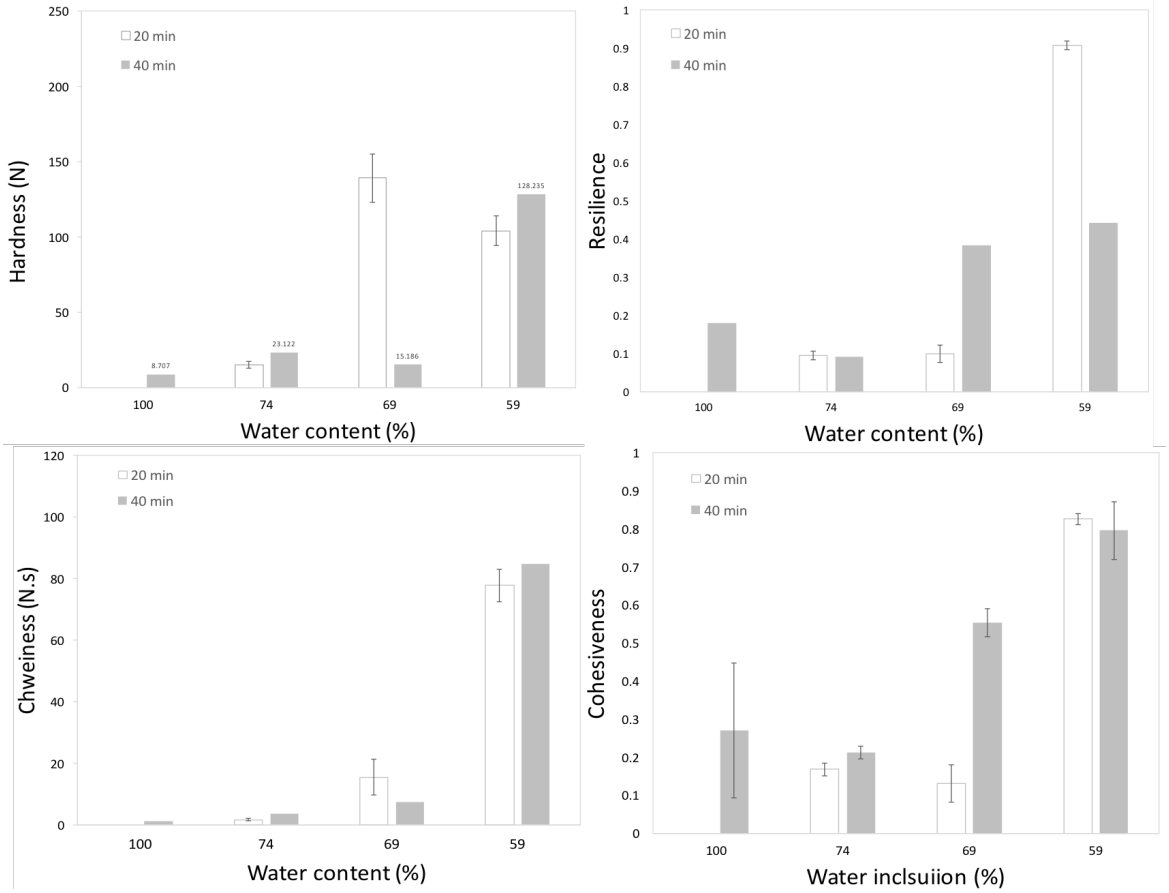

Fig. 6.6 Changes in the mechanical properties (hardness, cohesiveness, resilience and chewiness ± SD (n=4))of gluten free breads as a function of water and proofing period, in the gfb after 1 hour of baking.

at, $1.53x10^{-07}$ m/s, followed by condition 8 (59%H and 40PT) $1.11x10^{-07}$m/s. These were 1 order of magnitude (OoM) faster than the rest of breads as shown in Figure.6.10. The only system that displayed a faster mass transfer rate was glucose-control system ($1.1x10^{-06}$ m/s; data not displayed on the figure) which was 1 OoM faster than breads in conditions 2 and 8 described earlier and 2 OoM faster than the rest of the breads.

Baking temperatures, and proofing times also showed significant variability in the final starch digestion rates. The slowest digestibility rates were observed from doughs that were prepared by condition 1 (100%H, 35 minutes of proofing time and baked at 180^0C), resulting with 13% of its starch digested after 5 hours, and a overall mass transfer coefficient of $6.47x10^{-08}$m/s. This was identical to the slow mass transfer rates observed from wheat bread-control systems which occurred at $5.94x10^{-08}$m/s ; data not displayed on the figure. Reducing the proofing time by one half will cause a reduction in specific volumes when the hydration

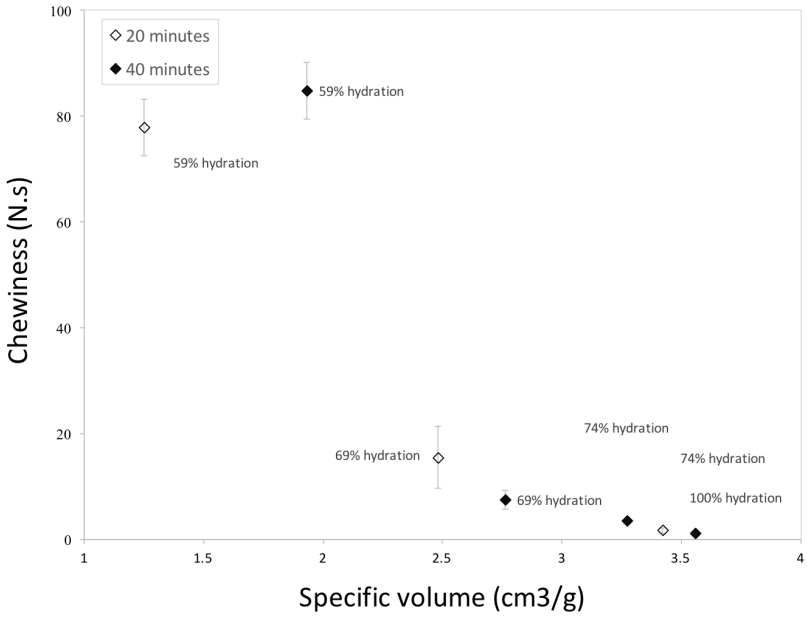

Fig. 6.7 Impact of specific volume on simulated chewiness behaviour for crumb of gfb (chewiness= hardness*cohesiveness*springiness)

is 69%. This reflects a digestibility of ~20% over 5 hours. The predicted overall mass transfer rates for the remaining conditions: 3-10, were all in the same OoM; $x10^{-08}$ m/s with insignificant differences, as shown in figure .

Eventhough, there might be similar chewiness of specific volume greater than 2.5 cm3/g, as shown in Figure.6.7, the digestibility rates may still be different, evidenced by breads digestion from condition 2 (Figures; 6.9.& 6.10.). The very fast overall mass transfer rates of glucose may be explained by the effortless non-reactive system, and homogenous solution which allows infinitely small resistance to mass transport of glucose diffusion through the membrane. The other systems were bio-reactive and heterogenous in its form, and were prone to diffusional resistances, such as binding of enzymes to starch and release of products/glucose from the food matrix and through the luminal medium through the membrane interface.

The differences observed in digestibility among the breads may be explained by the water content hydration levels before baking and specific volume levels reached after the baking process. The low level of digestion reached under condition 1, may be a result of the baking temperature, where it was 20 units less during the baking process. Accrodoing to Bjorck et al., (1994), processes that derange and break up the foods' physical structure, will result in elevated plasma glucose and insulin responses. Brand and others (1985), have also found

that cooking will enhance bioavailability of starch, by splitting starch molecules and increase the chance of amylase to bind to it.

Fardet et al. (2006), studies on wheat breads that contains gluten, has taken into account that the physical structure, is the most influential variable on postprandial glycemic responses (in-vivo), noting that the more condensed the structure, the more diminished is the glycemic response. The structure of the dough may also affect heat transfer during the cooking process, therefore the extent to which starch is gelatinised may be influenced by these operations, resulting in vastly different degree of starch damage in the final bread product (Borczak et al., 2017; Parada et al., 2011). Additionally, the less dense loafs suggest that the structure may be easily break down in the physical mixing of the digesta, as the cohesive forces holding the particles together may be weaker. This will increase amylase to starch interaction during digestion. Also, the behaviour of glutelin, the major protein found in rice flour, may behave differently, under specified hydration levels and proofing temperature (Ju et al., 2001), in the dough, resulting in different digestibility profiles of starch.

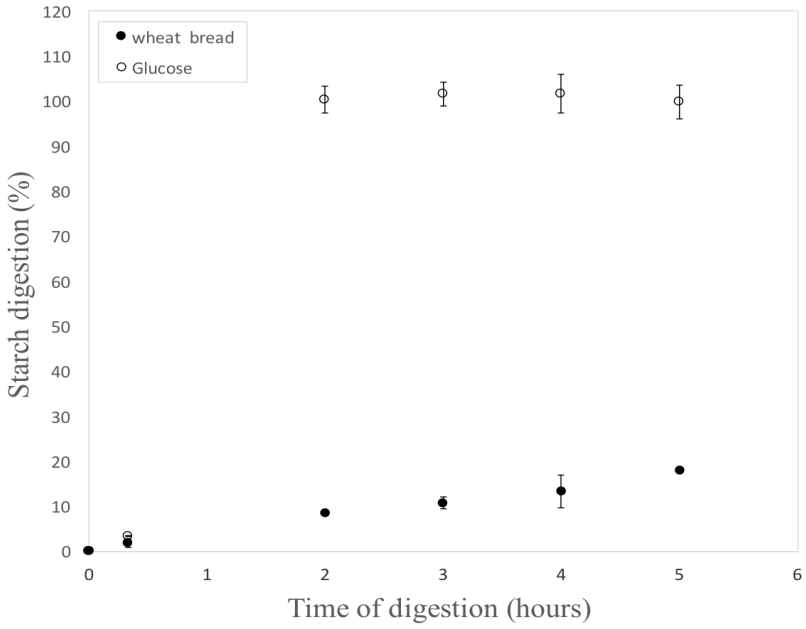

Fig. 6.8 Digestion rate plot of glucose and wheat under small intestine digestion.

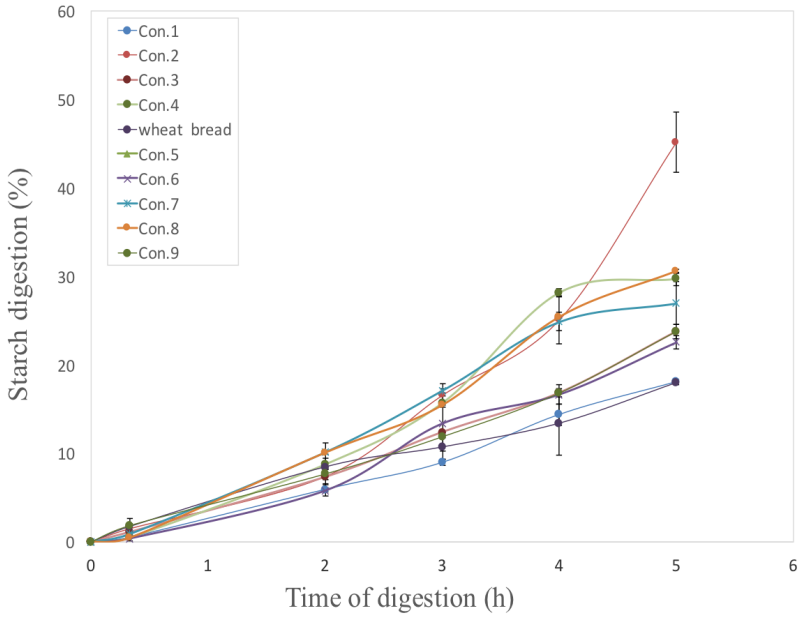

Fig. 6.9 In vitro digestion rate plots of In-vitro starch breakdown in gfb. (% digested starch-g glucose/100g total digestible carbohydrate)

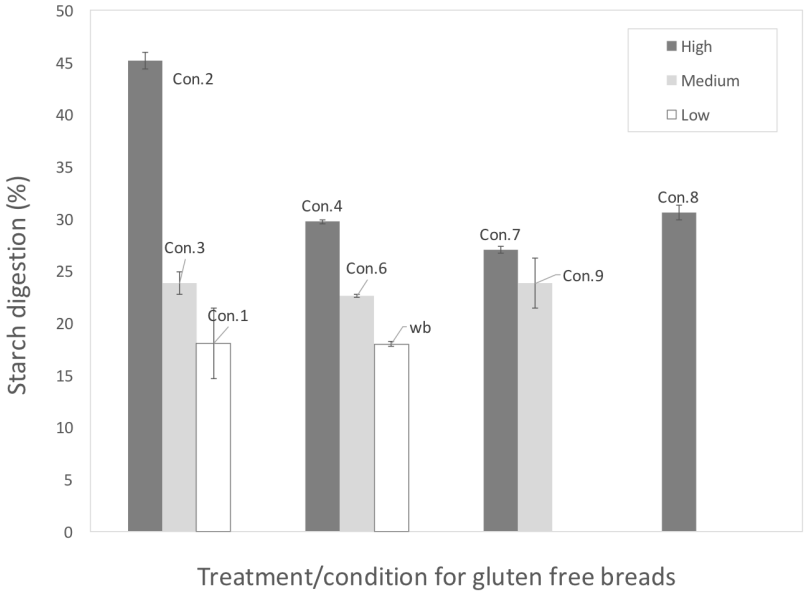

Fig. 6.10 Categorical overall percentage of starch digested at the end of 5 hours: High digestion (26-45 %), medium (20-24%) and low digestion (16-18%).

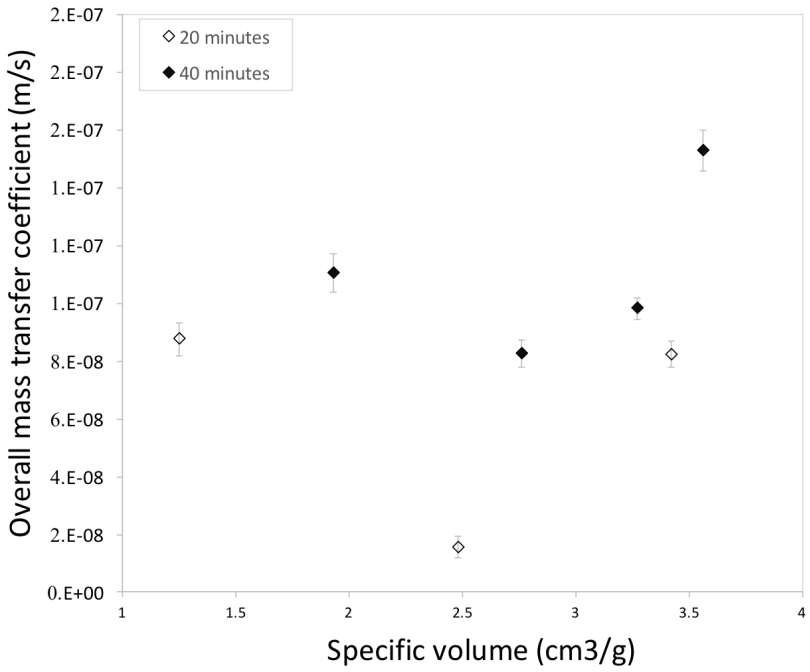

Fig. 6.11 Dependence of overall mass transfer rate on the loaf's specific volumes.

6.3.4 Optimisation of loaf specific volume: response surface method (RSM) - first steps

Having loaves with maximised specific volume are imporatant sensory parameters for consumer preferences. In order to achieve loafs with maximised specific volumes, a first step response surface method approach, was taken to derive optimised water ratio hydration levels and fermenting proofing times. Figure.6.12. shows the Pareto plot, indicating the main effect contributing to the outcome maximise specific volumes, when a $2K^2$ full factorial experiments were carried out. The main effect came from the water ratio hydration level, with the effect of fermenting/proofing times are important but not as important. There was also a negative effect coming from the interactions of these two variables. Since these are early stages optimisation time stamps, this negative effect will not be ignored for the purpose of deriving an appropriate predictive model.

Figure.6.13. illustrates the corresponding contour plots, indicating little curvature within the constrains of the experimental design. A base value/central point of 0,0, corresponding to 79.5% hydration and 30 minutes of proofing times were used. The coded variables and real world units used to generate these plots are shown in Table.6.2. The data was fitted to generate a first order predictive model as shown in equation.6.2. and take the form in

		Coded variables		
Variable	*Symbol*	-1	0	$+1$
Hydration level	XA	59	79.5	100
Proofing period	XB	20	30	40

Table 6.2 Variables and their levels for RSM

	Estimate	*Std.Error*	$t-value$	$Pr(>\|t\|)$
Intercept	2.38600	0.08800	27.114	0.0235*
H	0.84000	0.09839	8.538	0.0742
T	0.31500	0.09839	3.202	0.1927
H:T	-0.02500	0.09839	-0.254	0.8416

Table 6.3 Regression coefficients for first order model

equation.6.3. Once more, the interaction coefficient is not important relative to the main effect of water ration hydration levels. The maxima response surface for specific volume of loaves, suggest that optimal gluten free breads can be prepared from 100% water hydration and and 40 min proofing times. Lowering of proofing times may also improve the specific volumes.

$$y = \beta + \beta_A + \beta_B - \beta_{AB} \tag{6.2}$$

$$\tilde{y} = 2.386 + 0.84_{X_A} + 0.315_{X_B} - 0.025_{X_A X_B} \tag{6.3}$$

This model provide good guidance (with regression coefficients shown in Table.6.3) in the next steps, such a central composition design quadratic models, to improve the production of a new factorial that will enable better fit to the surface, in manufacturing breads with increased specific volume for reduced digestibility. It should however be used with caution as the model does not account for the complex chemical reaction and heat transfers occurring at various stages of the manufacturing process, which highlight the opportunity to include these parameters in future experiments to develop more robust predictive models developed for gluten free breads.

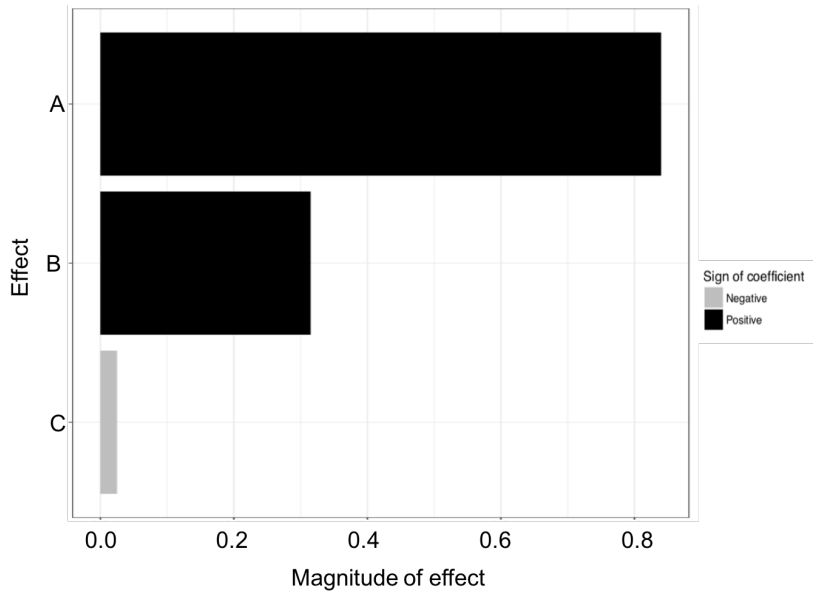

Fig. 6.12 Main effect affecting gluten free loaf specific volume: A - water level, B - dough fermentation time and C, interaction of A and B.

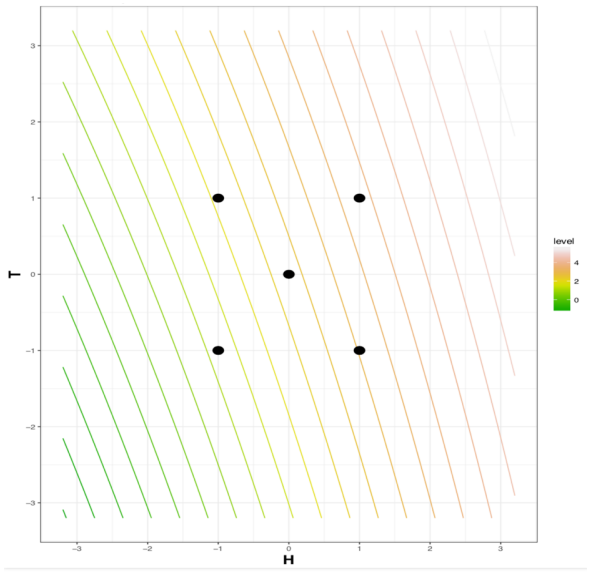

Fig. 6.13 Contour plot (Response surface method): T- dough fermentation time, H- hydration water level. Centre point- 2.21 cm3/g. coded values.

6.4 Conclusion

The hypothesis was that the manufacturing parameters for baking breads can be manipulated to vary the structures of breads, which may affect their digestibility kinetics. The specific volume of loaves, structured through different proofing times, hydration levels and baking temperatures altered starch digestibility in breads. The loaf specific volume can be optimised through increase hydration and fermentation times. However, increased loaf specific volume may not lead to a reduction in starch digestibility, suggesting, that, other processing factors could be manipulated to increase loaf specific volume which may still lower starched digestion, such as; the ratio of rice flour to corn starch, baking temperature and proofing rates. The preliminary predictive first order model promises good indication to further optimise the manufacturing of gluten free breads under these parameters. The next steps would be to perform digestion near real, including simulating oral digestion, and intestinal digestion to understand how gluten free breads may digest differently under the effect of gut motility using the dynamic duodenal model.

Chapter 7

Structure-mechanics-digestion: bolus breakdown

This Chapter was designed by myself in full. Prof. Serafim Bakalis gave advice to detail the experimental design and procedures. This chapter came from observations from static experiments after realising that the breads collapse under its own weight, during digestion in stirred tank reactor (conical flask). The early experimental was done by Dr. O. Gouseti via optical imaging.

Abstract

A strong relationship exists between food structural changes and its physiological responses, such as; satiety and molecular release, in flow in the intestinal tract. We wish to understand how and why structurally different breads can impart similar or different glycemic responses, or speed up or prolong satiety during gastric digestion. The mechanism behind bread resistance to breakdown under gastric gut constrains, if understood, can be used to clarify strategies bread used to regulate bread digestion in vivo. To study the kinetics of the breakdown and subsequent disintegration phenomenon occurring in bread, boluses; white, whole meal and multi-seed, were prepared by in vitro and in vivo methods, placed under acidic and neutral free diffusive systems and acidic shear system (multi-seed) and then optically captured by a novel one-dimensional approach. Bread bolus breakdown may be influenced by the technique of bolus preparation, swelling and the fluid transport into its matrix, as described by the effective diffusional coefficients. The kinetics of swelling was favoured by whole meal boluses, displaying 7% and 46% faster swelling rates than white and multi-seed boluses in acidic systems respectively, but decreased by 5% and 11% for white and multi grain boluses in neutral systems. Fickian diffusion indicated that fluid transport into bolus matrix are regulated by diffusion limited and degradation limited processes (Case I and Case II transport). Weibull's swelling food model best represented bread boluses swelling phenomena, compared to Peleg's swelling food model..

7.1 Introduction

Most of the foods we eat daily have a defined structure. Furthermore, there is growing knowledge on the interaction between food structure and its functions on digestion, starting from oral mastication. The effects of food structure on its breakdown is crucial to understand when designing novel foods as nutrient delivery carriers, and trying to regulate gut function and digestion (Gao et al., 2015). Most real foods are structurally complex, making their physical and mechanical properties poorly clarified, and difficult to produce. While some

foods structures are a result of nature, such as milk, grains and nuts, others such as; creams, spreads, cakes, buns and breads, are reliant on the science and engineering of restructuring and assembly, by food formulators and manufacturers (Grundy et al., 2016; Norton et al., 2014). Among manufactured foods frequently consumed, breads are known to contribute to postprandial hyperglycemia responses, because of their complex microstructure that arises from both formulation and processing (Khatkar et al., 1995; Nicolas et al., 2016; Singh et al., 2010). Consequently, efforts to understand bread digestion as a high GI (glycemic index) food, are mostly rooted in the study of starch hydrolysis kinetics by analytical investigations, for example, the release and uptake of glucose (bioavailability) (Rosell et al., 2001; Koh et al., 2009), while microscopy and visualisation techniques on bread digestion to understand nature of the degraded mechanics have been seldom done.

The most suitable reason to explain why solid foods, such as breads are chewed in the mouth is that it is required for rapid absorption (Prinz et al.,1997). Chewing or mastication is the first stage of the food digestion processes in transforming foods into fuel. But, before it can be digested further, it is first modified into a bolus through a series of complex operations of the mouth (tongue, teeth and saliva); whereby, the food matrix is simultaneously destroyed and reconstructed into a 'soft-safe' bolus to be swallowed (Woda et al., 2010; Prinz et al.,1997). Once the bolus is formed, it usually contains particles ranging from 0.8 to 2.29 mm, which is then swallowed, conveyed to the stomach by the oesophagus and begins to breakdown in size to micro length scales (μm). The combined effects of peristaltic contraction forces from the stomach walls, chemical penetration (acid hydrolysis), enzymatic activities and forces holding the particles together during gastric digestion are responsible for this complex disintegration phenomena (Schulze 2006, Hall 2011, Bornhorst 2016). The degree of chewing will influence the extent of gastric bolus disintegration, and subsequent emptying rates, affecting the kinetics of nutrient uptake and transport in the digestive tract (Kong et al., 2008; Kong et al., 2008a; Bornhorst et al., 2013; Guo et al., 2015; Yurkstas, 1965; Rey et al., 2007). Forexample, Ranawana et al. (2013), studied in vivo the mastication and particle size effect on blood glucose levels, and found that shorter chew cycles attenuate glycemic index during rice digestion. Similarly, acid uptake into chewed rice boli with essentially different structures, has been found to influence rice breakdown and further carbohydrate digestibility during gastric digestion (Mennah-Govela et al., 2015). In the same way, it is expected that different breads should similarly control digestion based on their different structures, by either facilitating faster or slower acid diffusivity in their structures to modulate digestion.

In breads, the microstructure is highly influenced by cellular foam networks of gluten proteins, formed during the baking processes, giving rise to breads with different compressibility and porosities. The porosity of breads has been recognised to be the main element as to why breads have a high GI overall Hera et al. (2014) and Mishra et al. (2012). Some work has been reported on the effect of bread structure on digestion in the oral phase (Gao et al., 2015 and Hoebler et al., 1998); however, little is known about the structural changes causing breads to disintegrate, or its behaviour upon contact with digestive fluids after oral processing and during gastric digestion. Consequently, to describe and characterise the structure changes of bread bolus during break down and disintegration is difficult to undertake. Disintegration studies of foods in humans has been mainly done by non-invasive methods (Moore 1984, Hausken 2001). For example, Marciani et al. (2001) studied disintegration in relation to gastric emptying, by means of echoplanar imaging, using a bolus of viscous locust bean, where tiny pieces were reported to fall off the surface, but the exact breakdown events was never quantified. Some studies have investigated disintegration from studying individual particles during digestion in-vitro Kong et al. (2008). However, food is delivered in the stomach as a bolus before it begins to digest into particles and should therefore be considered on this scale. Recently, Bornhorst et al. (2013) has use different bread systems to study the link between kinetics of bolus disintegration and glycemic indices response. The method measures the rate of hydration (bolus mass retention), which assumes that once the bolus is fully hydrated, then disintegration will take effect. This is not always the case, as disintegration may follow the mechanisms; (a) swelling due to surrounding fluid penetration and (b) erosion and breakdown phenomena, which can occur independent or concurrently. Since breads contains protein networks their breakdown mechanisms may follow some of the events described by Mercadrieto et al. (2007) who studied the swelling of proteins.

Swelling and erosion are important elements in digestion, because if swelling is suppressed, nutrients will remain trapped inside some food structures. Prolonged suppression of swelling can increase satiety. Swelling studies on food are largely done prior to digestion, with aims to fit data through numerical modelling. For example, Joshi et al., (2015), study the swelling of tea particles by optical measurements and Malumba et al. (2013) studied wheat starch granules behaviour under different thermal treatments. Mercadrieto et al. (2007), described the swelling of b-lactoglobulin and Oztop et al. (2011), described the swelling of whey protein gels at high moisture content. Few studies have been done that describe and quantify swelling of food bolus during digestion in the stomach. However, Gaserod, Haraldsen, and Lynch (2008) describe ”gastro-activated” swelling of alginate fibres at low pH’s in the stomach, which increase the viscosity of the surrounding fluids, tested by different

bread formulations. Disintegration was not accounted for in swelling of alginate fibres study, which is a part of the breakdown mechanism that exists in the stomach for solid foods. The contribution of swelling and erosion of compact soft matter - solid meals for the release and metabolism of starch and its role in glycaemic responses and satiety, still remains an area to be exploited. It will improve knowledge on the strategies taken by food structures during gastric digestion and its effect on gut function to regulate food digestion. The objective of this is to explore how food bolus is destructed in various breads, under simulated physiological chemical conditions, by varying the pH. This draws on a novel approach to capture the phenomena by one dimensional optical means. Ultimately, these data can be used to develop numerical models that can describe structure function behaviour in carbohydrate foods digestion.

7.2 Material and methods

The chemicals used in these studies were sourced from Sigma Aldrich Chemical Company UK unless otherwise stated.

7.2.1 Sample preparation

Three bread types; white, wholemeal and multi-seed, were procured from the local store to be investigated *in vitro* in line with Table.7.1. Foods were selected to include a range of structural differences with essentially varying glycemic index values (Eelderink et al, 2015).

7.2.2 Simulated salivary fluids (ssf)

The ssf, was prepared according to the methods of Chapter 3 of the thesis; section 3.1.3. The ssf, contains 0.15 M NaCl and the pH adjusted to 7 using 1.0 M HCl if required, α-amylase from hog pancreas (50 U/mg) and 6μg/ml lysozyme solution, both added on the day of digestion, after pre-warmed to 37^0C (Mandalari et al., 2009 ; Moreno et al., 2009).

7.2.3 Simulated intestinal fluid (sif) preparation (Gastric and Duodenal)

The sif was prepared according to the method used by Symonds and Brennan (2006).The sif contains; 20mM NaH_2PO_4; and 10mM NaC, adjusted to pH 7 (neutral) using $NaHC0_3$ or to pH2 (acidic) using 0.1 M HCl. For experiments that require enzymes in surrounding

Bread type	In-vivo chew (cycles)	In-vitro chew (seconds)
White bread (wb)	20	8
whole meal bread (wmb)	20	8
Multi seed bread (msb)	30	8

Table 7.1 Experimental design for bolus swelling and erosion under static digestion

digestive solutions, α-amylase from hog pancreas (50 U/mg), was added at a rate of 0.2g per litre on the day of digestion. The setup is shown in Fig.(7.1).

7.2.4 Bolus preparation and experimental setup

Chewing - *in vivo*

Bread samples, 3.5g of each, with the crust removed, were chewed until the urge of swallowing (reflected by the chew cycles-Table.7.1.), by one volunteer with normal dentition in the un-fed state. The chews were expectorated, then the boluses were shaped ex-vivo into spheres of ~16mm diameter, using an appropriate mould. It takes around 10 -30 seconds to have the bolus spheres to be ready, somewhat reflecting the time it takes to swallow *in vivo*. The volunteer thoroughly rinsed the mouth with drinking water between each sample.

Simulated Chewing

Bread samples, 75.0 g each, with the crust removed, were diced nto 4cm^3 bite sizes. 24.5ml ssf, pre-warmed at 370C, containing enzymes; α-amylase, 0.018g and lysozyme 14.7 μl and water 50 ml, was poured onto the bread and placed in a Kenwood food processor Kenwood, FPP210 series, (Designed and Engineered in the UK, Made in China), then artificially chewed for 8 seconds, acceptable to reach the requirements for swallowing. According to Hoebler et al., (2000), once the desired particle size is achieved (< 1mm), the bolus is safe to move to the gastric stage of digestion similarly done according to the methods section of Chapter 3 of the thesis. The chew was collected, and was shaped into bolus spheres of ~16mm diameter, using an appropriate mould, similarly to the *in vivo* chewed.

7.2.5 In vitro digestion

The boluses were then suspended by a hook into the *in vitro* model, after which simulated intestinal fluids (sif), 500ml at 37^{0}C (pH's 2 or 7), were added "on bottom" upwards via

syringe. This 'on bottom' set up was important to reduce turbulence generated from the inflow of digestive fluid to fill the the *in vitro* model, avoiding premature fluid permeation and bolus deformation. After filling to the 500 ml mark, recording with a high speed camera (Nikon Coolpix 5400, Nikon Corp., Tokyo, Japan) at 120f/s was done up to 1 hour. Figure.(7.1) illustrates the experimental setup followed. This experiment is about intra-gastric fluid diffusion into food matrix. Internal diffusion of intestinal fluids into food polymer systems may be influenced by several factors; the penetrant's (gastric juices) speed into structures and the physical properties (glassy state and relaxation capabilities) of the components/polymer. As a result the movement and diffusivity that occurs into polymer systems can be described and categorised as Case 1 (Fickian diffusion) and/or Case 11 (anomalous diffusion) to set out the relative importance of the mechanism of transport. The transport mechanism can derived from Fick's Law of diffusion which will later be discussed in the results section of this Chapter.

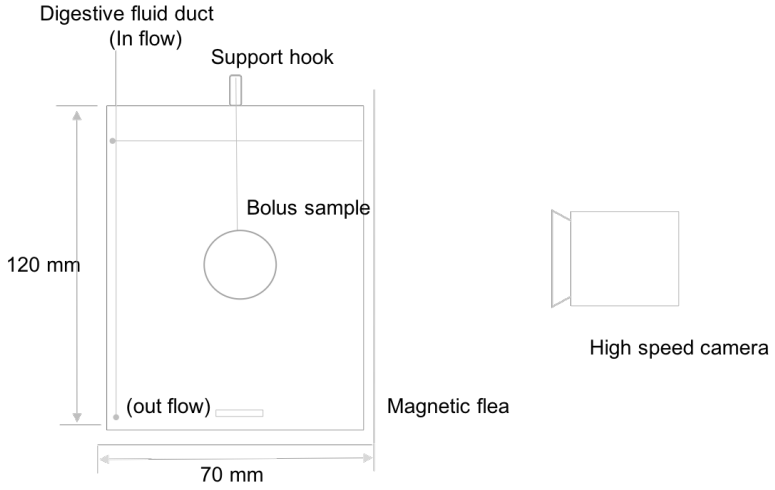

Fig. 7.1 Schematic of *in vitro* bolus breakdown under static conditions in *in vitro* model which is 70 X 120 mm in L x H dimensions.

7.2.6 Image analysis and processing

The videos were extracted into individual frames of still pictures and analysed using ''video to JPG converter" software. The images of the bolus structures obtained over time were associated with their diameter (and radius) by utilising image analysis similar to the method of Joshi et al. (2015). The ImageJ2x software estimates the projected surface area of the particle by summing the number of pixels it occupies. Since the bolus particles were moulded

into a sphere, its projected image on a 2-dimensional plane (2DP), is a circle, and the starting radius (δ_0 or r_0) of each bolus was established at time zero (t_0), 8.120 $\pm$0.198 mm.

7.2.7 Particle image velocimetry (PIV) to derive velocity profile

The velocity profile of the mixing was evaluated using PIV similar to the method of Chung et al.,(2009). The stirred tank was a rectangular glass flat bottom vessel with a magnetic flea at the bottom, and the working fluid was digestive components that were seeded with iron- Fe^{+} tracer particles. The tank dimensions were: (70mmX120mm). The magnetic flea impeller had a diameter, *D*=0.158 m, and length of 0.05m. A schematic view of the PIV experimental apparatus is shown in Figure.(7.3).

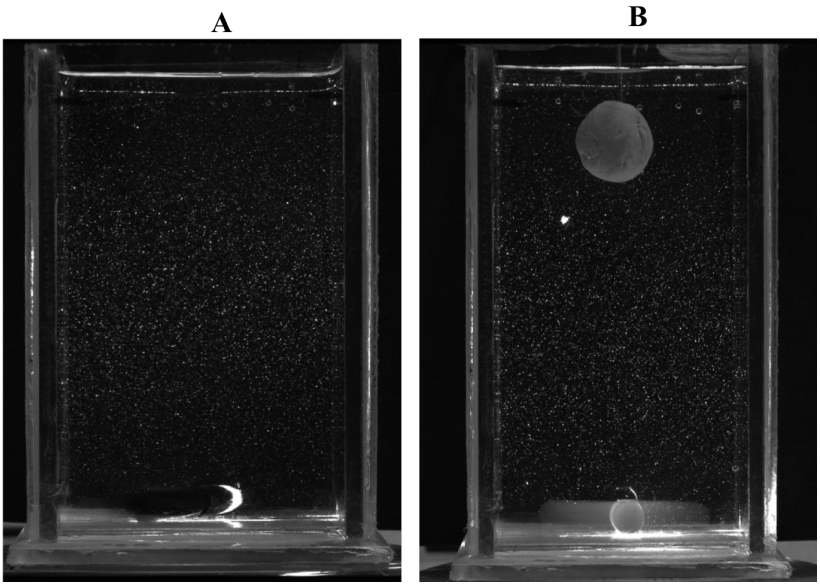

Fig. 7.2 Digestive fluid seeded with tracer particles; (a) without bolus (b) with multi seed bolus bolus, to understand the effect of mixing on bolus dissolution.

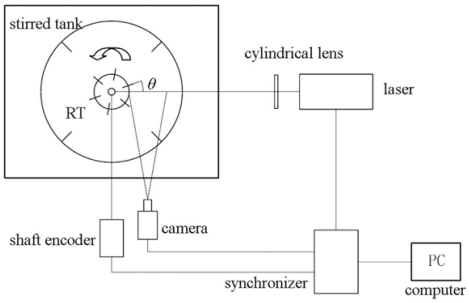

Fig. 7.3 PIV set up, to determine the velocity profiles in the digestion stirred tank under shear mixing at 100 rpm by magnetic flea.

7.3 Results and Discussion

7.3.1 Simulated chew and human chewing: breakdown mechanics

The morphological and structural changes on the mm scale of the two masticated methods on white bread were revealed using image analysis, described in subsection.7.2.6. Figure.(7.4)., shows typical images of white bread boluses when submerged and kept in gastric fluids at pH 2. There were a remarkable differences in the bolus structure breakdown between the two treatments (bread types). Fig.(7.4).A., shows bread bolus prepared by simulated mastication using a chopper food processor and Fig.(7.4).B.,shows bread bolus prepared by the healthy volunteer (in-vivo chew). In-vivo chewed bolus displayed a "cloud" like "puffing" characteristic deformation during the penetration of intestinal fluids into its matrix, which was not displayed by the in vitro chew. After an hour of submerged digestion, in vitro chew had the slowest swelling and erosion trends. This is an indication that the type of in vitro chew carried out in masticating the bread, to form a bolus can compromise structural digestion by slowing the swelling and erosion rates. Conversely, in-vivo masticated bolus during submerged digestion, showed rapid swelling, degradation, and deformations of its structure, which took approximately 25 minutes to complete. Swelling will initiate when the solid-liquid structure of the bread boli make contact with the liquid interface. In-vivo chew was used to establish the ”near-real" breakdown pathway under purely diffusive conditions.

Three key stages were identified in the typical breakdown mechanism, when the white bread images in Figure.7.4.B., were processed over the digestive times to capture the radius changes of the bolus, and is illustrated in Figure.7.5.A.,; The identified stages are used in the description, computation and analysis for the rest of bread bolus disintegration studies.

- A linear swelling stage, lasting approximately 10 minutes in Figure.7.5.A and involving a change in radius thickness (δ, 9.8 X10^{-03} m), while also displaying some surface erosion.
- An "almost" plateauing stage, where the velocity of swelling is nearly balanced to the velocity of erosion, giving approximated constant diameter of 0.02 m, leading to a net swelling effect lasting between 10-25 minutes of digestion. Additionally, in this stage, one can notice up to ~10 disruptions, removing the material from the parent bolus (erosion): identified on Figure.7.4..(B-C) which is related to the plateauing section of Figure.7.5.A.
- A major removal and disruption stage in image E on Fig.7.4.A, at the 25th minute, and is represented by the red locust on Fig.7.5.A. As the materials continue to be removed (radius change (-1.01 X10^{-03} m)), the structure is weakened and move into the final disintegration stages. The bolus undergoes structural damage, breaking down, increasing the digesta in to a much larger exposed surface area (tiny particles).

Differences observed during the structure-mechanistic-digestion between the two boluses may be explained by the mastication method. The 8 seconds of chopping with the blades of the food processor may have "masticated" the bread with particles of much smaller sizes compared to in-vivo chew bolus, which was formed from a more "kneading" method. When food bolus is constructed; real (in the mouth) or simulated (model), they are transformed into solid-liquid systems. Each system formed, may be hydrated with saliva at different degrees. Evidence exist indicating that the grinding mechanism used to conduct the chew for the same foods can bring about different types of compression that will cause different ranges of fracture and particle size for the same food material (Fontijn-Tekamp 2000, Chen 2009, Engelen 2005). Therefore, the very small particles formed by the in-vitro chew may stick to each other readily. Consequently, the cohesive forces between particles for the same bread created by the two different mastication methods will vary significantly and may be broken down differently for each bolus, due to the differences in structure at the microscale (μm). Unlike the in-vitro bolus, the ex vivo bolus which is impregnated with human saliva during reassembly, may have larger liquid bridges available between each particle or and cluster of particles within the bolus itself. This may be a precursor for easy diffusion of fluids into the bolus matrix and allow faster penetration for bolus breakdown. i.e. pre-existing liquid bridges created by saliva. The pre-existing liquid bridges, may play a role in the type of capillary function in each chewing method and essentially each bolus type (white,

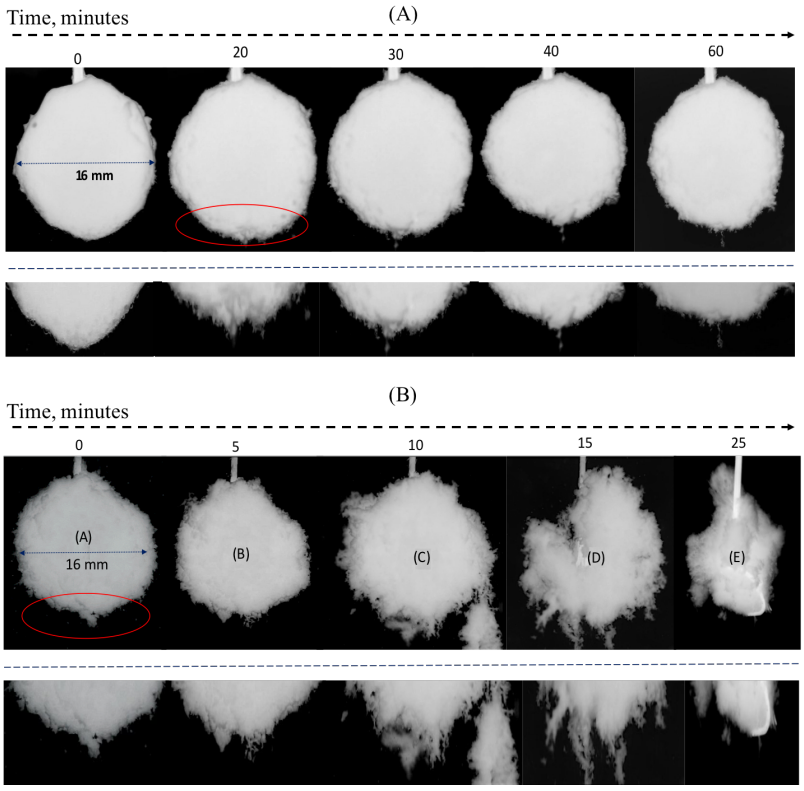

Fig. 7.4 Structure-mechanics-digestion: progression of white bread bolus breaking apart in *in vitro*; (a) simulated in-vitro chew (b) human in-vivo chew

wholemeal and multi-grain). This may be the reason for in vivo chew to "puff" relatively faster; ~10 min for wb, ~2 min for wmb and ~20 min for msb in Fig.7.5, compared to the in vitro chewed white bread bolus which took and more than 60 minutes to puff and to break apart, as this bolus had more liquid bridges (smaller and more particles) per unit area (~823 mm^2). This will establish a stronger capillary state, as the chewed bolus ill have the ability to exert stronger adhesive forces between connecting particles and particle clusters due to capillary and surface tension effects, similarly described by Iveson et al., (2002). The extent of the capillary and surface tension effects may have an impact on the diffusivity of intestinal fluids, either reducing or increasing mass transfer of the diffusion front, thereby establishing different permeation rates when covered with, and submerged in digestive fluids.

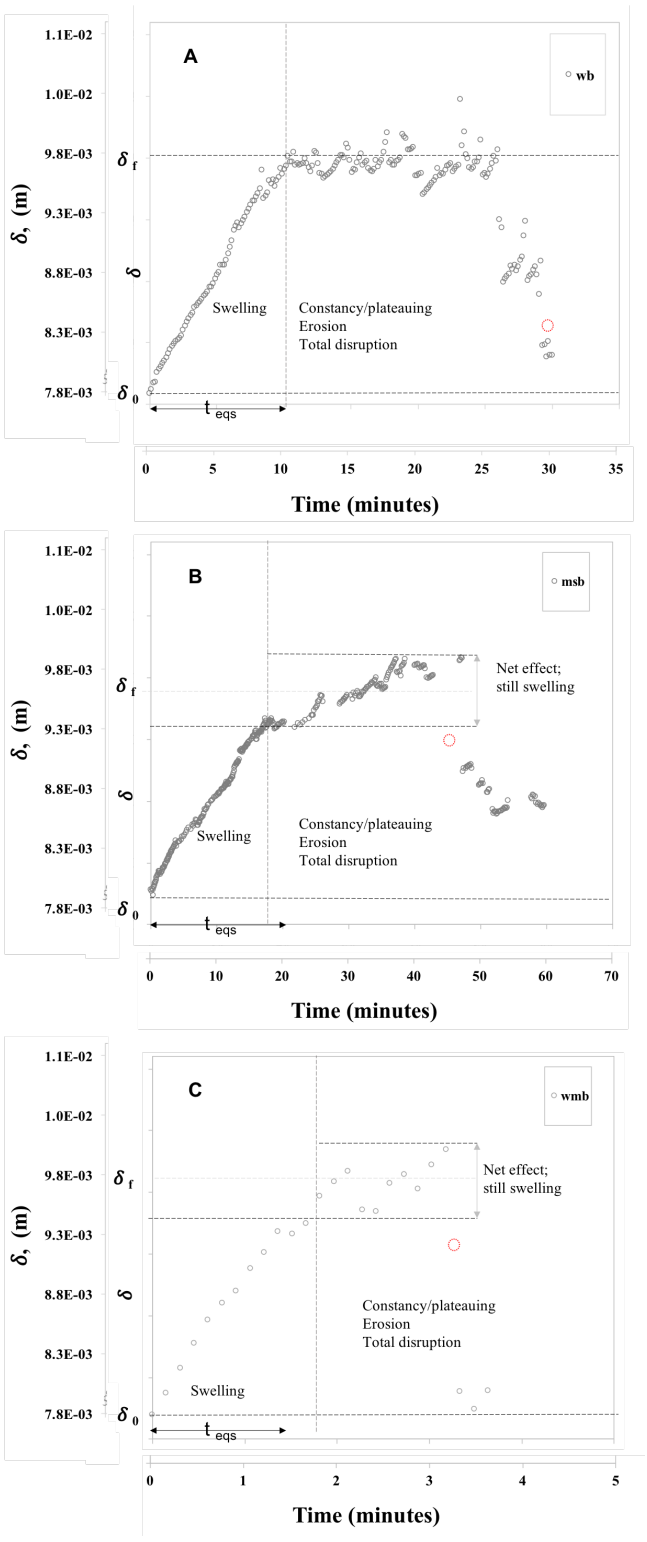

Fig. 7.5 Schematic of a typical structural changes pathway (swelling and erosion, constancy/plateauing and then disintegration) undergone by human chewed white bread bolus (wb)-A, processed from direct observed images on Fig.7.4.B, multi-seed bread (msb)-B and whole meal bread (wmb)-C, when in contact with digestive fluids at 37 ^{o}C at pH2. The hashed horizontal lines were used to determine δ, and dimensionless swelling ratio, f; t_s is the time to reach equilibrium/plateauing, δ_f is the final radius thickness of the boli at equilibrium $\delta_e q$. The doted red locus shows region and point of total destruction during the bolus lifetime.

7.3.2 Effect of pH on swelling rate behaviour: mechanism driving bolus swelling under pure diffusion

Herein, the bread bolus discussed are based on human masticated breads, where the different bread boluses were shaped ex-vivo, and placed in a digestive chamber with varying pH (2 or 7), described in section.7.4.1. Figure.7.6., illustrates the swelling and erosion behviour of three breads bolus types: white, whole meal and multiseed under acidic-pH2 (Figure.7.6.(A)) and neutral-pH7(Figure.7.6.(B)), conditions in a static system. All displayed similar characteristic breakdown mechanism of; swelling, plateauing/ equilibrium and erosion, however, occurring at very different time scales. These break down mechanisms occurs faster in pH2 than pH7 conditions. For example, the swelling phenomena under pH2 conditions, went on for 2, 10 and 20 minutes for wmb, wb and msb respectively and under pH7 conditions, it went for 10, 15 and 30 minutes for wmb, wb and msb respectively, which will be discussed in detail onwards. Figure.7.7., shows the swelling rates extracted from Figure.7.6., by taking the values from the starting radius (δ_0), until the establishment of a net swelling/equilibrium (δ_{eq}). Swelling kinetics, will give some insight on the bread boluses behavioural responses when initially in contact with the continuous phase of the intestinal fluids. The data from Figure.7.6, were fitted to a linear model in Figure.7.7., by plotting the change in radius vs the digestive time, with intercept on the y-axis. The gradient was taken as the rate at which each bolus took to reach its equilibrium swelling radius, to determine the swelling rate (m/s), which is recorded in Table.7.2.. This was defined as the equilibrium swelling velocity V_{eq}, computed from equation.7.1., where δ, is the change in radius thickness, and t_s, is the equilibrium swelling time during digestion.

$$V_{eq} = \frac{\delta_0 - \delta_{eq}}{t_s} \tag{7.1}$$

Boluses from whole meal breads are the most sensitive in all pH conditions. It had a change in swelling radius thickness of 1.8 x1 0^{-03} m, in 2 minutes in pH2. However, it took a longer time (10 min) in pH7 than pH2, to reach its maximum radius, having a thickness of 9.65x10^{-02} m as shown in Figure.7.7. Boluses from white bread was the second most sensitive to swelling and erosion in both pH conditions. It took about 10 minutes to reach its maximum swelling radius of 1.9 x 10^{-02} m in pH2 and approximately 15 minutes in pH7 reaching a thickness of 9.67 x 10^{-02} m. Multi-seed bread boluses in pH2, reached its maximum swelling in about 20 minutes, and took ~10 minutes longer in pH 7, having radius thickness changes of 1.3 x 10^{-03} m and 1.7 x 10^{-03} m respectively during swelling (Figure.7.7.). Additionally, msb boluses in both pHs? had very similar swelling equilibrium

and erosion patterns as depicted in Figure.7.6. These results suggest that msb with the less inclined slopes of swelling, behaved the least sensitive among the wb and wmb boluses.

Even with the similarities in bolus chew (same individual) and pH treatment, plateauing trends and erosion patterns behaved very different for each bolus type. The Equilibrium established was very short for whole meal boluses in pH2 acidic system in Figure.7.6.A, where the equilibrium seemed to may have never established, as there was no observable net swelling occurring over time, in comparison to neutral system at pH7 as shown in Figure.7.6.B, where a net swelling was established for 2-3 minutes before major erosion occurred, removing a thickness of -1.9 X 10^{-03} m initiated at 12 minutes into digestion. The boluses from white breads in pH7 displayed in Figure.7.6.B, had the plateauing effect lasting only 2-3 minutes and major erosion occurring at 15 minutes of digestion while, removing -4.0 X 10^{-04} m of thickness. White bread bolus in pH2 however, had a longer plateauing lasting around 15 minutes and began major erosion around 25^{th} minute in submerged digestion, removing -4.0X10^{-04}m of thickness, in Figure.7.6.A. The multiseed breads (msb), displayed profiles of prolong swelling and equilibrium, longer than any of the other two types of boluses and the bulk erosions are seen close to an hour of digestion in Figure.7.6. The equilibrium pattern for the msb boluses were not extremely different, however major bulk erosion time points varied; in pH2, major bulk erosion begins at the 47th minute of digestion removing -8.6 X10^{-04}m (Figure.7.6..A), which is a 53 % decrease when in conditions of pH7, which occurred around the 54^{th} minute of digestion, removing -4.0 X 10^{-04}m of thickness (Figure.7.6.B).

On one hand, swelling rates that were computed from equation.7.1.,using Figure.7.7., and recorded in Table.7.2., were evidently occurring faster in lower pH treatments, (pH2) than higher pH's (pH7) for wmb and msb boluses, reaching equilibrium swelling at 5 times and 2 times faster for wmb and msb respectively. For wmb, the swelling rate was increased from 3.29 X 10^{-06} m/s to 1.51 X 10^{-05} m/s which is an magnitude of order faster under acidic conditions. Similarly, for msb, the swelling rates increased by an order of magnitude faster in acidic conditions, moving from 7.05 X 10^{-07} m/s to 1.125 X 10^{-06} m/s. After reaching its swelling equilibrium capacity, wmb had fated in ~3 minutes, making it the fastest disintegrated bolus at the lower pH treatment. Additionally, it was also the fastest doomed once more in pH7 treatment, disintegrating just under ~17 minutes. On the other hand, white breads (wb), swelling rates were occurring almost identical, 2.29 X 10^{-06} and 2.79 X 10^{-06} m/s with only an infinitesimal increase of 4%, when the pH was raised from 2 to 7. The only

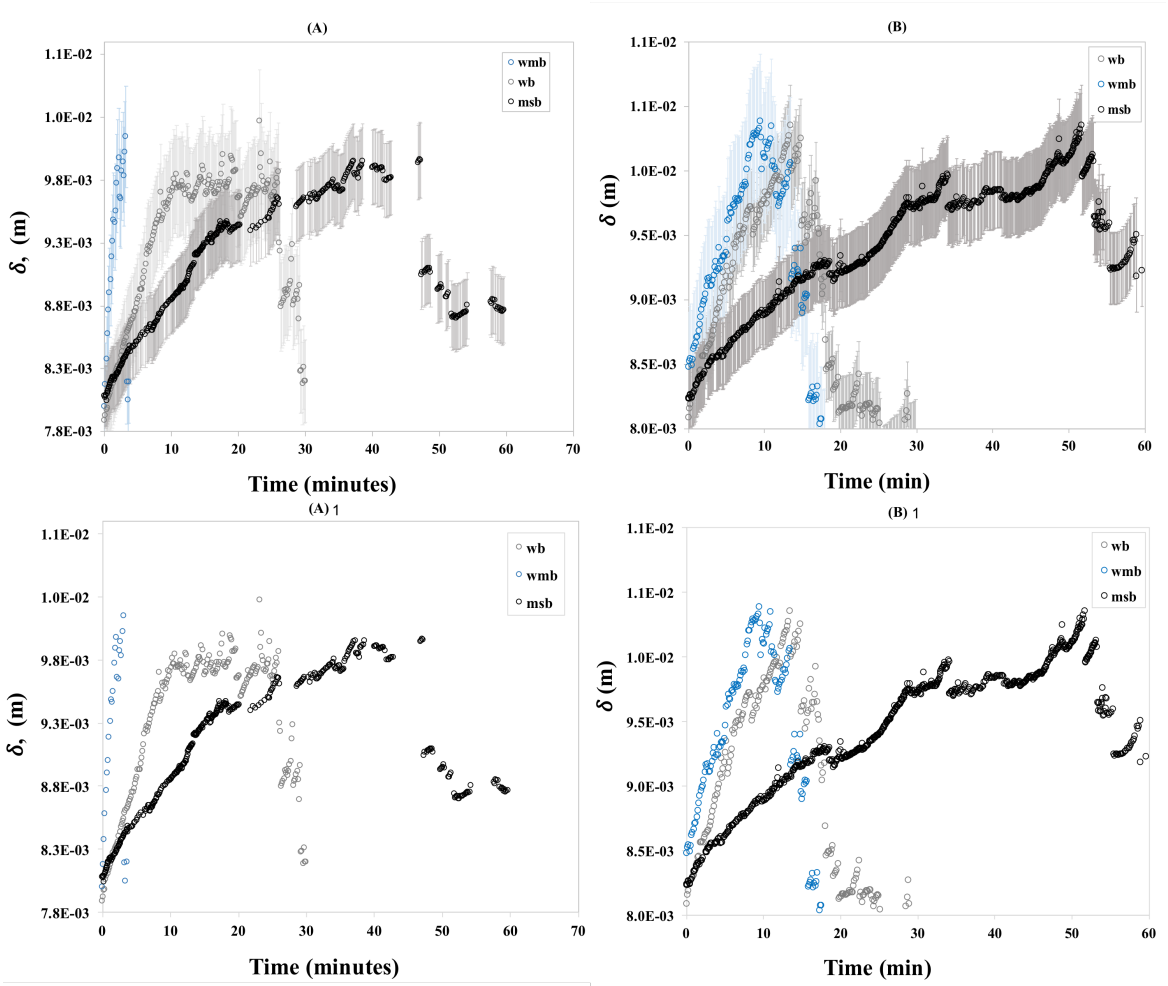

Fig. 7.6 Bolus response to swelling and erosion in static pH systems; (A) boli in ph2 (B) boli in pH7, (wb-white bread, wmb-whole meal bread, msb-multi-seed bread). A1 and B1 are the same profiles fitted without error bars (slightly better resolution on charts). Error bars are standard deviation from four replicas.

major evidently difference seen between wb response is the disintegration, which fated just under ~20 minutes at pH7 and just under ~30 min in pH2 (Fig.7.6 and Fig.7.7).

As boluses had similar geometry, intestinal fluid has to travel the same distance in order to reach the centre-core of the bolus. Therefore, bolus origin impacts the extent of response, the response times and its behaviour to lowering or increasing pH's. The differences may be explained from the effect of food properties on both the chewing process and oral digestion, that manipulate and reorganise the microstructure during the bolus formation. For example, the msb?s were the most resistant to the liquid, because the whole and partially intact grains in the multi-seed breads (msb), could have been broken during the chewing process at different

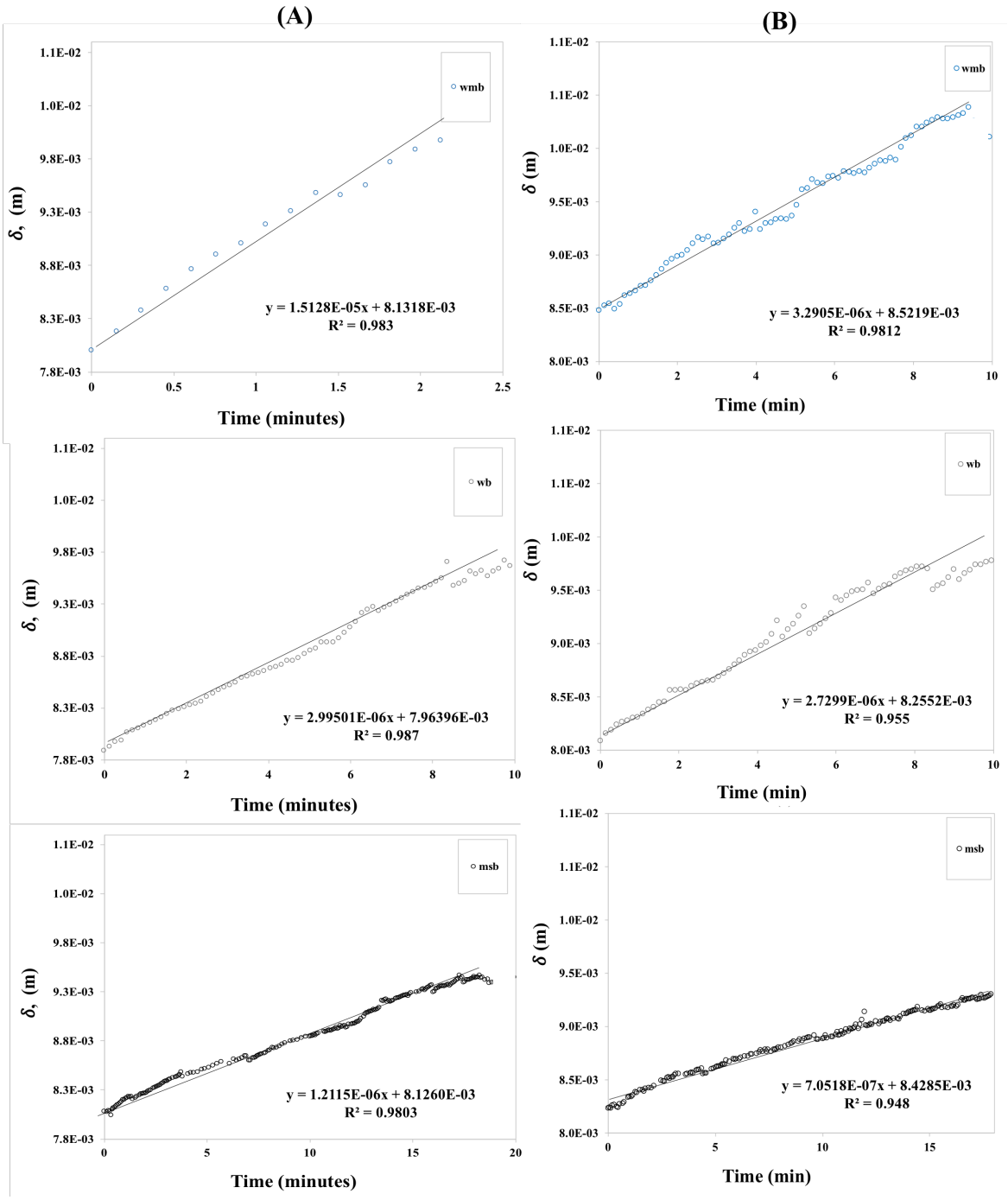

Fig. 7.7 Extracted swelling rates of bread boli in (A) acidic and (B) neutral systems from Figure.7.6.

extents, enough to release plant cell wall components that can alter the inter particle and bolus cohesive forces as well as the viscous effect form of the continuous phase (saliva) (Grundy et

al., 2016) and hence slower swelling and longer retention times to bulk erosion. In the case of the whole meal breads (wmb), the gluten structure and network were already weakened by the multi particulate wheat bran in the baking process (Dikeman et al., 2006). As a result, a weak gluten network in the structure of breads will cause starches to be exposed easily under oral shear, and exposed starch molecules are known to swell in great extent. Rodrigues et al., (2014) demonstrated that starch was heavily exposed after biscuits were chewed and spat out for cryo-sem analysis of the biscuit bolus structure. This might be a reason as to why wmb, displayed rapid swelling in both conditions of pH. For the white breads (wb), the gluten may have been more intact (well formed during the baking process and hence less damaged from mastication), and was able to display more resistance to swelling compared to the whole meal breads. Low swelling rate suggests low fluid penetration. As a result, the resistance of the food matrix changes with increased intestinal fluid penetration will cause different swelling pattern and rates.

7.3.3 Modes of fluid transport into bolus structure

The structural changes and rates of breakdown pathways were evidently different in each bread bolus. The differential swelling rates that were computed from equation.7.1, and shown in Table.7.2., suggest that the microstructure of each bolus may modulate the permeation rates by a peculiar mechanism, in addition to the already existing capillary effect. The systems were therefore examined to make clear, which physical factor/s may determine the type of fluid transport mechanism into the bread boluses. The diffusion mechanism defined by the diffusional coefficient, 'n',can be computed from the simple empirical power law model described by Buckley et al., (1962) and Ritger and Peppas 1987), in equation.7.2. It is usually the first method used to evaluate time dependent swelling in most polymer systems, during hydration. In the same way, the complex bread formulations, containing starch and proteins may behave similar to polymer systems, due to the polymeric constituencies (amylose, amylopectin and gluten) making up the bread at the molecular level. According to Peppas et al., (1994),, the change in geometry/in thickness during hydration may cause the estimated values of the diffusional coefficient 'n', to vary. These changes may be brought about by the behaviour of polymeric constituencies in the bread under different pH.

$$F = kt^n \tag{7.2}$$

Where; F is the amount of penetrant that entered the polymer system and can be defined in several ways (F_c and F_k see below), k, is a constant correlated to the network formed by

In vitro conditions (pH2)	White bread (wb)	Wholemeal bread (wmb)	Multi-seed bread (msb)
Swelling velocity x 10^{-6}(m/s)	2.99 ± 0.65	15.13 ± 3.78	1.125 ± 0.75
Diffusional exponent, n-F_c	0.0502	0.119	0.0559
Diffusional exponent, n-F_k	0.9339	0.7213	0.8687
Fitted to Peleg's model, R^2	0.99129	0.93467	0.982
Fitted to Weibull's model, R^2	0.964	0.96563	0.930

the macromolecular system and swelling medium, and n, is the diffusional exponent, which is an indication of the mechanism of transport.

The equation (.7.2.), is of course based on Fick's Laws of diffusion, by predicting how diffusion will change concentration with time (a diffusion dependent process). The change in concentration can be represented by the change in radius δ_t , at some time (t), as a result of the fluid penetration into the bolus. The equation, (.7.2.), was modified by Crank (1956), Fc, to equation.7.3., and later by Karadag et al. (2000), Fk, to equation.7.4., in simplified forms (Ritger and Peppas (1987) and Korsmeyer and Peppas (1984))

$$F_C = \frac{\delta_t}{\delta_{eq}} = kt^n \tag{7.3}$$

$$F_k = \frac{\delta_t - \delta_0}{\delta_0} = kt^n \tag{7.4}$$

Where; F_c is a fractional measure of the bolus swelling at a given time t with respect to equilibrium swelling; F_k represents the radius ratio at a given time t directly demonstrating how many times the bolus has swollen in the permeate and (δ, is the change in radius thickness as defined in section 7.3.2. This is very similarly used to the swelling ratio or degree of swelling, f, in studies conducted by Mercadrieto et al., (2009), and Wilson (2009), who extensively study protein swelling in different pH?s; where δ_f is the radius at equilibrium and δ_0 is the initial starting radius, similarly used in equation.7.3., and equation.7.4.

It is expect that estimation of the diffusional exponent, n, defined by either F_c (Equation.7.3.) and F_k (Equation.7.4.) from for each of the same bolus in Fig.7.7., would have given similar results, because the physical factors controlling the mechanism of internal diffusion during static digestion were unchanged, but this was not so. For example; the diffusional exponent, n for wb under pH2 condition was 0.05, when defined by F_c, and 0.93 when defined by F_k, (19 time greater). The greater value for "n" when defined by F_k was the established trend, regardless of the bread bolus type and pH conditions, when linear

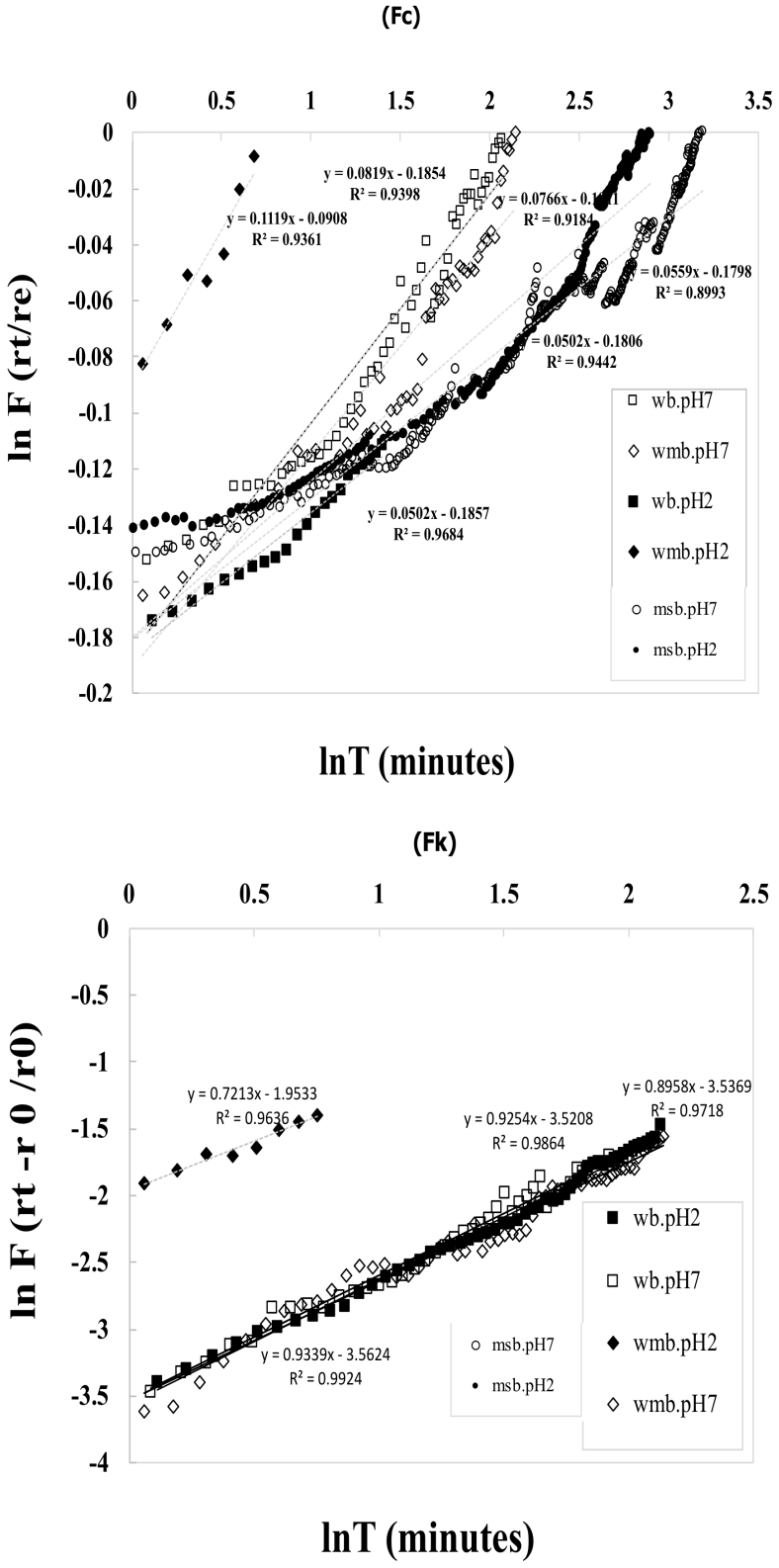

Fig. 7.8 Extracted swelling data for bread boluses in Fig.7.7., fitted, to Crank, (Fc) and Karadag, (Fk), models to generate the plots to estimate the diffusion exponent character 'n', under pH2 and pH7 conditions, (r = δ).

In vitro conditions (pH7)	White bread (wb)	Wholemeal bread (wmb)	Multi-seed bread (msb)
Swelling velocity x 10^{-6}(m/s)	2.79 $\pm$ 0.89	3.29$\pm$0.87	0.700$\pm$0.320
Diffusional exponent, n-F_c	0.0434	0.0766	0.0476
Diffusional exponent, n-F_k	0.9254	0.8958	0.7019
Fitted to Peleg's model, R^2	0.9955	0.9919	0.996
Fitted to Weibull's model, R^2	0.9668	0.893	0.960

Table 7.2 Estimated fluid dynamics parameters when human chewed, bread boluses were immersed in digestive fluids. The diffusional exponent, n were estimated from modified forms of Fick's Law (Equations, 7.3. and 7.4.and R^2's were estimated using Pelegs's and Weibull's mathematical models, from extracted swelling data in Fig.7.6.

data (swelling ratios) were fitted to Equations 7.3. and 7.4, and illustrated in Figure.7.8 and Table.7.2. Two important circumstances were revealed. Evaluation of F_k, indicated that transport in all bread types under all treatments displayed an anomalous Case II behaviour (all n values were >0.5). Values of "n" between 0.5-1.0 indicate that the transport mechanism was anomalous behaviour, which develops from the influence of two associated processes; polymer relaxation and Fickian diffusion by the fluid/water (defined as the movement of polymer chains causing water diffusion into the network)- to the overall transport mechanism (Siepmann and Peppas, 2001). Estimation of F_c, showed that under both pH treatments, for all bread types, the transport mechanism was a less Fickian-Case I behaviour (all n values were < 0.5). There are several limits of 'n' to expect to defines the type of transport. When n; is equal to 0.5, it implies that the transport process was Fickian diffusion controlled. This occurs when water permeates into the network, through free spaces between polymer chains i.e., occurs when the diffusion rate is extremely faster than the relaxation rate of the polymer chains (Siepmann and Peppas, 2001). The Case I and II difference suggests that both modes of mechanism might be taking place and may be occurring at different stages of the breakdown pathways, since the polymeric components of bread gluten proteins and starch may be influenced by the pH of the permeating fluids. Dissolution and formation of gluten proteins found in wheat can be influence by the solvent's pH (Larsson and Hedlund, 2004). Overall, F_k plots gave linear trends with fairly better coefficient of determination, (R^2) values than F_c plots, which may be a better fit model. One explanation for this might be that the enzymes added to the bread bolus in the salivary fluids during the chewing process, may behave differently in each bolus due to its origin and therefore the resistance to access starch and gluten protein in the presence of intestinal fluid and its interaction will therefore affects the overall permeation rates.

Mathematical models describing swelling in bolus systems

Diffusion and external resistance are two of the mechanisms that govern fluid uptake during the permeation transport phenomena. Rehydration and water uptake in biological systems (internal diffusion) are frequently modelled by the Weibull and Peleg approaches. Weibull's model has been used to report sorption kinetics of varying food structures such as cereals for breakfast (Machado et al.,1998), and pasta (Cunningham et al., 2007), and the Peleg model had been a model for moisture sorption kinetics of rice soaking and milk powder (Peleg, 1988). Recently the model was altered to describe the swelling phenomenon occurring in starch granules (Malumba et al., 2013). Since boluses are chewed food systems, movement of digestive fluids into their structures should operate similarly, and hence can be fitted to the Peleg's (Equation.7.5.) and Weibull's (Equation.7.6.) simplified models (Joshi et al., 2015).

$$ln(-ln(1-\alpha)) = \phi lnt + \phi ln\lambda \tag{7.5}$$

Where; α, is the swelling fraction that can be estimated by normalizing the radius by dividing the radius (δ_t), at some time (t) by the equilibrium radius (δ_{eq}), ϕ and λ are the Weibull's constants/parameters. The parameter, ϕ, can be used to specify the shape of the curve (parabolic, s-shaped or exponential) which tells the nature of the process, and the constant λ, can be used to described the rate of bolus swelling with respect to the level of acidity (pH). The temperature was constant throughout the experiments. A plot of ln(-ln(1-α)) vs. lnt, when experimental data were fitted to expressions from the simplified Weibull equation (7.5.), will produce a linear regression as shown in Fig.7.9.B. and gives a slope of ϕ and intercept of $\phi \ln \lambda$, for Weibull's model, which were used to determine the model's parameters.

Equation.7.6. shows the Peleg's model. Where; α, is the swelling fraction that can be estimated by normalizing the radius by dividing the radius δ_t at some time (t) by the equilibrium radius $\delta_e q$, estimated similar to the Weibull's model. P1 and P2 are Peleg's constants. Reciprocal P1 is related to the rate constant for the entire swelling process and reciprocal P2 is related to the maximum achievable swelling. Likewise, a plot of $1/\alpha$ vs. 1/t as shown in Figure.7.9.A, which produces a slope of P1 and intercept of P2, for Peleg's model, and used to determine the model parameters. The coefficient of determination (R^2), results for all bread types were computed and tabulated in Table.7.2.

$$1/\alpha = P1/t + P2 \tag{7.6}$$

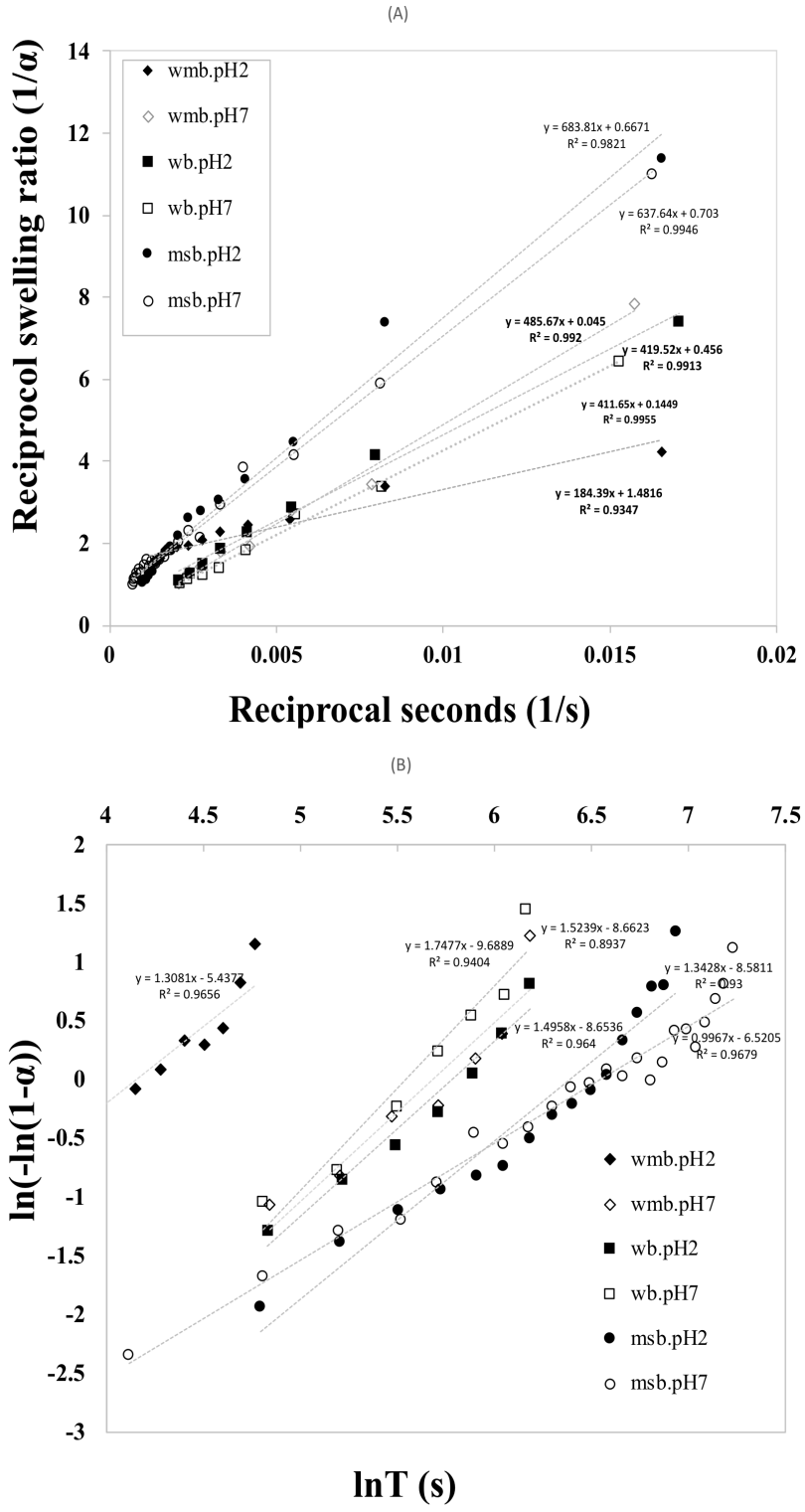

Fig. 7.9 Bread boluses swelling data from Figure.7.7., fitted to; (A) Peleg and (B) Weibull, food hydration models.

	Weibull's parameter			
Fluid's pH	pH 2		pH 7	
Bolus type	λ (s-1)	ϕ	λ (s-1)	ϕ
wmb (whole meal bread)	0.0167	1.31	0.004	1.75
wb (white bread)	0.0031	1.50	0.0034	1.52
msb (multi seed bread)	0.0012	1.34	0.0019	1.01

Table 7.3 Effect of pH on λ (s-1) and ϕ parameters from Weibull's model, as a function of fluid acidity (pH).

The kinetic Weibull's parameter showed mixed results as a function of pH as seen in Table.7.3. Values for λ, for whole meal bread (wmb) in acidic systems (pH2), was ~4 times that than when in neutral system (pH7). While, for white bread (wb) and muilti seed bread (msb) boluses, the values for λ, increased by 1.10 and 1.58 times for each bolus type in pH7 respectively. The values for the shape parameters (ϕ), increased for wmb and wb when the pH was raised from 2 to 7, by 1.34 and 1.01 times respectively. However, it fell for msb by 0.75 times. The values of the shape parameter can be used to predict the level of internal diffusional limitations during food hydration (Machado et al., 1998). When ϕ, is equal to or greater than 1, there is internal diffusional resistance. The shape parameters, (ϕ values) in Table 7.3, suggest that regardless of the type of bolus and the level of acidity (pH), internal diffusional limitations are active in the absorption of intestinal fluids of the bread boluses.

The rate parameter P1, evaluated from Peleg's model also showed mixed results as function of the penetrating fluids acidity level (pH) for different bread boluses. P1 was increased 2.6 times when the acidity of the penetrating fluid at pH7. However, the value of P1 fell to 0.98 nd 0.93 times for wb and msb respectively as seen in Table.7.4. Despite the parameters differences observed for the bread bolus on the Peleg and Weibull plots, the estimated coefficient of determination (R^2), in Table.7.2. were analysed. The Peleg model overall gave better R^2 values, for the swelling of bread boluses under both pH treatments, with the exception of wmb at pH2, albeit the data points are pretty scattered, compared to the Weibull's plot. The initial data are closely spaced, while the latter ones are wider spaced. This inconsistency makes, Peleg's model less worthy to describe bread bolus swelling under static in vitro digestion.

Bolus forces

The bolus maintains its structural integrity due to the cohesive forces holding its particles together. This force is known as the maximum cohesive force, F_C, and is brought about at

	Peleg's parameter			
Fluid's pH	pH 2		pH 7	
Bolus type	P1 (s)	P2	P1 (s)	P2
wmb (whole meal bread)	184	1.48	486	0.05
wb (white bread)	420	0.46	412	0.15
msb (multi seed bread)	684	0.67	638	0.71

Table 7.4 Effect of pH on P1 and P2 parameters from Peleg's model, as a function of fluid acidity (pH).

the threshold of swallowing, as described by the optimum swallow model (Prinz et al., 1997). Prinz et al. (1997) in this model, also describes that, a food bolus at the point of swallowing has two distinct tendencies; to stick to the wall lining as a result of surface tension of the film covering the bolus, in which case it is denoted as the adhesive force, F_A, Equation.7.7., (Prinz et al., 1997), and sticking between particles, as a function of the saliva's viscosity and is denoted as the F_V, Equation.7.8., (Prinz et al., 1997). The cohesive force, F_C, is the difference between viscous force F_A, and adhesive force F_A. Since the static digestion experiments does not presently include wall lining studies and the boluses freely suspended on a hook, the F_A, term can be ignored. As a result, the cohesive force, F_C, can now be modelled as a function of the viscous force, F_V, and data illustrated in Figure.7.11.

$$F_A = 4\pi r\gamma \tag{7.7}$$

$$F_v = \frac{3\pi\eta R^4}{64d^2t} \tag{7.8}$$

Where; η is the zero shear viscosity of human whole saliva, (3.6 x 10^{-3} $Pa.s$; Park et al., (2007)); γ is the surface tension of saliva, (0.053 N/m; Bowden and Taylor (1950)); R /r is the radius of the disc bolus (m); t is the time span over which the particles are separated/disintegrated in (s), extracted from Figure.7.6., and d, is the average distance, between particles separated by a thin film of saliva (2.5 x 10^{-6} m; Malone, Appelqvist, and Norton (2003)). The model works under the following assumptions;

1. The food bolus is a sphere, attached by two discs like surfaces on each other (attractive force, F_A), Figure.7.10.

	Viscous force, Fv (N)	
Bolus type	pH2	pH7
white bread (wb)	2.15 x10^8	2.52 x10^8
whole meal bread (wmb)	1.26x10^9	3.51x10^8
multi-seed bread (msb)	1.07x10^8	1.06 x10^8

Table 7.5 Bolus viscous forces (N), under the influence of pH, estimated from Equation.7.8.

2. Human saliva used was at zero shear viscosity, as bread boli were in static purely diffusive systems.

3. The distance between each particle is separated by the level of lubrication that determines the bolus slippiness at the point of swallowing (thin film).

4. The particles within the bolus are spherical.

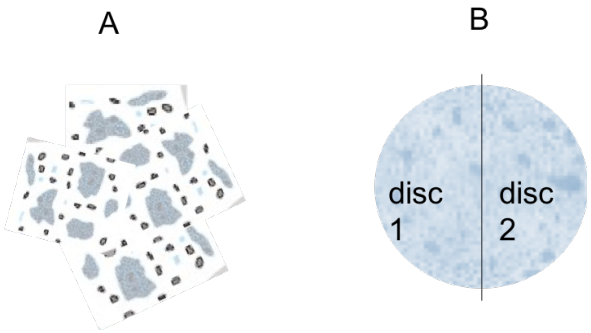

Fig. 7.10 Schematic of food transformation to bolus held together by cohesive for (Fc). A; food particles and saliva and B- mouled bolus by two disc halves.

The pH influences the disintegration time as earlier seen in Figure.7.6, and any increase in digestive time will indicate the type of bread bolus which are held together by weak or strong viscous/cohesive forces as is illustrated in Figures.7.11. The viscous forces holding the whole meal bread bolus was one order higher (1.26 x10 ^{09} N), than white and muti-seed bread boluses viscous forces, which were 2.15 x 10^{08} and 1.07 x 10^{08} N respectively under acidic conditions. However, under neutral conditions, the viscous forces fell significantly for wmb, all occurring within the same OoM, as the white and multi seeded bread boluses, albiet slightly higher. The bread boluses viscous forces evaluated form the Prinz et al., (1997)

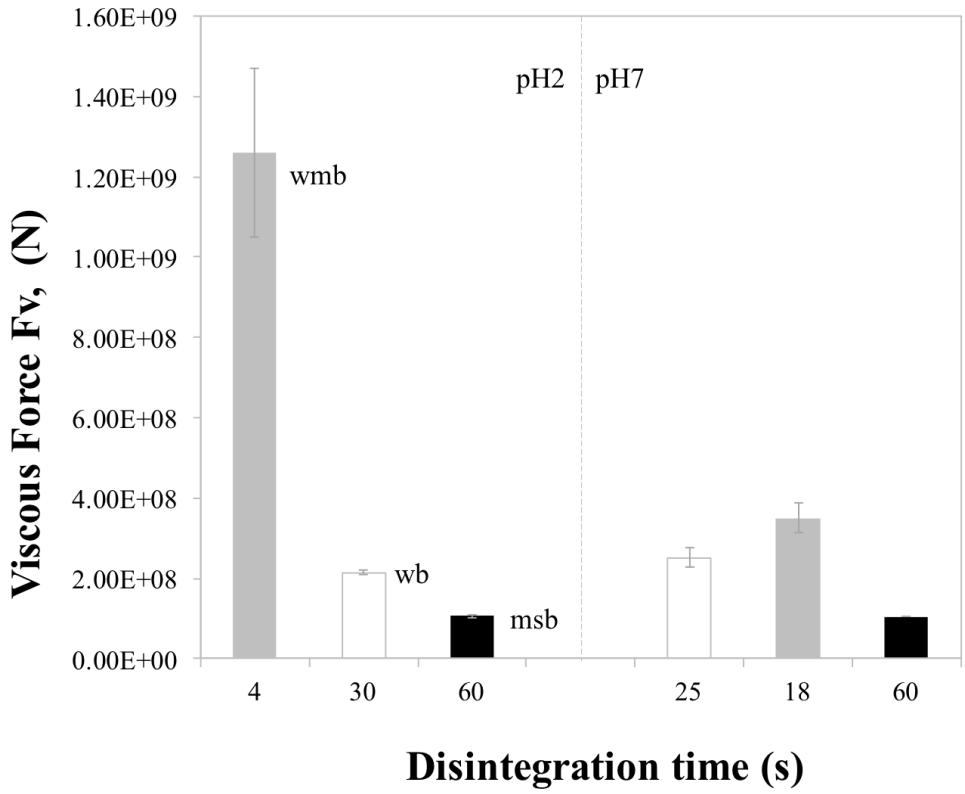

Fig. 7.11 Dependence of bolus cohesive forces (Fv) on pH, as a function of disintegration time from human chewing process; wb-white breads bolus, wmb-whole meal bolus and msb-multi-seed bolus. Error bars are the standard deviation of three measurements.

model in Equation.7.8, were not as expected; msb boluses were less viscous than wb and wmb boluses. This was not the case, as msb bolus was more sticky and pasty from direct observations compared to wb or wmb boluses as noted by the volunteer after each chew. The same model was also used to numerically solve bolus cohesive forces by Prinz et al., (1997) for which chewed carrots and brazil nuts gave better results (brazil nuts was more viscous than carrots), compared to these bread boluses. The time span parameter (t), over which particles separate was held constant during their studies ~0.25 s, which describes the late jaw opening period during real chew (in vivo). The time span variable in our bread bolus study however, was extracted from Figures.7.6., and describes the disintegration times, where the expectorated moulded bolus begins to tear apart completely for total destruction, and varied based on pH and bolus type (Figures.7.6.A and B). This may be the reason for the unexpected values for the bolus forces after they were numerically solved. The values indicate that the model may not be appropriate to describe the viscous forces in bread boluses in static gastric

systems as the numerically solved values were of high orders and inversely related to the type of food material (reduce viscosity by increased dietary fibres in multi seed bread).

Overall trends and results

The pH is important to the overall bolus rate swelling and disintegration. Figure.7.12., shows the effect of pH on the final degree of swelling, and swelling rate. For wb, the swelling rate was almost identical, but the extent of swelling was higher when the pH was lowered. Whole meal bread displayed a noticeable threshold, where in pH2, it had the highest swelling rate and highest final degree of swelling, this was inversely true for msb which had its highest swelling rate and final degree of swelling under pH7 conditions. Under pure diffusion, whole meal bread demonstrated the highest differences among all three bread types, having the highest degree of swelling, 2.45X10 $^{-1}$ and fastest swelling rate, 1.513X10 $^{-5}$m/s at pH2. At pH7, the degree of swelling was 2.11X10^{-01} and the swelling rate was 3.29 X10^{-05}m/s. In pH2, the swelling rate was 7% faster than wb and 46% faster than msb. While in pH7. the swelling rate was 5% faster than wb and 11 faster than msb. For white breads, the swelling rates were almost identical in both pH conditions, 2.29X10^{-06}m/s in pH2 and 2.79X10^{-06} m/s in pH7. A higher degree of swelling takes place when the conditions are more acidic 2.3X10^{-01}m/s.

7.3.4 Effect of shear on bolus swelling and break down rates

To estimate the relative velocity profiles under the effect of mixing, PIV experimentation was carried out in the absence and presence of bolus material.

The velocities were determined from equation.7.9.

$$V_{max} = \sqrt{U_{x^2} + U_{y^2}} \tag{7.9}$$

Where the maximum velocity, is V max, Ux is the velocity in the x-direction and Uy is the velocity in the y-direction. The amount of force (drag force) brought onto food structure under the velocity profiles was determined from equation.7.10.

$$D = C_d.A.\frac{\rho.U_0^2}{2} \tag{7.10}$$

Where D is the drag force, P is the fluid density: U_o is the flow velocity of the incoming flow fluid unaffected by the bolus, A is the projected area of the body on the plane of normal flow, and C_d is the drag coefficient.

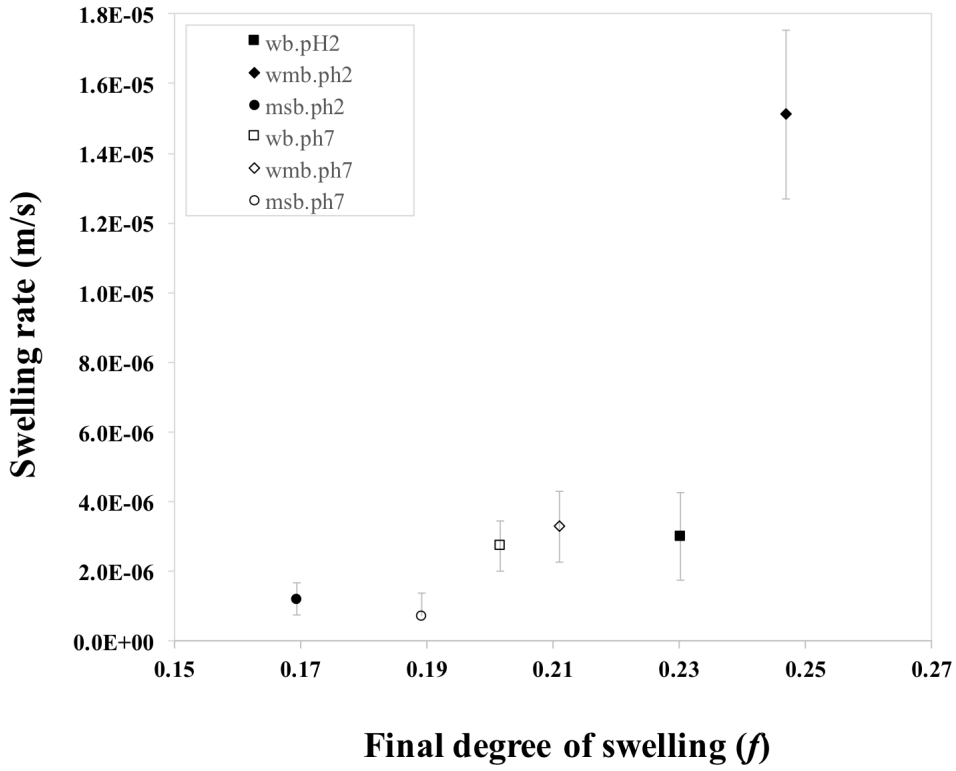

Fig. 7.12 Overall effect of swelling rate on the final degree of boli swelling when the pH was varied. Error bars shows the standard deviation of the three measurements.

The maximum velocity was set at 0.26 m/s without the bolus Fig.7.13-A. In the presence of the bolus, the velocity at the tip was 0.054 m/s Fig.7.13-B, indicating over 80% decrease in velocity profile. The bolus was able to absorb the incoming shear forces generated by the fluid phase of the medium, the impact of these forces are observed from Figure.7.14. At 100 rpm, the Reynolds' number of the system indicated that the flow inside the rig was turbulent - white Re ~4.16 X 10^3, with the average shear stress acting on the surface of the bolus, was estimated to be 1.45 X10^{-3}N, and was deduced as a function of the Reynolds' number.

Fig.7.14. illustrate two outcomes from the effect of force on the swelling rate of bread bolus. There is an instantaneous swelling velocity depicted that was never observed in pure diffusive systems. As a result, the swelling velocity was separated into; (a) instantaneous swelling velocity and (b) equilibrium swelling velocity computed using Equation.7.5. above and the data was also fitted to a 3rddegree polynomial. The instantaneous swelling velocity was happening 3 times faster than the overall equilibrium swelling velocity (5.8X10^{-7}m/s).

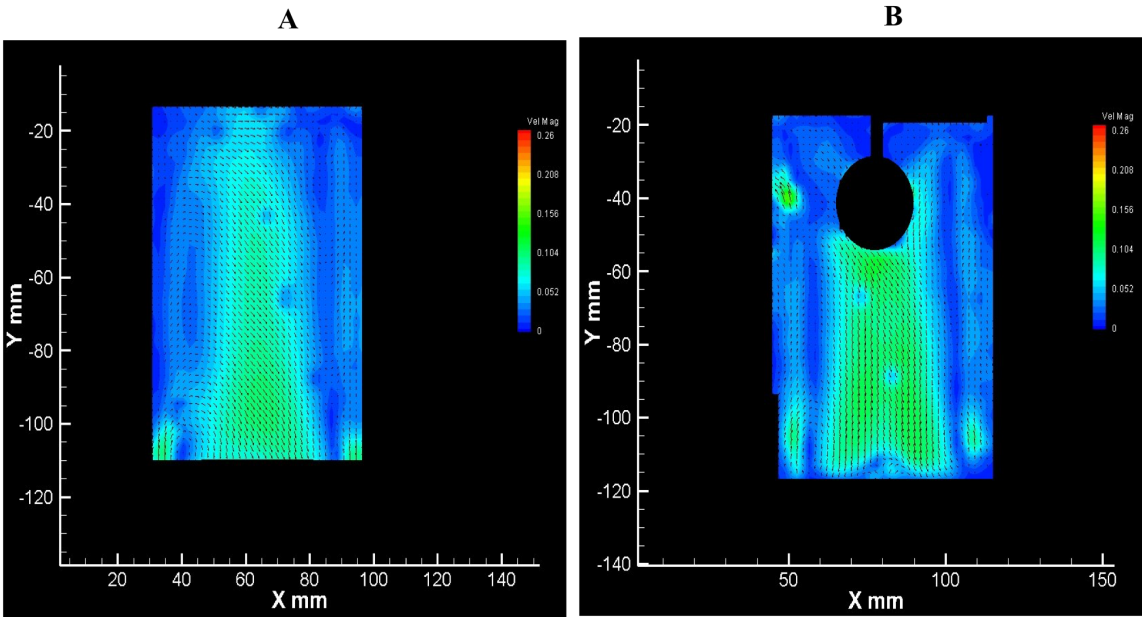

Fig. 7.13 Velocity vectors of flow fields generated in rig at 100 rpm:(A) without bolus (B) with multi-seed bread bolus. The velocities were used to estimate the Drag coefficient from Equation 7.10.

This may be explained by the effect of the permeation overcame the capillary forces and hence the cohesive forces holding the bolus together i.e. convective controlling process rather than diffusive control (non-Fickian behaviour). The equilibrium swelling velocity under shear was surprisingly not significantly higher than the same bolus without shear ($7X10^{-7}$m/s). This might be due to the continuous shear that did not allow sufficient changes for the extent of swelling (f), after the occurrence of the instantaneous stage. As a result, the rate of removal of surface thickness d, may have been greater than the rate of intestinal fluid permeation. Subsequently, leading to very small expansion of bolus radius with time. Additionally, it is known that gluten increase in strength under mechanical stress and this might be an additional reason for the small difference of the swelling rates with or without shear stress.

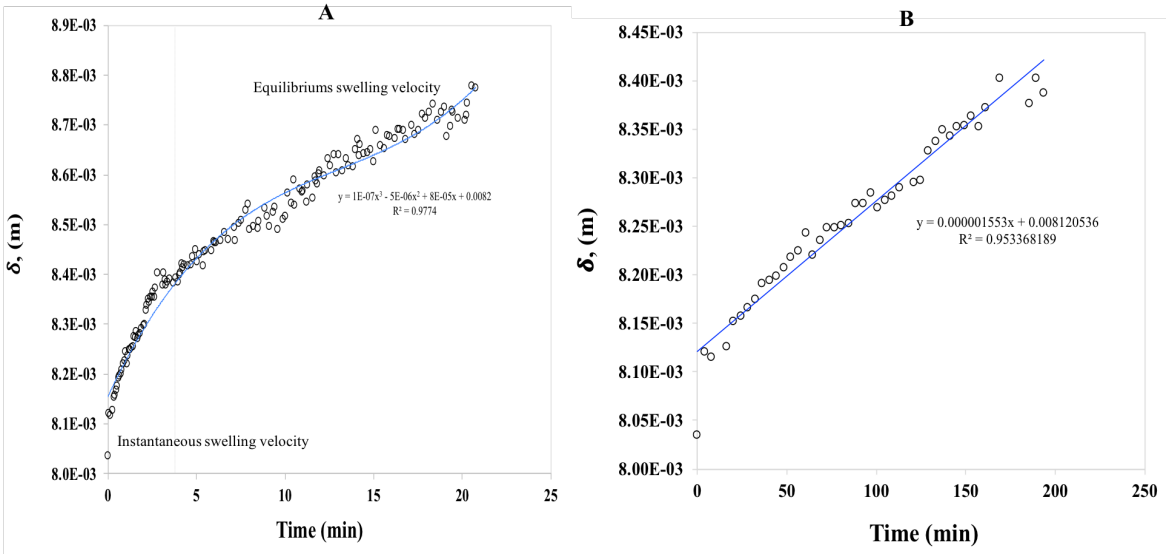

Fig. 7.14 Swelling velocity profiles of msb bolus under the effect of shear at 100 rpm in pH7; A - overall swelling profile and, B - extracted instantaneous swelling velocity.

7.4 Conclusion

The model was successful to visualise bolus break down on the mm scale, similarly expected in the human stomach. This study also showed the importance of human oral processing and the effect of food structure on the regulation of the degree of structure-mechanics-digestion (bolus disintegration) reached. It was demonstrated that there are different fluid mechanics strategies responsible for the kinetics of breakdown pathways (swelling, plateauing and erosion/ disintegration), and swelling rates were very critical to bolus breakdown in breads. Food structure and pH were identified as the key factors driving the swelling process especially for whole meal breads (favoured by very low pH's (2)). The application of the power-law model implied a Case 1 and 11 Fickian transport mechanism, regardless of the influence of pH, and bread structures, and that bread are swellable controlled release systems. This observed discrepancy suggest that a more advance fluid mechanics study is required - possibly at smaller length scales. The swelling kinetics modelled by the Weibul's approach gave overall better representation of bread bolus swelling based on the distribution of data points, rather than the Peleg's model. Also, the Weibull's model indicated that strong internal diffusional resistance is active for all bread bolus systems regardless of the level of fluid acidity it is being digested in.

Application of shear forces onto bread food structure, may lead to faster fluid penetration. However, the ability of the same level of force to damage food structure, may be co related

to other factors such as the degree of chew and hence level of breakage it had sustained in the oral phase of digestion.

Chapter 8

Conclusion

8.1 Chapter 8. Conclusions and future recommendations

The research presented here was concerned with simulating in vitro digestion done 'near real', to understand the impact of food structure/ viscosity and hydrodynamics on the digestive processes in the upper regions of the gastrointestinal tract. In particular, relating duodenal gut contractile motilities and food structure/digesta viscosity to food digestion kinetics (dissolution and absorption). Overall, three (3) in-vitro tool box models were developed (the salient- dynamic duodenal model, the stirred tank reactor model and the bolus dissolution model) to understand the underlying mechanism controlling food digestion, more specifically, how different breads impart different digestion profiles under 'near real' gut environment. Knowledge that may help in the design of healthy foods that may control food digestion.

It was confirmed/proven that different breads digest in such a way that it alters the viscosity of the surrounding fluids: a change in resistance to flow can influence the digestion rate. The dissolution phenomena of the breads were also studied and has led to new ideas on how breads are digested. The main deductions and recommendations from this thesis are summarised as follows;

8.1.1 Chapter 3. A small intestine dynamic model to study the effect of motility on transport and digestion

In this chapter, a bio relevant in vitro model (DDM) was developed to use real foods, breads as reactive systems and model fluids, soluble fibres as the non reactive systems to mimic in vivo digestion. The tool's salient physiological features were successfully reproduced to

induce gut motility to simulate flow and mixing similar to the human duodenum and up to 12 contractions per minute.

The work shows the significance of mass transfer on the absorption of bioavailable sugars by varying the viscosity of the surrounding fluids. This suggest that soluble fibres can be used as food ingredients for their antiglycaemic effects when used as viscogenic agents. Mass transfer operations showed that addition of these fibres such as guar gum reduces digestibility and glucose/reducing sugar absorption, regardless of the mixing conditions. However, gut wall movements of segmentation increase mass transfer of sugars during simulated intestinal absorption.

Furthermore, the model was able to allow for selection of wheat varieties (cultivars; Hereward and Yumai) with specific traits for bread making. Wheat varieties giving rise to different levels of arabinoxylan contents and consequently different viscosities, could influence the bread's carbohydrate metabolism and subsequently its post- prandial blood glucose levels (glycaemic index value). Further investigations are however, required to test if the decline in mass transfer can clarify the post-prandial blood glucose levels observed in vivo when soluble fibres are in the diets.

Two important limitations were considered when simulating the digestion and absorption process using this model: (i) the magnitude of shear forces by the gut wall contraction on the digesta during simulated *in-vitro* mixing compared to *in-vivo* mixing shear forces, and (ii) the membrane in the dynamic duodenal model does not account for the brush border villi and intestinal epithelial cell membrane.

Measuring the extent and amount of force going into the system, would give a good indication in engineering terms of the total energy input and also the amount of shear required for each food type. This can be done by altering the design to include pressure sensors on each segmenting pistons used to induce mixing of the gut walls. In addition, since the current lumen is inert, there is a likely hood and opportunity to use a biological membrane such as those from pig intestine (ex vivo), to study more closely the effect of mixing while incorporating the complexity of the gut wall architecture (villi and mucus entities). There is also opportunity to fabricate the duodenum in a C-shaped manner that is observed in vivo. The shape and orientation is known to influence fluid flow and subsequently digestion (Wright et al., 2016).

8.1.2 Chapter 4. Fluid mixing and transport process in the gut model

This chapter investigated the flow and mixing undertaken by the in vitro dynamic duodenal model to perform food digestion i.e. how deposited pancreatic enzymes and other intestinal fluids are distributed and "mixed in" with freshly added food systems in the lumen. Flow visualisation techniques were used to observe the flow paths. Positron Emission Tomography (PET), images revealed that fluid flow and mechanisms rely on fluid viscosity.

Spreading and oscillation were the two main mass transfer mechanism observed to achieve mixing by segmentation. When the luminal content was of high viscosity, the secretion from the duct follows a spreading path before it is chopped into pieces and repeatedly transfer (oscillate) around the length/geometry of the gut model, .i.e., axial mixing is the first event, then radial mixing. This transport of this mass is not observed in self-diffusion systems with regards to high viscosity fluid system.

An increase in viscosity under self-diffusion mixing mechanism indicates a decreased mixedness, conversely, an increased viscosity under segmentation mixing indicated and decreased mixedness. The more viscous the fluids the larger the difference in mixedness between segmented and self-diffuse systems. The RTD function curve in the small intestine model indicated tailing and stagnation which was extended significantly when the systems motility was a combination of peristaltic and segmentation motion. This was indicative of strong internal recirculation. This was more pronounced in more viscous fluids (1% guar gum concentration). Less viscous model systems displayed a smooth curve which meant that materials exited from the peristaltic flow current without backflow resistance. This was evident under mixing and no mixing, however extremely slower under segmentation.

The velocity flow profiles for two different bread particulate systems, during segmentation motility were estimated from PET. The faster velocity profiles in wholemeal bread are a result of the level of fine bran that is able to allow faster penetration of fluids. For future studies, smaller times scales can be used to study the distribution of fluids into more mixed particulate systems. Additionally, PEPT can be used to track more precisely the velocity distribution in axial and radial dispersions during mixing.

Further improvement is needed to understand flow when the model is not restricted. In this model, the entry and exit ends were sealed and fixed, and did not contract (Figure.4.1.B.). This lack of wall motion does not allow for more accurate fluid transit to be captured. This could be partially solved through a design change of the model, by increasing the length of the tube lumen and C-shaped orientation. This will enable more realistic reproduction of the fluid flow from gut wall contraction and extent of fluid back flow. For example, we could

understand the nature of velocity and pressure profile during gut relaxation and contraction (Figure.8.1).

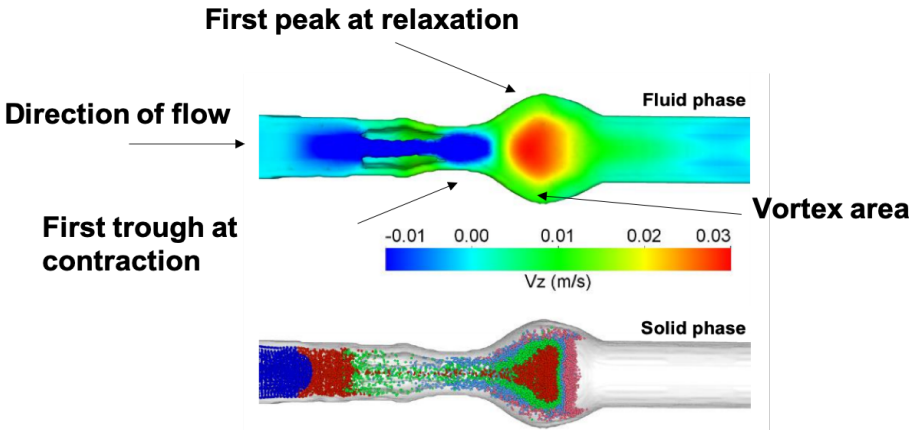

Fig. 8.1 Pressure gradients and velocity that occur at the contraction and relaxation boundary in the human duodenum (Sinnot et al., 2015).

8.1.3 Chapter 5. A unique stirred tank reactor n vitro model for food applications

The aim of this chapter was to design and use a simple stirred vessel as a new digestion system, an *in-vitro* tool. The model successfully carried out digestion and absorption of model fluids and real foods using methodologies developed on the dynamic model. Xanthan gum model fluids delayed absorption significantly, compared to guar gum model fluids/foods when used at the same concentration. This may be because xanthan gum physiochemical properties, evident from viscosity shear profiles (Table.5.1.), was able to reduce the mixing effect and hence slow both convection and diffusion phenomena. Therefore, food formulators, formulating to reduce blood sugar levels with these soluble fibres based on percentages in food recipes should understand that it may not give the same results during in vivo starch digestion.

Starch digestibility in breads are also improved through enhanced mixing. Different fibres behave differently under the same mixing and digestion constraints. The differences

arising in digestibility are a result of botanical origins. Further, when they are manipulated by varying the concentration they have a profound impact on digestibility as reflected by the mass transfer rates. For example, the digested bran bread. Benefits of consuming bran fibre in the diet, may not work by the same mechanism in vivo, attenuating glucose absorption and subsequent postprandial responses (insulin and glucose in blood plasma), as we have observed in vitro that increasing the bran content, increases digestibility (Figure 5.5).

Data has shown that the stirred vessel oversimplify the in vivo mixing processes (Figure 5.5). The hypothesis was that different mixing modes may impart different kinetics on breads digested, i.e., gut wall squeeze-flow mixing (segmentation) and rotation mixing by an impeller, and hence digestion of low and high viscosity breads were compared at different mixing frequencies (Figure 5.9). Comparing the two models were difficult due to the their differences in design and configuration. As stated earlier, the wall motion from the gut wall is in a discontinuous mode, while that of the stirred vessel was continuous motion by the impeller. The velocities and shear rates below the impeller's shaft in a stirred vessel are usually low at low mixing speeds, and does not change as the speed increases (Bai et al., 2011). Therefore the digesta was not truly exposed to a dynamic environment, in contrast to the digesta in the DDM where disintegration occurs under the influence of dynamic oscillation of the flexible gut wall tube.

The study indicated that the dynamic duodenal model provided a near real duodenal environment to improve understanding of the phenomena that are complex to evaluate in vivo. Using the dynamic model it is feasible to evaluate both the digestive kinetic behaviour of different food formulations but also how they are will be distributed during digestion, as seen in Chapter4. More work is needed to understand dissolution, food structure breakdown from mm to nm scales during digestion and its impact on reducing sugar mass transfer. Faster mixing speed in the stirred vessel resulted in faster mass transfer rates (Figure 5.9), which may be because of different food structure dissolution rates.

8.1.4 Chapter 6. Development of gluten-free bread under optimised conditions to understand in-vitro starch digestion.

The aim of this chapter was to design bread structures from the manufacturing stage that may essentially impart different levels of digestibility through the design of the same gluten-free bread recipes. Manipulating various processing conditions in the bread manufacturing process were able to produce bread with varying microstructure thereby enabling different in vitro starch digestibility under that same in vitro conditions.

The water content and the proofing time are two of the most important variable to manipulate to optimised bread with increased bread specific volume. The system model that was developed could predict the, optimised use of water to produce bread with increased specific volume - a property that is desirable based on consumer preferences. In vivo studies are needed to validate the in vitro digestibility mechanisms arising from producing gluten-free bread in this manner.

Overall, this study highlights the importance of water on digestion - essentially the moisture content of the food material consumed. This was evident by the 100% hydration level and 40 minutes proofing time, having a faster in vitro starch digestibility than that all other bread, as it displayed a 45% starch digestion over the incubation period.

8.1.5 Chapter 7. Structure-mechanics-digestion: bolus breakdown

The aim of this study was to identify the mechanism of the breakdown pathways undergone by food bolus in different simulated chemical and shear environments. The objective was to first compare an if in-vivo chew- bolus broke down differently from in-vitro mastication.

in-vitro simulation of the oral process compromise disintegration rates under acidic and neutral conditions. Bread are swelling particulate systems. This may be due to the fact that they are soft condensed matter (SCM). Multi-seed bread showed more stability for swelling and disintegration under all conditions, while white bread bolus broke down faster in acidic conditions. Under circular shear forces, an instantaneous swelling velocity is first observed after which a more linear like velocity is dominant. The distinction between the mechanism of permeate transport into bolus still remains unclear i.e. Fickian or non-Fickian behaviour. It is clear that a mathematical model that could represent the swelling and breakdown of the bolus under gastric construing could and should be developed for in-vitro systems to better understand other relevant physical feature of digestion

This is a very promising study, and a milestone closer to understanding food as soft matter and how the phenomena of swelling and erosion contribute to release and delayed rates of nutrients under digestive conditions. This might offer an alternative explanation for differences in GI when carbohydrate foods are digested. Information on the porosity and tortuosity using CT-scan technology might be useful to understand and compute the Thiele modulus, ϕ especially when the complexity of the study incorporates the use of external enzymes.

In reaction engineering, the physical interpretation of ϕ english2 is analogous to the Damkohler number, $\phi =$ ka2/DA i.e. reaction rate/diffusion rate. And for reaction limited

regime ϕ 2>> 1, and for diffusion-limited regime ϕ 2<< 1. Additionally, the mechanical force can be more realistic in shear studies, such as the use of sonic waves to generate pulses in the rig mirroring peristaltic waves in the gut. There is also the need for a numerical model that is dedicated to swelling and erosion of bolus in a digestive environment, and inline measurement measuring the rate of nutrient release.

Chapter 9

References

Aguilera, J. M. (2005). Why food microstructure Journal of Food Engineering, 67(1-2):3-11. 28

Akhtar, M., STENZEL, J., MURRAY, B., and DICKINSON, E. (2005). Factors affecting the perception of creaminess of oil-in-water emulsions. Food Hydrocolloids, 19(3):521526.

Alloncle, M. and Doublier, J.-L. (1991). Viscoelastic properties of maize starch/hydrocolloid pastes and gels. Food Hydrocolloids, 5(5):455467.

Alminger, M. L., Eklund-Jonsson, C., Kidman, S., and Langton, M. (2012). Starch Microstructure and Starch Hydrolysis in Barley and Oat Tempe During In Vitro Digestion. Food Digestion, 3(1-3):5362.

Amidon, G., Kou, J., Elliott, R., and Lightfoot, E. (1980). Analysis of models for determining intestinal wall permeabilities. Journal of Pharmaceutical Sciences, 69(12):1369 1373.

Anderson, G. H., Cho, C. E., Akhavan, T., Mollard, R. C., Luhovyy, B. L., and Finocchiaro, E. T. (2010). Relation between estimates of cornstarch digestibility by the Englyst in vitro method and glycemic response subjective appetite, and short-term food intake in young men. The American Journal of Clinical Nutrition, 91(4):932939.

Andersson, R., Westerlund, E., Tilly, A.-C., and an, P. (1993). Natural Variations in the Chemical Composition of White Flour. Journal of Cereal Science, 17(2):183189.

Angioloni, A. and Collar, C. (2011). Physicochemical and nutritional properties of reduced-caloric density high-fibre breads. LWT - Food Science and Technology, 44(3):747 758.

Anne Berghfer and Tobias Pischon and Thomas Reinhold and Caroline M Apovian and Arya M Sharma and Stefan N Willich (2008). Obesity prevalence from a European perspective: a systematic review. BMC Public Health, 8(1).

Anton, A. A. and Artfield, S. D. (2008). Hydrocolloids in gluten-free breads: A review. International Journal of Food Sciences and Nutrition, 59(1):11 -23.

Arendt, E. K., Morrissey, A., Moore, M. M., and Bello, F. D. (2008). Gluten-free breads. In Gluten-Free Cereal Products and Beverages, pages 289 VII. Elsevier.

Argent, B. E. and Gray, M. A. (1990). Pancreatic Ducts: Isolation Culture and Bicarbonate Transport. In Epithelia, pages 69 -97. Springer Netherlands.

Atuma, C., Strugala, V., Allen, A., and Holm, L. (2001). The adherent gastrointestinal mucus gel layer: thickness and physical state in vivo. American Journal of Physiology-Gastrointestinal and Liver Physiology, 280(5):G922G929.

Bakalis, S., COX, P. W., WANG-NOLAN, W., PARKER, D., and RYER, P. J. F. (2003). Use of Positron-Emission Particle Tracking (PEPT) Technique for Velocity Measurements in Model Food Fluids. Journal of Food Science, 68(9):26842692.

Baldyage and Bourne (1986). Flow phenomena and measurement. Encyclopedia of Fluid Mechanics (Cheremisinoff NP, eds), Vol 1, p 148201. -

Ball, S., Guan, H.-P., James, M., Myers, A., Keeling, P., Mouille, G., Bul, A., Colonna, P., and Preiss, J. (1996a). From Glycogen to Amylopectin: A Model for the Biogenesis of the Plant Starch Granule. Cell, 86(3):349352.

Ball, S., Guan, H.-P., James, M., Myers, A., Keeling, P., Mouille, G., Bul, A., Colonna, P., and Preiss, J. (1996b). From Glycogen to Amylopectin: A Model for the Biogenesis of the Plant Starch Granule. Cell, 86(3):349352.

Bellmann, S., Lelieveld, J., Gorissen, T., Minekus, M., and Havenaar, R. (2016). Development of an advanced in vitro model of the stomach and its evaluation versus human gastric physiology. Food Research International, 88:191198.

Benini, L., Castellani, G., Brighenti, F., Heaton, K., Brentegani, M., Casiraghi, M., Sembenini, C., Pellegrini, N., Fioretta, A., and Minniti, G. (1995). Gastric emptying of a solid meal is accelerated by the removal of dietary fibre naturally present in food. Gut, 36:82530.

Benjamin, O., Silcock, P., Kieser, J., Waddell, J., Swain, M., and Everett, D. (2012a). Development of a model mouth containing an artificial tongue to measure the release of volatile compounds. Innovative Food Science & Emerging Technologies, 15:96103.

Benshitrit, R. C., Levi, C. S., Tal, S. L., Shimoni, E., and Lesmes, U. (2012). Development of oral food-grade delivery systems: Current knowledge and future challenges. Food Funct., 3(1):1021.

Berg, T., Singh, J., Hardacre, A., and Boland, M. J. (2012). The role of cotyledon cell structure during in vitro digestion of starch in navy beans. Carbohydrate Polymers, 87(2):16781688.

Berti, C., Riso, P., Monti, L., and Porrini, M. (2004). In vitro starch digestibility and in vivo glucose response of gluten free foods and their gluten counterparts. European Journal of Nutrition, 43(4).

Bharucha, A. E. and Brookes, S. J. (2012). Neurophysiologic Mechanisms of Human Large Intestinal Motility. In Physiology of the Gastrointestinal Tract, pages 9771022. Elsevier.

Bloch, H. (1987). Man -s curiosity about food digestion: an historical overview. J Natl Med Assoc, 79:12237.

Boland, M. (2016). Human digestion - a processing perspective. Journal of the Science of Food and Agriculture, 96(7):2275 -2283.

Borczak, B., Sikora, M., Sikora, E., Dobosz, A., and Kapusta-Duch, J. (2017). Glycaemic index of wheat bread. page 1700022.

Bornhorst, G. M., Gouseti, O., Wickham, M. S., and Bakalis, S. (2016). Engineering Digestion: Multiscale Processes of Food Digestion. Journal of Food Science, 81(3):R534 R543.

Bornhorst, G. M. and Singh, R. P. (2013). Kinetics of in Vitro Bread Bolus Digestion with Varying Oral and Gastric Digestion Parameters. Food Biophysics, 8(1):50 59.

Bourlieu, C., Mrd, O., Bouzerzour, K., Mandalari, G., Macierzanka, A., Mackie, A. R., and Dupont, D. (2014). Specificity of Infant Digestive Conditions: Some Clues for Developing Relevant In Vitro Models. Critical Reviews in Food Science and Nutrition, 54(11):14271457.

Brenelli, S., Campos, S., and Saad, M. (1997). Viscosity of gums in vitro and their ability to reduce postprandial hyperglycemia in normal subjects. Brazilian Journal of Medical and Biological Research, 30(12):14371440.

Brennan, C., Blake, D., Ellis, P., and Schofield, J. (1996a). Effects of Guar Galactomannan on Wheat Bread Microstructure and on theIn vitroandIn vivoDigestibility of Starch in Bread. Journal of Cereal Science, 24(2):151160.

Brennan, C. S. and Tudorica, C. M. (2008). Evaluation of potential mechanisms by which dietary fibre additions reduce the predicted glycaemic index of fresh pastas. International Journal of Food Science & Technology, 43(12):2151 -2162.

Brownlee, I., Dettmar, P., Strugala, V., and Pearson, J. (2006). The Interaction of Dietary Fibres with the Colon. Current Nutrition & Food Science, 2(3):243 -264.

Brownlee, I. A. (2011). The physiological roles of dietary fibre. Food Hydrocolloids, 25(2):238 -250.

Buckley, D. J. and Berger, M. (1962). The swelling of polymer systems in solvents. II. Mathematics of diffusion. Journal of Polymer Science, 56(163):175 -188.

Burns, H. D., Hamill, T. G., si Eng, W., Francis, B., Fioravanti, C., and Gibson, R. E. (1999). Positron emission tomography neuroreceptor imaging as a tool in drug discovery research and development. Current Opinion in Chemical Biology, 3(4):388 -394.

Burton-Freeman, B. (2000). Dietary Fiber and Energy Regulation. The Journal of Nutrition, 130(2):272S -275S.

Butterworth, P. J., Warren, F. J., and Ellis, P. R. (2011). Human –amylase and starch digestion: An interesting marriage. 63(7):395 -405.

Cai, L., Lu, S., and Pike, V. W. (2008). ChemInform Abstract: Chemistry with [18F]Fluoride Ion. ChemInform, 39(37).

Calbet, J. A. and MacLean, D. A. (1997). Role of caloric content on gastric emptying in humans. The Journal of Physiology, 498(2):553 -559.

Camilleri, M., Malagelada, J. R., Brown, M. L., Becker, G., and Zinsmeister, A. R. (1985). Relation between antral motility and gastric emptying of solids and liquids in humans. American Journal of Physiology-Gastrointestinal and Liver Physiology, 249(5):G580 -G585.

Camilleri, M. and Prather, C. M. (1994). Axial forces during gastric emptying in health and models of disease. Digestive Diseases and Sciences, 39(S12):14S -17S.

Cauvain, S. and Young, L. (2003). Water control in baking. In Bread Making, pages 447 -466. Elsevier.

Cauvain, S. P. and Young, L. S. (2008). Bakery Food Manufacture and Quality. Wiley-Blackwell.

Cengel, Y. A., Ghajar, A. J. & Kanoglu, M. (2011). Heat and mass transfer: fundamentals and applications. Singapore: McGraw-Hill. XXI, 902 s. : ill. pp.

Chang, E. B., Sitrin, M. D., and Black, D. D. (1996). Gastrointestinal, hepatobiliary, and nutritional physiology. J.B. Lippincott Company.

Chen, J. (2009a). Food oral processing -A review. Food Hydrocolloids, 23(1):1 -25.

Chen, J. (2014). Food oral processing: Some important underpinning principles of eating and sensory perception. Food Structure, 1(2):91 -105.

Chen, J., Gaikwad, V., Holmes, M., Murray, B., Povey, M., Wang, Y., and Zhang, Y. (2011). Development of a simple model device for in vitro gastric digestion investigation. Food & Function, 2(3-4):174.

Chivers, D. J. and Langer, P. (1994). Food form and function: interrelationships and future needs iAll contributors (operating in three groups)/i. In Chivers, D. J. and Langer, P., editors, The Digestive System in Mammals, pages 411 -430. Cambridge University Press.

Cohen, M. H. and Turnbull, D. (1959). Molecular Transport in Liquids and Glasses. The Journal of Chemical Physics, 31(5):1164 -1169.

Collar, C., Santos, E., and Rosell, C. M. (2006). Significance of Dietary Fiber on the Viscometric Pattern of Pasted and Gelled Flour-Fiber Blends. Cereal Chemistry Journal, 83(4):370 -376.

Collins, P. J., Houghton, L. A., Read, N. W., Horowitz, M., Chatterton, B. E., Heddle, R., and Dent, J. (1991). Role of the proximal and distal stomach in mixed solid and liquid meal emptying. Gut, 32(6):615 -619.

Courtin, C. and Delcour, J. (2002a). Arabinoxylans and Endoxylanases in Wheat Flour Bread-making. Journal of Cereal Science, 35(3):225 -243.

Crank (1956). The Mathematics of Diffusion. Oxford University Press, Clarendon Press, p. 239.

Curto, A. L., Pitino, I., Mandalari, G., Dainty, J. R., Faulks, R. M., and Wickham, M. S. J. (2011a). Survival of probiotic lactobacilli in the upper gastrointestinal tract using an in vitro gastric model of digestion. Food Microbiology, 28(7):1359 -1366.

Cussler, E. L. (2009c). Theories of Mass Transfer. In Diffusion, pages 274 -303. Cambridge University Press.

De la Hera, E., Rosell, C. M., and Gomez, M. (2014). Effect of water content and flour particle size on gluten-free bread quality and digestibility. Food Chemistry, 151:526 -531.

De Loubens, C., Lentle, R. G., Love, R. J., Hulls, C., and Janssen, P. W. M. (2013a). Fluid mechanical consequences of pendular activity segmentation and pyloric outflow in the proximal duodenum of the rat and the guinea pig. Journal of The Royal Society Interface, 10(83):20130027 -20130027.

De Loubens, C., Panouill., Saint-Eve, A., Dris, I., Tra, I., and Souchon, I. (2011). Mechanistic model of in vitro salt release from model dairy gels based on standard- ized breakdown test simulating mastication. Journal of Food Engineering, 105(1):161 - 168.

De Wijk, R. A., Janssen, A. M., and Prinz, J. F. (2011). Oral movements and the perception of semi-solid foods. Physiology & Behavior, 104(3):423 -428.

Decuypere, J. A., Dendooven, R. M., and Henderickx, H. K. (1986). Stomach Emptying of Milk Diets in Pigs. A Mathematical Model Allowing Description and Comparison of the Emptying Pattern. 36(8):679 -696.

Delcour, J., Courtin, C., Verbeke, K., Broekaert, W., and Arnaut, F. (2012). Wheat bran-derived arabinoxylan oligosaccharides: A novel soluble dietary fibre with prebiotic properties. CFW Plexus, (AACCI 2011 Annual Meeting).

Delzenne, N., Blundell, J., Brouns, F., Cunningham, K., Graaf, K. D., Erkner, A., Lluch, A., Mars, M., Peters, H. P. F., and Westerterp-Plantenga, M. (2010). Gastrointestinal targets of appetite regulation in humans. Obesity Reviews, 11(3):234 -250.

Demirkesen, I., Mert, B., Sumnu, G., and Sahin, S. (2010). Rheological properties of gluten-free bread formulations. Journal of Food Engineering, 96(2):295 -303.

Deng, R., Pang, L., Xu, Y., Li, L., Wu, X., and Chen, X. D. (2014). Investigation on a Soft Tubular Model Reactor Based on Bionics of Small Intestine - Residence Time Distribution. International Journal of Food Engineering, 10(4).

Deng, R., Selomulya, C., Wu, P., Woo, M. W., Wu, X., and Chen, X. D. (2016). A soft tubular model reactor based on the bionics of a small intestine - Starch hydrolysis. Chemical Engineering Research and Design, 112:146 -154.

Dhital, S., Dolan, G., Stokes, J. R., and Gidley, M. J. (2014). Enzymatic hydrolysis of starch in the presence of cereal soluble fibre polysaccharides. Food & Function, 5(3):579.

Dikeman, C. L., Murphy, M. R., and Fahey, G. C. (2006b). Dietary Fibers Affect Viscosity of Solutions and Simulated Human Gastric and Small Intestinal Digesta. The Journal of Nutrition, 136(4):913 -919.

Dikeman, C. L., Murphy, M. R., and Fahey, G. C. (2007). Diet type affects viscosity of ileal digesta of dogs and simulated gastric and small intestinal digesta. Journal of Animal Physiology and Animal Nutrition, 91(3-4):139 -147.

Dona, A. C., Pages, G., Gilbert, R. G., and Kuchel, P. W. (2010). Digestion of starch: In vivo and in vitro kinetic models used to characterise oligosaccharide or glucose release. Carbohydrate Polymers, 80(3):599 -617.

Dreher, M. L. (2017). Introduction to Dietary Fiber. In Dietary Fiber in Health and Disease, pages 1 -18. Springer International Publishing.

Du, P., Paskaranandavadivel, N., Angeli, T. R., Cheng, L. K., and O'Grady, G. (2015). The virtual intestine: in silico modeling of small intestinal electrophysiology and motility and the applications. Wiley Interdisciplinary Reviews: Systems Biology and Medicine, 8(1):69 -85.

Duda, J. L. (1985). Molecular diffusion in polymeric systems. Pure and Applied Chemistry, 57(11):1681 -1690.

Dupont, D. (2016). In Vitro Digestion Models. In Reference Module in Food Science. Elsevier.

Dupont, D. and Mackie, A. R. (2015). Static and dynamic in vitro digestion models to study protein stability in the gastrointestinal tract. Drug Discovery Today: Disease Models, 17-18:23 -27.

Eastwood, M. and Morris, E. (1992). Physical properties of dietary fiber that influence physiological function: a model for polymers along the gastrointestinal tract. Am J Clin Nutr, 55:436 -42.

Edgar, . W. M. (1990). Saliva and dental health. Clinical implications of saliva: report of a consensus meeting. British Dental Journal, 169(4):96 -98. -

Edwards, C. H., Grundy, M. M., Grassby, T., Vasilopoulou, D., Frost, G. S., Butterworth, P. J., Berry, S. E., Sanderson, J., and Ellis, P. R. (2015). Manipulation of starch bioaccessibility in wheat endosperm to regulate starch digestion postprandial glycemia, insulinemia, and gut hormone responses: a randomized controlled trial in healthy ileostomy participants. American Journal of Clinical Nutrition, 102(4):791 -800.

Eelderink, C., Noort, M. W. J., Sozer, N., Koehorst, M., Holst, J. J., Deacon, C. F., Rehfeld, J. F., Poutanen, K., Vonk, R. J., Oudhuis, L., and Priebe, M. G. (2015). The structure of wheat bread influences the postprandial metabolic response in healthy men. Food & Function, 6(10):3236 -3248.

[104] Ehrlein, H. and Scheemann, M. (2005). Gastrointestinal motility. Technical report.

Ehrlein, H. J., Schemann, M., and Siegle, M. L. (1987). Motor patterns of small intestine determined by closely spaced extraluminal transducers and videofluoroscopy. American Journal of Physiology-Gastrointestinal and Liver Physiology, 253(3):G259 - G267.

Elliott, R., Amidon, G., and Lightfoot, E. (1980). A convective mass transfer model for determining intestinal wall permeabilities: laminar flow in a circular tube. Journal of Theoretical Biology, 87(4):757 -771.

Ellis, P. R., Dawoud, F. M., and Morris, E. R. (1991). Blood glucose plasma insulin and sensory responses to guar-containing wheat breads: effects of molecular weight and particle size of guar gum. British Journal of Nutrition, 66(03):363.

Engelen, L., Fontijn-Tekamp, A., and van der Bilt, A. (2005). The influence of product and oral characteristics on swallowing. Archives of Oral Biology, 50(8):739 -746.

Englyst, H., Kingman, S., and Cummings, J. (1992). Classification and measurement of nutritionally important starch fractions. Eur J Clin Nutr, 46 Suppl 2:S33 -50.

Englyst, H. N., Veenstra, J., and Hudson, G. J. (1996). Measurement of rapidly available glucose (RAG) in plant foods: a potential in vitro predictor of the glycaemic response. British Journal of Nutrition, 75(03):327.

Ertekin, C. and Aydogdu, I. (2003). Neurophysiology of swallowing. Clinical Neurophysiology, 114(12):2226 -2244.

Fardet, A., Leenhardt, F., Lioger, D., Scalbert, A., and Rsy, C. (2006a). Parameters controlling the glycaemic response to breads. Nutrition Research Reviews, 19(01):18.

Fardet, A., Leenhardt, F., Lioger, D., Scalbert, A., and Rsy, C. (2006b). Parameters controlling the glycaemic response to breads. Nutrition Research Reviews, 19(01):18. Feher, J. (2012). The Stomach. In Quantitative Human Physiology, pages 701 -710. Elsevier.

- Ferrer-Mairal, A., Pea-Lapuente, C., Iglesia, I., Urtasun, L., Miguel-Etayo, P. D., Rem., Cort E., and Moreno, L. A. (2011). In vitro and in vivo assessment of the glycemic index of bakery products: influence of the reformulation of ingredients. European Journal of Nutrition, 51(8):947 -954.

Fiszman, S. and Varela, P. (2013). The role of gums in satiety/satiation. A review. Food Hydrocolloids, 32(1):147 -154.

Fonseca, M. R. J. (2011). An Engineering Understanding of the Small Intestine. PhD thesis, The University of Birmingham.

Fontijn-Tekamp, F., Slagter, A., Bilt, A. V. D., Hof, M. V. '., Witter, D., Kalk, W., and Jansen, J. (2000). Biting and Chewing in Overdentures Full Dentures, and Natural Dentitions. Journal of Dental Research, 79(7):1519 -1524.

Fowler, J. S. and Ido, T. (2005). Design and Synthesis of 2-Deoxy-2-[18F]Fluoro-D-Glucose (18FDG). In Handbook of Radiopharmaceuticals, pages 307 -321. John Wiley & Sons Ltd.

Gallagher, E., Gormley, T., and Arendt, E. (2004). Recent advances in the formulation of gluten-free cereal-based products. Trends in Food Science & Technology, 15(3-4):143 - 152.

Gambaro, A., Varela, P., Gimenez, A., Aldrovand, A., Fisman, S. M., and Hough, G. (2002). TEXTURAL QUALITY OF WHITE PAN BREAD BY SENSORY AND INSTRUMENTAL MEASUREMENTS. Journal of Texture Studies, 33(5):401 -413.

Gan, Z., Galliard, T., Ellis, P., Angold, R., and Vaughan, J. (1992). Effect of the outer bran layers on the loaf volume of wheat bread. Journal of Cereal Science, 15(2):151 -163.

Gao, J., Wong, J. X., Lim, J. C.-S., Henry, J., and Zhou, W. (2015). Influence of bread structure on human oral processing. Journal of Food Engineering, 167:147 -155.

Gidley, M. J. (2013). Hydrocolloids in the digestive tract and related health implica- tions. Current Opinion in Colloid & Interface Science, 18(4):371 -378.

Gil-Humanes, J., Pist., Altamirano-Fortoul, R., Real, A., Comino, I., Sousa, C., Rosell, C. M., and Barro, F. (2014). Reduced-Gliadin Wheat Bread: An Alternative to the Gluten-Free Diet for Consumers Suffering Gluten-Related Pathologies. PLoS ONE, 9(3):e90898.

Giuberti, G., Fortunati, P., and Gallo, A. (2016). Can different types of resistant starch influence the in vitro starch digestion of gluten free breads - Journal of Cereal Science, 70:253 -255.

Goesaert, H., Brijs, K., Veraverbeke, W., Courtin, C., Gebruers, K., and Delcour, J. (2005). Wheat flour constituents: how they impact bread quality and how to impact their functionality. Trends in Food Science & Technology, 16(1-3):12 -30.

Goni, I., Garcia-Alonso, A., and Saura-Calixto, F. (1997). A starch hydrolysis procedure to estimate glycemic index. Nutrition Research, 17(3):427 -437.

Gould, J. T. (1998). Baking around the world. In Technology of Breadmaking, pages 197 -213. Springer US.

Gouseti, O., Jaime-Fonseca, M., Fryer, P., Mills, C., Wickham, M., and Bakalis, S. (2014a). Hydrocolloids in human digestion: Dynamic in-vitro assessment of the effect of food formulation on mass transfer. Food Hydrocolloids, 42:378 -385.

Gray, H., Gray, H., and Lewis, W. H. (1918). Anatomy of the human body. Lea & Febiger,.

Grundy, M. M.-L., Edwards, C. H., Mackie, A. R., Gidley, M. J., Butterworth, P. J., and Ellis, P. R. (2016a). Re-evaluation of the mechanisms of dietary fibre and implications for macronutrient bioaccessibility digestion and postprandial metabolism. British Journal of Nutrition, 116(05):816 -833.

Guerra, A., Etienne-Mesmin, L., Livrelli, V., Denis, S., Blanquet-Diot, S., and Alric, M. (2012a). Relevance and challenges in modeling human gastric and small intestinal digestion. Trends Biotechnol, 30:591 -600.

Guinard, J.-X. and Mazzucchelli, R. (1996). The sensory perception of texture and mouthfeel. Trends in Food Science & Technology, 7(7):213 -219.

Gularte, M. A. and Rosell, C. M. (2011). Physicochemical properties and enzymatic hydrolysis of different starches in the presence of hydrocolloids. Carbohydrate Polymers, 85(1):237 -244.

Gunness,P.andGidley,M.J.(2010).Mechanismsunderlyingthecholesterol-lowering properties of soluble dietary fibre polysaccharides. Food & Function, 1(2):149.

Guo, Q., Ye, A., Lad, M., Ferrua, M., Dalgleish, D., and Singh, H. (2015). Disintegration kinetics of food gels during gastric digestion and its role on gastric emptying: an in vitro analysis. Food & Function, 6(3):756 -764.

Guri, A., Haratifar, S., and Corredig, M. (2014). Bioefficacy of Tea Catechins Associated with Milk Caseins Tested Using Different In Vitro Digestion Models. Food Digestion, 5(1-3):8 -18.

Guyton and Hall (2012). Physiology of Gastrointestinal Disorders. In Pocket Companion to Guyton and Hall Textbook of Medical Physiology, pages 502 -505. Elsevier.

-Hall, J. E. and Guyton, A. C. (2011a). Gastrointestinal physiology. In Guyton and Hall Physiology Review, pages 191 -210. Elsevier.

-Han, H. M., Cho, J. H., Kang, H. W., and Koh, B. K. (2011). Rice varieties in relation to rice bread quality. Journal of the Science of Food and Agriculture, 92(7):1462 -1467. [Haralampu] Haralampu, S. G. In-vivo andIn-vitro Digestion of Resistant Starch. In Advanced Dietary Fibre Technology, pages 413 -423. Blackwell Science Ltd.

Hartmann, H., Derksen, J., and van den Akker, H. (2006a). Numerical simulation of a dissolution process in a stirred tank reactor. Chemical Engineering Science, 61(9):3025 -3032.

Hartmann, H., Derksen, J. J., and van den Akker, H. E. A. (2006b). Mixing times in a turbulent stirred tank by means of LES. AIChE Journal, 52(11):3696 -3706.

Hausken, T., Mundt, M., and Samson, M. (2001). The contribution of antral peristalsis in gastric emptying of a low-caloric liquid meal in man is of minor importance. Gastroenterology, 120(5):A464 -A464.

Heaton, K., Marcus, S., Emmett, P., and Bolton, C. (1988). Particle size of wheat, maize, and oat test meals: effects on plasma glucose and insulin responses and on the rate of starch digestion in vitro. Am J Clin Nutr, 47:675 -82.

Hemdane, S., Jacobs, P. J., Dornez, E., Verspreet, J., Delcour, J. A., and Courtin, C. M. (2015a). Wheat (Triticum aestivum L.) Bran in Bread Making: A Critical Review. Comprehensive Reviews in Food Science and Food Safety, 15(1):28 -42.

Hemdane, S., Leys, S., Jacobs, P. J., Dornez, E., Delcour, J. A., and Courtin, C. M. (2015b). Wheat milling by-products and their impact on bread making. Food Chemistry, 187:280 -289.

Hemery, Y. M., Anson, N. M., Havenaar, R., Haenen, G. R., Noort, M. W., and Rouau, X. (2010). Dry-fractionation of wheat bran increases the bioaccessibility of phenolic acids in breads made from processed bran fractions. Food Research International, 43(5):1429 - 1438.

Hernot, D. C., Boileau, T. W., Bauer, L. L., Swanson, K. S., and Fahey, G. C. (2008). In Vitro Digestion Characteristics of Unprocessed and Processed Whole Grains and Their Components. Journal of Agricultural and Food Chemistry, 56(22):10721 -10726.

Hettiaratchi, U.P.K., E. S. W. J. (2012). Prediction of glycaemic indices (GI) of meals by starch hydrolysis indices. International Food Research Journal, 19, 1153-1159.

Hoebler, C., Lecannu, G., Belleville, C., Devaux, M.-F., Popineau, Y., and Barry, J.-L. (2002). Development of anin vitrosystem simulating bucco-gastric digestion to assess the physical and chemical changes of food. International Journal of Food Sciences and Nutrition, 53(5):389 -402.

Hollebeeck, S., Borlon, F., Schneider, Y.-J., Larondelle, Y., and Rogez, H. (2013). Development of a standardised human in vitro digestion protocol based on macronutrient digestion using response surface methodology. Food Chemistry, 138(2-3):1936 -1944.

Hooser, S. and Earnest, D. (2010). Introduction: The Gastrointestinal Tract -.InComprehensiveToxicology,pa - -2.Elsevier.

Houghton, D., Wilcox, M. D., Chater, P. I., Brownlee, I. A., Seal, C. J., and Pearson, J. P. (2015). Biological activity of alginate and its effect on pancreatic lipase inhibition as a potential treatment for obesity. Food Hydrocolloids, 49:18 -24.

Humphrey, S. P. and Williamson, R. T. (2001a). A review of saliva: Normal composition flow, and function. The Journal of Prosthetic Dentistry, 85(2):162 -169.

Hur, S. J., Lim, B. O., Decker, E. A., and McClements, D. J. (2011a). In vitro human digestion models for food applications. Food Chemistry, 125(1):1 -12.

Iveson, S. M., Beathe, J. A., and Page, N. W. (2002). The dynamic strength of partially saturated powder compacts: the effect of liquid properties. Powder Technology, 127(2):149 -161.

Izydorczyk,M.(2009).Arabinoxylans. In Handbook of Hydrocolloids,pages653 -692. Elsevier.

Izydorczyk, M. S. and Biliaderis, C. G. (1995). Cereal arabinoxylans: advances in structure and physicochemical properties. Carbohydrate Polymers, 28(1):33 -48.

Jaime-Fonseca, M. R., Gouseti, O., Fryer, P. J., Wickham, M. S. J., and Bakalis, S. (2015a). Digestion of starch in a dynamic small intestinal model. European Journal of Nutrition, 55(8):2377 -2388.

James, B. (2014a). Food Microstructure Analysis. In Engineering Properties of Foods Fourth Edition, pages 63 -92. CRC Press.

Janssen, P., Berghe, P. V., Verschueren, S., Lehmann, A., Depoortere, I., and Tack, J. (2011). Review article: the role of gastric motility in the control of food intake. Alimentary Pharmacology & Therapeutics, 33(8):880 -894.

Janssen, P. W. M., Lentle, R. G., Asvarujanon, P., Chambers, P., Stafford, K. J., and Hemar, Y. (2007). Characterization of flow and mixing regimes within the ileum of the brushtail possum using residence time distribution analysis with simultaneous spatio-temporal mapping. The Journal of Physiology, 582(3):1239 -1248.

Jenkins, D. J., Kendall, C. W., Axelsen, M., Augustin, L. S., and Vuksan, V. (2000). Viscous and nonviscous fibres nonabsorbable and low glycaemic index carbohydrates, blood lipids and coronary heart disease. Current Opinion in Lipidology, 11(1):49 -56.

Jenkins, D. J. A. (1977). Decrease in Postprandial Insulin and Glucose Concentrations by Guar and Pectin. Annals of Internal Medicine, 86(1):20.

Jenkins, G. (1978). The physiology and biochemistry of the mouth (4th ed.). Oxford: Blackwell.

Johnson, L. R. (2012a). Preface to the First Edition. In Physiology of the Gastrointestinal Tract, page xv. Elsevier.

Johnson, L. R. (2014a). Gastrointestinal physiology (8th ed.). Philadelphia, PA: Elsevier Mosby.

Johnston, K. L., Thomas, E. L., Bell, J. D., Frost, G. S., and Robertson, M. D. (2010). Resistant starch improves insulin sensitivity in metabolic syndrome. Diabetic Medicine, 27(4):391 -397.

Jones, K. L., Russo, A., Stevens, J. E., Wishart, J. M., Berry, M. K., and Horowitz, M. (2001). Predictors of Delayed Gastric Emptying in Diabetes. Diabetes Care, 24(7):1264 -1269.

Joshi, B. S., Farakte, R. A., Yadav, G. U., Patwardhan, A. W., and Singh, G. (2015a). Swelling kinetics of tea in hot water. Journal of Food Science and Technology, 53(1):315 -325.

Ju, Z., Hettiarachchy, N., and Rath, N. (2001). Extraction denaturation and hydrophobic Properties of Rice Flour Proteins. Journal of Food Science, 66(2):229 -232.

Jumars, P. A. (2000). Animal Guts as Ideal Chemical Reactors: Maximizing Absorption Rates. The American Naturalist, 155(4):527 -543.

Kam, J., Puranik, S., Yadav, R., Manwaring, H. R., Pierre, S., Srivastava, R. K., and Yadav, R. S. (2016). Dietary Interventions for Type 2 Diabetes: How Millet Comes to Help. Frontiers in Plant Science, 7.

Karadag, E., Saraydin, D., -aldiran, Y., and G -ven, O. (2000). Swelling studies of copolymeric acrylamide/crotonic acid hydrogels as carriers for agricultural uses. Polymers for Advanced Technologies, 11(2):59 -68.

Kararli, T. T. (1995). Comparison of the gastrointestinal anatomy physiology, and biochemistry of humans and commonly used laboratory animals. Biopharmaceutics & Drug Disposition, 16(5):351 -380.

Kellett, G. L. and Brot-Laroche, E. (2005). Apical GLUT2: A Major Pathway of Intestinal Sugar Absorption. Diabetes, 54(10):3056 -3062.

Kellow, J., Borody, T., Phillips, S., Tucker, R., and Haddad, A. (1986). Human interdigestive motility: Variations in patterns from esophagus to colon. Gastroenterology, 91(2):386 -395.

Kendall, C. W., Esfahani, A., and Jenkins, D. J. (2010). The link between dietary fibre and human health. Food Hydrocolloids, 24(1):42 -48.

Kerlin, P., Zinsmeister, A., and Phillips, S. (1982). Relationship of motility to flow of contents in the human small intestine. Gastroenterology, 82:701 -6.

Khatkar, B., Bell, A., and Schofield, J. (1995). The dynamic rheological properties of glutens and gluten sub-fractions from wheats of good and poor bread making quality. Journal of Cereal Science, 22(1):29 -44.

Khattak,W.A.,Ul-Islam,M.,andPark,J.K.(2012).Prospectsofreusableendogenous hydrolyzing enzymes in bioethanol production by simultaneous saccharification and fermentation. Korean Journal of Chemical Engineering, 29(11):1467 -1482.

Koh, L. W., Kasapis, S., Lim, K. M., and Foo, C. W. (2009). Structural enhancement leading to retardation of in vitro digestion of rice dough in the presence of alginate. Food Hydrocolloids, 23(6):1458 -1464.

Kong,F.andSingh,R.(2008a).AModelStomachSystemtoInvestigateDisintegration Kinetics of Solid Foods during Gastric Digestion. Journal of Food Science, 73(5):E202 - E210.

Kong, F. and Singh, R. (2008b). A Model Stomach System to Investigate Disin- tegration Kinetics of Solid Foods during Gastric Digestion. Journal of Food Science, 73(5):E202 -E210.

Kong,F.andSingh,R.(2008c).AModelStomachSystemtoInvestigateDisintegration Kinetics of Solid Foods during Gastric Digestion. Journal of Food Science, 73(5):E202 - E210.

Koziolek, M., Garbacz, G., Neumann, M., and Weitschies, W. (2013). Simulating the Postprandial Stomach: Physiological Considerations for Dissolution and Release Testing. Molecular Pharmaceutics, 10(5):1610 -1622.

Kristensen, M. and Jensen, M. G. (2011). Dietary fibres in the regulation of appetite and food intake. Importance of viscosity. Appetite, 56(1):65 -70.

Kritchevsky, D. (1982). Fiber Obesity, and Diabetes. In Dietary Fiber in Health and Disease, pages 133 -137. Springer US.

Kukukova, A., Aubin, J., and Kresta, S. M. (2009a). A new definition of mixing and segregation: Three dimensions of a key process variable. Chemical Engineering Research and Design, 87(4):633 -647.

Lairon, D., Play, B., and JOURDHEUILRAHMANI, D. (2007). Digestible and indigestible carbohydrates: interactions with postprandial lipid metabolism. The Journal of Nutritional Biochemistry, 18(4):217 -227.

Lazaridou, A., Duta, D., Papageorgiou, M., Belc, N., and Biliaderis, C. (2007). Effects of hydrocolloids on dough rheology and bread quality parameters in gluten-free formulations. Journal of Food Engineering, 79(3):1033 -1047.

Leadbeater, T. W., Parker, D. J., and Gargiuli, J. (2012). Positron imaging systems for studying particulate granular and multiphase flows. Particuology, 10(2):146 -153.

Leeds, A. R. (1982). Modification of Intestinal Absorption by Dietary Fiber and Fiber Components. In Dietary Fiber in Health and Disease, pages 53 -71. Springer US.

Lehmann, U. and Robin, F. (2007). Slowly digestible starch - its structure and health implications: a review. Trends in Food Science & Technology, 18(7):346 -355.

Lentle, R. and Janssen, P. (2010). Manipulating digestion with foods designed to change the physical characteristics of digesta. Crit Rev Food Sci Nutr, 50:130 -45.

Lentle,R.G.,Hemar,Y.,Hall,C.E.,andStafford,K.J.(2005).Periodic fluid extrusion and models of digesta mixing in the intestine of a herbivore the common brushtail possum (Trichosurus vulpecula). Journal of Comparative Physiology B, 175(5):337 -347.

Lentle, R. G. and Janssen, P. W. M. (2008a). Physical characteristics of digesta and their influence on flow and mixing in the mammalian intestine: a review. Journal of Comparative Physiology B, 178(6):673 -690.

Lentle, R. G. and Janssen, P. W. M. (2011a). Contractile Activity and Control of the Physical Process of Digestion Within a Gut Segment. In The Physical Processes of Digestion, pages 121 -153. Springer New York.

Lentle, R. G. and Janssen, P. W. M. (2011b). Flow Mixing and Absorption at the Mucosa. In The Physical Processes of Digestion, pages 221 -274. Springer New York.

Lentle, R. G. and Janssen, P. W. M. (2011c). Physical Aspects of the Digestion of Protein Particles. In The Physical Processes of Digestion, pages 47 -61. Springer New York.

Lentle, R. G., Loubens, C. D., Hulls, C., Janssen, P. W. M., Golding, M. D., and Chambers, J. P. (2012). A comparison of the organization of longitudinal and circular contractions during pendular and segmental activity in the duodenum of the rat and guinea pig. Neurogastroenterology & Motility, 24(7):686 -e298.

Levenspiel, O. (1973). Chemical reaction engineering Octave Levenspiel, Wiley, New York(1972). 578 pages.$16.95. AIChE Journal, 19(1):206 -207.

Levenspiel, O. (1999a). Chemical Reaction Engineering. Industrial & Engineering Chemistry Research, 38(11):4140 -4143.

Levenspiel, O. (1999b). Chemical Reaction Engineering. Industrial & Engineering Chemistry Research, 38(11):4140 -4143.

[Li, Q., Liu, R., Wu, T., and Zhang, M. (2017). Aggregation and rheological behavior of soluble dietary fibers from wheat bran. Food Res Int, 102:291 -302.

Liao, Y. and Lucas, D. (2010). A literature review on mechanisms and models for the coalescence process of fluid particles. Chemical Engineering Science, 65(10):2851 -2864.

Liddle, R. A. (2012). Regulation of Pancreatic Secretion. In Physiology of the Gastrointestinal Tract, pages 1425 -1460. Elsevier.

Lim, Y. F., de Loubens, C., Love, R. J., Lentle, R. G., and Janssen, P. W. M. (2015). Flow and mixing by small intestine villi. Food & Function, 6(6):1787 -1795.

L, A. C. B., Pereira, A. J. G., and Junqueira, R. G. (2004). Flour mixture of rice flour corn and cassava starch in the production of gluten-free white bread. Brazilian Archives of Biology and Technology, 47(1):63 -70.

Lu, Z. X., Walker, K. Z., Muir, J. G., Mascara, T., and O'Dea, K. (2000b). Arabinoxylan fiber a byproduct of wheat flour processing, reduces the postprandial glucose response in normoglycemic subjects. The American Journal of Clinical Nutrition, 71(5):1123 -1128.

Lu, Z. X., Walker, K. Z., Muir, J. G., and O'Dea, K. (2004). Arabinoxylan fibre improves metabolic control in people with Type II diabetes. European Journal of Clinical Nutrition, 58(4):621 -628.

Lund, E., Farleigh, C., and Johnson, I. (2005). DO OATS LOWER BLOOD CHOLESTEROL - In Dietary Fibre, pages 296 -299. Elsevier.

Lvova, L., Denis, S., Barra, A., Mielle, P., Salles, C., Vergoignan, C., Natale, C. D., Paolesse, R., Temple-Boyer, P., and Feron, G. (2012a). Salt release monitoring with specific sensors in -in vitro - oral and digestive environments from soft cheeses. Talanta, 97:171 -180.

Lvova, L., Denis, S., Barra, A., Mielle, P., Salles, C., Vergoignan, C., Natale, C. D., Paolesse, R., Temple-Boyer, P., and Feron, G. (2012b). Salt release monitoring with specific sensors in -in vitro - oral and digestive environments from soft cheeses. Talanta, 97:171 -180.

Macritchie, F. (1992). Physicochemical Properties of Wheat Proteins in Relation to Functionality. In Advances in Food and Nutrition Research, pages 1 -87. Elsevier.

Mahadevan, V. (2014a). Anatomy of the small intestine. Surgery (Oxford), 32(8):391 -395.

Mahadevan, V. (2017). Anatomy of the small intestine. Surgery (Oxford), 35(8):407 -412.

Maldonado-Valderrama, J., Terriza, J. A. H., Torcello-G, A., and Cabrerizo- Vhez, M. A. (2013). In vitro digestion of interfacial protein structures. Soft Matter, 9(4):1043 -1053.

Malone, M., Appelqvist, I., and Norton, I. (2003). Oral behaviour of food hydrocol- loids and emulsions. Part 1. Lubrication and deposition considerations. Food Hydrocol- loids, 17(6):763 -773.

Malumba,P.,Jacquet,N.,Delimme,G.,Lefebvre,F.,andB,F.(2013).Theswelling behaviour of wheat starch granules during isothermal and non-isothermal treatments. Journal of Food Engineering, 114(2):199 -206.

Mandala, I. and Kapsokefalou, M. (2011). Gluten-Free Bread. In Flour and Breads and their Fortification in Health and Disease Prevention, pages 161 -169. Elsevier.

Mandalari, G., Adel-Patient, K., Barkholt, V., Baro, C., Bennett, L., Bublin, M., Gaier, S., Graser, G., Ladics, G., Mierzejewska, D., Vassilopoulou, E., Vissers, Y., Zuidmeer, L., Rigby, N., Salt, L., Defernez, M., Mulholland, F., Mackie, A., Wickham, M., and Mills, E. (2009b). In vitro digestibility of -casein and -lactoglobulin under simulated human gastric and duodenal conditions: A multi-laboratory evaluation. Regulatory Toxicology and Pharmacology, 55(3):372 -381.

Marciani, L., Gowland, P. A., Spiller, R. C., Manoj, P., Moore, R. J., Young, P., and Fillery-Travis, A. J. (2001). Effect of meal viscosity and nutrients on satiety intragastric dilution, and emptying assessed by MRI. American Journal of Physiology-Gastrointestinal and Liver Physiology, 280(6):G1227 -G1233.

Marco, C. and Rosell, C. M. (2008). Breadmaking performance of protein enriched gluten-free breads. European Food Research and Technology, 227(4):1205 -1213.

-Mario, F. D. and Goni, E. (2014). Gastric acid secretion: Changes during a century. Best Practice & Research Clinical Gastroenterology, 28(6):953 -965.

-Marlett, J. (2001). Dietary Fiber and Cardiovascular Disease. In Handbook of Dietary Fiber, pages 17 -30. CRC Press.

Marteau, P., Minekus, M., Havenaar, R., and Veld, J. H. I. (1997). Survival of Lactic Acid Bacteria in a Dynamic Model of the Stomach and Small Intestine: Validation and the Effects of Bile. Journal of Dairy Science, 80(6):1031 -1037.

MartAlfonso, J., Cuadri, A., Berta, M., and Stading, M. (2018). Relation be- tween concentration and shear-extensional rheology properties of xanthan and guar gum solutions. Carbohydrate Polymers, 181:63 -70.

Maughan, R. J. and Vise, G. E. (1992). GASTRIC EMPTYING OF DILUTE GLUCOSE SOLUTIONS IN MAN. Medicine & Science in Sports & Exercise, 24 (Supplement):S40.

McClements, D. J. and Li, Y. (2010). Review of in vitro digestion models for rapid screening of emulsion-based systems. Food & Function, 1(1):32.

McPherson, K., Marsh, T., and Brown, M. (2007a). Tackling Obesities: Future Choices -Modelling Future Trends in Obesity & Their Impact on Health. American Psychological Association (APA).

Mennah-Govela, Y. A., Bornhorst, G. M., and Singh, R. P. (2015). Acid Diffusion into Rice Boluses is Influenced by Rice Type Variety, and Presence of -Amylase. Journal of Food Science, 80(2):E316 -E325.

Mercadrieto,R.,Falconer,R.J.,Paterson,W.R.,and Wilson,D.I.(2007).Swelling and Dissolution of -Lactoglobulin Gels in Alkali. Biomacromolecules, 8(2):469 -476.

Mercadrieto, R., Paterson, W. R., and Wilson, D. I. (2009). Effect of salts on the alkaline degradation of -lactoglobulin gels and aggregates: Existence of a dissolution threshold. Food Hydrocolloids, 23(6):1587 -1595.

Mercuri, A., Passalacqua, A., Wickham, M. S. J., Faulks, R. M., Craig, D. Q. M., and Barker, S. A. (2011). The Effect of Composition and Gastric Conditions on the Self-Emulsification Process of Ibuprofen-Loaded Self-Emulsifying Drug Delivery Systems: A Microscopic and Dynamic Gastric Model Study. Pharmaceutical Research, 28(7):1540 -1551.

Meullenet, J.-F. and Gandhapuneni, R. (2006). Development of the BITE Master II and its application to the study of cheese hardness. Physiology & Behavior, 89(1):39 -43.

Meyer, J. H., Gu, Y., Elashoff, J., Reedy, T., Dressman, J., and Amidon, G. (1986). Effects of viscosity and fluid outflow on postcibal gastric emptying of solids. American Journal of Physiology-Gastrointestinal and Liver Physiology, 250(2):G161 -G164.

Miller, G. L. (1959). Use of Dinitrosalicylic Acid Reagent for Determination of Reducing Sugar. Analytical Chemistry, 31(3):426 -428.

Mills, T., Spyropoulos, F., Norton, I. T., and Bakalis, S. (2011). Development of an in-vitro mouth model to quantify salt release from gels. Food Hydrocolloids, 25(1):107 -113.

Minekus, M., e. a. (1995.). A Multicompartmental Dynamic Computer-Controlled Model Simulating the Stomach and Small-intestine. Alternatives to Laboratory Animals, 2: p. 197-209.

Minekus, M., Alminger, M., Alvito, P., Ballance, S., Bohn, T., Bourlieu, C., Carri, F., Boutrou, R., Corredig, M., Dupont, D., Dufour, C., Egger, L., Golding, M., Karakaya, S., Kirkhus, B., Feunteun, S. L., Lesmes, U., Macierzanka, A., Mackie, A., Marze, S., McClements, D. J., Mrd, O., Recio, I., Santos, C. N., Singh, R. P., Vegarud, G. E., Wickham, M. S. J., Weitschies, W., and Brodkorb, A. (2014a). A standardised static in vitro digestion method suitable for food - an international consensus. Food Funct., 5(6):1113 -1124.

Minekus, M., Smeets-Peeters, M., Bernalier, A., Marol-Bonnin, S., Havenaar, R., Marteau, P., Alric, M., Fonty, G., and in't Veld, J. H. J. H. (1999a). A computer-controlled system to simulate conditions of the large intestine with peristaltic mixing water absorption and absorption of fermentation products. Applied Microbiology and Biotechnology, 53(1):108 -114.

Minekus, M., Smeets-Peeters, M., Bernalier, A., Marol-Bonnin, S., Havenaar, R., Marteau, P., Alric, M., Fonty, G., and in't Veld, J. H. J. H. (1999b). A computer-controlled system to simulate conditions of the large intestine with peristaltic mixing water absorption and absorption of fermentation products. Applied Microbiology and Biotechnology, 53(1):108 -114.

Mishra, S., Hardacre, A., and Monro, J. (2012). Food Structure and Carbohydrate Digestibility. In Carbohydrates - Comprehensive Studies on Glycobiology and Glycotechnology. InTech.

Moore, J. G., Christian, P. E., Brown, J. A., Brophy, C., Datz, F., Taylor, A., and Alazraki, N. (1984). Influence of meal weight and caloric content on gastric emptying of meals in man. Digestive Diseases and Sciences, 29(6):513 -519.

Moran, T. H., Wirth, J. B., Schwartz, G. J., and McHugh, P. R. (1999). Interactions between gastric volume and duodenal nutrients in the control of liquid gastric emptying. American Journal of Physiology-Regulatory Integrative and Comparative Physiology, 276(4):R997 -R1002.

Moreno, F., Mackie, A., and Mills, E. (2005a). Phospholipid interactions protect the milk allergen alpha-lactalbumin from proteolysis during in vitro digestion. J Agric Food Chem, 53:9810 -6.

Moreno, F. J., Mackie, A. R., and Mills, E. N. C. (2005b). Phospholipid Interac- tions Protect the Milk Allergen -Lactalbumin from Proteolysis during in Vitro Digestion. Journal of Agricultural and Food Chemistry, 53(25):9810 -9816.

Muir, J. and O -Dea, K. (1992). Measurement of resistant starch: factors affecting the amount of starch escaping digestion in vitro. Am J Clin Nutr, 56:123 -7.

Munoz, J. M. (1982). Interactions of Dietary Fiber and Nutrients. In Dietary Fiber in Health and Disease, pages 85 -89. Springer US.

Nicolas, V., Vanin, F., Grenier, D., Lucas, T., Doursat, C., and Flick, D. (2016). Modeling bread baking with focus on overall deformation and local porosity evolution. AIChE Journal, 62(11):3847 -3863.

Norton, I., Moore, S., and Fryer, P. (2007a). Understanding food structuring and breakdown: engineering approaches to obesity. Obesity Reviews, 8(s1):83 -88.

Norton, I., Moore, S., and Fryer, P. (2007b). Understanding food structuring and breakdown: engineering approaches to obesity. Obesity Reviews, 8(s1):83 -88.

Norton, J. E., Wallis, G. A., Spyropoulos, F., Lillford, P. J., and Norton, I. T. (2014). Designing Food Structures for Nutrition and Health Benefits. Annual Review of Food Science and Technology, 5(1):177 -195.

Ogden, C., Carroll, M., Fakhouri, T., Hales, C., Fryar, C., Li, X., and Freedman, D. (2018). Prevalence of Obesity Among Youths by Household Income and Education Level of Head of Household - United States 2011-2014. MMWR Morb Mortal Wkly Rep, 67:186 -189.

Ogden, C. L., Carroll, M. D., Curtin, L. R., McDowell, M. A., Tabak, C. J., and Flegal, K. M. (2006). Prevalence of Overweight and Obesity in the United States 1999-2004. JAMA, 295(13):1549.

Oomen, A. G., Rompelberg, C. J. M., Bruil, M. A., Dobbe, C. J. G., Pereboom, D. P. K. H., and Sips, A. J. A. M. (2003). Development of an In Vitro Digestion Model for Estimating the Bioaccessibility of Soil Contaminants. Archives of Environmental Contamination and Toxicology, 44(3):281 -287.

Oztop, M. H. and McCarthy, K. L. (2011). Mathematical modeling of swelling in high moisture whey protein gels. Journal of Food Engineering, 106(1):53 -59.

Pal.A, K, I., W, S., B, A., Fried, M., and Brasseur, J. G. (2004). Gastric flow and mixing studied using computer simulation. Proceedings of the Royal Society B: Biological Sciences, 271(1557):2587 -2594.

Pallotta, N., Corazziari, E., Scopinaro, F., Bonino, R., Schillaci, O., Vignoni, A., Mangano, M., and Torsoli, A. (1998). Noninvasive estimate of bile flux through the gallbladder in humans. The American Journal of Gastroenterology, 93(10):1877 -1885.

Parada, J. and Aguilera, J. (2011). Review: Starch Matrices and the Glycemic Response. Food Science and Technology International, 17(3):187 -204.

Park, I., Kim, Y. I., and Kim, S. W. (2016). 0929 Effects of dietary supplementation of -mannanase on digesta viscosity and intestinal health of nursery pigs. Journal of Animal Science, 94(supplement5):447.

Park, M.-S., Chung, J.-W., Kim, Y.-K., Chung, S.-C., and Kho, H.-S. (2007). Viscosity and wettability of animal mucin solutions and human saliva. Oral Diseases, 13(2):181 - 186.

Parker, D. J., Leadbeater, T. W., Fan, X., Hausard, M. N., Ingram, A., and Yang, Z. (2008). Positron imaging techniques for process engineering: recent developments at Birmingham. Measurement Science and Technology, 19(9):094004.

Penry, D. L. and Jumars, P. A. (1986a). Chemical Reactor Analysis and Optimal Digestion. BioScience, 36(5):310 -315.

Penry, D. L. and Jumars, P. A. (1987). Modeling Animal Guts as Chemical Reactors. The American Naturalist, 129(1):69 -96.

Peppas, N. A. and Brannon-Peppas, L. (1994). Water Diffusion and Sorption in Amorphous Macromolecular Systems and Foods. In Water in Foods, pages 189 -210. Elsevier.

Perry, D. W. G. R. H. (2008). Perry -s chemical engineers handbook. Choice Reviews Online, 45(08):45 -4393 -45 -4393.

Peyron, M.-A., Gierczynski, I., Hartmann, C., Loret, C., Dardevet, D., Martin, N., and Woda, A. (2011). Role of Physical Bolus Properties as Sensory Inputs in the Trigger of Swallowing. PLoS ONE, 6(6):e21167.

Primo-Mart C., van de Pijpekamp, A., van Vliet, T., de Jongh, H., Plijter, J., and Hamer, R. (2006). The role of the gluten network in the crispness of bread crust. Journal of Cereal Science, 43(3):342 -352.

Prinz, J. F. and Lucas, P. W. (1997a). An optimization model for mastication and swallowing in mammals. Proceedings of the Royal Society B: Biological Sciences, 264(1389):1715 -1721.

Ralet, M.-C., Thibault, J.-F., and Valle, G. D. (1990). Influence of extrusion-cooking on the physico-chemical properties of wheat bran. Journal of Cereal Science, 11(3):249 - 259.

Ranawana, V., Leow, M. K.-S., and Henry, C. J. K. (2013). Mastication effects on the glycaemic index: impact on variability and practical implications. European Journal of Clinical Nutrition, 68(1):137 -139.

Rey, A., Gonzz, R., de Juan, J. M., Benedito, J., and Mulet, A. (2007). EMG assess- ment of chewing behaviour for food evaluation: Influence of personality characteristics. Food Quality and Preference, 18(3):585 -595.

Ridgwell, J. (1986). Food Around the World. Oxford University Press, 126 Pages.

Roberts, F., Smith, H., Low, A., and Ellis, P. (2005). Influence of wheat breads containing guar flour supplements of high and low molecular weights on viscosity of jejunal digesta in the pig. In Dietary Fibre, pages 164 -168. Elsevier.

Roberts, K. (2011). The physiological and rheological effects of foods supplemented with guar gum. Food Research International, 44(5):1109 -1114.

Rodrigues,S.A.,Young,A.K.,James,B.J.,andMorgenstern,M.P.(2014).Structural Changes Within a Biscuit Bolus During Mastication. Journal of Texture Studies, 45(2):89 - 96.

Rosell, C., Rojas, J., and de Barber, C. B. (2001). Influence of hydrocolloids on dough rheology and bread quality. Food Hydrocolloids, 15(1):75 -81.

Salles, C., Tarrega, A., Mielle, P., Maratray, J., Gorria, P., Liaboeuf, J., and Liodenot, J.-J. (2007a). Development of a chewing simulator for food breakdown and the analysis of in vitro flavor compound release in a mouth environment. Journal of Food Engineering, 82(2):189 -198.

Sams, L., Paume, J., Giallo, J., and Carri, F. (2016). Relevant pH and lipase for in vitro models of gastric digestion. Food Funct., 7(1):30 -45.

Sarna, S. K. (1985). Cyclic motor activity migrating motor complex: 1985. Gastroenterology, 89(4):894 -913.

Saulnier, L., Peneau, N., and Thibault, J.-F. (1995a). Variability in grain extract viscosity and water-soluble arabinoxylan content in wheat. Journal of Cereal Science, 22(3):259 -264.

Savoie, L. (1994). Digestion and absorption of food: usefulness and limitations of in vitro models. Canadian Journal of Physiology and Pharmacology, 72(4):407 -414.

Schober, T. J. (2009). Manufacture of Gluten-Free Specialty Breads and Confectionery Products. In Gluten-Free Food Science and Technology, pages 130 -180. Wiley-Blackwell.

Schulze, K. (2006a). Imaging and modelling of digestion in the stomach and the duodenum. Neurogastroenterology and Motility, 18(3):172 -183.

Segura, M. E. M. and Rosell, C. M. (2011). Chemical Composition and Starch Digestibility of Different Gluten-free Breads. Plant Foods for Human Nutrition, 66(3):224 -230.

Shan, L. (2002). Structural Basis for Gluten Intolerance in Celiac Sprue. Science, 297(5590):2275 -2279.

Shewry, P. and Ward, J. (2009). PREFACE. In HEALTHGRAIN Methods, page iii. Elsevier.

Shewry, P. R., Halford, N. G., Belton, P. S., and Tatham, A. S. (2002). The structure and properties of gluten: an elastic protein from wheat grain. Philosophical Transactions of the Royal Society B: Biological Sciences, 357(1418):133 -142.

Siegel, J. A., Urbain, J. L., Adler, L. P., Charkes, N. D., Maurer, A. H., Krevsky, B., Knight, L. C., Fisher, R. S., and Malmud, L. S. (1988). Biphasic nature of gastric emptying. Gut, 29(1):85 -89.

Singh, J., Berg, T., Hardacre, A., and Boland, M. J. (2014). Cotyledon Cell Structure and In Vitro Starch Digestion in Navy Beans. In Food Structures Digestion and Health, pages 223 -242. Elsevier.

Singh, J., Dartois, A., and Kaur, L. (2010). Starch digestibility in food matrix: a review. Trends in Food Science & Technology, 21(4):168 -180.

Skandalakis, J. E., Skandalakis, P. N., and Skandalakis, L. J. (1995). Duodenum. In Surgical Anatomy and Technique, pages 311 -326. Springer US.

Skandalakis, L. J. and Skandalakis, J. E. (2013). Duodenum. In Surgical Anatomy and Technique, pages 345 -360. Springer New York.

Skandalakis, L. J., Skandalakis, J. E., and Skandalakis, P. N. (2009a). Surgical Anatomy and Technique. Springer New York.

Slavin, J. (2013). Fiber and Prebiotics: Mechanisms and Health Benefits. Nutrients, 5(4):1417 -1435.

Slavin, J. and Jacobs, D. R. (2009). Dietary Fiber: All Fibers are not Alike. In Nutrition Guide for Physicians, pages 13 -24. Humana Press.

Slavin, J. L. (2005). Dietary fiber and body weight. Nutrition, 21(3):411 -418.

Smithson, K., Millar, D., Jacobs, L., and Gray, G. (1981). Intestinal diffusion barrier: unstirred water layer or membrane surface mucous coat - Science, 214(4526):1241 -1244.

Sobotta, J. (1907). volume 157. New England Journal of Medicine (NEJM/MMS). [328] Southgate, D. (2001). The Southgate Method of Dietary Fiber Analysis. In CRC Handbook of Dietary Fiber in Human Nutrition Third Edition, pages 83 -86. CRC Press.

Stankovic, I., Miletic, I., and Miletic, V. (1995). INVESTIGATION OF HYPER- SENSITIVITY TO WHEAT GLIADIN FROM GLUTEN-FREE DIETARY PRODUCTS USING DOT-BLOT ASSAY. In Wheat Structure, pages 189 -191. Elsevier.

Stoll, B. R., Batycky, R. P., Leipold, H. R., Milstein, S., and Edwards, D. A. (2000a). A theory of molecular absorption from the small intestine. Chemical Engineering Science, 55(3):473 -489.

Stoll, B. R., Batycky, R. P., Leipold, H. R., Milstein, S., and Edwards, D. A. (2000b). A theory of molecular absorption from the small intestine. Chemical Engineering Science, 55(3):473 -489.

Sugano, K. (2009). Introduction to computational oral absorption simulation. Expert Opinion on Drug Metabolism & Toxicology, 5(3):259 -293.

Symons, L. and Brennan, C. (2006). The Influence of (1-3) (1-4)-beta-D-Glucan-rich Fractions from Barley on the Physicochemical Properties and In Vitro Reducing Sugar Release of White Wheat Breads.

Takahashi, T. (2011). Flow Behavior of Digesta and the Absorption of Nutrients in the Gastrointestine. Journal of Nutritional Science and Vitaminology, 57(4):265 -273.

Takahashi, T., Noborikawa, M., ichi Oda, S., Maruyama, S., Koda, T., Tokunaga, M., Naoi, M., and Kitamori, K. (2012). Digesta Viscosity and Glucose Behavior in the Small Intestine Lumen. In Dietary Fiber and Health, pages 185 -196. CRC Press.

Takahashi, T. and Sakata, T. (2004). Viscous properties of pig cecal contents and the contribution of solid particles to viscosity. Nutrition, 20(4):377 -382.

Tharakan, A., Norton, I., Fryer, P., and Bakalis, S. (2010a). Mass transfer and nutrient absorption in a simulated model of small intestine. J Food Sci, 75:E339 -46.

Tharakan, A., Norton, I., Fryer, P., and Bakalis, S. (2010b). Mass Transfer and Nutrient Absorption in a Simulated Model of Small Intestine. Journal of Food Science, 75(6):E339 -E346.

Thomas, K., Aalbers, M., Bannon, G., Bartels, M., Dearman, R., Esdaile, D., Fu, T., Glatt, C., Hadfield, N., Hatzos, C., Hefle, S., Heylings, J., Goodman, R., Henry, B., Herouet, C., Holsapple, M., Ladics, G., Landry, T., MacIntosh, S., Rice, E., Privalle, L., Steiner, H., Teshima, R., van Ree, R., Woolhiser, M., and Zawodny, J. (2004). A multi-laboratory evaluation of a common in vitro pepsin digestion assay protocol used in assessing the safety of novel proteins. Regulatory Toxicology and Pharmacology, 39(2):87 -98.

Thuenemann, E. C., Mandalari, G., Rich, G. T., and Faulks, R. M. (2015). Dynamic Gastric Model (DGM). In The Impact of Food Bioactives on Health, pages 47 -59. Springer International Publishing.

Topping, D. L. and Clifton, P. M. (2001). Short-Chain Fatty Acids and Human Colonic Function: Roles of Resistant Starch and Nonstarch Polysaccharides. Physiological Reviews, 81(3):1031 -1064.

Torsdottir, I., Alpsten, M., Andersson, H., and Einarsson, S. (1989a). Dietary Guar Gum Effects on Postprandial Blood Glucose Insulin and Hydroxyproline in Humans. The Journal of Nutrition, 119(12):1925 -1931.

Tungland, B. and Meyer, D. (2002). Nondigestible Oligo- and Polysaccharides (Dietary Fiber): Their Physiology and Role in Human Health and Food. Comprehensive Reviews in Food Science and Food Safety, 1(3):90 -109.

Ulleberg, E. K., Comi, I., Holm, H., Herud, E. B., Jacobsen, M., and Vegarud, G. E. (2011). Human Gastrointestinal Juices Intended for Use in In Vitro Digestion Models. Food Digestion, 2(1-3):52 -61.

Urbain, J.-L., Siegel, J., Charkes, N., Maurer, A., Malmud, L., and Fisher, R. (1989). The two-component stomach: effects of meal particle size on fundal and antral emptying. European Journal of Nuclear Medicine, 15(5).

Vardakou, M., Mercuri, A., Barker, S. A., Craig, D. Q. M., Faulks, R. M., and Wickham, M. S. J. (2011). Achieving Antral Grinding Forces in Biorelevant In Vitro Models: Comparing the USP Dissolution Apparatus II and the Dynamic Gastric Model with Human In Vivo Data. AAPS PharmSciTech, 12(2):620 -626.

Vassallo, M. J., Camilleri, M., Prather, C. M., Hanson, R. B., and Thomforde, G. M. (1992). Measurement of axial forces during emptying from the human stomach. American Journal of Physiology-Gastrointestinal and Liver Physiology, 263(2):G230 -G239.

Verhoeckx, K. (2015). The Impact of Food Bio-Actives on Gut Health. Springer Open.

Vieira, M. L. T., Kirby, B., Ragueneau-Majlessi, I., Galetin, A., Chien, J. Y. L., Einolf, H. J., Fahmi, O. A., Fischer, V., Fretland, A., Grime, K., Hall, S. D., Higgs, R., Plowchalk, D., Riley, R., Seibert, E., Skordos, K., Snoeys, J., Venkatakrishnan, K., Waterhouse, T., Obach, R. S., Berglund, E. G., Zhang, L., Zhao, P., Reynolds, K. S., and Huang, S.-M. (2013). Evaluation of Various Static In Vitro -In Vivo Extrapolation Models for Risk Assessment of the CYP3A Inhibition Potential of an Investigational Drug. Clinical Pharmacology & Therapeutics, 95(2):189 -198.

Virtual.Medical.Centre. (2018). Virtual Medical Centre as the source material. Technical report.

Vist, G. E. and Maughan, R. J. (1995). The effect of osmolality and carbohydrate content on the rate of gastric emptying of liquids in man. The Journal of Physiology, 486(2):523 -531.

Wagner, H. N. (1991). Molecular medicine: From science to service. J. Nucl. Med, 32, 561 -564.

Wang, Y., Brasseur, J. G., Banco, G. G., Webb, A. G., Ailiani, A. C., and Neuberger, T. (2010). A multiscale lattice Boltzmann model of macro- to micro-scale transport with applications to gut function. Philosophical Transactions of the Royal Society A: Mathematical, Physical and Engineering Sciences, 368(1921):2863 -2880.

Wasserman, D. H. (2009). Four grams of glucose. American Journal of Physiology-Endocrinology and Metabolism, 296(1):E11 -E21.

Wey, A. V., Cookson, A., Roy, N., McNabb, W., Soboleva, T., Wieliczko, R., and Shorten, P. (2014a). A mathematical model of the effect of pH and food matrix composition on fluid transport into foods: An application in gastric digestion and cheese brining. Food Research International, 57:34 -43.

Wey, A. V., Cookson, A., Roy, N., McNabb, W., Soboleva, T., Wieliczko, R., and Shorten, P. (2014b). A mathematical model of the effect of pH and food matrix composi- tion on fluid transport into foods: An application in gastric digestion and cheese brining. Food Research International, 57:34 -43.

Wickham, M. J. S., Faulks, R. M., Mann, J., and Mandalari, G. (2012). The Design Operation, and Application of a Dynamic Gastric Model. Dissolution Technologies, 19(3):15 -22.

Wilde, P. and Chu, B. (2011). Interfacial & colloidal aspects of lipid digestion. Advances in Colloid and Interface Science, 165(1):14 -22.

Woda, A., Mishellany-Dutour, A., Batier, L., Frans, O., Meunier, J.-P., Reynaud, B., Alric, M., and Peyron, M.-A. (2010). Development and validation of a mastication simulator. Journal of Biomechanics, 43(9):1667 -1673.

Wolter,A.,Hager,A.-S.,Zannini,E.,andArendt,E.K.(2014).Influenceofsourdough on in vitro starch digestibility and predicted glycemic indices of gluten-free breads. Food & Function, 5(3):564.

Woolnough, J. W., Monro, J. A., Brennan, C. S., and Bird, A. R. (2008a). Sim- ulating human carbohydrate digestionin vitro: a review of methods and the need for standardisation. International Journal of Food Science & Technology, 43(12):2245 -2256. -

Woolnough, J. W., Monro, J. A., Brennan, C. S., and Bird, A. R. (2008b). Sim- ulating human carbohydrate digestionin vitro: a review of methods and the need for standardisation. International Journal of Food Science & Technology, 43(12):2245 -2256.

Wright, N. D., Kong, F., Williams, B. S., and Fortner, L. (2016). A human duodenum model (HDM) to study transport and digestion of intestinal contents. Journal of Food Engineering, 171:129 -136. Wyrwisz,M.K.J.(2015).TheApplicationofDietaryFiberinBreadProducts.Journal of Food Processing & Technology, 06(05).

Yamatoya, K., Kuwano, K., and Suzuki, J. (1997). Effects of hydrolyzed guar gum on cholesterol and glucose in humans. Food Hydrocolloids, 11(2):239 -242.

Yoon, H., Sharp, K., Hill, D., Adrian, R., Balachandar, S., Ha, M., and Kar, K. (2001). Integrated experimental and computational approach to simulation of flow in a stirred tank. Chemical Engineering Science, 56(23):6635 -6649.

Yu, L., Ramaswamy, H. S., and Boye, J. (2013). Protein rich extruded products prepared from soy protein isolate-corn flour blends. LWT - Food Science and Technology, 50(1):279 -289.

Yurkstas, A. A. (1965). The masticatory act. The Journal of Prosthetic Dentistry, 15(2):248 -260.

Zhu, Y. (2011). Response to the article -In vitro human digestion models for food application -. Food Chemistry, 128(3):820 -821.

Zijlstra, N., de Wijk, R., Mars, M., Stafleu, A., and de Graaf, C. (2009). Effect of bite size and oral processing time of a semisolid food on satiation. American Journal of Clinical Nutrition, 90(2):269 -275.

Zijlstra, N., Mars, M., Stafleu, A., de Wijk, R., and de Graaf, C. (2010). Investigating the effect of texture differences in 3 pairs of solid foods on satiation. Appetite, 55(1):169 - 170.

Zuidmeer, L., Goldhahn, K., Rona, R. J., Gislason, D., Madsen, C., Summers, C., Sodergren, E., Dahlstrom, J., Lindner, T., Sigurdardottir, S. T., McBride, D., and Keil, T. (2008). The prevalence of plant food allergies: A systematic review. Journal of Allergy and Clinical Immunology, 121(5):1210 -1218.e4.